

# Regulation of the mannitol utilization genes in *Bacillus subtilis*

Von der Fakultät Energie-, Verfahrens- und Biotechnik der Universität Stuttgart  
zur Erlangung der Würde eines Doktors der Naturwissenschaften (Dr. rer. nat.)  
genehmigte Abhandlung

vorgelegt von

**Kambiz Morabbi Heravi**

aus Teheran, IRAN

Hauptberichter: Prof. Dr. Ralf Mattes

Mitberichter: Prof. Dr. Dieter Jendrossek

Tag der mündlichen Prüfung: 08.02.2013

Institut für Industrielle Genetik der Universität Stuttgart  
2013



I hereby assure that I performed the present study independently without further help or other materials than stated.

Stuttgart, 15<sup>th</sup> June 2012



## Acknowledgements

- ❖ I would like to thank my doctoral advisor, *Prof. Dr. Ralf Mattes*, for his support during the past four years, and his critical suggestions for the correction of this dissertation. Additionally, I would like to thank *Prof. Dr. Dieter Jendrossek*, co-examiner of this doctoral thesis.
- ❖ I also appreciate *Prof. Dr. Andreas Stolz* and *Prof. Dr. Jens Kurreck* for their helpful recommendation letters during the study.
- ❖ I would like to express my deepest gratitude to my supervisor, *Dr. Josef Altenbuchner*, whose expertise and guidance inspired me to develop new ideas during this project. His caring and trust provided an excellent chance for the accomplishment of my research. I have learned a lot from him.
- ❖ I also wish to thank *Dr. Hildegard Watzlawick*, whose unforgettable efforts in August 2008 made it possible for me to begin this study in Germany. I appreciate her support during this study and her suggestions for improving the biochemical trials.
- ❖ Special thanks should be given to my colleagues in the *Bacillus subtilis* research group, *Dr. Tianqi Sun*, *Marian Wenzel* and others.
- ❖ Special thanks to *Silke Weber* and *Gisella Kwiatkowski* for their assistance in this research.
- ❖ I would like to thank my colleagues and friends *Dr. Jana Hoffmann* and *Dr. Stefan Söllner* for their support, help, and guidance during this study.
- ❖ Special thanks to my colleagues in laboratory 3 of Institut für Industrielle Genetik, *Marina Boose* and *Lei Wang* for providing a friendly atmosphere during this study.
- ❖ Last but not the least, I would like to thank all other colleagues whose names are not mentioned here, but their friendly criticism, advice and suggestions have always been constructive.

*This work was accomplished with a financial support from DAAD (Deutscher Akademischer Austausch Dienst) under the index number A/07/80803*



# Table of Contents

<b>Related publication</b> .....	<b>13</b>
<b>List of abbreviations</b> .....	<b>15</b>
<b>Summary</b> .....	<b>19</b>
<b>Zusammenfassung</b> .....	<b>22</b>
<b>1. Introduction</b> .....	<b>25</b>
1.1. <i>B. subtilis</i> as an industrial host .....	25
1.2. The choice of plasmid for cloning and gene expression in <i>B. subtilis</i> .....	28
1.3. Promoters used for gene expression in <i>B. subtilis</i> .....	29
1.3.1. Transcription initiation at the promoter .....	31
1.3.2. Transcription initiation repression .....	33
1.3.3. Transcription initiation activation .....	33
1.4. Carbohydrate uptake systems in <i>Bacillus subtilis</i> .....	34
1.5. Phosphoenolpyruvate-dependent phosphotransferase system (PTS).....	35
1.6. PTS encoding operons and their specific regulators in <i>B. subtilis</i> .....	36
1.6.1. Regulation of GlcT and other PRD-containing antiterminators.....	37
1.6.2. Regulation of PRD-containing activators in <i>B. subtilis</i> .....	39
1.7. PTS and CcpA-dependent carbon catabolite repression in <i>B. subtilis</i> .....	41
1.8. CcpA-independent carbon catabolite repression.....	43
1.8.1. Catabolite control mediated by catabolite control proteins.....	43
1.8.2. Catabolite control mediated by HPr(H15~P) .....	44
1.9. Mannitol utilization system in <i>B. subtilis</i> .....	45
1.10. Aim of the study .....	46
<b>2. Materials and Methods</b> .....	<b>47</b>

2.1. Strains.....	47
2.2. Plasmids.....	48
2.3. Oligonucleotides.....	53
2.4. Media.....	58
2.5. Antibiotics .....	60
2.6. Buffers and solutions.....	60
2.7. Chemicals and enzymes .....	64
2.8. Instruments .....	65
2.9. Growth conditions .....	66
2.10. DNA manipulation .....	67
2.10.1. DNA isolation .....	67
2.10.2. PCR .....	68
2.10.3. Hybridization of complementary oligonucleotides .....	70
2.10.4. Restriction digestion of PCR fragments and plasmids.....	70
2.10.5. Isopropanol precipitation of DNA.....	71
2.10.6. Agarose gel electrophoresis .....	71
2.10.7. Purification of the DNA from agarose gel .....	71
2.10.8. Alkaline phosphatase treatment .....	72
2.10.9. DNA concentration .....	72
2.10.10. Ligation .....	72
2.10.11. DNA sequencing .....	73
2.11. RNA manipulation .....	73
2.11.1. RNase-free equipment.....	73
2.11.2. RNA isolation.....	74
2.11.3. Formaldehyde agarose gel electrophoresis .....	74



2.11.4. Isopropanol precipitation of RNA.....	74
2.11.5. Primer Extension.....	75
2.12. Transformation of <i>E. coli</i> JM109.....	75
2.13. Electroporation of <i>E. coli</i> DH5 $\alpha$ .....	76
2.14. Transformation of <i>B. subtilis</i> .....	77
2.15. Electroporation of <i>B. subtilis</i> .....	77
2.16. Protein analysis methods.....	78
2.16.1. Cell disruption.....	78
2.16.2. SDS-PAGE.....	79
2.16.3. Native PAGE electrophoresis.....	80
2.16.4. Bradford assay.....	80
2.16.5. Affinity chromatography by Ni-NTA agarose column.....	81
2.16.6. Buffer exchange by PD MidiTrap G-25 column.....	81
2.16.7. Ion-exchange chromatography (IEC).....	81
2.16.8. Electrophoretic mobility shift.....	82
2.17. $\beta$ -galactosidase assay (Miller's assay).....	83
2.18. Fluorescence measurement.....	83
2.19. Bioinformatic.....	84
<b>3. Results .....</b>	<b>85</b>
3.1. Activity of the <i>mtlAFD</i> promoter ( $P_{mtlA}$ ).....	85
3.2. Identification of the $P_{mtlA}$ transcription start site.....	87
3.3. Shortening of the $P_{mtlA}$ sequence.....	88
3.4. $P_{mtlA}$ activity in minimal and rich medium.....	89
3.5. Activity of the <i>mtlR</i> promoter ( $P_{mtlR}$ ).....	90
3.6. Identification of the $P_{mtlR}$ transcription start site.....	91

3.7.	Shortening of the 5' untranslated region of $P_{mtlR}$ - <i>lacZ</i> mRNA .....	92
3.8.	Comparison of $P_{mtlA}$ and $P_{mtlR}$ .....	93
3.9.	HPr(H15~P)-dependent activity of $P_{mtlA}$ .....	94
3.10.	Deletion of the mannitol utilization genes in <i>B. subtilis</i> .....	95
3.10.1.	Deletion of the activator encoding gene ( <i>mtlR</i> ) .....	95
3.10.2.	Deletion of the mannitol-specific enzyme II encoding genes ( <i>mtlAF</i> ) .....	96
3.10.3.	Deletion of <i>mtlF</i> by a new markerless deletion system .....	99
3.10.4.	Disruption of the mannitol 1-phosphate dehydrogenase encoding gene ( <i>mtlD</i> )....	102
3.10.5.	Deletion of the <i>mtlAFD</i> operon .....	103
3.11.	Regulation of $P_{mtlA}$ and $P_{mtlR}$ by glucitol .....	104
3.11.1.	$P_{mtlA}$ induction by glucitol .....	104
3.11.2.	Induction of $P_{mtlR}$ by glucitol.....	105
3.11.3.	Deletion of the <i>gutRBP</i> genes encoding glucitol utilization system .....	106
3.11.4.	Growth of the <i>mtl</i> and <i>gut</i> mutants in minimal medium .....	107
3.12.	Carbon catabolite repression of $P_{mtlA}$ and $P_{mtlR}$ .....	109
3.12.1.	$P_{mtlA}$ activity in the presence of different PTS sugars .....	109
3.12.2.	Activity of $P_{mtlA}$ in CcpA-dependent CCR mutants .....	109
3.12.3.	$P_{mtlR}$ activity in CcpA-dependent CCR mutants .....	111
3.12.4.	Deletion of the glucose-PTS transporter .....	112
3.13.	Regulation of the MtlR activity via phosphorylation of MtlR domains.....	113
3.13.1.	Integration of $P_{mtlA}$ - <i>lacZ</i> into the chromosome .....	113
3.13.2.	Mutation of the PRDI domain.....	114
3.13.3.	Mutation of the PRDII domain.....	116
3.14.	Operators of $P_{mtlA}$ and $P_{mtlR}$ .....	117
3.14.1.	Alignment of the $P_{mtlA}$ and $P_{mtlR}$ putative activator binding sites .....	117

3.14.2.	Fusion of the $P_{mtlA}$ upstream sequence to the $P_{mtlR}$ core elements.....	118
3.14.3.	Shortening of the 5'-end of $P_{mtlA}$ .....	118
3.14.4.	Mutations between the MtlR binding site and -35 box of $P_{mtlA}$ .....	119
3.14.5.	Construction of hybrid promoters .....	121
3.14.6.	<i>In vitro</i> activity of MtlR .....	129
3.14.7.	Function of the $P_{mtlA}$ and $P_{mtlR}$ <i>cre</i> sites and their mutants.....	140
3.14.8.	Fusion of $P_{groE}$ to <i>cre</i> sites.....	143
3.15.	Expression system based on mannitol regulatory elements .....	145
3.15.1.	Optimization of -10 box in $P_{mtlA}$ .....	145
3.15.2.	Shortening the 5'UTR in $P_{mtlA}$ - <i>lacZ</i> mRNA.....	146
3.15.3.	Construction of expression vectors based on pUB110.....	147
3.15.4.	Improvement of the expression vector based on $P_{mtlA}$ .....	149
<b>4.</b>	<b>Discussion.....</b>	<b>152</b>
4.1.	Structure and transcription activation of $P_{mtlA}$ and $P_{mtlR}$ .....	152
4.2.	Regulation of $P_{mtlA}$ and $P_{mtlR}$ .....	155
4.3.	Carbon catabolite repression of $P_{mtlA}$ and $P_{mtlR}$ .....	159
4.4.	Translation initiation and construction of an expression system .....	162
<b>5.</b>	<b>Conclusion and perspectives .....</b>	<b>166</b>
<b>6.</b>	<b>References .....</b>	<b>167</b>
<b>7.</b>	<b>Appendices .....</b>	<b>185</b>



## Related publication

Morabbi Heravi, K., M. Wenzel, and J. Altenbuchner. 2011. **Regulation of *mtl* operon promoter of *Bacillus subtilis*: Requirements of its use in expression vectors.** *Microbial Cell Factories* 10:83.

Morabbi Heravi K., Altenbuchner A. **Construction of an expression system based on mannitol PTS in *Bacillus subtilis* and its regulation.** Annual Conference of the Association for General and Applied Microbiology (VAAM), 18–21 March 2012, Tübingen, Germany. (Poster OTP087)  
Published abstract in: VAAM Biospektrum Sonderausgabe 2012.



## List of abbreviations

$\alpha$ CTD	C-terminus of the $\alpha$ subunit of RNA polymerase
a.k.a.	also known as
amp	ampicillin
A	adenine (for DNA)/ alanine (for protein)
AMV-RT	avian myeloblastosis virus reverse transcriptase
APS	ammonium persulfate
ATP	adenosine triphosphate
bla	$\beta$ -lactamase
bp	base pair
BSA	bovine serum albumin
cDNA	complementary DNA
cat	chloramphenicol acetyltransferase
<i>cre</i>	catabolite responsive element
C	cytosine
Cm	chloramphenicol
Cy5	cyanine dye5
CCR	carbon catabolite repression
CRP	cyclic AMP receptor protein
dNTP	deoxyribonucleotide
ddATP	2',3'-Dideoxyadenosine-5'-triphosphate
ddCTP	2',3'-Dideoxycytidine-5'-triphosphate
ddGTP	2',3'-Dideoxyguanosine-5'-triphosphate
ddH <sub>2</sub> O	double-distilled water
ddTTP	2',3'-Dideoxythymidine-5'-triphosphate
ddNTP	dideoxyribonucleotide
Da	dalton
DEPC	diethylpyrocarbonate
DHAP	dihydroxyacetone phosphate
DMSO	dimethyl sulfoxide
DNA	deoxyribonucleic acid
DTT	dithiothreitol
e.g.	for example
erm	erythromycin
<i>et al.</i>	<i>et alii</i>
<i>etc.</i>	<i>et cetera</i>
eGFP	enhanced green fluorescent protein
EDTA	ethylenediaminetetraacetic acid

Fig.	figure
FBP	fructose 6-phosphate
G	guanine
Glc	D-glucose
h	hour
H	histidine
His	histidine
HEPES	4-(2-hydroxyethyl)-1-piperazineethanesulfonic acid
HF	high fidelity
HTH	helix-turn-helix
<i>i.e.</i>	<i>id est</i> (that is)
<i>in vitro</i>	within glass
<i>in vivo</i>	within the living
kb	kilobase pair
kDa	kilodalton
kPa	kilopascal
LB	lysogeny broth
Mtl	D-mannitol
MOPS	3-(N-morpholino)propanesulfonic acid
M.U.	Miller unit
N	any nucleotide (adenine, cytosine, guanine, thymine)
Ni-NTA	nickel-nitrilotriacetic acid
ori	origin of replication
OD <sub>600</sub>	optical density of a sample measured at a wavelength of 600 nm
ppGpp	guanosine pentaphosphate
PAGE	polyacrylamide gel electrophoresis
PCR	polymerase chain reaction
PEG	polyethylene glycol
PEP	phosphoenolpyruvate
PHA	polyhydroxyalkanoates
PMSF	phenylmethanesulfonylfluoride
PRD	PTS-regulatory domains
PTS	phosphoenolpyruvate-dependent phosphotransferase system
rha	rhamnose
rpm	revolutions per minute
RBS	ribosomal binding site
RFU	relative fluorescence units
RNase	ribonuclease
RNA	ribonucleic acid
RNAP	DNA-dependent RNA polymerase



RT	room temperature
ssDNA	single-stranded DNA
ScFv	single-chain variable fragment
Spc	spectinomycin
S	serine
SDS	sodium dodecyl sulfate
T	thymine
Tris	tris(hydroxymethyl)aminomethane
T <sub>m</sub>	DNA melting temperature
TAE	Tris-acetate-EDTA
TB	terrific broth
TCA	tricarboxylic acid cycle
TCEP	tris(2-carboxyethyl)phosphine
TEMED	<i>N,N,N',N'</i> -tetramethylethylenediamine
TIR	translation initiation region
TSS	transcription start site
TSS (solution)	transformation and storage solution
UTR	untranslated region of mRNA
UV	ultraviolet



## Summary

*Bacillus subtilis* takes up mannitol by a phosphoenolpyruvate-dependent phosphotransferase system (PTS). The mannitol utilization system is encoded by the *mtlAFD* operon consisting of *mtlA* (encoding membrane-bound EIICB<sup>Mtl</sup>), *mtlF* (encoding phosphocarrier EIIA<sup>Mtl</sup>), and *mtlD* (encoding mannitol 1-phosphate dehydrogenase). This operon is activated by MtlR whose coding gene is located approx. 14.4 kb downstream of the operon. The regulation of the mannitol utilization genes in *B. subtilis* was studied by fusion of the promoters of *mtlAFD* ( $P_{mtlA}$ ) and *mtlR* ( $P_{mtlR}$ ) to *lacZ* as a reporter gene. Both the  $P_{mtlA}$  and  $P_{mtlR}$  were inducible by mannitol and glucitol, while glucose reduced their activities. The promoter strength of  $P_{mtlA}$  was about 4.5-fold higher than that of  $P_{mtlR}$ . Identification of the transcription start sites of  $P_{mtlA}$  and  $P_{mtlR}$  revealed that both of these promoters contain a  $\sigma^A$ -type promoter structure. The promoter -35 and -10 boxes in  $P_{mtlA}$  were TTGTAT and TAACAT and in  $P_{mtlR}$  TTGATT and TATATT, respectively. Catabolite responsive elements (*cre*) were detected in the sequences of  $P_{mtlA}$  and  $P_{mtlR}$  overlapping the -10 boxes. Shortening the mRNA 5' untranslated region (5'UTR) increased the  $P_{mtlA}$  activity, whereas  $P_{mtlR}$  activity was decreased by shortening of its mRNA 5'UTR. Alignment of the -35 upstream sequences of  $P_{mtlA}$  and  $P_{mtlR}$  revealed the putative MtlR binding site. This sequence comprised a similar incomplete inverted repeat in both the  $P_{mtlA}$  and  $P_{mtlR}$  sequences (TTGNCACAN<sub>4</sub>TGTGNCAA). This sequence was encompassed by two 11 bp distal and proximal flanking sequences. Construction of  $P_{mtlA}$ - $P_{licB}$  hybrid promoters and shortening of the 5'-end of  $P_{mtlA}$  indicated the probable boundaries of putative MtlR binding site in  $P_{mtlA}$ . Increasing the distance between the putative MtlR binding site and -35 box lowered the  $P_{mtlA}$  maximal activity, although  $P_{mtlA}$  remained inducible by mannitol.  $P_{mtlA}$  became inactive by disruption of the TTGNCACAN<sub>4</sub>TGTGNCAA sequence. In contrast, manipulation of the distal and proximal flanking sequences only reduced the maximal activity of  $P_{mtlA}$ , whereas  $P_{mtlA}$  remained highly inducible. These flanking sequences contained AT-rich repeats similar to the consensus sequence of  $\alpha$ CTD binding sites. It is assumed that MtlR binds to the TTGNCACAN<sub>4</sub>TGTGNCAA sequence, whereas two  $\alpha$ CTD monomers bind to AT-rich sequences upstream and downstream of MtlR binding site. In this way, the mechanism of class I activation was proposed for  $P_{mtlA}$  and  $P_{mtlR}$  transcription initiation.

Regulation of  $P_{mnlA}$  and  $P_{mnlR}$  was investigated by deletion of  $mnlAF$ ,  $mnlF$ ,  $mnlD$ , and  $mnlR$ . Deletion of the  $mnlAF$  genes rendered  $P_{mnlA}$  and  $P_{mnlR}$  constitutive showing the inhibitory effect of EIICB<sup>Mtl</sup> and EIIA<sup>Mtl</sup> (PTS transporter components) on MtlR in the absence of mannitol. The constitutive activity of  $P_{mnlA}$  was increased by the deletion of  $mnlF$ . In contrast, the deletion of  $mnlAFD$  showed a significant reduction in the  $P_{mnlA}$  constitutive activity. Disruption of  $mnlD$  made *B. subtilis* sensitive to mannitol in a way that addition of mannitol or glucitol to the bacterial culture ended in cell lysis. Besides,  $P_{mnlA}$  and  $P_{mnlR}$  were similarly induced by glucitol and mannitol in a  $mnlD::erm$  mutant. Also, deletion of  $mnlR$  rendered  $P_{mnlA}$  and  $P_{mnlR}$  uninducible by mannitol or glucitol. In contrast, deletion of the glucitol utilization genes had no influence on the inducibility of  $P_{mnlA}$  or  $P_{mnlR}$  by glucitol. The  $P_{mnlA}$  activity was drastically reduced in  $ptsH$ -H15A (HPr-H15A) mutant similar to the  $\Delta mnlR$  mutant. The mutation of histidine 289 in the PRDI domain of MtlR to alanine reduced the activity of  $P_{mnlA}$ , whereas the  $P_{mnlA}$  activity in the  $mnlR$ -H230A mutant was almost similar to wild type. In contrast, mutation of the PRDII domain of MtlR to H342D mainly relieved  $P_{mnlA}$  from glucose repression. Moreover, MtlR double mutant H342D C419A which was produced in *E. coli* was shown to be active *in vitro*. These results represent the positive regulation of MtlR via phosphorylation of the PRDII domain by HPr(H15~P). Also, dephosphorylation of the domains EIIB<sup>Gat</sup>- and EIIA<sup>Mtl</sup>-like of MtlR by EIIA<sup>Mtl</sup> and EIICB<sup>Mtl</sup> transporter components causes activation. The  $P_{mnlA}$  activity was repressed in the presence of glucose and fructose, while sucrose and mannose had no influence on the  $P_{mnlA}$  activity. Therefore, catabolite repression of  $P_{mnlA}$  and  $P_{mnlR}$  were studied by CcpA-dependent carbon catabolite repression mutants, such as  $ptsH$ -S46A,  $\Delta crh$ ,  $\Delta hprK$ , and  $\Delta ccpA$ . Induction of  $P_{mnlA}$  and  $P_{mnlR}$  in these mutants did not result in a complete loss of catabolite repression. Therefore, the catabolite responsive elements (*cre* sites) of  $P_{mnlA}$  and  $P_{mnlR}$  were investigated. Using a constitutive promoter,  $P_{groE}$ , it was shown that the *cre* sites of  $P_{mnlA}$  and  $P_{mnlR}$  were weakly functional. In contrast, deletion of the glucose PTS transporter, encoded by  $ptsG$ , resulted in a complete loss of glucose repression in  $P_{mnlA}$  and  $P_{mnlR}$ . Thus, the main glucose repression of mannitol PTS function at the posttranslational level in a HPr-mediated manner via MtlR-H342 and at transcriptional level by CcpA-dependent carbon catabolite repression.

Finally,  $P_{mnlA}$  was tested for its application as a heterologous gene expression system based on a derivative of pUB110 with high copy number in the cell. Further studies showed that a

single copy of *mtlR* controlled by its own promoter ( $P_{mtlR-mtlR}$ ) on the chromosome was not enough for the activity of  $P_{mtlA}$  on a high copy number vector. Thus,  $P_{mtlR-mtlR}$  was inserted into the same vector. In this case, the induced  $P_{mtlA}$  activity and its basal activity increased. Ultimately, a highly inducible expression system based on mannitol as a cheap inducer was constructed.

## Zusammenfassung

*Bacillus subtilis* nimmt Mannitol mit Hilfe eines Phosphoenolpyruvat-abhängigem Phosphotransferasesystems auf. Dieses wird durch das *mtlAFD*-Operon codiert, welches aus *mtlA* (codiert das Membran-gebundene EIICB<sup>Mtl</sup>), *mtlF* (codiert das Phosphorylgruppen-übertragende EIIA<sup>Mtl</sup>) und *mtlD* (codiert die Mannitol-1-phosphat-Dehydrogenase) besteht. Das Operon wird durch MtlR aktiviert, dessen Gen ca. 14,4 kb stromabwärts des Operons lokalisiert ist. Die Regulation der Gene für die Mannitol-Verwertung in *B. subtilis* wurde mit Hilfe des Reportergens *lacZ* untersucht, welches an die Promotoren vom *mtlAFD* ( $P_{mtlA}$ ) sowie *mtlR* ( $P_{mtlR}$ ) fusioniert wurde. Sowohl  $P_{mtlA}$  als auch  $P_{mtlR}$  wurden durch Mannitol und Glucitol induziert, während Glucose die Promotoraktivitäten reprimierte. Im Vergleich zu  $P_{mtlR}$  zeigte  $P_{mtlA}$  eine ca. 4,5-fach höhere Promotorstärke. Die Analyse der Transkriptionsinitiations-Sequenzen durch Transkriptionsstartbestimmung von  $P_{mtlA}$  und  $P_{mtlR}$  ergab, dass es sich um  $\sigma^A$ -abhängige Promotoren handelt. Die -35 und -10 Promotorsequenzen von  $P_{mtlA}$  und  $P_{mtlR}$  wurden als TTGTAT und TAACAT bzw. TTGATT und TATATT identifiziert. In beiden Promotoren wurden *cre*-Sequenzen (catabolite responsive element) gefunden, welche mit den -10 Regionen überlappen. Eine Verkürzung der 5'-untranslatierten Region (5'UTR) von  $P_{mtlA}$  erhöhte dessen Aktivität, wohingegen die Aktivität von  $P_{mtlR}$  durch die Verkürzung der 5'UTR reduziert wurde. Durch Sequenzalignment der stromaufwärts von  $P_{mtlA}$  und  $P_{mtlR}$  gelegenen Sequenzen konnte die mutmaßliche MtlR-Bindestelle identifiziert werden. Diese Bindestelle ist in beiden Sequenzen durch eine unvollständig ausgeprägte, invertierte Wiederholungssequenz (TTGNCACAN<sub>4</sub>TGTGNCAA) charakterisiert, welche ihrerseits von jeweils zwei 11 bp langen Sequenzen flankiert wird. Die Konstruktion von  $P_{mtlA}$ - $P_{licB}$  Hybrid-Promotoren und eine Verkürzung des 5'-Terminus von  $P_{mtlA}$  brachte Erkenntnisse bezüglich des Bereichs der mutmaßlichen MtlR-Bindestelle innerhalb von  $P_{mtlA}$ . Eine Vergrößerung der Distanz zwischen der mutmaßlichen MtlR-Bindestelle und der -35 Region verringerte die maximale Aktivität von  $P_{mtlA}$ , welcher aber noch Mannitol-induzierbar blieb. Eine Unterbrechung der Sequenz TTGNCACAN<sub>4</sub>TGTGNCAA verursachte eine Inaktivierung von  $P_{mtlA}$ . Im Gegensatz dazu hatte die Veränderung flankierender Sequenzen nur eine Reduktion der maximalen Aktivität von  $P_{mtlA}$  zur Folge, wobei die Induzierbarkeit des  $P_{mtlA}$  erhalten blieb. In den flankierenden Sequenzen

wurden AT-reiche Wiederholungen identifiziert, welche Ähnlichkeit zu der Konsensus-Sequenz von  $\alpha$ CTD aufweisen. Es wird angenommen, dass MtlR an die Sequenz TTGNACAN<sub>4</sub>TGTGNCAA bindet und zwei  $\alpha$ CTD Monomere an AT-reichen Sequenzen, die sich jeweils stromaufwärts bzw. stromabwärts dieser MtlR-Bindestelle befinden. Dies lässt auf einen Mechanismus der Klasse I schließen.

Die Regulation von  $P_{mtlA}$  und  $P_{mtlR}$  wurde mit Hilfe von *mtlAF*-, *mtlF*-, *mtlD*- und *mtlR*-Deletionen in *B. subtilis* untersucht. Die Deletion von *mtlAF* führte zu einer konstitutiven Aktivität von  $P_{mtlA}$  und  $P_{mtlR}$ , wodurch der inhibitorische Effekt von EIICB<sup>Mtl</sup> und EIIA<sup>Mtl</sup> (Untereinheiten des PTS-Transporters) auf MtlR bei Abwesenheit von Mannitol gezeigt werden konnte. Die konstitutive Aktivität von  $P_{mtlA}$  wurde durch die Deletion von *mtlF* noch verstärkt. Im Gegensatz dazu verursachte die Deletion von *mtlAFD* eine signifikante Reduktion der konstitutiven Aktivität von  $P_{mtlA}$ . Die Mutation von *mtlD* resultierte in einer Sensitivität von *B. subtilis* gegenüber Mannitol und Glucitol. Kultivierung in Gegenwart dieser Zucker führte zu einer Lyse der Zellen. In der *mtlD::erm* Mutante wurden  $P_{mtlA}$  und  $P_{mtlR}$  durch Glucitol und Mannitol gleichermaßen induziert. Ferner führte die Deletion von *mtlR* zu einer Uninduzierbarkeit von  $P_{mtlA}$  und  $P_{mtlR}$  mit Mannitol und Glucitol, wohingegen die Deletion der Gene für die Glucitol-Verwertung keinen Einfluss auf die Induzierbarkeit von  $P_{mtlA}$  und  $P_{mtlR}$  mit Glucitol hatte. Wie auch in der  $\Delta$ *mtlR* Mutante war die Aktivität von  $P_{mtlA}$  in der *ptsH*-H15A (HPr-H15A) Mutante drastisch reduziert. Die Mutation des Histidin 289 in der PRDI-Domäne von MtlR zu einem Alanin reduzierte die Aktivität von  $P_{mtlA}$ , während die Aktivität von  $P_{mtlA}$  in der *mtlR*-H230A-Mutante ähnlich wie die des Wildtyps war. Im Gegensatz dazu führte die Mutation H342D der PRDII-Domäne von MtlR zu einer verminderten Glucose-Repression von  $P_{mtlA}$ . Eine MtlR Doppelmutante H342D C419A wurde in *E. coli* produziert und ihre Aktivität in einem Gelmobilityshiftassay *in vitro* bestätigt. Diese Ergebnisse zeigen, dass MtlR einer, durch die Phosphorylierung der PRDII-Domäne durch HPr(H15~P) stattfindenden, positiven Regulation unterliegt. Ferner kann eine Aktivierung von MtlR durch eine Dephosphorylierung der EIIB<sup>Gat</sup>- und EIIA<sup>Mtl</sup>-ähnlichen Domänen durch die EIIA<sup>Mtl</sup> und EIICB<sup>Mtl</sup> Transporter-Untereinheiten erreicht werden. Glucose und Fructose reprimieren die Aktivität von  $P_{mtlA}$  wohingegen Saccharose und Mannose keinen Einfluss auf die  $P_{mtlA}$ -Aktivität haben. Daher wurde die Kohlenstoff-Katabolit-Repression von  $P_{mtlA}$  und  $P_{mtlR}$  in CcpA-abhängigen Mutanten, wie

*ptsH-S46A*,  $\Delta$ *crh*,  $\Delta$ *hprK* und  $\Delta$ *ccpA*, untersucht. Da eine Induktion von  $P_{mtlA}$  und  $P_{mtlR}$  in den Mutanten nicht zu einem vollständigen Verlust der Katabolit-Repression führte, wurden die *cre*-Sequenzen (catabolite responsive element) der beiden Promotoren untersucht. Mit Hilfe des konstitutiven Promotors  $P_{groE}$  wurde gezeigt, dass die *cre*-Sequenzen von  $P_{mtlA}$  und  $P_{mtlR}$  nur schwach funktionsfähig waren. Im Gegensatz dazu führte die Deletion des Glucose-PTS-Transporters, welcher von *ptsG* codiert wird, zu einem vollständigen Verlust der Glucose-Repression von  $P_{mtlA}$  und  $P_{mtlR}$ . Folglich wird die Repression des Mannitol-PTS durch Glucose hauptsächlich posttranslational durch HPr *via* MtlR-H342 und auf transkriptionaler Ebene durch eine CcpA-abhängige Kohlenstoff-Katabolit-Repression vermittelt.

Die Anwendbarkeit des  $P_{mtlA}$  als Kontrollelement für eine homologe- oder heterologe Genexpression wurde untersucht. Hierzu wurde ein Expressionsvektor basierend auf dem pUB110 Vektor, der einer hohen Kopienzahl aufweist, konstruiert. Jedoch zeigte sich, dass für die Kontrolle des  $P_{mtlA}$  eine chromosomale Kopie von *mtlR* nicht ausreichend ist. Das Vorhandensein von  $P_{mtlR}$ -*mtlR* auf dem Vektor führte jedoch zu einer Erhöhung der Basalaktivität sowie der maximalen Aktivität. Letztendlich wurde ein gut regulierbares, auf dem günstigen Induktor Mannitol basierendes Expressionssystem konstruiert.



# 1. Introduction

The genus *Bacillus* was named by changing the name of Ehrenberg's "*Vibrio subtilis*" to *Bacillus subtilis* by Ferdinand Cohn in 1872 (33, 53, 85). However, it was only from about 1920 that the genus *Bacillus* was defined to include aerobic, endospore-forming, and rod-shaped bacteria (31). This genus is one of the most diverse and commercially useful groups of the bacteria (85). Among them, *Bacillus subtilis* is an ubiquitous microorganism found in soil, water, and air (50). Development of *B. subtilis* as a bacterial model system began over 60 years ago with the pioneering mutagenesis studies (25). Later, it was found that *B. subtilis* 168, a tryptophan auxotrophic mutant, produced naturally competent cells relevant for genetic transformation (206). *B. subtilis* as a Gram-positive bacterium belongs to the Firmicutes with a low G + C content. At first, the entire genome of *B. subtilis* 168 was published in 1997 (117). A decade later, *B. subtilis* genome was resequenced and the data are readily available in GenoList database (<http://genodb.pasteur.fr/cgi-bin/WebObjects/GenoList>) (9). Whole genome sequencing of *B. subtilis* 168 showed that this bacterium has 4,214,810 base pairs comprising of 4,100 protein-coding frames (117). Several characteristics of *B. subtilis* including biofilm formation, cannibalism, natural competence, motility, as well as endospore formation turned *B. subtilis* into a reference model for research applications (50, 78, 138, 205).

## 1.1. *B. subtilis* as an industrial host

Production and secretion of homologous extracellular enzymes, such as  $\alpha$ -amylase, alkaline protease, alkaline phosphatase, esterase, *etc.*, at gram per liter concentrations made *B. subtilis* an important source for industrial enzymes. Due to the presence of such a huge capacity for protein secretion, *B. subtilis* was also exploited as a workhorse for production and secretion of heterologous proteins in order to facilitate the downstream processing (87, 134, 201). Heterologous enzymes, such as acid-stable  $\alpha$ -amylase from *B. licheniformis* (3.1 g/l), as well as pharmaceutical proteins, e.g. human interleukin-3 (100 mg/l), were successfully produced and secreted into the growth medium (92, 243). The mentioned proteins are two examples of the

successfully produced enzymes, pharmaceutical proteins, and vaccine components summarized in table 1.1 (57, 188, 219, 244).

**Table 1. 1.** Some of the heterologous and homologous proteins produced by *B. subtilis* (244).

Product	Product origin	Yield (mg/l)	Reference
$\alpha$ -amylase	<i>Bacillus amyloliquefaciens</i>	1,000 – 3,000	(168)
Epidermal growth factor	human	7	(121)
Interferon- $\alpha$ 2	human	0.5 – 1.0	(169)
Lipase A	<i>Bacillus subtilis</i> 168	600	(133)
Penicillin G acylase	<i>Bacillus megaterium</i>	n.d.	(256)
PHA depolymerase A	<i>Paucimonas lemoignei</i>	1.9	(15)
Proinsulin	human	1,000	(166)
ScFv	human	10 – 15	(250)
Staphylokinase	<i>Staphylococcus aureus</i>	337	(261)
Streptavidin	<i>Streptomyces avidinii</i>	35 – 50	(249)
Thioredoxin	<i>Alicyclobacillus acidocaldarius</i>	500	(2)

Indeed, there are some advantages in employing *B. subtilis* as an expression host for secreted proteins rather than *E. coli*, especially for production of pharmaceutical proteins. As a Gram-negative member, *E. coli* possesses lipopolysaccharide, a.k.a. endotoxin, and secretes the proteins into the periplasm both of which make the downstream processing costly and laborious (134). In contrast, *B. subtilis* has a huge capacity for secretion of the proteins into the medium. It is also a non-pathogen microorganism generally recognized as safe (GRAS). Finally, it has no significant biased codon usage. Nevertheless, there are some bottlenecks using *B. subtilis* as an expression host including: (i) plasmid instability, (ii) lack of proper expression systems, (iii) low level of protein productions due to inefficient DNA transcription, mRNA translation, protein translocation, or protein folding, and (iii) the presence of 44 known and 27 putative proteases and peptidases (Fig. 1.1) (134). The latter obstacle was highly solved by deletion of the protease encoding genes (listed in table 1.2). In fact, deletion of the *aprE* (serine alkaline protease) and *nprE* (neutral protease) resulted in reduction of the extracellular protease activity of *B. subtilis* to less than 4% of the wild type strain (110).

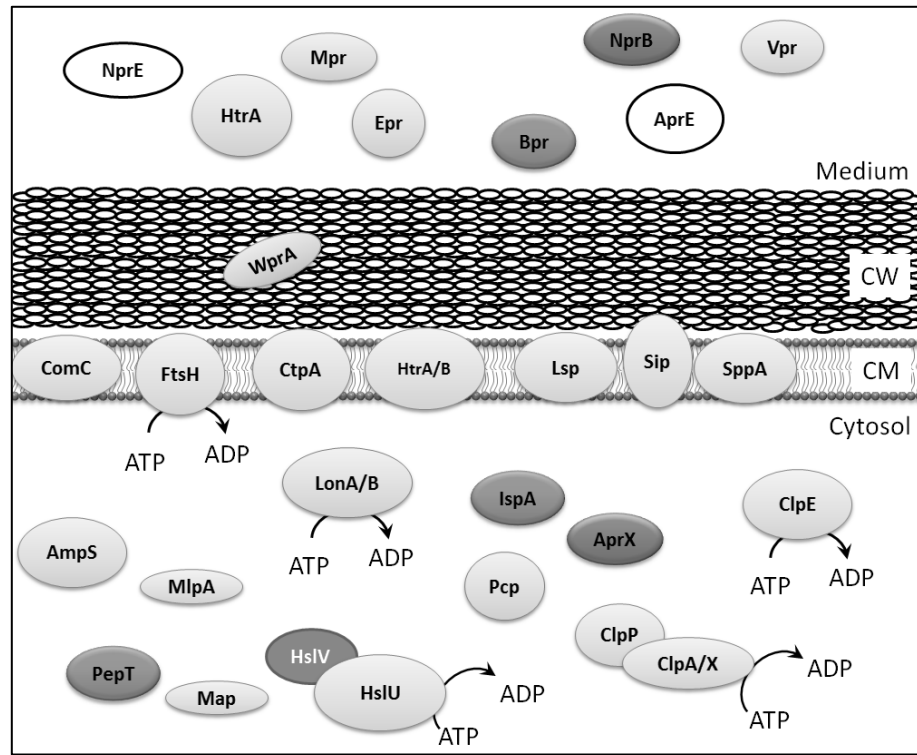


**Fig. 1. 1.** Some of the proteases and peptidases of *B. subtilis* during the vegetative growth are depicted according to Westers *et al.* (244). The sporulation proteases and peptidases as well as the proteases involved in peptidoglycan maturation are not demonstrated.

**Table 1. 2.** Some of the protease-deficient *B. subtilis* strains reviewed by Westers *et al.* (244)

<i>B. subtilis</i> strain	Protease mutation	Reference
BG2054	$\Delta nprE-522$ ; $\Delta aprE-684$	(254)
DB104	<i>nprR2</i> ; <i>nprE18</i> ; $\Delta aprE3$	(110)
DB105	<i>nprR2</i> ; <i>nprE18</i> ; $\Delta aprE3$	(110)
WB600	<i>nprE</i> ; <i>nprB</i> ; <i>aprE</i> ; <i>epr</i> ; <i>mpr</i> ; <i>bpr</i>	(251)
WB700	<i>nprE</i> ; <i>nprB</i> ; <i>aprE</i> ; <i>epr</i> ; <i>mpr</i> ; <i>bpr</i> ; <i>vpr</i>	(260)
LB700	<i>nprE</i> ; <i>nprB</i> ; <i>aprE</i> ; <i>epr</i> ; <i>mpr</i> ; <i>bpr</i> ; <i>wprA</i>	(129)
WB800	<i>nprE</i> ; <i>nprB</i> ; <i>aprE</i> ; <i>epr</i> ; <i>mpr</i> ; <i>bpr</i> ; <i>vpr</i> ; <i>wprA</i>	(250)

Co-expression of the chaperones, and thio-disulfide oxidoreductases, stabilizing the 5'- and 3'-ends of the mRNA, improvement of the translational initiation by changing the Shine-Dalgarno enhanced the production of some proteins (60, 134, 198, 233, 244). Nonetheless, all of the mentioned strategies are dependent on a strong and tightly regulated gene expression system.

## 1.2. The choice of plasmid for cloning and gene expression in *B. subtilis*

Enhancement of gene expression based on stable plasmids and tightly regulated promoters is the first step of heterologous (or homologous) protein overproduction. *B. subtilis* 168, the common laboratory strain, does not contain any plasmid. However, several cryptic rolling circle plasmids were isolated from *B. subtilis* isolates. These cryptic plasmids are classified in six groups, represented by pTA1015, pTA1020, pTA1030, pTA1040, pTA1050, pTA1060 (149, 228). These isolated plasmids do not confer any selectable phenotypes to their host. Therefore, most cloning vectors for *B. subtilis* are based on rolling circle-type replication plasmids from other Gram-positive bacteria such as Staphylococci or Streptococci (Table 1.3) (19-21, 81, 149, 164). For instance, pUB110 is a rolling circle-type plasmid originating from *Staph. aureus*. The derivatives of pUB110 are commonly used for gene expression in *B. subtilis*. Generally, a plasmid comprises two origins of replication in the rolling circle replication: a plus origin, which is responsible for formation of ssDNA, and a minus origin, which is the initiation site for complementary strand replication. The minus origin is not necessary for the replication of the plasmid (81). Therefore, this site was accidentally deleted in many plasmids during the vector construction. Consequently, these plasmids are frequently unstable due to the formation of ssDNA or by accumulation of high molecular weight linear head to tail DNA (21). In addition to rolling circle-type plasmids, theta-type plasmids are also widely applied for the cloning of desired genes in *B. subtilis*. Among them, pAM $\beta$ 1 is widely employed. Plasmid pAM $\beta$ 1 originates from *Enterococcus faecalis* and replicates in an unidirectional theta-type replication (24, 32, 127). However, this plasmid has a large size (approx. 26.5 kb) and low copy number (1 – 5 copies per chromosome) (32). In addition to pAM $\beta$ 1, a low-copy theta-type plasmid, called pBS72, is also used for construction of vectors in *B. subtilis*. Plasmid pBS72 was isolated from a *B. subtilis* strain (220). Due to the low copy number or low transformation frequency of the rolling circle-type and theta-type vectors in *B. subtilis*, several *E. coli/B. subtilis* shuttle vectors have been constructed based on the mentioned replicons to facilitate the plasmid propagation. Most of the constructed shuttle vectors are based on pUB110 or pBS72 origins of replication for *B. subtilis* and pBR322 for *E. coli* (198).

**Table 1. 3.** Plasmids used as the parental vectors for construction of *E. coli*/*B. subtilis* shuttle vectors are listed as stated by Schumann (198).

Plasmid	Marker	Modes of replication	Original host	Reference
pUB110	Kanamycin	Rolling circle	<i>Staphylococcus aureus</i>	(119)
pC194	Chloramphenicol	Rolling circle	<i>Staphylococcus aureus</i>	(102)
pE194	Erythromycin	Rolling circle	<i>Staphylococcus aureus</i>	(101)
pE194-cop6	Erythromycin	Rolling circle	<i>Staphylococcus aureus</i>	(241)
pT181	Tetracycline	Rolling circle	<i>Staphylococcus aureus</i>	(101)
pTA1015	Cryptic <sup>1</sup>	Rolling circle	<i>Bacillus subtilis</i>	(149)
pTA1060	Cryptic	Rolling circle	<i>Bacillus subtilis</i>	(228)
pAM $\beta$ 1	Erythromycin	Theta-type	<i>Enterococcus faecalis</i>	(32)
pBS72	Cryptic	Theta-type	<i>Bacillus subtilis</i>	(220)
pIP404	Chloramphenicol	Theta-type	<i>Clostridium perfringens</i>	(17)
	Tetracycline			
pIP501	Chloramphenicol	Theta-type	<i>Streptococcus agalactiae</i>	(96)
	Erythromycin			
pLS20	Cryptic	Theta-type	<i>Bacillus subtilis</i> var. <i>natto</i>	(217)
pLS32	Cryptic	Theta-type	<i>Bacillus subtilis</i> var. <i>natto</i>	(218)
pSM19035	Erythromycin	Theta-type	<i>Streptococcus pyogenes</i>	(27)
pTB19	Tetracycline	Theta-type	<i>Geobacillus stearothermophilus</i>	(99)
	Kanamycin			

<sup>1</sup>Cryptic plasmids do not confer selectable marker.

### 1.3. Promoters used for gene expression in *B. subtilis*

Constitutive promoters, such as the promoter of *amyQ* from *B. amyloliquifaciens*, were among the first promoters exploited to express  $\alpha$ -amylase,  $\beta$ -lactamase and human interferon  $\alpha 2$  (IFN-  $\alpha 2$ ) in *B. subtilis* (168-170). By expanding the knowledge of regulatory systems in *B. subtilis*, several inducible promoters have been later employed for gene expression in *B. subtilis* (Table 1.4). These inducible promoters could be classified into three major classes: (i) inducer-specific promoters, (ii) growth phase- and stress-specific promoters, and (iii) autoinducible promoters. Among them, inducer-specific promoters are the most widely used (198). So far, the expression systems in *B. subtilis* are mostly based on xylose or IPTG as the inducers. Basically, xylose-inducible expression systems comprise the promoter of the *xylAB* operon ( $P_{xylA}$ ). The *xylAB* operon encodes the components of the xylose utilization system in *B. subtilis*. The expression of *xylAB* is negatively regulated by a repressor, XylR. The inducer xylose binds and inactivates XylR (66). IPTG-inducible expression systems are based on *lac* operator and LacI, the repressor of the *lacZYA* operon in *E. coli* (71). IPTG-inducible  $P_{spac}$  is a well-known

promoter in which the promoter of *B. subtilis* phage SPO-1 and *E. coli lac* operator are fused (258). IPTG inactivates LacI and thereby induces  $P_{spac}$  activity. Nevertheless,  $P_{spac}$  has some disadvantages including the high cost of IPTG and its toxicity. Besides,  $P_{spac}$  activity is not strong enough and not tightly-controlled for large-scale protein production (198). Hence, construction of the sugar-inducible expression systems are highly attended in recent years (163, 198). A summary of used promoters are listed in table 2.4.

**Table 1. 4.** Promoters used for gene expression in *B. subtilis*.

Promoter	Inducer	Type	Reference
$P_{59}$	-	Constitutive	(18)
$P_{HpaII}$	-	Constitutive	(18)
$P_{amyQ}$	-	Constitutive	(170)
$P_{APase}$	Phosphate concentration	Autoinducible	(128)
$P_{aprE}$	-	Stationary growth phase-specific	(104)
$P_{araA}$	Arabinose	Inducer-specific	(39)
$P_{citM}$	Citrate	Inducer-specific	(63)
$P_{des}$	-	Cold-inducible	(126)
$P_{gev}$	Glycine	Inducer-specific	(175)
$P_{malA}$	Maltose	Inducer-specific	(255)
$P_{grac}$	IPTG	Inducer-specific	(174)
$P_{gsiB}$	Heat and acid shock, ethanol	Autoinducible, Stress-specific	(161)
$P_{hyper-spark}$	IPTG	Inducer-specific	(179)
$P_{lepA}$	-	Constitutive	(161)
$P_{manP}$	Mannose	Inducer-specific	(214)
$P_{N25}$	IPTG	Inducer-specific	(125)
$P_{P43}$	-	Constitutive	(264)
$P_{PhoD}$	Phosphate concentration	Autoinducible	(52)
$P_{pst}$	Phosphate concentration	Autoinducible	(111)
$P_{rpsF}$	-	Exponential growth phase-specific	(163)
$P_{sacB}$	Sucrose	Inducer-specific	(265)
$P_{spac}$	IPTG	Inducer-specific	(259)
$P_{spaS}$	Subtilin	Late exponential growth phase-specific	(14)
$P_{T7}$	Xylose, rifampicin	Inducer-specific	(35)
$P_{tet}$	Anhydrotetracycline	Inducer-specific	(69)
$P_{veg}$	IPTG	Inducer-specific	(121)
$P_{xylA}$	Xylose	Inducer-specific	(13)
$P_{yxiE}$	-	Constitutive	(263)

The sugar-inducible promoters are generally activated by an activator or repressed by a repressor both of which regulate the gene expression at transcription initiation level. Prior to review the

carbohydrate uptake systems in *B. subtilis*, the promoter activation and repression must be explained.

### 1.3.1. Transcription initiation at the promoter

Transcription initiation requires the interaction of a multi-subunit DNA binding protein, *i.e.* DNA-dependent RNA polymerase (RNAP), with the promoter sequence (23). Three steps are defined for transcription initiation. Formation of a closed complex by binding of the RNAP to the promoter region, formation of an open complex by melting the DNA around transcription start site (also called isomerization), and finally transition from initiation to elongation phase in a process called promoter escape or clearance (235). RNAP is a holoenzyme ( $E\sigma$ ) consisting of a sigma factor ( $\sigma$ ) and the multi-subunit core enzyme (E). In most of the bacteria, core enzyme comprises  $\alpha_2$ ,  $\beta$ ,  $\beta'$ , and  $\omega$  subunits. The  $\alpha$  dimer subunits assemble a crab-claw structure formed by  $\beta$  and  $\beta'$  subunits. The  $\beta$  subunit polymerizes the nascent RNA strand. The small  $\omega$  subunit is likely a chaperone protein assisting the folding of  $\beta'$  subunit (23). In *B. subtilis*, there is an extra auxiliary subunit, called  $\delta$ , which is likely to be an integral RNAP subunit (47, 172). *In vitro* studies showed that this subunit increases the specificity of transcription in *B. subtilis* (98). Sigma factors have three major functions: (i) to ensure the recognition of specific promoter sequences, (ii) to position the RNA polymerase at the target promoter, and (iii) to facilitate the unwinding of the DNA duplex near the transcription start site. Different sigma factors are usually encoded by the genome of a bacterium each of which enables the recognition of different sets of promoters (23, 167, 246). For instance, *B. subtilis* contains at least 14 known variants of sigma factors (83, 117). Many promoters in *B. subtilis* including most of the sugar-inducible promoters are recognized by the housekeeping sigma factor, called  $\sigma^A$ . The  $\sigma^A$ -type promoters contain two principal elements called core promoter elements: -10 hexamer (or box), a.k.a. Pribnow box, and -35 hexamer. The -10 box (TATAAT) is located about 10 bp upstream of the transcription start site (shown by +1), while the -35 box (TTGACA) is placed 35 bp upstream of the transcription start site (Fig. 1.2) (23, 167, 247).

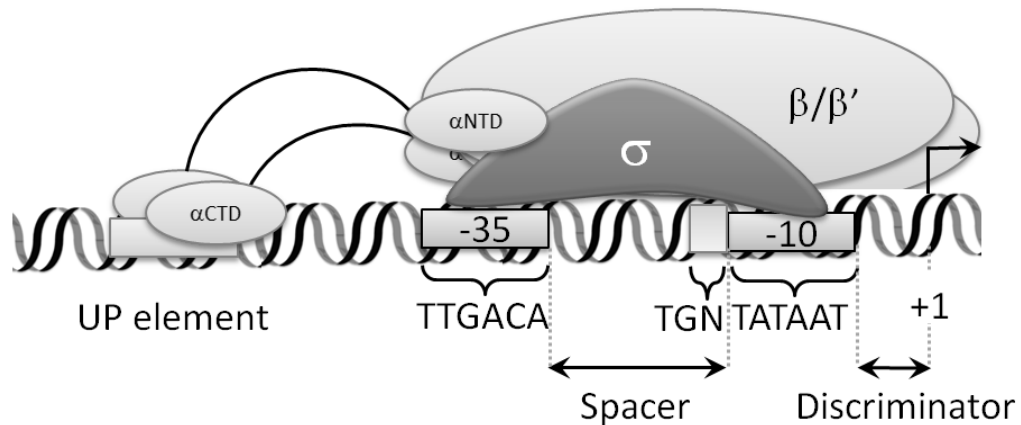


**Fig. 1. 2.** The schematic view of the interaction between RNA polymerase holoenzyme and a  $\sigma^A$ -type promoter (23).

The distance between -10 and -35 boxes, called spacer sequence, is 17 bp long in an optimal  $\sigma^A$ -type promoter (83). The domain 2 of the sigma factor binds to promoter -10 box and -35 box is recognized by the domain 4 of the sigma factor (48, 70). In addition to core elements, there are two extra elements in the promoter sequence. The first one is an AT rich sequence, called the UP element, where the C-terminus of the  $\alpha$  subunit ( $\alpha$ CTD) binds (54, 89, 184). The second extra element is called the extended -10 box, where the domain 3 of the sigma factor binds (70). By binding of the RNAP holoenzyme to the promoter sequence, the DNA strand is unwound from -10 to +2 positions to generate the open complex (23, 83). This isomerization, transition of the closed complex to the open complex, results in binding of the non-template strand to the domain 2 of the sigma factor. Next steps are initiation of RNA synthesizing and transcription elongation if the promoter clearance occurs (Fig. 2.3). However, the number of RNA polymerases and sigma factors in the cell are limited. For prudent distribution of the RNAP holoenzyme, some mechanisms regulate the transcription initiation. These include optimal sequence of the promoter core elements, presence of the anti-sigma factors, binding of small ligands such as ppGpp to RNAP, and transcription factors (23, 88, 167, 246). Among them, the sequence of the promoter core elements and transcription factors are more specific for the regulation of an operon. The conventional transcription factors are classified in two groups: transcriptional repressors and activators (88).



### 1.3.2. Transcription initiation repression

Some promoters require no additional factors for their activity due to the optimal sequence of their core elements. In general, the activity of such promoters is controlled by transcriptional repressors (77). Transcriptional repressors act in different ways (Fig. 1.3.A). The simplest way is the steric hindrance of RNA polymerase. In this case, the repressor binding site is often located between the core promoter elements or close to them. Binding of the repressor constraints the binding of RNAP to the promoter core elements (23, 183, 230). Binding of the LacI repressor to O<sub>1</sub> operator at *lac* promoter of *E. coli* is an example for this mechanism (191). In another case, the repressor binding site is upstream and downstream of the promoter core elements. Binding of the repressor molecules to their binding site is followed by protein-protein interactions which causes DNA looping. The DNA looping inhibits the formation of closed complex (23, 183, 230). Repression of the *gal* promoter by GalR in *E. coli* is a well-known example (68). Finally, repression by modulation of an activator or anti-activation happens when the repressor binding site overlaps an activator binding site (23, 183, 230). The latter mechanism is observed between cytidine catabolism regulator (CytR) and cyclic AMP receptor protein (CRP) in *E. coli* (229). The three mechanisms are depicted in Fig. 1.3.A.

### 1.3.3. Transcription initiation activation

Most of the promoters lack a good match to the consensus sequence of housekeeping promoter core elements. These group require ancillary proteins, known as transcriptional activators (77). In general, activators bind upstream of the target promoter and recruit RNAP by direct protein-protein interaction (10). The simple promoter activation is categorized to four mechanisms (3 mechanisms are shown in Fig. 1.3.B) (23). In class I activation, the activator binds upstream of the -35 box and interacts with  $\alpha$ CTD of RNAP. The flexible linker of  $\alpha$ CTD and  $\alpha$ NTD enables the Class I activators to bind at different distances upstream of the -35. The activator binding site in class I activation is usually located near positions -61 to -91 (10, 23, 77). The most prominent example of this class is the CRP binding site at the *lac* promoter (51). In the second class, the activator binds directly adjacent to the -35 box. Thus, the activator directly

contacts domain 4 of the sigma factor (10, 23, 77). This is found in the  $P_{RM}$  promoter of bacteriophage  $\lambda$  where CI binding site is close to the promoter core (162). In the third class, the activator binds to the core promoter and changes the conformation of the promoter by twisting the DNA. This DNA twisting enables the promoter to be bound by a sigma factor (23). For instance, the MerR-type activators bind to the spacer sequence and twist the DNA to reorientate the -10 and -35, thereby the sigma factor can bind (22, 90). In the fourth mechanism, the activator modulates the repression in a process, called anti-repression (230). This was shown in the promoter of competence transcription factor (ComK) in *B. subtilis*. Binding of the ComK activator to the minor groove at *comK* promoter results in physical displacement of the repressors Rok and CodY by which the repression effect will be removed (203). All of the mentioned mechanisms are simple activation and repression mechanisms. There are, however, other mechanism which have more complicated regulations (10, 23, 77, 88, 137, 183, 230).

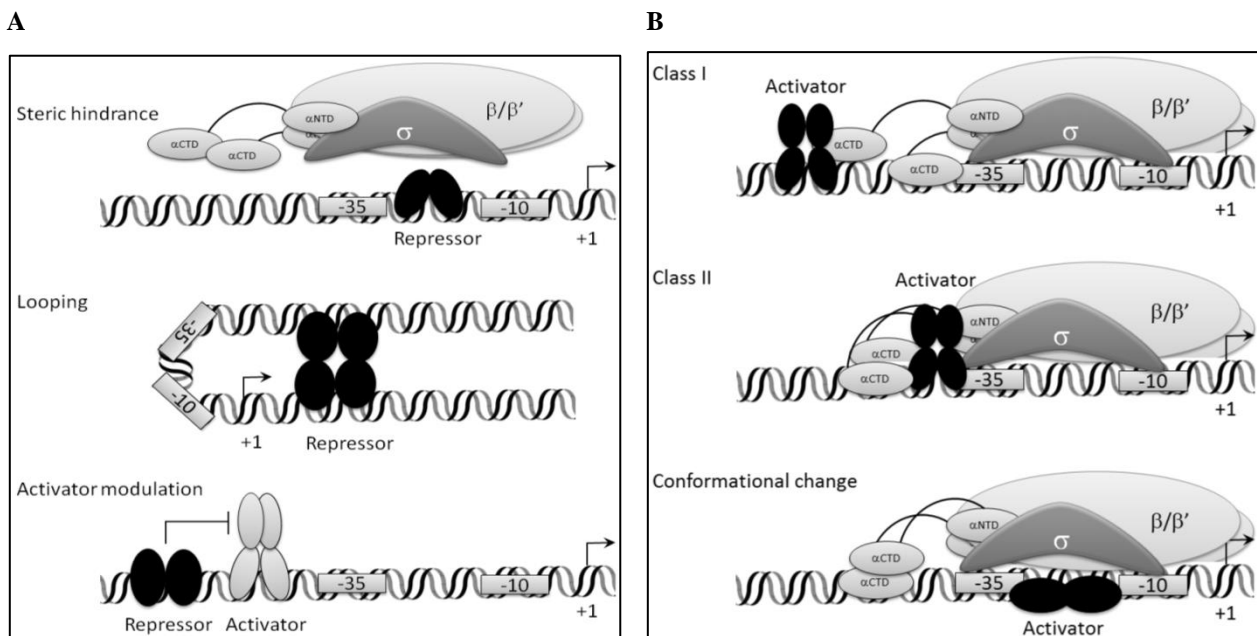


**Fig. 1.3.** (A) Schematic view of the different mechanisms of the transcription repression. (B) Different mechanisms of the transcription activation (10, 23).

#### 1.4. Carbohydrate uptake systems in *Bacillus subtilis*

*B. subtilis* is able to degrade several plant-derived polysaccharides by secretion of extracellular enzymes, such as  $\alpha$ -amylase (*amyE*) (216), levansucrase (*sacB*) (132), and levanase

(*sacC*) (118, 236). The resulting oligo-, di- and monosaccharides are then transported into the cell and catabolized. At least 18 different mono- or disaccharides can be used by *B. subtilis* as a carbon source (113, 210). For uptake of carbohydrates, different transport systems can be employed by *B. subtilis* (summarized in table 1.5). These carbohydrate uptakes systems include: ATP-binding cassette (ABC), phosphoenolpyruvate (PEP): sugar phosphotransferase system (PTS), facilitators and secondary active transporters (44, 210). Among them, PTS is the main carbohydrate uptake system in *B. subtilis* (180, 237).

**Table 1. 5.** Some of the main carbohydrate uptake systems in *B. subtilis* (44).

Carbohydrate uptake system	Carbohydrate
PTS	fructose, maltose, mannitol, glucose, sucrose, trehalose, salicin, N-acetylglucoseamine, mannose, glucomannan
Facilitators	glycerol
ABC	arabinose, ribose, rhamnogalacturonan, acetoin, galactose, maltodextrin
Other transporters	arabinose, glucose, inositol, glucitol

### 1.5. Phosphoenolpyruvate-dependent phosphotransferase system (PTS)

PTS is a phosphotransfer system by which a carbohydrate is simultaneously transported across the cytoplasmic membrane and phosphorylated (114). This carbohydrate uptake system comprises two general proteins, enzyme I (EI; 63 kDa) and a histidine-containing phosphocarrier protein (HPr; 9 kDa), as well as a multidomain sugar-specific transporter, called enzyme II (EII) (73, 165). The phosphoryl group transferred by PTS is originated from phosphoenol pyruvate (PEP). The EI protein is the first component of this cascade which becomes autophosphorylated using PEP as the phosphoryl donor. In the next step, EI phosphorylates the phosphocarrier HPr protein at His15. Finally, this phosphoryl group is transferred to the sugar specific EII located at the cytoplasmic membrane. The phosphorylated sugar is then catabolized in glycolysis in which two PEP will be generated (Fig. 1.4) (44, 75, 114, 176).

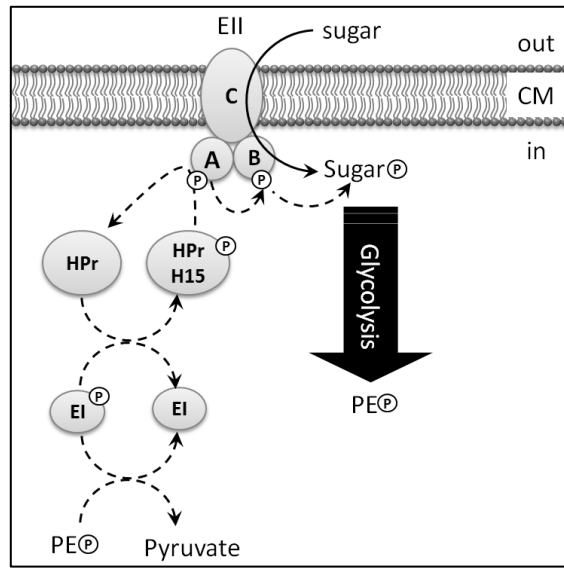


**Fig. 1. 4.** The schematic view of a phosphoenolpyruvate-dependent phosphotransferase system (PTS) (75).

### 1.6. PTS encoding operons and their specific regulators in *B. subtilis*

Generally, the operons encoding PTS in *B. subtilis* consist of one or two encoding genes for sugar-specific EII (transporter) and phosphosugar modifying enzymes (listed in Table 1.6). The PTS transporters are composed of three (or four) domains, where the soluble domains IIA and IIB being part of the phosphorylation chain, while IIC is the membrane-bound domain which transports the carbohydrate. Operons encoding PTS are usually regulated by their specific regulator encoded by a gene located within or outside the PTS operon (45, 180). These regulators function in different ways, such as transcription activation, transcription repression, and transcription antitermination (see Table 1.6). According to their function, transcriptional activators and repressors contain DNA binding domains, while antiterminators contain RNA binding domains (45). Some of the regulators are directly activated in the presence of their phosphosugar. For instance, the repressor of the trehalose PTS-encoding operon, TreR, loses its DNA binding affinity by trehalose 6-phosphate (26). Besides, the activator of the maltose PTS-encoding operon, MalR, is supposed to bind its operator only in a complex with maltose 6-phosphate (253). Other regulators contain extra duplicated PTS-regulatory domains (PRD). *B. subtilis* 168 contains eight PRD-containing regulators including PRD-containing antiterminators

(GlcT, LicT, SacT, and SacY, a.k.a. BglG/SacY family) and PRD-containing activators (LicR, MtlR, and ManR, a.k.a. DeoR-type activator family, and LevR) (79, 208, 231). Phosphorylation or dephosphorylation of the PRD domains activates or deactivates the regulator. However, this activation mechanism is somewhat different between the PRD-containing activators and antiterminators.

**Table 1. 6.** Phosphoenolpyruvate-dependent phosphotransferase systems of *B. subtilis* (44).

Sugar	Operon	Regulator (gene)	Regulation	Reference
$\beta$ -glucoside	<i>bglPH, bglS</i>	<b>LicT</b> * ( <i>licT</i> )	Antitermination	(124, 135, 136, 194, 226, 232)
fructose	<i>levDEFGsacC</i>	<b>LevR</b> ( <i>levR</i> )	Activator	(29, 41, 145, 211)
fructose	<i>fruRKA</i>	FruR	Repressor	(67, 173, 180)
Glucose	<i>ptsGHI</i>	<b>GlcT</b> ( <i>glcT</i> )	Antitermination	(7, 72, 74, 123, 124, 190, 192, 212)
Glucosamine	<i>nagBB gamP</i>	YbgA ( <i>ybgA</i> )	(?)	(180)
Maltose	<i>malARP</i>	MalR	Activator	(196, 253)
Mannitol	<i>mtlAFD</i>	<b>MtlR</b> ( <i>mtlR</i> )	Activator	(107, 154)
Mannose	<i>manPA</i>	<b>ManR</b> ( <i>manR</i> )	Activator	(214)
N-acetylglucosamine	<i>nagP, nagABR</i>	NagR	Repressor	(11)
Oligo $\beta$ -glucoside	<i>licBCAH</i>	<b>LicR</b> ( <i>licR</i> )	Activator	(177, 221, 222)
Oligo $\beta$ -mannoside	<i>gmuBACDREFG</i>	GmuR	Repressor	(185)
Sucrose	<i>sacPA</i>	<b>SacT</b> ( <i>sacT</i> )	Antitermination	(3, 4, 40, 59, 143)
Sucrose	<i>sacXY, sacB</i>	<b>SacY</b>	Antitermination	(36, 143, 207, 225)
Trehalose	<i>trePAR</i>	TreR	Repressor	(26, 91, 195)

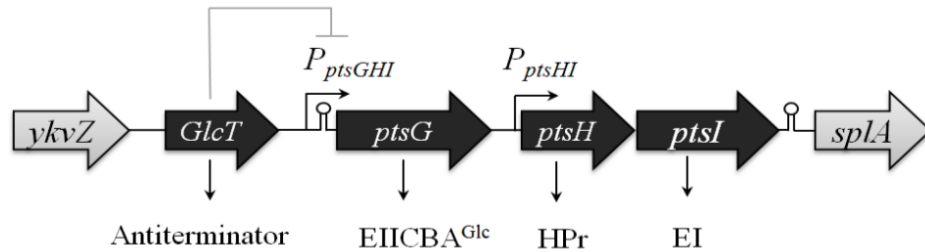
\* The PRD-containing regulators are shown by bold letters.

### 1.6.1. Regulation of GlcT and other PRD-containing antiterminators

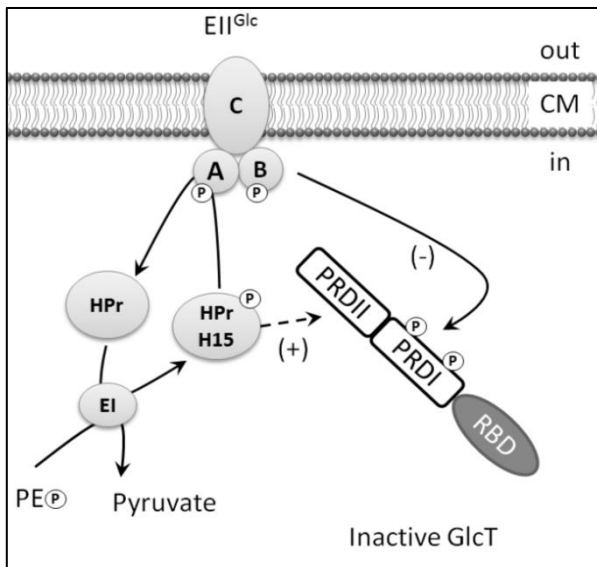
Glucose is the preferred carbon and energy source for many bacteria. In *B. subtilis*, glucose is mainly taken up via a phosphoenolpyruvate-dependent phosphotransferase system encoded by *ptsGHI* operon (Fig. 1.5.A). The *ptsG* gene encodes for specific EIICBA<sup>Glc</sup> transporter, while *ptsH* and *ptsI* encode for general HPr and EI proteins of the PTS pathway (73, 74). The EIICBA<sup>Glc</sup> protein consists of two hydrophilic domains, EIIB<sup>Glc</sup> and EIIA<sup>Glc</sup>, which are involved in the phosphorylation of glucose and of domain C, a membrane-bound domain, which transports glucose (215). The *ptsHI* genes are constitutively expressed by a promoter, *P<sub>ptsHI</sub>*, located downstream of *ptsG*. Therefore, general proteins of the PTS pathway, *i.e.* HPr and EI, are

always present in the cytoplasm. In addition to  $P_{ptsHI}$ , an inducible promoter, denoted  $P_{ptsGHI}$ , directs the expression of the *ptsGHI* operon (Fig. 1.5.A).

A



B



C

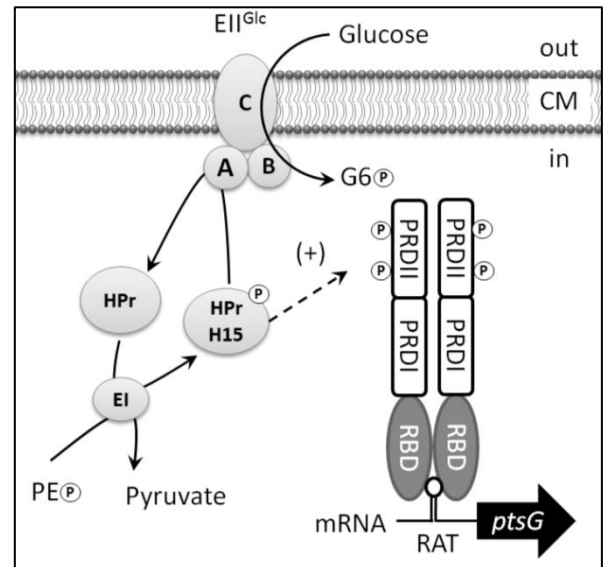


**Fig. 1. 5.** (A) Genetic organization and regulation of the *ptsGHI* operon and its antiterminator, GlcT. (B) Deactivation of GlcT by EII<sup>Glc</sup> in the absence of glucose. (C) Activity of GlcT in the presence of glucose. (CM: Cytoplasmic membrane; EI: Enzyme I; G6P: Glucose 6-phosphate; HPr: Histidine-containing phosphocarrier protein; PRD: PTS-regulatory domain; RBD: RNA binding domain) (192).

$P_{ptsGHI}$  is regulated by GlcT antiterminator. This protein belongs to the BglG/SacY antiterminator family in *B. subtilis*. The *glcT* gene is located upstream of the *ptsGHI* operon (74, 212). GlcT consists of an N-terminal RNA binding domain, and the PRDI and PRDII domains.

Phosphorylation of the PRD domains of GlcT modulates the protein activity in response to the availability of the glucose (7). In the absence of glucose, GlcT is phosphorylated by EII<sup>Glc</sup> in PRDI (Fig. 1.5.B). This phosphorylation deactivates GlcT. In this case, the transcription of *ptsGHI* operon is early terminated due to the presence of a terminator structure in the leader sequence of *ptsG*. This terminator is overlapped by an inverted repeat, called ribonucleotide antiterminator (RAT). This overlap forms a protein-dependent riboswitch. When glucose is present in the extracellular milieu, uptake of glucose leads to dephosphorylation of EII<sup>Glc</sup> (Fig. 1.5.C). This dephosphorylation competes with the phosphorylation of GlcT by the EII<sup>Glc</sup>. Thus, GlcT becomes active and binds to RAT. Upon binding of GlcT, a new stem-loop structure forms preventing the early transcription termination of the *ptsGHI* mRNA (7, 123, 190, 212). In addition to EII<sup>Glc</sup>-dependent phosphorylation in PRDI, there is a second phosphorylation in PRDII domain of GlcT mediated by HPr(H15~P). The PRDII phosphorylation slightly stimulates the GlcT activity. In other words, GlcT is still active when PRDII is dephosphorylated; however, the full activity is only observed when PRDII is phosphorylated and PRDI is dephosphorylated (192). Similarly, all members of the BglG/SacY antiterminator family of *B. subtilis* are negatively affected by the cognate transporter. However, the role of phosphorylation via HPr(H15~P) varies among these antiterminators (231). Similar to GlcT, SacY is still functional in the absence of HPr (36). In contrast, other transcriptional antiterminators such as LicT or SacT absolutely require the phosphorylation of the PRDII by HPr(H15~P) for activity (3, 45, 115, 136).

### 1.6.2. Regulation of PRD-containing activators in *B. subtilis*

PRD-containing activators in *B. subtilis* are basically divided into two groups. The first group is called DeoR-type activators including MtlR, ManR, and LicR. The second group with LevR, as the only member, comprises NifA/NtrC-type activators. The DeoR-type activators usually interact with the  $\sigma^A$ -containing RNAP holoenzyme, whereas LevR interacts with RNA polymerase containing  $\sigma^L$  (45, 61). Therefore, domain organization in these groups are different (Fig. 1.6) (79). DeoR-type activators contain a helix-turn-helix (HTH) motif in their N-terminus resembling the DNA binding domain in transcriptional activators of the *E. coli* DeoR family

(231). This DNA binding domain is followed by two PRDs each of which contains two conserved histidyl residues. The PRDs are followed by an EIIB<sup>Gat</sup>-like domain containing a conserved cysteyle residue and an EIIA-like domain belonging to the mannitol/fructose class PTS (45, 79).

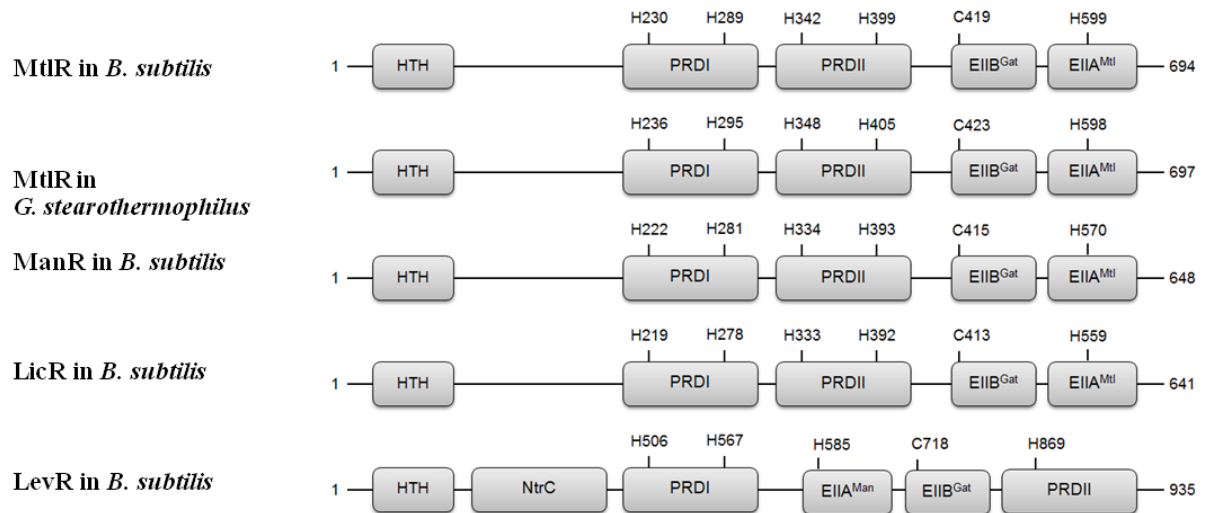


**Fig. 1. 6.** Domain organization of the PRD-containing transcription activators. HTH represents helix-turn-helix motif in the DNA binding domain (45, 107, 213).

Early knowledge dealing with regulation of a DeoR-type activator was achieved by studying *Geobacillus stearothermophilus* MtlR. This DeoR-type activator is phosphorylated by HPr(H15~P) in PRDII which activates MtlR. In the absence of mannitol, domain B of EIICB<sup>Mtl</sup> phosphorylates the EIIA<sup>Mtl/Fru</sup>-like domain of MtlR to deactivate it (93, 94). Similar to *G. stearothermophilus* MtlR, phosphorylation by HPr(H15~P) is essential for the activity of ManR, while removal of EIICBA<sup>Man</sup> leads to constitutive activity of the *manPA* promoter (214). LicR in *B. subtilis* is regulated by the same mechanism (221). Lately, it has been shown that the EIIB<sup>Gat</sup>-like domain of *B. subtilis* MtlR also interacts with the EIIA<sup>Mtl</sup> (107). Phosphorylation of LevR is different from DeoR-type activators. This NifA/NtrC-type activator, LevR, is the best studied PRD-containing activator in *B. subtilis*. LevR contains an N-terminal helix-turn-helix motif followed by a NifA/NtrC-like domain. The latter domain probably interacts with RNAP associated with  $\sigma^L$  (45, 147). The central NifA/NtrC-like domain is followed by a complete PRD



containing two conserved histidyl residues. There is also another truncated PRD containing only one conserved histidyl residue at the C terminus of LevR. Between the two PRDs, EIIA<sup>Man</sup>- and EIIB<sup>Gat</sup>- like domains are located (45). HPr(H15~P)-mediated phosphorylation occurs in the EI<sup>Man</sup>-like domain which positively regulates the activity of LevR. In the absence of fructose, the second phosphorylation in PRDII inactivates LevR. This phosphorylation is mediated by EIIB<sup>Lev</sup> (144, 211). Briefly, the PRDI domain in PRD-containing antiterminators is phosphorylated by specific transporter, while EIIA- and EIIB-like domains in PRD-containing activators interact with the specific transporter domains. The role of PRDI in the PRD-containing activators remains unknown. It is supposed that PRDI might transfer the signal from PRDII to the DNA binding domain (45).

### **1.7. PTS and CcpA-dependent carbon catabolite repression in *B. subtilis***

PTS is not only serving as a carbohydrate transport system, but also as a signal transducer for carbon catabolite repression (CCR) (209). In fact, the general PTS component, HPr, plays an important role in carbon catabolite repression in *B. subtilis*. HPr contains two phosphorylation sites including histidine 15 and serine 46. Histidine 15 is the PEP-dependent phosphorylation site transferring the phosphoryl group between EI and EII (114). In contrast, Serine 46 is phosphorylated in an ATP-dependent reaction by a homohexameric enzyme, called HPr kinase/phosphorylase (HPrK/P; 34 kDa) (65, 182). HPrK/P is a bifunctional enzyme which phosphorylates HPr-Ser46 at a high concentration of fructose 1,6-bisphosphate (FBP), while its phosphorylase activity is stimulated by a high inorganic phosphate concentration inside the cell caused by nutrient limitation (182). The presence of glucose or a PTS sugar in the nutrient medium results in a high level of FBP which is an intermediate product of glycolysis. HPr(S46~P) act as an effector for the pleiotropic transcription regulator, catabolite control protein A (CcpA) (45, 139). CcpA is a master transcription regulator which binds to different operons in *B. subtilis* and activates or represses the expression of these operons (204). Binding of the CcpA (36 kDa) dimer to its binding site is triggered in the presence of HPr(S46~P). Interestingly, the interaction between CcpA and HPr(S46~P) is also enhanced by the presence of FBS and glucose 1-phosphate (Fig. 1.7.A) (45, 75, 139). Rather than HPr(S46~P), another cofactor protein can



responsive element (*cre*) (240). Most of the *cre* sites are located at the promoter core elements or upstream of the promoter core elements. However, there are also some examples where the *cre* site is located at the 5'UTR region of mRNA or even inside the coding sequence (61). Several bioinformatics and practical analysis revealed the consensus sequence of *cre* comprising WTGNAARCGNNCA sequence (152). Recently, a detailed comparison of the *cre* sites in the genome of *B. subtilis* showed two groups of functional *cre* sites harboring the consensus sequences WTGNAANCGNWWNCA and WTGAAARCGYTTWNN (61). Regarding the position of the *cre* site, binding of the CcpA complex can repress or activate the operon. For *ackA* (acetate kinase), *pta* (phosphotransacetylase), and *ilv-leu* (biosynthesis of branched-chain amino acids) genes, the *cre* site is located upstream of the promoter core elements and activates their gene expression (178, 200, 224, 227). These genes are required for the excretion of acetate when the cells are grown in the excess of carbon source. The *cre* site located inside the promoter core elements or downstream of the promoter region can repress gene expression by steric hindrance mechanism or elongation roadblock, respectively (45, 61).

## **1.8. CcpA-independent carbon catabolite repression**

### **1.8.1. Catabolite control mediated by catabolite control proteins**

In addition to CcpA-dependent CCR in *B. subtilis*, many genes are regulated by other catabolite control proteins, such as CcpB, CcpC, and CcpN. CcpB is a paralogous protein of CcpA and regulates some operons including *gnt*, *xyl*, and *fad* genes. The latter genes encode the fatty acid degradation (30, 61). CcpC represses the *citB* and *citZCH* genes encoding the first three steps of the TCA cycle (106). CcpN represses *pckA* encoding the phosphoenolpyruvate carboxykinase and *gapB* encoding the glyceraldehyde-3-phosphate dehydrogenase during glycolysis. In fact, CcpN is active when the cells are growing on a glycolytic substrate, even if the medium also contains a gluconeogenic substrate (199). CggR is another regulatory protein influencing the central glycolytic genes. This protein represses the *gapA* operon, *i.e.* *cggR-gapA-pgk-tpi-pgm-eno*. The *gapA* operon encodes the enzymes responsible for the conversion of three-carbon intermediates of glycolysis. FBP is an inhibitor of CggR (46, 140).

### 1.8.2. Catabolite control mediated by HPr(H15~P)

The phosphorylated HPr-H15 can also play an important role in the carbon catabolite repression of many operons. HPr-H15 is not only a phosphocarrier protein for the specific enzyme II of many PTS systems, but also it is capable of phosphorylation of the glycerol kinase, RNA-binding antiterminators and DNA-binding transcription activators of the PTS-sugar utilization systems (45, 61, 75).

#### 1.8.2.1. Inducer exclusion in glycerol utilization system

In *B. subtilis*, glycerol is taken up by a facilitator, called GlpF, and converted to glycerol 3-phosphate by the glycerol kinase (GlpK). The *glpFK* operon is induced by binding of glycerol 3-phosphate and GlpP, an antiterminator, to the mRNA leader sequence of *glpFK*. This binding prevents the early transcription termination. Glycerol kinase (GlpK) is activated by a phosphoryl transfer from HPr(H15~P) (Fig. 1.7.A). In the presence of glucose, HPr(H15~P) is mainly dephosphorylated by EIICBA<sup>Glc</sup> leading to prevention of GlpK phosphorylation. The unphosphorylated GlpK is less active than its phosphorylated form. Therefore, transcription of *glpFK* operon is terminated due to the low amount of glycerol 3-phosphate in the cell. This mechanism of repression is called inducer exclusion (38).

#### 1.8.2.2. Induction prevention of the PRD-containing regulators

Several PTS operons are regulated by transcription regulators comprising PTS-regulatory domains (PRD). The activity of these PRD-containing regulators (activator or antiterminator) is modulated by PTS-dependent phosphorylation of their PRDs. This type of regulation is based on the sugar-specific EII and HPr(H15~P). In the absence of sugar, the related specific EII phosphorylates PRDI in antiterminators or EIIA- and EIIB-like domains in activators. In addition to EII-dependent phosphorylation, HPr(H15~P) also catalyzes the phosphorylation of PRDII in the absence of glucose. HPr(H15~P) is efficiently used in the presence of a preferred PTS-

carbohydrate, such as glucose. This constitutes a CCR mechanism that downregulates the activities of PRD-containing regulators (45, 61, 75).

### 1.9. Mannitol utilization system in *B. subtilis*

Mannitol is taken up via a PTS in *B. subtilis*. In mannitol PTS pathway, mannitol passes through the domain C and becomes phosphorylated by the domain B of membrane-bound EIICB<sup>Mtl</sup>. This phosphate is provided by the cytoplasmic EIIA<sup>Mtl</sup> protein which has been already phosphorylated by HPr(H15~P). The mannitol 1-phosphate dehydrogenase enzyme converts the uptaken mannitol 1-phosphate to fructose 6-phosphate which is an intermediate compound of glycolysis pathway. The mannitol utilization system is encoded by the *mtlAFD* operon located at 449.72 – 452.73 kb of the chromosome of *B. subtilis* 168 (Fig. 1.8). The *mtlA* gene (1437 bp) is the first gene of the operon encoding the EIICB<sup>Mtl</sup> protein (50 kDa) (9, 117). The *mtlF* gene (432 bp) encodes the cytoplasmic phosphocarrier protein, EIIA<sup>Mtl</sup> (15 kDa) (9, 107). Finally, the *mtlD* gene (1122 bp) encodes the mannitol 1-phosphate dehydrogenase enzyme (41 kDa) (9, 117). Transcription of the operon is activated by the activator, MtlR (78 kDa). The *mtlR* gene (2085 bp) encoding the activator is located 14.1 kb downstream of the *mtlAFD* operon. Interestingly, expression of *mtlAFD* operon is induced by glucitol in addition to mannitol which is the main inducer. Besides, the presence of mannitol 1-phosphate dehydrogenase is essential for assimilation of glucitol (239). Glucitol is a non-PTS sugar taken up by a H<sup>+</sup>-symporter (GutP) and oxidized to fructose by glucitol dehydrogenase (GutB) inside the cytoplasm. However, a weak uptake of glucitol by mannitol-specific EII has been already observed (28).

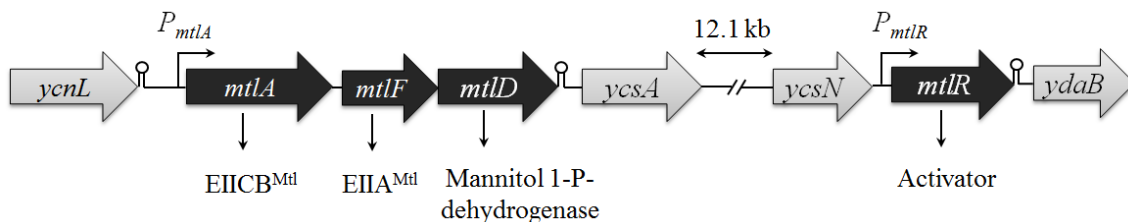


**Fig. 1. 8.** Genetic map of the *mtl* operon and its regulator on the chromosome of *B. subtilis* 168.

### **1.10. Aim of the study**

In order to construct an expression vector for heterologous and homologous genes in *B. subtilis* based on low cost inducer, the mannitol utilization system was chosen. In *B. subtilis*, mannitol is taken up via a phosphoenolpyruvate-dependent phosphotransferase system (PTS). So far, regulation by PRD-containing antiterminators has been mainly studied in *B. subtilis*. Among the PRD-containing activators, regulation of LevR and LicR has been also investigated. Besides, the mannose PTS in *B. subtilis* has been recently characterized and its regulation is being studied. Prior to this study, activation of the *mtlAFD* operon, encoding mannitol utilization system, and the location of its activator, *mtlR*, has been reported. Nevertheless, the exact regulation of the *mtlAFD* operon as well as its activator encoding gene (*mtlR*) is unknown. Thus, the promoter structure of the *mtlAFD* operon and *mtlR* in *B. subtilis* will be characterized in this study. Next, regulation of these promoters in several mannitol utilization deficient mutants will be studied. Also, regulation of MtlR, as a PTS-containing regulator, will be investigated. A challenge in application of a sugar-inducible system is caused by glucose catabolite repression. Therefore, catabolite repression of the promoters of mannitol PTS encoding operon and its activator will be investigated. Finally, a highly inducible expression vector based on mannitol will be constructed which can be used for expression of heterologous and homologous genes in *B. subtilis*.

## 2. Materials and Methods

### 2.1. Strains

Strain	Genotype	Source or reference
<i>E. coli</i>		
DH5 $\alpha$	<i>fhuA2</i> $\Delta$ ( <i>argF-lacZ</i> )U169 <i>phoA glnV44</i> $\Phi$ 80	(12)
JM109	$\Delta$ ( <i>lacZ</i> )M15 <i>gyrA96 recA1 relA1 endA1 thi-1 hsdR17 mcrA recA1 supE44 endA1 hsdR17</i> ( $r_{\kappa}^{-}$ $m_{\kappa}^{+}$ ) <i>gyrA96 relA1 thi</i> $\Delta$ ( <i>lac-proAB</i> ) F' [ <i>traD36 proAB<sup>+</sup> lacI<sup>f</sup> lacZ</i> $\Delta$ M15]	(257)
JW2409-1	F', $\Delta$ ( <i>araD-araB</i> )567, $\Delta$ <i>lacZ</i> 4787( $::rrnB-3$ ), $\lambda$ ', $\Delta$ <i>ptsI</i> 745:: <i>kan</i> , <i>rph-1</i> , $\Delta$ ( <i>rhaD-rhaB</i> )568, <i>hsdR</i> 514	(5)
<i>B. subtilis</i>		
168	<i>trpC2</i>	Bacillus Genetic Stock Center
3NA	<i>spo0A3</i>	(150)
QB5223	<i>trpC2 ptsH-S46A</i>	(146)
TQ303	<i>spo0A3</i> , $\Delta$ <i>ccpA::erm</i>	(214)
TQ308	<i>spo0A3</i> , $\Delta$ <i>hprK::erm</i>	(214)
TQ338	<i>spo0A3</i> , $\Delta$ <i>crh::erm</i>	(214)
TQ338_S46	<i>trpC2 ptsH-S46A</i> $\Delta$ <i>crh::erm</i>	(214)
TQ432	<i>trpC2 ptsH-H15A amyE::cat</i>	(214)
MW373	<i>spo0A3</i> $\Delta$ <i>ptsG</i>	(154)
KM12	<i>spo0A3</i> $\Delta$ <i>mtlAF::ermC</i>	3NA transformed with pKAM5
KM13	<i>spo0A3</i> $\Delta$ <i>mtlAFD::ermC</i>	3NA transformed with pKAM6
KM15	<i>spo0A3</i> $\Delta$ <i>mtlR::ermC</i>	3NA transformed with pKAM4
KM37	<i>spo0A3</i> <i>mtlD::ermC</i>	3NA transformed with pKAM14
KM39	<i>spo0A3</i> $\Delta$ <i>gutRBP</i> ydjE:: <i>cat</i>	3NA transformed with pKAM13
KM40	<i>spo0A3</i> $\Delta$ <i>mtlAFD::ermC</i> $\Delta$ <i>gutRBP</i> ydjE:: <i>cat</i>	KM13 transformed with pKAM13
KM103	<i>spo0A3</i> $\Delta$ <i>mtlF</i>	3NA transformed with pKAM47
KM162	<i>spo0A3</i> $\Delta$ <i>mtlR::ermC</i> <i>his'</i> , <i>spc</i>	KM15 transformed with pHM30
KM165	<i>spo0A3</i> <i>mtlR-H289A</i>	KM162 transformed with pKAM68
KM176	<i>spo0A3</i> <i>amyE::ter-P<sub>mtlA</sub>-lacZ-spc</i>	3NA transformed with pKAM123
KM179	<i>spo0A3</i> <i>mtlR-H289A amyE::ter-P<sub>mtlA</sub>-lacZ-spc</i>	KM165 transformed with pKAM123
KM209	<i>spo0A3</i> <i>mtlR-H342D</i>	KM15 transformed with pKAM126
KM210	<i>spo0A3</i> <i>mtlR-H230A</i>	KM15 transformed with pKAM127

Strain	Genotype	Source or reference
KM212	<i>spo0A3 mtlR</i> -H230A H289A	KM15 transformed with pKAM129
KM213	<i>spo0A3 mtlR</i> -H342D <i>amyE::ter-P<sub>mtlA</sub>-lacZ-spc</i>	KM209 transformed with pKAM123
KM214	<i>spo0A3 mtlR</i> -H230A <i>amyE::ter-P<sub>mtlA</sub>-lacZ-spc</i>	KM210 transformed with pKAM123
KM216	<i>spo0A3 mtlR</i> -H230A H289A <i>amyE::ter-P<sub>mtlA</sub>-lacZ-spc</i>	KM212 transformed with pKAM123

## 2.2. Plasmids

**Table 2. 1.** Parental plasmids used in this study. The plasmid maps are represented in appendices.

Plasmid	Genotype	Source or reference
pDG1730	<i>erm, bla, amyE'</i> - <i>spc-amyE'</i>	(82)
pHM30	<i>hisF, hisI', spc, yvcA, yvcB, bla</i>	(158)
pHM31	<i>hisF, hisI, yvcA, yvcB, bla</i>	(158)
pIC20HE	<i>lacZ, bla, ori<sub>pUC18</sub></i>	(1)
pJOE4786.1	<i>lacPOZ', bla, ori<sub>pUC18</sub></i>	(105)
pJOE6089.4	<i>ori<sub>pBR322</sub>, rop, cer, rhaP<sub>BAD</sub>, eGFP-strep, rrnB, bla</i>	Laboratory stock
pJOE6732.1	<i>ori<sub>pAMβ1</sub>, repDE, P<sub>xyI</sub>-cre<sub>P1</sub>, spc, ori<sub>pUC18</sub>, bla</i>	Laboratory stock
pMW168.1	<i>ter-'manR-P<sub>manP</sub>-TIR<sub>gsiB</sub>-eGFP-ter, ori<sub>pUC18</sub>, rep, ori<sub>pUB110</sub>, spc</i>	(242)
pMW363.1	<i>'manP-cat-yjdA-yjdB', bla, spc, ori<sub>pUC18</sub></i>	(154)
pSUN284.1	<i>ter-ΔmanR-P<sub>manP</sub>-lacZ-ter, repA, ori<sub>pUC18</sub>, ori<sub>pBS72</sub>, bla, spc</i>	(214)
pSUN279.2	<i>ter-P<sub>manR</sub>-manR-P<sub>manP</sub>-lacZ-ter, repA, ori<sub>pUC18</sub>, ori<sub>pBS72</sub>, spc</i>	(214)
pSUN308.3	<i>'lgt-ermC-nagA', bla, spc, ori<sub>pUC18</sub></i>	Laboratory stock

**Table 2. 2.** Plasmids constructed in this study.

Plasmid	Partial genotype	Parental vector (cut)	Insert/PCR (cut)
<i>Cloning Vectors</i>			
pKAM01	<i>P<sub>mtlR</sub>-mtlR</i>	pJOE4786.1 ( <i>Sma</i> I)	s5656/s5657
pKAM05	<i>'lgt-ermC-ydaB'</i>	pSUN308.3 ( <i>Spe</i> I/ <i>Stu</i> I)	s5860/s5812 ( <i>Spe</i> I/ <i>Stu</i> I)
pKAM08	<i>'nagA-ermC-P<sub>mtlA</sub>-mtlD'</i>	pSUN308.3 ( <i>Eco</i> RV/ <i>Bgl</i> II)	s5918/s5919 + s5920/s5921 F <sup>β</sup> .s5918/s5921 ( <i>Eco</i> RV/ <i>Bgl</i> II)
pKAM011	<i>'lgt-ermC-ycsA'</i>	pSUN308.3 ( <i>Spe</i> I/ <i>Stu</i> I)	s5994/s5995 ( <i>Spe</i> I/ <i>Stu</i> I)
pKAM014	<i>'ydcC-cat- yjdA-yjdB'</i>	pMW363.1 ( <i>Eco</i> RI/ <i>Nhe</i> I)	s6302/s6303 ( <i>Eco</i> RI/ <i>Nhe</i> I)



## Materials and Methods

Plasmid	Partial genotype	Parental vector (cut)	Insert/PCR (cut)
pKAM015	<i>mtlD'</i>	pSUN308.3 ( <i>EcoRV/NdeI</i> )	s6344/s6345 ( <i>EcoRV/NdeI</i> )
pKAM020	<i>mtlA' mroxP-cat-mroxP</i>	pKAM19 ( <i>BamHI/XhoI</i> )	s6759/s6760 ( <i>BamHI/XhoI</i> )
pKAM024	<i>P<sub>mtlR</sub>-mtlR-H342D</i>	pJOE4786.1 ( <i>SmaI</i> )	s6949/s6865 + s6866/s6867 F.s6949/s6867
pKAM025	<i>P<sub>mtlR</sub>-mtlR-H230A</i>	pJOE4786.1 ( <i>SmaI</i> )	s6949/s6868 + s6869/s6867 F.s6949/s6867
pKAM026	<i>P<sub>mtlR</sub>-mtlR-H289A</i>	pJOE4786.1 ( <i>SmaI</i> )	s6949/s6870 + s6871/s6867 F.s6949/s6867
pKAM027	<i>P<sub>mtlR</sub>-mtlR-H230A H289A</i>	pJOE4786.1 ( <i>SmaI</i> )	s6949/s6870 + s6871/s6867 F.s6949/s6867
<i>Expression Vectors</i>			
pKAM1	<i>ter-P<sub>mtlA</sub>(-181 → -1)<sup>α</sup>-lacZ-ter</i>	pSUN279.2 ( <i>NheI/AflIII</i> )	s5526/s5527 ( <i>NheI/AflIII</i> )
pKAM3	<i>ter-P<sub>mtlR</sub>(-200 → -1)-lacZ-ter</i>	pSUN279.2 ( <i>NheI/AflIII</i> )	s5799/s5800 ( <i>NheI/AflIII</i> )
pKAM9	<i>ter-P<sub>mtlA</sub>(-161 → -1)-lacZ-ter</i>	pSUN279.2 ( <i>NheI/AflIII</i> )	s6209/s5527 ( <i>NheI/AflIII</i> )
pKAM12	<i>ter-P<sub>mtlA</sub>'(-161 → -32)-lacZ-ter</i>	pSUN279.2 ( <i>NheI/AflIII</i> )	s6209/s6213 ( <i>NheI/AflIII</i> )
pKAM18	<i>ter-P<sub>mtlR</sub>'(-200 → -15)-lacZ-ter</i>	pSUN279.2 ( <i>NheI/AflIII</i> )	s5799/s6392 ( <i>NheI/AflIII</i> )
pKAM21	<i>ter-P<sub>HP7</sub>-lacZ-ter</i>	pSUN279.2 ( <i>NheI/AflIII</i> )	s6504/s6505 + s6506/s6507 F.s6504/s6507 ( <i>NheI/AflIII</i> )
pKAM23	<i>ter-P<sub>HP9</sub>-lacZ-ter</i>	pSUN279.2 ( <i>NheI/AflIII</i> )	s6504/s6510 + s6511/s6507 F.s6504/s6507 ( <i>NheI/AflIII</i> )
pKAM25	<i>ter-P<sub>HP11</sub>-lacZ-ter</i>	pSUN279.2 ( <i>NheI/AflIII</i> )	s6504/s6508 + s6509/s6507 F.s6504/s6507 ( <i>NheI/AflIII</i> )
pKAM27	<i>ter-P<sub>mtlA</sub>(-161 → -32) *[cttta → gaaat]-lacZ-ter</i>	pSUN279.2 ( <i>NheI/AflIII</i> )	s6688/s6213 ( <i>NheI/AflIII</i> )
pKAM29	<i>ter-P<sub>HP12</sub>-lacZ-ter</i>	pSUN279.2 ( <i>NheI/AflIII</i> )	s6504/s6608 + s6609/s6507 F.s6504/s6507 ( <i>NheI/AflIII</i> )
pKAM30	<i>ter-P<sub>HP13</sub>-lacZ-ter</i>	pSUN279.2 ( <i>NheI/AflIII</i> )	s6504/s6652 + s6653/s6507 F.s6504/s6507 ( <i>NheI/AflIII</i> )
pKAM31	<i>ter-P<sub>mtlA cre+</sub>-lacZ-ter</i>	pSUN279.2 ( <i>NheI/AflIII</i> )	s6209/s6654 + s6655/s6213 F.s6209/s6213 ( <i>NheI/AflIII</i> )

## Materials and Methods

Plasmid	Partial genotype	Parental vector (cut)	Insert/PCR (cut)
pKAM32	<i>ter-P<sub>mtlA cre-</sub>-lacZ-ter</i>	pSUN279.2 ( <i>NheI/AflII</i> )	s6209/s6656 + s6657/s6213 F.s6209/s6213 ( <i>NheI/AflII</i> )
pKAM33	<i>ter-P<sub>mtlR cre+</sub>-lacZ-ter</i>	pSUN279.2 ( <i>NheI/AflII</i> )	s5799/s6664 + s6665/s6392 F.s5799/ s6392 ( <i>NheI/AflII</i> )
pKAM34	<i>ter-P<sub>mtlR cre-</sub>-lacZ-ter</i>	pSUN279.2 ( <i>NheI/AflII</i> )	s5799/s6666 + s6667/ s6392 F.s5799/ s6392 ( <i>NheI/AflII</i> )
pKAM39	<i>ter-P<sub>mtlA-mtlR</sub>-His<sub>6</sub></i>	pKAM12 ( <i>AflII/XmaI</i> )	s6686/ s6687 ( <i>AflII/XmaI</i> )
pKAM40	<i>ter-P<sub>mtlA cre*(-35 and -10)</sub>-lacZ-ter</i>	pSUN279.2 ( <i>NheI/AflII</i> )	s6209/s6709 + s6710/s6213 F.s6209/s6213 ( <i>NheI/AflII</i> )
pKAM41	<i>ter-P<sub>mtlR cre*(-35 and -10)</sub>-lacZ-ter</i>	pSUN279.2 ( <i>NheI/AflII</i> )	s5799/s6711 + s6712/ s6392 F.s5799/s6392 ( <i>NheI/AflII</i> )
pKAM42	<i>ter-P<sub>mtlA</sub>*[taacat→tataat]-lacZ-ter</i>	pSUN279.2 ( <i>NheI/AflII</i> )	s6209/s6713 + s6714/s6213 F.s6209/s6213 ( <i>NheI/AflII</i> )
pKAM43	<i>ter- 'P<sub>mtlA</sub>(-157 → -32)-lacZ-ter</i>	pSUN279.2 ( <i>NheI/AflII</i> )	s6726/s6213 ( <i>NheI/AflII</i> )
pKAM44	<i>ter-P<sub>mtlA</sub>'(-161 → -52)-lacZ-ter</i>	pSUN279.2 ( <i>NheI/AflII</i> )	s6209/s6727 ( <i>NheI/AflII</i> )
pKAM45	<i>ter-P<sub>mtlA</sub>(-161 → -32) *[ctttc→gaaag]-lacZ-ter</i>	pSUN279.2 ( <i>NheI/AflII</i> )	s6209/s6728 + s6729/s6213 F.s6209/s6213 ( <i>NheI/AflII</i> )
pKAM48	<i>ter- 'P<sub>mtlA</sub>(-159 → -32)-lacZ-ter</i>	pSUN279.2 ( <i>NheI/AflII</i> )	s6792/s6213 ( <i>NheI/AflII</i> )
pKAM49	<i>ter- 'P<sub>mtlA</sub>(-155 → -32)-lacZ-ter</i>	pSUN279.2 ( <i>NheI/AflII</i> )	s6793/s6213 ( <i>NheI/AflII</i> )
pKAM50	<i>ter-P<sub>mtlA</sub>'(-161 → -42)-lacZ-ter</i>	pSUN279.2 ( <i>NheI/AflII</i> )	s6209/s6794 ( <i>NheI/AflII</i> )
pKAM51	<i>ter-P<sub>mtlA</sub>'(-161 → -107)-'P<sub>mtlR</sub>(-110 → -15)-lacZ-ter</i>	pSUN279.2 ( <i>NheI/AflII</i> )	s6209/s6798 + s6799/s6392 F.s6209/s6392 ( <i>NheI/AflII</i> )
pKAM52	<i>ter-P<sub>mtlA</sub>(-161 → -32) *[ttcaa→aagtt]-lacZ-ter</i>	pSUN279.2 ( <i>NheI/AflII</i> )	s6209/s6800 + s6801/s6213 F.s6209/s6213 ( <i>NheI/AflII</i> )
pKAM57	<i>ter- 'P<sub>mtlA</sub>(-153 → -32)-lacZ-ter</i>	pSUN279.2 ( <i>NheI/AflII</i> )	s6829/s6213 ( <i>NheI/AflII</i> )
pKAM58	<i>ter- 'P<sub>mtlA</sub>(-149 → -32)-lacZ-ter</i>	pSUN279.2 ( <i>NheI/AflII</i> )	s6830/s6213 ( <i>NheI/AflII</i> )
pKAM59	<i>ter- 'P<sub>mtlA</sub>(-151 → -32)-lacZ-ter</i>	pSUN279.2 ( <i>NheI/AflII</i> )	s6210/s6213 ( <i>NheI/AflII</i> )
pKAM62	<i>ter-P<sub>HP20</sub>-lacZ-ter</i>	pSUN279.2 ( <i>NheI/AflII</i> )	s6504/s6855 + s6856/ s6507 F.s6504/ s6507 ( <i>NheI/AflII</i> )
pKAM65	<i>ter-P<sub>HP23</sub>-lacZ-ter</i>	pSUN279.2 ( <i>NheI/AflII</i> )	s6209/s6861 + s6862/s6954 F.s6209/s6954 ( <i>NheI/AflII</i> )

## Materials and Methods

Plasmid	Partial genotype	Parental vector (cut)	Insert/PCR (cut)
pKAM84	<i>ter-P<sub>mtlA</sub></i> (-161 → -32) *[gtcct→cagga]- <i>lacZ-ter</i>	pSUN279.2 ( <i>NheI/AfIII</i> )	s7065/s6213 ( <i>NheI/AfIII</i> )
pKAM86	<i>ter-P<sub>mtlR</sub>'</i> (-200 → -37)- <i>lacZ-ter</i>	pSUN279.2 ( <i>NheI/AfIII</i> )	s5799/s7066 ( <i>NheI/AfIII</i> )
pKAM87	<i>ter-P<sub>mtlR</sub>'</i> (-200 → -47)- <i>lacZ-ter</i>	pSUN279.2 ( <i>NheI/AfIII</i> )	s5799/s7067 ( <i>NheI/AfIII</i> )
pKAM88	<i>ter-P<sub>groE</sub></i> ( <i>cre<sub>PmtlA</sub></i> )-UTR <sub><i>mtlR</i></sub> - <i>lacZ-ter</i>	pSUN279.2 ( <i>NheI/AfIII</i> )	s7098/s7189 + s7190/s6392 F.s7098/s6392 ( <i>NheI/AfIII</i> )
pKAM89	<i>ter-P<sub>groE</sub></i> ( <i>cre<sub>PmtlR</sub></i> )-UTR <sub><i>mtlR</i></sub> - <i>lacZ-ter</i>	pSUN279.2 ( <i>NheI/AfIII</i> )	s7098/s7191 + s7192/s6392 F.s7098/s6392 ( <i>NheI/AfIII</i> )
pKAM90	<i>ter-P<sub>groE</sub></i> ( <i>cre<sub>PacsA</sub></i> )-UTR <sub><i>mtlR</i></sub> - <i>lacZ-ter</i>	pSUN279.2 ( <i>NheI/AfIII</i> )	s7098/s7193 + s7194/s6392 F.s7098/s6392 ( <i>NheI/AfIII</i> )
pKAM91	<i>ter-P<sub>groE</sub></i> ( <i>cre<sub>mtlA</sub></i> )-UTR <sub><i>mtlR</i></sub> - <i>lacZ-ter</i>	pSUN279.2 ( <i>NheI/AfIII</i> )	s7098/s7195 + s7196/s6392 F.s7098/s6392 ( <i>NheI/AfIII</i> )
pKAM92	<i>ter-P<sub>mtlA</sub></i> (-161 → -32) *[ccaaa→ggttt]- <i>lacZ-ter</i>	pSUN279.2 ( <i>NheI/AfIII</i> )	s7091/s6213 ( <i>NheI/AfIII</i> )
pKAM93	<i>ter-P<sub>mtlA</sub></i> - <i>mtlR</i> -H342D-His <sub>6</sub>	pKAM12 ( <i>AfIII/XmaI</i> )	s6686/s6865 + s6866/s6687 F.s6686/s6687 ( <i>NheI/AfIII</i> )
pKAM96	<i>ter-P<sub>mtlR</sub>'</i> (-200 → -78)-UTR <sub><i>mtlA</i></sub> - <i>lacZ-ter</i>	pSUN279.2 ( <i>NheI/AfIII</i> )	s5799/s7149 + s7150/s6213 F.s5799/s6213 ( <i>NheI/AfIII</i> )
pKAM101	<i>ter-P<sub>groE</sub></i> -UTR <sub><i>mtlR</i></sub> - <i>lacZ-ter</i>	pSUN279.2 ( <i>NheI/AfIII</i> )	s7098/s7237 + s7238/s6392 F.s7098/s6392 ( <i>NheI/AfIII</i> )
pKAM114	<i>ter-P<sub>mtlA</sub>'</i> (-161 → -42)- <i>gsiB</i> * [aaa→cat]- <i>eGFP-ter</i>	pMW168.1 ( <i>AgeI/BamHI</i> )	s7355/s7356 ( <i>AgeI/BamHI</i> )
pKAM144	<i>ter-P<sub>mtlA</sub>'</i> (-161 → -42)- <i>gsiB</i> - <i>eGFP-ter</i>	pMW168.1 ( <i>AgeI/AfIII</i> )	s7355/s7356 ( <i>AgeI/AfIII</i> )
pKAM145	<i>ter-P<sub>mtlA+10</sub></i> - <i>lacZ-ter</i>	pKAM12 ( <i>NheI/MunI</i> )	s6209/s7548 ( <i>NheI/MunI</i> )
pKAM160	<i>ter-P<sub>licB</sub></i> - <i>lacZ-ter</i>	pSUN279.2 ( <i>NheI/AfIII</i> )	s7614/s7615 ( <i>NheI/AfIII</i> )
pKAM161	<i>ter-P<sub>HP41</sub></i> - <i>lacZ-ter</i>	pSUN279.2 ( <i>NheI/AfIII</i> )	s6209/s7617 + s7616/s7615 F.s6209/s7615 ( <i>NheI/AfIII</i> )
pKAM162	<i>ter-P<sub>HP42</sub></i> - <i>lacZ-ter</i>	pSUN279.2 ( <i>NheI/AfIII</i> )	s6209/s7618 + s7619/s7615 F. s6209/s7615 ( <i>NheI/AfIII</i> )
pKAM163	<i>ter-P<sub>mtlA</sub>'</i> (-161 → -72)-UTR <sub><i>manP</i></sub> - <i>gsiB-eGFP-ter</i>	pMW168.1 ( <i>AgeI/BglII</i> )	s7355/s7620 ( <i>AgeI/BglII</i> )

## Materials and Methods

Plasmid	Partial genotype	Parental vector (cut)	Insert/PCR (cut)
pKAM164	<i>ter-P<sub>mtlR</sub>'(-200→-78)-UTR<sub>manP</sub>-gsiB-eGFP-ter</i>	pMW168.1 ( <i>AgeI/BglII</i> )	s7621/s7622 ( <i>AgeI/BglIII</i> )
pKAM167	<i>ter-P<sub>mtlA+11</sub>-lacZ-ter</i>	pKAM12 ( <i>NheI/MunI</i> )	s6209/s7678 ( <i>NheI/MunI</i> )
pKAM168	<i>ter-P<sub>mtlA+9</sub>-lacZ-ter</i>	pKAM12 ( <i>NheI/MunI</i> )	s6209/s7679 ( <i>NheI/MunI</i> )
pKAM169	<i>ter-P<sub>mtlA</sub>'(-161→-42)-gsiB*</i> [aaa→cat]- <i>eGFP-ter-mtlR-P<sub>mtlR</sub></i>	pKAM114 ( <i>PvuII</i> )	pKAM01 ( <i>BamHI</i> )
pKAM176	<i>ter-P<sub>HP43</sub>-lacZ-ter</i>	pSUN279.2 ( <i>NheI/AfIII</i> )	s7714/s7615 ( <i>NheI/AfIII</i> )
pKAM182	<i>rhaP<sub>BAD</sub>-mtlR-H3242D C419A</i>	pJOE6089.4 ( <i>AflIII/XmaI</i> )	s7303/s7301 + s7302/s7304 F.s7303/s7304 ( <i>AfIII/XmaI</i> )
pKAM185	<i>ter-P<sub>HP44</sub>-lacZ-ter</i>	pSUN279.2 ( <i>NheI/AfIII</i> )	s7800/s6954 ( <i>NheI/AfIII</i> )
<i>Integration vectors</i>			
pKAM4	<i>ycsN-ermC-ydaB'</i>	pKAM05 ( <i>EcoRV/BglII</i> )	s5809/s5810 ( <i>EcoRV/BglII</i> )
pKAM5	<i>ycnL-ermC-P<sub>mtlA</sub>-mtlD'</i>	pKAM08 ( <i>SpeI/StuI</i> )	s6067/s6079 ( <i>SpeI/StuI</i> )
pKAM6	<i>ycnL-ermC-ycsA'</i>	pKAM011 ( <i>EcoRV/BglII</i> )	s6068/s6080 ( <i>EcoRV/BglII</i> )
pKAM13	<i>'ydjC-cat-psiA'</i>	pKAM014 ( <i>AflIII/NdeI</i> )	s6304/s6305 ( <i>AflIII/NdeI</i> )
pKAM14	<i>mtlD'-ermC-mtlD'</i>	pKAM015 ( <i>HincII</i> )	s5069/s5070
pKAM19	<i>mroxP-cat-mroxP</i>	pIC20HE ( <i>XhoI/EcoRI</i> )	s6465/s6466 ( <i>XhoI/EcoRI</i> )
pKAM47	<i>mtlA'-mroxP-cat-mroxP-mtlD'</i>	pKAM020 ( <i>NheI/SacI</i> )	s6761/s6762 ( <i>NheI/SacI</i> )
pKAM68	<i>hisF-hisI-P<sub>mtlR</sub>-mtlR-H289A-yvcA-</i> <i>yvcB</i>	pHM31 ( <i>XmaI/NheI</i> )	pKAM026 ( <i>XmaI/SpeI</i> )
pKAM123	<i>amyE'-ter-P<sub>mtlA</sub>-lacZ-<i>spc</i>-amyE'</i>	pDG1730 ( <i>HindIII/EcoRI</i> )	s7455/s7481 ( <i>HindIII/EcoRI</i> )
pKAM126	<i>ycsN-P<sub>mtlR</sub>-mtlR-H342D-ydaB'</i>	pKAM4 ( <i>XmaI/SpeI</i> )	pKAM024 ( <i>XmaI/SpeI</i> )
pKAM127	<i>ycsN-P<sub>mtlR</sub>-mtlR-H230A-ydaB'</i>	pKAM4 ( <i>XmaI/SpeI</i> )	pKAM025 ( <i>XmaI/SpeI</i> )
pKAM129	<i>ycsN-P<sub>mtlR</sub>-mtlR-H230A H230A-</i> <i>ydaB'</i>	pKAM4 ( <i>XmaI/SpeI</i> )	pKAM027 ( <i>XmaI/SpeI</i> )

<sup>α</sup> The numbers are showing the base pair position with respect to start codon of the wild type gene.

<sup>β</sup> The fusion PCRs are shown by (F.) sign.

\*[\*→\*]: the asterisk and bracket show the base pair exchange in the sequence.

## 2.3. Oligonucleotides

Primer	Sequence (5'→3')	Direction	Application
s5069	AAA AAA GAA TTC GAT ATC AGA TCT ACG CGT TAA CCC GGG C	Fwd.	Amplification of <i>ermC</i>
s5070	AAA AAA CAA TTG AAT CGA TTC ACA AAA AAT AGG	Rev.	Amplification of <i>ermC</i>
s5526	AAA AAA GCT AGC GGC TCC TGA AAC CAG GAG	Fwd.	Amplification of <i>P<sub>mtlA</sub></i>
s5527	AAA AAC TTA AGA TAT AAA CCC TCC CTG TTT TG	Rev.	Amplification of <i>P<sub>mtlA</sub></i>
s5656	AAC TGC AGT ACG ATA TTC CAT AAA AAG C	Fwd.	Amplification of <i>P<sub>mtlR</sub></i>
s5657	AAA GAT CTC AGG TTT ACA GTA TGT TTT TT	Rev.	Amplification of <i>P<sub>mtlR</sub></i>
s5799	AAG CTA GCT ACG ATA TTC CAT AAA AAG C	Fwd.	Amplification of <i>P<sub>mtlR</sub></i>
s5800	AA CTT AAG AAA AAA GAC CTC CTA GCC	Rev.	Amplification of <i>P<sub>mtlR</sub></i>
s5809	AAA AAA GAT ATC AAC GCC CTT GCC CTT TC	Fwd.	Amplification of <i>ycsN</i>
s5810	AAA AAA AGA TCT GCA TCA GCT GGT AAA CTG AT	Rev.	Amplification of <i>ycsN</i>
s5812	AAA AAA AGG CCT AAC ACA AAT GTT GTT TCT GC	Rev.	Amplification of <i>ydaB</i>
s5860	AAA AAA ACT AGT ACC TGC ATG GCA CAC GT	Fwd.	Amplification of <i>ydaB</i>
s5918	AAA GAT CTA ACC AGG AGC CTT TTT ATT TT	Fwd.	Amplification of <i>P<sub>mtlA</sub></i>
s5919	CGA AAT GTA AGG CGA TCA TAT ATA AAC CCT CCC TGT T	Rev.	Amplification of <i>P<sub>mtlA</sub></i>
s5920	AAC AGG GAG GGT TTA TAT ATG ATC GCC TTA CAT TTC G	Fwd.	Amplification of <i>mtlD</i>
s5921	AAG ATA TCG ACC GTA AAC AGC TTC CGT T	Rev.	Amplification of <i>mtlD</i>
s5959	Cy5-GCT GCA AGG CGA TTA AGT TGG	Rev.	Hybridized to <i>lacZ</i>
s5960	Cy5-CCA GTC ACG ACG TTG TAA AAC	Rev.	Hybridized to <i>lacZ</i>
s5994	AAA CTA GTA AGA AAC TTA ATC AAT AAC CGA C	Fwd.	Amplification of <i>ycsA</i>
s5995	AAA GGC CTT CTC GAT TCC GCT ATA ATC AG	Rev.	Amplification of <i>ycsA</i>
s6067	CCT GAA AGA AAC ACC ATG CCC GAA C	Fwd.	Amplification of <i>yncL</i>
s6068	AAG ATA TCG AAA GAA ACA CCA TGC CCG AAC	Fwd.	Amplification of <i>yncL</i>
s6079	AAA AAA ACT AGT CTT TGG CAC ATG ACT GTG ACA	Rev.	Amplification of <i>yncL</i>
s6080	AAA GAT CTC TTT GGC ACA TGA CTG TGA CA	Rev.	Amplification of <i>yncL</i>
s6209	AAA AAA GCT AGC TTT TTA TTT TTA AAA AAT TGT CAC AGT CA	Fwd.	Amplification of <i>P<sub>mtlA</sub></i>
s6210	AAA AAA GCT AGC TAA AAA ATT GTC ACA GTC ATG TGC	Fwd.	Amplification of <i>P<sub>mtlA</sub></i>
s6213	AAA AAA CTT AAG TAA GAT ACA AAA ATA TGT TCA GAG A	Rev.	Amplification of <i>P<sub>mtlA</sub></i>
s6302	AAA AAA GAA TTC GGT ATC TAT CTT TTA TGC CAA	Fwd.	Amplification of <i>ydjC</i>
s6303	AAA AAA GCT AGC TAC GTA GTT CTG TCA GCA ATC	Rev.	Amplification of <i>ydjC</i>
s6304	AAA AAA CTT AAG ATC ATT GAA GAT GTT TCT TGA	Fwd.	Amplification of <i>pspA</i>

## Materials and Methods

Primer	Sequence (5'→3')	Direction	Application
s6305	AAA AAA CAT ATG CAG CAA TTT GAT TCG CCG C	Rev.	Amplification of <i>pspA</i>
s6344	AAA AAA GAT ATC GAT CGC CTT ACA TTT CGG TGC	Fwd.	Amplification of <i>mtlD</i>
s6345	AAA AAA CAT ATG TTA AAA TGA TGG CGT GCA ACG	Rev.	Amplification of <i>mtlD</i>
s6392	AAA AAA CTT AAG AGC CAA TCT TGA TGT GCG G	Rev.	Amplification of $P_{mtlR}$
s6465	AAA AAA CTC GAG TCT GGC TCT TGA TAA TGT ACA CTA TAC GAA GTT ATA CTA GTA GCA CGC CAT AGT GAC TG	Fwd.	Amplification of <i>mroxP-cat-mroxP</i>
s6466	AAA AAA GAA TTC TCT GGC TCT TGA TAA TGT ACA CTA TAC GAA GTT ATA CTA GTA GTT ATT GGT ATG ACT GGT TT	Rev.	Amplification of <i>mroxP-cat-mroxP</i>
s6504	AAA AAA GCT AGC GTT ATA GGG AAA AAT GCC TTT ATT	Fwd.	Fusion $P_{manP}$ - $P_{mtlA}$
s6505	ACG CTT ACA GTC CCT ATA CAA TTT TTT TAC CAT AGG TTC CG	Rev.	Fusion $P_{manP}$ - $P_{mtlA}$
s6506	CGG AAC CTA TGG TAA AAA AAT TGT ATA GGG ACT GTA AGC GT	Fwd.	Fusion $P_{manP}$ - $P_{mtlA}$
s6507	AAA AAA CTT AAG TAA GAT ACA AAA ATA TGT TCA GAG AAT G	Rev.	Fusion $P_{manP}$ - $P_{mtlA}$
s6508	ACG CTT ACA GTC CCT ATA CAA CGC TTT TTT TAC CAT AGG TT	Rev.	Fusion $P_{manP}$ - $P_{mtlA}$
s6509	AAC CTA TGG TAA AAA AAG CGT TGT ATA GGG ACT GTA AGC GT	Fwd.	Fusion $P_{manP}$ - $P_{mtlA}$
s6510	AAA ACG CTT ACA GTC CCT TAA AAT CGC TTT TTT TAC C	Rev.	Fusion $P_{manP}$ - $P_{mtlA}$
s6511	GGT AAA AAA AGC GAT TTT AAG GGA CTG TAA GCG TTT T	Fwd.	Fusion $P_{manP}$ - $P_{mtlA}$
s6608	ACG CTT ACA GTC CCT ATA AAT CGC TTT TTT TAC CAT AGG TT	Rev.	Fusion $P_{manP}$ - $P_{mtlA}$
s6609	AAC CTA TGG TAA AAA AAG CGA TTT ATA GGG ACT GTA AGC GT	Fwd.	Fusion $P_{manP}$ - $P_{mtlA}$
s6652	ACG CTT ACA GTC CCT ATA CAT CGC TTT TTT TAC CAT AGG TT	Rev.	Fusion $P_{manP}$ - $P_{mtlA}$
s6653	AAC CTA TGG TAA AAA AAG CGA TGT ATA GGG ACT GTA AGC GT	Fwd.	Fusion $P_{manP}$ - $P_{mtlA}$
s6654	TTT GAA AAC GCT TAC ATT CCC TAT ACA ATT GAA AGT AAA G	Rev.	$P_{mtlA}$ cre site improvement
s6655	AAT GTA AGC GTT TTC AAA TAG AGT CAA AGG GAA GCA TCA	Fwd.	$P_{mtlA}$ cre site improvement
s6656	TGT TAA AAG CCT TAG TGT CCC TAT ACA ATT GAA AGT AAA G	Rev.	$P_{mtlA}$ cre site disruption
s6657	ACA CTA AGG CTT TTA ACA TAG AGT CAA AGG GAA GCA TCA	Fwd.	$P_{mtlA}$ cre site disruption
s6664	ATT GAA AAC GCT TTC AAA AAA GAA TCA ATC ACT TAT AAA TG	Rev.	$P_{mtlR}$ cre site improvement
s6665	TTT GAA AGC GTT TTC AAT TAA AAG GAA ACC TCT CTA TAT CC	Fwd.	$P_{mtlR}$ cre site improvement
s6666	ATA TAA AAG CCT TTG TAG AAA GAA TCA ATC ACT TAT AAA TG	Rev.	$P_{mtlR}$ cre site disruption
s6667	CTA CAA AGG CTT TTA TAT TAA AAG GAA ACC TCT CTA TAT CC	Fwd.	$P_{mtlR}$ cre site disruption

## Materials and Methods

Primer	Sequence (5'→3')	Direction	Application
s6686	AAA AAA CTT AAG AGG AGG TCT TTT TTA TGT ATA TGA	Fwd.	Amplification of <i>mtlR-His<sub>6</sub></i>
s6687	AAA AAA CCC GGG TTA GTG GTG GTG GTG GTG GTG CAG TAT GTT TTT TTC TTT CAT CC	Rev.	Amplification of <i>mtlR-His<sub>6</sub></i>
s6688	AAA AAA GCT AGC TTT TTA TTT TTA AAA AAT TGT CAC AGT CAT GTG CCA AAG TCC TGA AAT CTT TCA ATT GTA TAG GGA CTG	Fwd.	Amplification of <i>P<sub>mtlA</sub></i>
s6709	ATG TTA TTG AAA ACG CTT ACA TTA TAC AAT TGA AAG TAA AGA GGA C	Rev.	Relocating <i>P<sub>mtlA</sub> cre</i> site
s6710	AAT GTA AGC GTT TTC AAT AAC ATA GAG TCA AAG GGA AG	Fwd.	Relocating <i>P<sub>mtlA</sub> cre</i> site
s6711	TTG AAA ACG CTT TCA AAA ATC AAT CAC TTA TAA ATG GTA AT	Rev.	Relocating <i>P<sub>mtlR</sub> cre</i> site
s6712	TTT GAA AGC GTT TTC AAT ATA TTA AAA GGA AAC CTC TCT AT	Fwd.	Relocating <i>P<sub>mtlR</sub> cre</i> site
s6713	CCC TTT GAC TCT ATT ATA AAA CGC TTA CAG TCC CT	Rev.	Changing the <i>P<sub>mtlA</sub> -10</i> box
s6714	AAG CGT TTT ATA ATA GAG TCA AAG GGA AGC AT	Fwd.	Changing the <i>P<sub>mtlA</sub> -10</i> box
s6726	AAA AAA GCT AGC TAT TTT TAA AAA ATT GTC ACA GT	Fwd.	Amplification of <i>P<sub>mtlA</sub></i>
s6727	AAA AAA CTT AAG AGA GAA TGA TGC TTC CCT TTG	Rev.	Amplification of <i>P<sub>mtlA</sub></i>
s6728	ATA CAA TTC TTT CTA AAG AGG ACT TTG GCA CAT G	Rev.	Amplification of <i>P<sub>mtlA</sub></i>
s6729	CCT CTT TAG AAA GAA TTG TAT AGG GAC TGT AAG CGT	Fwd.	Amplification of <i>P<sub>mtlA</sub></i>
s6759	AAA AAA GGA TCC CAT CCA TTT CTT CGG AGG	Fwd.	Amplification of ' <i>mtlA</i>
s6760	AAA AAA CTC GAG GAC AAT CAC TCT CTT TCT ATA AGA T	Rev.	Amplification of ' <i>mtlA</i>
s6761	AAA AAA GCT AGC CAT TTT CAA CGA GGT GAA CT	Fwd.	Amplification of <i>mtlD'</i>
s6762	AAA AAA GAG CTC TTT GAC CGT TTT GAG TCC G	Rev.	Amplification of <i>mtlD'</i>
s6792	AAA AAA GCT AGC TTT ATT TTT AAA AAA TTG TCA CA	Fwd.	Amplification of <i>P<sub>mtlA</sub></i>
s6793	AAA AAA GCT AGC TTT TTA AAA AAT TGT CAC AGT C	Fwd.	Amplification of <i>P<sub>mtlA</sub></i>
s6794	AAA AAA CTT AAG AAA TAT GTT CAG AGA ATG ATG C	Rev.	Amplification of <i>P<sub>mtlA</sub></i>
s6798	CGC TTT CAA GAA AGA ATC AAT TGA AAG TAA AGA GGA CTT TGG	Rev.	Fusion of operator of <i>P<sub>mtlA</sub></i> to <i>P<sub>mtlR</sub></i>
s6799	CCA AAG TCC TCT TTA CTT TCA ATT GAT TCT TTC TTG AAA GCG	Fwd.	Fusion of operator of <i>P<sub>mtlA</sub></i> to <i>P<sub>mtlR</sub></i>
s6800	CGC TTA CAG TCC CTA TAC AAA ACT TAG TAA AGA GGA CTT TGG CAC	Rev.	Amplification of <i>P<sub>mtlA</sub></i>
s6801	CCA AAG TCC TCT TTA CTA AGT TTT GTA TAG GGA CTG TAA GCG	Fwd.	Amplification of <i>P<sub>mtlA</sub></i>
s6829	AAA AAA GCT AGC TTT AAA AAA TTG TCA CAG TCA T	Fwd.	Amplification of <i>P<sub>mtlA</sub></i>
s6830	AAA AAA GCT AGC AAA AAT TGT CAC AGT CAT GTG	Fwd.	Amplification of <i>P<sub>mtlA</sub></i>

## Materials and Methods

Primer	Sequence (5'→3')	Direction	Application
s6855	AAA ACG CTT ACA GTC CCT AAA AAT CGC TTT TTT TAC CA	Rev.	Fusion $P_{manP}$ - $P_{mtlA}$
s6856	TGG TAA AAA AAG CGA TTT TTA GGG ACT GTA AGC GTT TT	Fwd.	Fusion $P_{manP}$ - $P_{mtlA}$
s6861	CTG TAT ACC GAA ATC AGC TCA TAT ACA ATT GAA AGT AAA GAG GAC T	Rev.	Fusion $P_{mtlA}$ - $P_{manP}$
s6862	CAA AGT CCT CTT TAC TTT CAA TTG TAT ATG AGC TGA TTT CGG TAT ACA G	Fwd.	Fusion $P_{mtlA}$ - $P_{manP}$
s6865	GCT GAC GGC CGG CTC CAG ATC TGC AAT CAA GCC TTC ATA TAA	Rev.	Mutation $mtlR$ -H342D
s6866	TTA TAT GAA GGC TTG ATT GCA GAT CTG GAG CCG GCC GTC AGC	Fwd.	Mutation $mtlR$ -H342D
s6867	AAA AAA ACT AGT TTA CAG TAT GTT TTT TTC TTT CAT	Rev.	Amplification of $mtlR$
s6868	TCG TTC GAT CGC ATA CGT TAA CGC GAC GAC GAG CGC TAT ATA G	Rev.	Mutation $mtlR$ -H230A
s6869	CTA TAT AGC GCT CGT CGT CGC GTT AAC GTA TGC GAT CGA ACG A	Fwd.	Mutation $mtlR$ -H230A
s6870	CGA TTG GCG CTT CGA AGC GCT ATA GTA ATA TAG CCG ACC TCC G	Rev.	Mutation $mtlR$ -H289A
s6871	CGG AGG TCG GCT ATA TTA CTA TAG CGC TTC GAA GCG CCA ATC G	Fwd.	Mutation $mtlR$ -H289A
s6949	AAA AAA CCC GGG TAC GAT ATT CCA TAA AAA GC	Fwd.	Amplification of $P_{mtlR}$
s6954	AAA AAA CTT AAG AAA ATT ATT TCT AGA AAG TGT GAA	Rev.	Amplification of $P_{manP}$
s7065	AAA AAA GCT AGC TTT TTA TTT TTA AAA AAT TGT CAC AGT CAT GTG CCA AAC AGG ACT TTA CTT TCA ATT GTA TAG GG	Fwd.	Amplification of $P_{mtlA}$
s7066	AAA AAA CTT AAG AAG TCG CAA GGA GAT GC	Rev.	Amplification of $P_{mtlR}$
s7067	AAA AAA CTT AAG GAG ATG CAG TAG AGG ATA TAG A	Rev.	Amplification of $P_{mtlR}$
s7068	AAA AAA CTT AAG AGA GGA TAT AGA GAG GTT TCC	Rev.	Amplification of $P_{mtlR}$
s7091	AAA AAA GCT AGC TTT TTA TTT TTA AAA AAT TGT CAC AGT CAT GTG GGT TTG TCC TCT TTA CTT TCA ATT GTA TA	Fwd.	Amplification of $P_{mtlA}$
s7098	AAA AAA GCT AGC AGC TAT TGT AAC ATA ATC GGT	Fwd.	Fusion of $P_{groE}$ - $cre$ - $UTR_{mtlR}$
s7149	AGA ATG ATG CTT CCC TTT GTT TTA ATA TAA AAC GCT TTC AA	Rev.	Fusion of $P_{mtlR}$ and UTR of $mtlA$
s7150	TTG AAA GCG TTT TAT ATT AAA ACA AAG GGA AGC ATC ATT CT	Fwd.	Fusion of $P_{mtlR}$ and UTR of $mtlA$
s7189	CCT TAA AAC GCT TAC AGC AAT TCT TAT AAT AAA GAA TCT CC	Rev.	Fusion of $P_{groE}$ - $cre$ - $P_{mtlA}$ - $UTR_{mtlR}$
s7190	TGC TGT AAG CGT TTT AAG GAA ACC TCT CTA TAT CCT CTA	Fwd.	Fusion of $P_{groE}$ - $cre$ - $P_{mtlA}$ - $UTR_{mtlR}$
s7191	CCA TAA AAC GCT TTC AAC AAT TCT TAT AAT AAA GAA TCT CC	Rev.	Fusion of $P_{groE}$ - $cre$ - $P_{mtlR}$ - $UTR_{mtlR}$
s7192	TGT TGA AAG CGT TTT ATG GAA ACC TCT CTA TAT CCT CTA	Fwd.	Fusion of $P_{groE}$ - $cre$ - $P_{mtlR}$ - $UTR_{mtlR}$
s7193	CCT GGT AAC GCT TTC AAC AAT TCT TAT AAT AAA GAA TCT CC	Rev.	Fusion of $P_{groE}$ - $cre$ - $P_{acsA}$ - $UTR_{mtlR}$



## Materials and Methods

Primer	Sequence (5'→3')	Direction	Application
<b>s7194</b>	TGT TGA AAG CGT TAC CAG GAA ACC TCT CTA TAT CCT CTA	Fwd.	Fusion of $P_{groE-cre_{PacsA^-}}$ - $UTR_{mtlR}$
<b>s7195</b>	CCT GTT CAC GCT TTC AGC AAT TCT TAT AAT AAA GAA TCT CC	Rev.	Fusion of $P_{groE-cre_{mtlA^-}}$ - $UTR_{mtlR}$
<b>s7196</b>	TGC TGA AAG CGT GAA CAG GAA ACC TCT CTA TAT CCT CTA	Fwd.	Fusion of $P_{groE-cre_{mtlA^-}}$ - $UTR_{mtlR}$
<b>s7237</b>	GTA GAG GAT ATA GAG AGG TTT CCC AAT TCT TAT AAT AAA GAA TCT CC	Rev.	Fusion of $P_{groE}$ - $UTR_{mtlR}$
<b>s7238</b>	GGA GAT TCT TTA TTA TAA GAA TTG GGA AAC CTC TCT ATA TCC TCT AC	Fwd.	Fusion of $P_{groE}$ - $UTR_{mtlR}$
<b>s7301</b>	GAG CCG ATC CCG CTG CTC GCG ACG ACA AGC GCT TTC A	Rev.	Mutation $mtlR$ -C419A
<b>s7302</b>	TGA AAG CGC TTG TCG TCG CGA GCA GCG GGA TCG GCT C	Fwd.	Mutation $mtlR$ -C419A
<b>s7303</b>	AAA AAA CTT AAG AAG GAG ATA TAC ATA TGT ATA TGA CTG CCA GAG AAC	Fwd.	Amplification of $mtlR$
<b>s7304</b>	AAA AAA CCC GGG TTA CAG TAT GTT TTT TTC TTT CAT C	Rev.	Amplification of $mtlR$
<b>s7355</b>	AAA AAA ACC GGT TTT TTA TTT TTA AAA AAT TGT CAC AGT CA	Fwd.	Amplification of $P_{mtlA}$
<b>s7356</b>	AAA AAA GGA TCC TTT GTT ATT GTC TGC CAT ATG GAA TTC CTC CTT TAA TTC TTA AGA AAT ATG TTC AGA GAA TGA TGC	Rev.	Amplification of $P_{mtlA}$
<b>s7455</b>	AAA AAA GAA TTC TTA TTA TTA TTT TTG ACA CCA GAC	Fwd.	Amplification of $P_{mtlA}$ - $lacZ$
<b>s7481</b>	AAA AAA AAG CTT CGT CGA GAC CCC TGT GGG TCT CGT TTT TTG GAT CCG GCG CCC ACG T	Rev.	Amplification of $P_{mtlA}$ - $lacZ$
<b>s7548</b>	AAA AAC AAT TGA AAG AAA TTG AAA GTA AAG AGG ACT TTG G	Rev.	Amplification of $P_{mtlA}$
<b>s7614</b>	CCC CCC GCT AGC CAG CCT GTA TAT ACC TTT TTT CC	Fwd.	Amplification of $P_{licB}$
<b>s7615</b>	CCC CCC CTT AAG AGA GTT TGA TCA ATT TTG TAA TGT	Rev.	Amplification of $P_{licB}$
<b>s7616</b>	AAA AAA GGT CTC AAT GTT TAT GAA AGC GAT TTC	Fwd.	Fusion $P_{mtlA}$ - $P_{licB}$
<b>s7617</b>	AAA AAA GGT CTC AAC ATT GAA AGT AAA GAG GAC TT	Rev.	Fusion $P_{mtlA}$ - $P_{licB}$
<b>s7618</b>	GCT TTC ATA AAC ACT CAG GGT AAA GAG GAC TTT GGC ACA TGA CT	Rev.	Fusion $P_{mtlA}$ - $P_{licB}$
<b>s7619</b>	AGT CAT GTG CCA AAG TCC TCT TTA CCC TGA GTG TTT ATG AAA GC	Fwd.	Fusion $P_{mtlA}$ - $P_{licB}$
<b>s7620</b>	AAA AAA AGA TCT ACT CTA TGT TAA AAC GCT TAC AGT	Rev.	Amplification of $P_{mtlA}$
<b>s7621</b>	AAA AAA ACC GGT TAC GAT ATT CCA TAA AAA GCA T	Fwd.	Amplification of $P_{mtlR}$
<b>s7622</b>	CCC CCC AGA TCT TTT TAA TAT AAA ACG CTT TCA A	Rev.	Amplification of $P_{mtlR}$
<b>s7678</b>	AAA AAC AAT TGA AAG AAA ATT GAA AGT AAA GAG GAC TTT GG	Rev.	Amplification of $P_{mtlA}$
<b>s7679</b>	AAA AAC AAT TGA AAG AAT TGA AAG TAA AGA GGA CTT TGG	Rev.	Amplification of $P_{mtlA}$

Primer	Sequence (5'→3')	Direction	Application
<b>s7714</b>	AAA AAA GCT AGC TTT TTA TTT TTA AAA	Fwd.	Fusion $P_{mtA}$ - $P_{licB}$
	AAT TGT CAC AGT CAT GTG CCA AAG TCC		
	TCT TTA CTT TGA GTG TTT ATG AAA GCG		
	ATT TC		
<b>s7800</b>	AAA AAG CTA GCT TTT TAT TTT TAA AAA	Fwd.	Fusion $P_{mtA}$ - $P_{manP}$
	ATT GTC ACA GTC ATG TGC CAA AGT CCT		
	CTT TAC TTT GCG ATT TTA ATG AGC TGA TT		

## 2.4. Media

Medium	Component	Amount	Note (Reference)
Lysogeny broth (LB)	Trypton	10 g	pH was adjusted to 7.2 and autoclaved (142).
	Yeast extract	5 g	
	NaCl	10 g	
	H <sub>2</sub> O	to 1000 ml	
	Agar (added for LB medium)	20 g	
LB <sub>starch</sub> medium	LB	1000 ml	
	Starch	10 g	
	Agar	20 g	
Markerless gene integration into <i>B. subtilis</i> chromosome			
Mineral broth/medium	(NH <sub>4</sub> ) <sub>2</sub> H citrate	1 g	pH was adjusted to 7.2 and autoclaved. MgSO <sub>4</sub> , glucose, and TEL were separately autoclaved (245)
	Na <sub>2</sub> SO <sub>4</sub>	2 g	
	(NH <sub>4</sub> ) <sub>2</sub> SO <sub>4</sub>	2.68 g	
	NH <sub>4</sub> Cl	0.5 g	
	K <sub>2</sub> HPO <sub>4</sub>	1.46 g	
	NaH <sub>2</sub> PO <sub>4</sub> .H <sub>2</sub> O	0.4 g	
	Glucose (50% w/v)	10 ml	
	MgSO <sub>4</sub> .7H <sub>2</sub> O (stock 1 M)	1 ml	
	TEL	3 ml	
	H <sub>2</sub> O	to 1000 ml	
Trace elements (TEL)	Agar	20 g	
	CaCl <sub>2</sub> .2H <sub>2</sub> O	0.5 g	Added to the mineral medium after autoclaving (245).
	FeCl <sub>3</sub> .6H <sub>2</sub> O	16.7 g	
	Na <sub>2</sub> EDTA	20.1 g	
	ZnSO <sub>4</sub> .7H <sub>2</sub> O	0.18 g	
	MnSO <sub>4</sub> .H <sub>2</sub> O	0.1 g	
	CuSO <sub>4</sub> .5H <sub>2</sub> O	0.16 g	
	CoCl <sub>2</sub> .6H <sub>2</sub> O	0.18 g	
	H <sub>2</sub> O	to 1000 ml	

## Materials and Methods

Medium	Component	Amount	Note (Reference)
<b>Transformation of <i>B. subtilis</i></b>			
Spizizen's minimal salts (SMS)	(NH <sub>4</sub> ) <sub>2</sub> SO <sub>4</sub>	2 g	Glucose/ glucitol were added after autoclaving. (86, 206)
	K <sub>2</sub> HPO <sub>4</sub>	14 g	
	KH <sub>2</sub> PO <sub>4</sub>	6 g	
	Na <sub>3</sub> citrate.2H <sub>2</sub> O	1 g	
	MgSO <sub>4</sub> .7H <sub>2</sub> O	0.2 g	
	Glucose/Glucitol (50% w/v)	10 ml	
	H <sub>2</sub> O	to 1000 ml	
SMS + succinate and glutamate (SMS+SG)	(NH <sub>4</sub> ) <sub>2</sub> SO <sub>4</sub>	2 g	Sterile-filtered succinate salt and glutamate salts were added after autoclaving.
	K <sub>2</sub> HPO <sub>4</sub>	14 g	
	KH <sub>2</sub> PO <sub>4</sub>	6 g	
	Na <sub>3</sub> citrate.2H <sub>2</sub> O	1 g	
	MgSO <sub>4</sub> .7H <sub>2</sub> O	0.2 g	
	Na <sub>2</sub> succinate. 6H <sub>2</sub> O (20% w/v)	30 ml	
	K glutamate.H <sub>2</sub> O (20% w/v)	40 ml	
H <sub>2</sub> O	to 1000 ml		
Broth I	SMS (or SMS+SG)	96.5 ml	The components were separately autoclaved or sterile-filtered.
	Casamino acids (1% w/v)	2 ml	
	MgSO <sub>4</sub> .7H <sub>2</sub> O (1 M)	0.5 ml	
	Tryptophan (0.5% w/v)	1 ml	
	Na <sub>2</sub> succinate. 6H <sub>2</sub> O (20% w/v)	2.5 ml	
H <sub>2</sub> O	to 100 ml		
Broth II	SMS (or SMS+SG)	8 ml	The components were separately autoclaved or sterile-filtered.
	Casamino acids (1% w/v)	0.1 ml	
	MgSO <sub>4</sub> .7H <sub>2</sub> O (1 M)	0.05 ml	
	Tryptophan (0.5% w/v)	0.1 ml	
<b>Electroporation of <i>E. coli</i></b>			
Terrific broth (TB)	Bacto-trypton	12 g	KH <sub>2</sub> PO <sub>4</sub> -K <sub>2</sub> HPO <sub>4</sub> solution was separately dissolved and autoclaved (186).
	Bacto-yeast	24 g	
	Glycerol (100%)	4 ml	
	H <sub>2</sub> O	to 900 ml	
	KH <sub>2</sub> PO <sub>4</sub>	2.31 g	
	K <sub>2</sub> HPO <sub>4</sub>	12.54 g	
H <sub>2</sub> O	to 100 ml		
<b>Electroporation of <i>B. subtilis</i></b>			
LB <sub>glucitol</sub>	Trypton	1 g	pH was adjusted to 7.2 and autoclaved. Glucitol was separately autoclaved.
	Yeast extract	0.5 g	
	NaCl	1 g	
	Glucitol (2 M)	25 ml	
	H <sub>2</sub> O	to 100 ml	

## Materials and Methods

Medium	Component	Amount	Note (Reference)
Recovery broth	Trypton	1 g	pH was adjusted to 7.2 and autoclaved.
	Yeast extract	0.5 g	
	NaCl	1 g	
	Glucitol (2 M)	25 ml	Glucitol and mannitol were separately autoclaved (252).
	Mannitol (1 M)	38 ml	
	H <sub>2</sub> O	to 100 ml	

### 2.5. Antibiotics

Antibiotic	Stock solution	Final conc.
Ampicillin	100 mg/ml in 50% ethanol	100 µg/ml
Chloramphenicol	25 mg/ml in 50% ethanol	5 µg/ml
Erythromycin	10 mg/ml in 50% ethanol	5 µg/ml
Spectinomycin	100 mg/ml in H <sub>2</sub> O	100 µg/ml

The desired antibiotic was added to the autoclaved medium at 50°C.

### 2.6. Buffers and solutions

Buffer or solution	Components	Amount
TE 10.01	Tris-HCl (1 M, pH 8)	10 ml
	EDTA (0.5 M, pH 8)	0.2 ml
	H <sub>2</sub> O	to 1000 ml
<b>Plasmid isolation by alkaline lysis</b>		
Resuspension buffer	Glucose.H <sub>2</sub> O	9.9 g
	Tris-HCl (1 M, pH 8)	25 ml
	EDTA	3.72 g
	H <sub>2</sub> O	to 1000 ml
	RNase (freshly added before use)	10 µg/ml
Lysis solution	NaOH (2 M)	5 ml
	SDS solution (20% w/v)	2.5 ml
	H <sub>2</sub> O	to 50 ml
Neutralization solution	Ammonium acetate	231.24 g
	H <sub>2</sub> O	to 400 ml

## Materials and Methods

Buffer or solution	Components	Amount
<b>Isolation of chromosomal DNA from <i>B. subtilis</i></b>		
Resuspension buffer	Tris-HCl (1 M, pH 8)	2.5 ml
	EDTA (0.5 M, pH 8)	5 ml
	Sucrose (20% w/v)	50 ml
	Glycine (0.5 mM)	0.1 ml
	Lysozyme (freshly added just before use)	20 mg/ml
	H <sub>2</sub> O	to 100 ml
<b>Agarose gel electrophoresis</b>		
50x TAE	Tris base	242 g
	Acetic acid	57 ml
	EDTA	18.6 g
	H <sub>2</sub> O	to 1000 ml
Adjust pH to 8.0		
10x Sample loading buffer	Bromphenol blue	0.025 g
	Xylen cyanol FF	0.025 g
	Glycerol (100%)	3 ml
	H <sub>2</sub> O	7 ml
<b>Formaldehyde agarose gel electrophoresis for RNA</b>		
10x gel buffer	MOPS (1 M, pH 7.0)	200 ml
	Sodium acetate (3 M)	16.65 ml
	EDTA (0.5 M, pH 8.0)	20 ml
	H <sub>2</sub> O	to 1000 ml
	pH was adjust to 8.0 and treated with DEPC before autoclaving	
Running buffer	10x formaldehyde agarose gel buffer	50 ml
	Formaldehyd (37% or 12.3 M)	10 ml
	DEPC-treated H <sub>2</sub> O	to 500 ml
5x sample loading buffer	Saturated bromophenol blue aqueous solution	20 µl
	EDTA (0.5 M, pH 8.0)	8 µl
	Formaldehyd (37% or 12.3 M)	72 µl
	Glycerol (86%)	200 µl
	Formamide	300 µl
	10x formaldehyde agarose gel buffer	400 µl
<b>SDS-PAGE</b>		
10x running buffer	Tris base	30.2 g
	SDS	10 g
	Glycine	188 g
	H <sub>2</sub> O	to 1000 ml

Materials and Methods

Buffer or solution	Components	Amount
5x sample loading buffer	Tris-HCl (2 M, pH 6,8)	6.25 ml
	SDS (20% w/v)	12.5 ml
	EDTA	0.146 g
	Bromophenol blue	0.05 g
	$\beta$ -Mercaptoethanol	2.5 ml
	Glycerol (100%)	25 ml
	H <sub>2</sub> O	to 50 ml
Stored at $-20^{\circ}\text{C}$		
Coomassie stain solution	Coomassie Brilliant Blue R250	2 g
	Coomassie Brilliant Blue G250	0.5 g
	Methanol	50 ml
	Ethanol	425 ml
	Acetic acid	100 ml
	H <sub>2</sub> O	425 ml
Destain solution	Methanol (100%)	250 ml
	Acetic acid	100 ml
	H <sub>2</sub> O	to 1000 ml
<b>Affinity chromatography by Ni-NTA agarose column</b>		
Resuspension buffer 1	NaH <sub>2</sub> PO <sub>4</sub> .H <sub>2</sub> O	50 mM
	NaCl	300 mM
Adjust pH to 8		
Wash buffer 1	NaH <sub>2</sub> PO <sub>4</sub> .H <sub>2</sub> O	50 mM
	NaCl	300 mM
	Imidazole	20 mM
Adjust pH to 8		
Elution buffer 1	NaH <sub>2</sub> PO <sub>4</sub> .H <sub>2</sub> O	50 mM
	NaCl	300 mM
	Imidazole	250 mM
Adjust pH to 8		
Resuspension buffer 2	HEPES (pH 7.4)	50 mM
	NaCl	300 mM
	$\beta$ -mercaptoethanol (14.3 M)	3 mM
	PMSF	1 mM
Adjust pH to 7.4		
Wash buffer 2	HEPES (pH 7.4)	50 mM
	NaCl	300 mM
	$\beta$ -mercaptoethanol (14.3 M)	3 mM
	Imidazole	20 mM
Adjust pH to 7.4		
Elution buffer 2	HEPES (pH 7.4)	50 mM
	NaCl	300 mM
	$\beta$ -mercaptoethanol (14.3 M)	3 mM
	Imidazole	250 mM
Adjust pH to 7.4		

Materials and Methods

Buffer or solution	Components	Amount
<b>Electrophoretic mobility shift</b>		
2x Shift buffer A	Tris-HCl (1 M, pH 8)	4 $\mu$ l
	MgCl <sub>2</sub> (1 M)	2 $\mu$ l
	EDTA (0.02 M, pH 8)	20 $\mu$ l
	DTT (0.1 M)	10 $\mu$ l
	Glycerol (100%)	200 $\mu$ l
	BSA (10 mg/ml)	10 $\mu$ l
	Herring Sperm DNA (10 mg/ml)	10 $\mu$ l
	H <sub>2</sub> O	to 1 ml
Stored at 4°C		
5x Shift buffer B (238) with slight modification	Tris-HCl (1 M, pH 7.5)	50 $\mu$ l
	KCl (1 M)	250 $\mu$ l
	DTT (0.1 M)	100 $\mu$ l
	Glycerol (100%)	250 $\mu$ l
	BSA (10 mg/ml)	25 $\mu$ l
	Herring Sperm DNA (10 mg/ml)	2.5 $\mu$ l
	H <sub>2</sub> O	to 1 ml
Stored at 4°C		
5x Shift buffer C	Tris-HCl (1 M, pH 7.5)	50 $\mu$ l
	MgCl <sub>2</sub> (1 M)	250 $\mu$ l
	DTT (0.1 M)	100 $\mu$ l
	Glycerol (100%)	250 $\mu$ l
	BSA (10 mg/ml)	25 $\mu$ l
	Herring Sperm DNA (10 mg/ml)	2.5 $\mu$ l
	H <sub>2</sub> O	to 1 ml
Stored at 4°C		
2x Shift buffer D (94)	HEPES (1 M, pH 7.4)	20 $\mu$ l
	KCl (2 M)	40 $\mu$ l
	DTT (0.1 M)	20 $\mu$ l
	1 M MgCl <sub>2</sub>	8 $\mu$ l
	Glycerol (100%)	250 $\mu$ l
	BSA (10 mg/ml)	25 $\mu$ l
	Herring Sperm DNA (10 mg/ml)	25 $\mu$ l
	H <sub>2</sub> O	to 1 ml
Stored at 4°C		
10x TBE	Tris base	108 g
	Boric acid	55 g
	EDTA (0.5 M, pH 8)	40 ml
	H <sub>2</sub> O	to 1000 ml

## Materials and Methods

Buffer or solution	Components	Amount
<b>Transformation of <i>E. coli</i></b>		
TSS	LB, pH 6.5	82.5 ml
	PEG 6000	10 g
	DMSO	5 ml
	MgCl <sub>2</sub> (2 M)	2.5 ml
Autoclaved and stored at 4°C		
<b>Electroporation of <i>B. subtilis</i></b>		
EP buffer	Glycerol (100%)	10 ml
	Glucitol (2 M)	25 ml
	Mannitol (1 M)	50 ml
	H <sub>2</sub> O (sterile)	to 100 ml
<b>β-galactosidase assay (Miller's assay)</b>		
Z buffer	Na <sub>2</sub> HPO <sub>4</sub> (1 M)	60 ml
	NaH <sub>2</sub> PO <sub>4</sub> (1 M)	40 ml
	KCl (2 M)	5 ml
	MgSO <sub>4</sub> ·7H <sub>2</sub> O (1 M)	1 ml
	β-Mercaptoethanol (14.3 M)	2.7 ml
	H <sub>2</sub> O	to 1000 ml
Stored at 4°C		

### 2.7. Chemicals and enzymes

Company	Chemical or enzyme
Bio-Rad Laboratories, München	APS, TEMED, Bradford reagents
Boehringer Mannheim GmbH	Chloramphenicol, Erythromycin
Difco Laboratories, Detroit, USA	Bacto agar, Euro agar, Trypton
Fermentas Life Sciences, St. Leon-Rot	GeneRuler™ 1 kb Plus (#SM1331/2/3), High fidelity DNA polymerase, Unstained protein molecular weight marker (#SM0431)
Thermo Fisher Scientific Inc. (Finnzymes)	Phusion® Hot Start II
Fluka Chemie AG, Buchs, Schweiz	DMSO, EDTA, Fine chemicals
GE Healthcare	Fraction collector FRAC-200 GFX™ PCR DNA and gel band purification kit Liquid chromatography controller LCC-500 plus PD MidiTrap G-25 gel filtration column Sequencing kit
Millipore, Cork, Ireland	Amicon® Ultra - 0.5 ml 30K ultrafiltration column
Merck, Darmstadt	Fine chemicals
New England Biolabs, Frankfurt am Main	Restriction enzymes



Company	Chemical or enzyme
Promega, Mannheim	RNasin <sup>®</sup> RNase inhibitor, <i>Pfu</i> DNA polymerase
Qiagen, Hilden	DNeasy Blood & Tissue Kit Ni-NTA matrix QIAprep <sup>®</sup> Spin Miniprep Kit RNeasy Mini Kit
Roche Diagnostics, Mannheim	Restriction endonuclease, Reverse transcriptase (AMV), T4 DNA ligase, T7 DNA polymerase
Roth GmbH, Karlsruhe	Ampicillin, 30% Acrylamid-, 0,8% Bisacrylamid-stock solution (Rotiphorese Gel 30), dNTPs for PCR, Ethanol p.a., Isopropanol, RNase AWAY <sup>®</sup> , Roti <sup>®</sup> -Mark Standard, Sucrose, Tris
Sigma Chemie GmbH, Deisenhofen	Fine chemicals, Spectinomycin

## 2.8. Instruments

Company	Instrument
Avestin	EmulsiFlex <sup>®</sup> -C5 High Pressure Homogenizer
Biometra	SDS gel tray
Bio-Rad Laboratories	Gene Pulser <sup>®</sup> I (Electroporator)
MJ Research	PTC-200 Peltier Thermal Cycler
Eppendorf	Microcentrifuge 5415 D Thermomixer Compact
Heat Sytem & Ultrasonics Inc.	Sonicator Ultrasonic Processor W-385
Hereaus	Megafuge 1.0 Biofuge Fresco
IMPLEN	NanoPhotometer
Molecular Dynamics	Storm 860 Phosphorimager
Pharmacia Biotech (GE Healthcare)	ALFexpress DNA sequencer Liquid Chromatography Controller LCC-500 Plus Fraction collector FRAC-200 Mono Q <sup>®</sup> HR 5/5 column PD MidiTrap G-25 column Ultrospec 3000
Renner GmbH	Gel tray for agarose gel electrophoresis
Tecan Group Ltd.	SpectraFluor Microplate reader
Thermo Fisher Scientific	SORVALL <sup>®</sup> RC-5B PLUS Superspeed Centrifuge

## 2.9. Growth conditions

Propagation of the desired plasmid was performed by *E. coli* JM109 or *E. coli* DH5 $\alpha$ . For this purpose, a single colony of an *E. coli* transformant was cultivated in a glass tube with 5 ml LB containing the relevant antibiotic. The *E. coli* culture was incubated overnight at 37°C and used for plasmid isolation.

Unless otherwise specified, *B. subtilis* 3NA was used as a host microorganism. Knock-out mutants were selected on LB agar, supplemented by erythromycin (5  $\mu$ g/ml) or chloramphenicol (5  $\mu$ g/ml). Knock-out mutations were confirmed by cultivating the mutants in broth I with no trisodium citrate. Depending on the mutation, glucose was also replaced with 1% (w/v) sterile-filtered mannitol or glucitol. Tryptophan was added to the broth I for tryptophan auxotrophic *B. subtilis* 168 and its derivatives. All of the strains were incubated overnight at 37°C under a shaking condition at 200 rpm to compare the turbidity of the mutants cultures with the wild type strain as a control.

The activity of the promoters was measured by cultivation and induction of the *B. subtilis* 3NA harboring the desired plasmid in LB. For this purpose, 85 ml LB medium in a 500 ml Erlenmeyer flask was inoculated with an overnight culture in a dilution of 1:50 and incubated at 37°C under shaking (200 rpm). Then, aliquots of 8 ml with an OD<sub>600</sub> of 0.4 were divided into 100 ml Erlenmeyer flasks and different carbohydrates, *i.e.* mannitol, mannitol + glucose, glucose, glucitol, glucitol + glucose, were subsequently added to a final concentration of 0.2% (w/v). Cultures were harvested 1 h after the addition of sugars and used for the  $\beta$ -galactosidase enzyme assay. As a defined medium, Spizizen's minimal salts (SMS) supplemented by trace elements was also used to measure the promoter activities in the same procedure. All of the experiments were repeated at least 3 times and mean values were used for comparison.

## **2.10. DNA manipulation**

### **2.10.1. DNA isolation**

#### **2.10.1.1. Plasmid isolation by alkaline lysis**

Isolation of the plasmid from *E. coli* transformants was performed according to the method of Lee and Rashed (1990) with a slight modification (130). A single colony of *E. coli* transformants was inoculated into 5 ml LB broth and incubated overnight at 37°C. Afterwards, the overnight culture was centrifuged for 5 min at 4,500 rpm (Megafuge), and the pellet was resuspended in 200 µl resuspension buffer. Next, 300 µl of lysis solution was added to the cell suspension. The lysate was gently inverted 4 to 5 times and remained up to 5 min at room temperature. Subsequently, 400 µl of neutralization solution was added to the lysate and mixed thoroughly. The neutralized mixture was centrifuged for 10 min at 13,000 rpm (Microcentrifuge) and 600 µl of the clear supernatant was added to 600 µl of isopropanol in a new Eppendorf tube. Having thoroughly mixed, the mixture was centrifuged for 10 min at 13,000 rpm (Microcentrifuge) and the pellet washed twice with 70% and 100% ethanol, respectively. The pellet was air-dried and resuspended in 30 to 50 µl ddH<sub>2</sub>O.

#### **2.10.1.2. Plasmid isolation by QIAprep® Spin Miniprep Kit**

The plasmid DNA used for cloning, sequencing and storage were purified by QIAprep® Spin Miniprep Kit. The procedure was performed according to the manufacturer's manual. Plasmid isolation from *B. subtilis* was preceded by incubation of the bacterial suspension in resuspension buffer containing 20 mg/ml lysozyme in an Eppendorf thermomixer for 30 min at 37°C and shaken at 750 rpm. The protoplast suspension was then mixed with lysis solution and the plasmid isolation was accomplished according to manufacturer's manual. Plasmid DNA was finally eluted by 50 µl ddH<sub>2</sub>O.

### 2.10.1.3. Isolation of chromosomal DNA by DNeasy Blood & Tissue Kit

Isolation of the chromosomal DNA from *B. subtilis* was carried out using DNeasy Blood & Tissue Kit (Qiagen). An overnight culture of *B. subtilis* in LB medium (2 ml, 4 OD<sub>600</sub>) was centrifuged for 10 min at 4,500 rpm (Megafuge). The pellet was then resuspended in 180 µl resuspension buffer containing 20 mg/ml lysozyme and incubated in an Eppendorf thermomixer for 30 min at 37°C and shaken at 750 rpm. Further steps were performed according to the manufacturer's instructions. For final elution, 200 µl ddH<sub>2</sub>O was used.

## 2.10.2. PCR

### 2.10.2.1. DNA amplification

To amplify the desired gene from the *B. subtilis* 168 chromosome or a plasmid, polymerase chain reaction (PCR) was carried out using Phusion<sup>®</sup> Hot Start II, *Pfu* DNA Polymerase or High Fidelity Polymerase. All of the PCRs were performed in a final volume of 100 µl according to the Table 2.3.

**Table 2. 3.** Polymerase chain reaction (PCR).

Components	Volume
DNA template (chromosomal/plasmid)	1 µl (100 ng/10 ng)
dNTP-Mix (10 mM)	2 µl
DNA polymerase	1 µl
10x or 5x reaction buffer containing MgSO <sub>4</sub> or MgCl <sub>2</sub> *	10 – 20 µl
DMSO	0 – 10 µl
Forward primer (100 pmol/µl)	1 µl
Reverse primer (100 pmol/µl)	1 µl
ddH <sub>2</sub> O	to 100 µl

\* 5x reaction buffer contains 7.5 mM MgCl<sub>2</sub> used for reactions by Phusion<sup>®</sup> Hot Start II, while 10x reaction buffers containing 20 mM MgSO<sub>4</sub> and 15 mM MgCl<sub>2</sub> used for *Pfu* DNA Polymerase and High Fidelity Polymerase, respectively.

The PCR was performed in a MJ Research Peltier thermocycler PTC-200 according to the Table 2.4. The amplified fragments were afterwards analyzed on the 0.8% (w/v) agarose gel in order to check the length of the fragment as well as its purity.

**Table 2. 4.** PCR cycles.

Cycle step	Temperature (°C)	Time	Number of cycles
Initial denaturation	94	2 min	1
Denaturation	92	30 sec	30 – 35
Annealing	$T_m - 5$	30 sec	
Extension	72	30 sec	
Final extension	72	10	1

### 2.10.2.2. Fusion PCR

Two DNA sequences were fused to each other using fusion PCR. At first, the selected genes were separately amplified by primary oligonucleotides (a & b; c & d; Fig. 2.1). The reverse primer of upstream gene with respect to the fusion orientation and the forward primer of downstream gene included identical overhang sequences shown as in Fig. 2.1 by dashes with at least 17 bp length. After purification of the primary PCR products, 1  $\mu$ l of each PCR product was mixed in a new PCR without oligonucleotide primers. The annealing temperature was calculated according to the melting temperature of the identical sequence. After 10 cycles, the forward primer of the upstream gene and the reverse primer of the downstream gene were added and the PCR was continued for another 25 cycles with the annealing temperature of the primers (oligonucleotides a and d; Fig. 2.1).

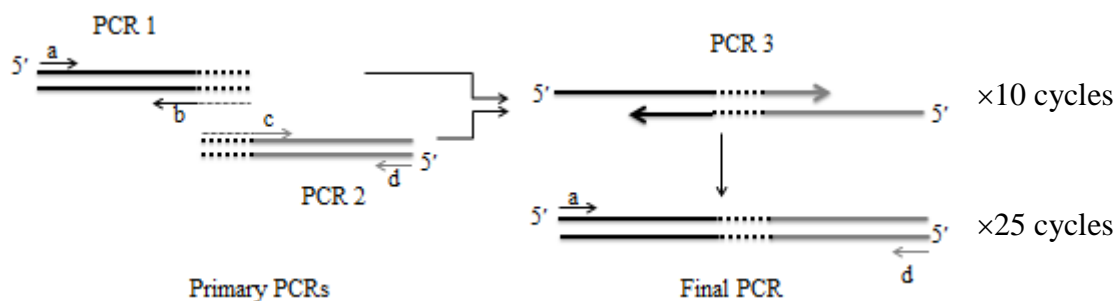


**Fig. 2. 1.** Schematic view of a fusion PCR is shown. PCRs using oligonucleotides a/b and c/d was followed by final PCR using a/d oligonucleotides and the primary PCR products. The dashes show the identical sequences with at least 17 bp length.

#### **2.10.2.3. Colony PCR**

Deletion and insertion of the chromosomal DNA in *B. subtilis* transformants were rapidly investigated by colony PCR. A single colony of *B. subtilis* was suspended in 100 µl sterile water and boiled for 10 min. The suspension was subsequently centrifuged for 3 min at 13,000 rpm (Microcentrifuge). 10 µl of the clear supernatant was used as the template in the PCR as described in 3.10.2.1. The PCR product was finally analyzed on agarose gel.

#### **2.10.2.4. Purification of PCR products**

PCR fragments were purified by the columns of GFX<sup>TM</sup> PCR DNA and Gel Band purification kit (GE Healthcare) according to manufactures' instructions.

### **2.10.3. Hybridization of complementary oligonucleotides**

Short fragments of dsDNA were constructed by hybridization reaction in which 5 µl of two complementary oligonucleotides (100 pmol/µl) were mixed with 1:1 ratio. The oligonucleotide mixture was denatured for 5 min at 92°C followed by annealing for 10 min at 65°C. The reaction was subsequently cooled to 4°C for 1 – 2 min and kept on ice. 5 µl of the dsDNA was used for the digestion reaction.

### **2.10.4. Restriction digestion of PCR fragments and plasmids**

Plasmids and PCR products were digested in a final volume of 20 µl. Either 7 µl of isolated plasmid or 5 µl of PCR fragment (approx. 0.5 µg) were digested by adding 2 µl of 10x restriction buffer and 1 µl of restriction enzyme (3 – 5 U). The reaction was incubated 1 to 2 h at the relevant temperature. In the case of double digestion, the DNA was first digested with an enzyme followed by isopropanol precipitation (see below). The precipitated DNA was resuspended in ddH<sub>2</sub>O and subjected to the second restriction enzyme with a final volume of

20 µl. Finally, the digested DNA was loaded to an agarose gel in order to cut and purify the desired fragment.

#### **2.10.5. Isopropanol precipitation of DNA**

To precipitate DNA, 2 µl sodium acetate (3 M, pH 6.3) and 20 µl isopropanol were added to 20 µl DNA solution and mixed thoroughly. After incubation for 5 min at room temperature, the solution was centrifuged for 5 min at 13,000 rpm (Microcentrifuge). The supernatant was discarded and pellet was washed twice by 40 µl 70% ethanol and 40 µl 100% ethanol. Finally, the pellet was air-dried at room temperature and dissolved in relevant amount of ddH<sub>2</sub>O.

#### **2.10.6. Agarose gel electrophoresis**

Confirmation of the correct PCR product, plasmid restriction pattern, or to isolate restriction fragments were performed by agarose gel electrophoresis. By this method, the DNA fragments are separated by the electric field according to their size. The gel was prepared by addition of 0.46 g agarose to 60 ml TAE buffer (short gel) and 1.2 g agarose to 150 ml TAE buffer (long gel) followed by boiling. Finally, 2.4 µl and 6 µl ethidium bromide (10 mg/ml) were added to the short and long gels, respectively, and poured into the gel tray. The DNA sample was mixed with 10x sample loading buffer and separated in TAE running buffer through agarose gel. For size determination, 3 µl of 1 kb DNA ladder (Fermentas) were loaded on a separate lane. Long gels were run by 100 – 120 V and short gels by 80 V. The DNA bands were detected by UV light with 302 nm wave length.

#### **2.10.7. Purification of the DNA from agarose gel**

After separating the DNA fragments on the agarose gel, the desired band was cut out under the UV light (366 nm) with a scalpel. The cut gel fragment was immersed in binding buffer

and melted at 70°C. The DNA was purified by the column of “GFX™ PCR DNA and Gel Band purification kit” (GE Healthcare) according to manufactures’ instructions.

#### **2.10.8. Alkaline phosphatase treatment**

The ligation efficiency of the digested vectors at a single restriction site was increased by the application of alkaline phosphatase (Roche). This enzyme removes the phosphate group from the 5'-end of the DNA, thereby inhibiting self-ligation of the parental vector. For this reaction, 25 µl purified vector DNA was mixed with 3 µl 10x buffer and 2 µl alkaline phosphatase (20 U/µl). The reaction incubated for 30 minutes at 37°C. Finally, the DNA was purified by the GFX™ PCR DNA and Gel Band purification kit and used for ligation.

#### **2.10.9. DNA concentration**

Concentration of the PCR products, digested DNA, and plasmids were measured using a NanoPhotometer (IMPLEN GmbH) at 260 nm. 1 OD<sub>260</sub> corresponds to 50 µg/ml dsDNA.

#### **2.10.10. Ligation**

Insertion of the desired gene into the plasmid vector was carried out by ligation. The desired insert and vector were mixed with 2 µl of the ligation buffer containing ATP and ddH<sub>2</sub>O in a final volume of 19 µl. Finally, 1 µl of T4 DNA ligase (Roche) was added to DNA solution. Cohesive end ligation was performed at 4°C, whereas the blunt end was incubated overnight at room temperature.



### **2.10.11. DNA sequencing**

The sequencing of DNA was performed according to Sanger's method (187) using a 5'-end Cy5-labeled oligonucleotide and ALF express Genetic analyzer (Amersham Pharmacia Biotech). As the template, desired plasmids were isolated by Miniprep Kit and precipitated by sodium acetate-isopropanol. After isopropanol precipitation, 5 to 10  $\mu\text{g}$  plasmid DNA was dissolved in 10  $\mu\text{l}$  ddH<sub>2</sub>O. Afterwards, 2  $\mu\text{l}$  of Cy5-labeled oligonucleotide (10 pmol/ $\mu\text{l}$ ) and 1.5  $\mu\text{l}$  NaOH (1 M) were added to 10  $\mu\text{l}$  ddH<sub>2</sub>O. The mixture was incubated for 5 min at 65°C followed by cooling at 37°C water bath. Next, 1.5  $\mu\text{l}$  HCl (1 M) and 2  $\mu\text{l}$  annealing buffer (AutoRead Sequencing kit, Amersham Pharmacia Biotech) were added to the mixture. Having incubated for 10 min at 37°C, the reaction was finally kept for 10 min at room temperature. Subsequently, 1  $\mu\text{l}$  extension buffer and 3.5  $\mu\text{l}$  DMSO were added to the reaction. Four 5.4  $\mu\text{l}$  aliquots of the reaction mixture were divided into four Eppendorf tubes each of which contained 2  $\mu\text{l}$  enzyme mix (1  $\mu\text{l}$  T7 DNA polymerase + 1  $\mu\text{l}$  enzyme dilution buffer with a concentration of 4 U/ $\mu\text{l}$ ) and 3  $\mu\text{l}$  ddNTP solution which contained either ddATP, ddCTP, ddGTP or ddTTP in combination with other three dNTPs. The reaction was incubated for 5 minutes at 37°C and stopped by the addition of 6  $\mu\text{l}$  stop solution. After incubation for 3 min at 80°C, the samples remained on ice before loading on the gel. The sequencing gel was prepared according to manufactures' instructions (Amersham Pharmacia Biotech). TBE buffer (0.5x) was used as running buffer. To analyze the sequences, 5  $\mu\text{l}$  of each reaction was loaded to the wells of the gel.

## **2.11. RNA manipulation**

### **2.11.1. RNase-free equipment**

During RNA-based experiments, all of the applied materials and equipment were prepared RNase-free. To do so, the solutions and glass wares were treated with 0.1% (v/v) DEPC and incubated overnight at 37°C. Subsequently, they were autoclaved for 45 min until the DEPC scent was gone. The instruments which could not be autoclaved were swabbed by RNase AWAY<sup>®</sup>.

### **2.11.2. RNA isolation**

20 ml of LB supplemented with 10 µg/ml spectinomycin was inoculated by overnight culture (400 µl) and incubated at 37°C. At the OD<sub>600</sub> of 0.4, the bacterial culture was divided into two 10 ml aliquots and one of them was induced by 0.8% (w/v) mannitol, while the other one incubated uninduced. The bacterial cultures were harvested 1 h after the addition of mannitol, and centrifuged for 5 min at 4,500 rpm (Megafuge). The supernatant was discarded to reduce the rest volume to less than 80 µl. Finally, total RNA was then extracted using RNeasy Mini Kit (QIAGEN) according to manufactures' instruction.

### **2.11.3. Formaldehyde agarose gel electrophoresis**

To control the quality of the extracted RNA, the isolated RNA was loaded on a 1.2% (w/v) formaldehyde agarose gel. The gel was prepared by dissolving of 0.6 g agarose in 45 ml DEPC-treated ddH<sub>2</sub>O and 5 ml of 10x formaldehyde gel buffer. The suspension was boiled and cooled to 60°C, and 0.9 ml formaldehyde (37%) was added. The solution was poured on a small gel tray. After solidification, the gel was equilibrated for 30 min in formaldehyde agarose running buffer. Next, 3 µg RNA was mixed with 5x sample loading buffer, heated for 15 min at 65°C, and immediately cooled on ice prior to electrophoresis. The electrophoresis was carried out by 100 V for 5 min which was then reduced to 60 V as long as the bromophenol blue bands passed the two third of the gel length. The formaldehyde agarose gel was stained in 200 ml formaldehyde running buffer containing 0.5 µg/ml ethidium bromide for 1 h at room temperature. Finally, the gel was observed under the UV light (302 nm).

### **2.11.4. Isopropanol precipitation of RNA**

50 µg of isolated RNA dissolved in 100 µl DEPC- treated ddH<sub>2</sub>O was mixed with 10 µl of sodium acetate (3 M, pH 6.3) and 220 µl of ethanol (100%). The mixture was incubated overnight at -20°C and then centrifuged for 10 min at 13,200 rpm (Microcentrifuge). After

discarding the supernatant, the pellet was washed twice with 100  $\mu$ l ethanol and dried at room temperature. The pellet was finally dissolved in 5  $\mu$ l DEPC-ddH<sub>2</sub>O.

#### **2.11.5. Primer Extension**

Cy5-labeled oligonucleotides were used to determine the transcription start site of the desired promoters in this study. As described in section 3.12.2, the total RNA (50  $\mu$ g) was isolated and precipitated by isopropanol and finally resuspended in 5  $\mu$ l ddH<sub>2</sub>O. To inhibit RNase activity, 0.5  $\mu$ l RNasin<sup>®</sup> Ribonuclease inhibitor (Promega, 40 U/ $\mu$ l) was added to the 5  $\mu$ l total RNA, followed by denaturation at 65°C for 3 min and cooling on ice. Subsequently, 0.5  $\mu$ l labeled oligonucleotide (10 pmol/ $\mu$ l), namely s5959 or s5960, and 2  $\mu$ l of 5x AMV-RT buffer were added to the RNA sample. The hybridization was performed for 20 min at 54°C (s5959) or 52°C (s5960). Afterwards, the RNA-oligonucleotide hybrid was cooled gradually within 5 minutes to room temperature. The reverse transcription reaction was started by the addition of 1  $\mu$ l dNTP (10 mM) and 1  $\mu$ l Avian Myeloblastosis Virus Reverse Transcriptase (AMV-RT; 20 U/ $\mu$ l). The reaction was incubated for 1 h at 42°C and stopped by the addition of 5  $\mu$ l of stop solution from the AutoRead sequencing Kit (Amershan Pharmacia Biotech) and incubation for 3 min at 80°C. The reactions were kept on ice or frozen at -20 before further analysis. To compare the obtained band of reverse transcription with the sequencing results, 5  $\mu$ l of each reaction was loaded onto the ALFexpress DNA polyacrylamide sequencing gel. The same labeled oligonucleotide was used in the sequencing reaction of the desired plasmid.

#### **2.12. Transformation of *E. coli* JM109**

*Escherichia coli* JM109 was transformed by the heat shock method (186). Competent cells were prepared by inoculation of 100 ml LB with an overnight culture (1:100) and incubation of the bacterial culture at 37°C. At the OD<sub>600</sub> of 0.35 to 0.40, the bacterial culture was centrifuged for 10 min at 4500 rpm in a SORVALL SS34 rotor. The cells were then resuspended in 4 ml ice-

cooled TSS. The ligation reaction was added to 200  $\mu$ l of competent cells and incubated on ice for 30 min. Alternatively, the competent cells could be stored at  $-70^{\circ}\text{C}$  and thawed before addition of the ligation mixture or desired plasmid. The bacteria-DNA mixture was heat shocked for 60 sec at  $42^{\circ}\text{C}$  followed by further incubation on ice for 2 – 3 min. 2 ml of LB medium was added to the bacteria and the bacterial culture was incubated in a roller drum for 30 min at  $37^{\circ}\text{C}$ . After incubation, the culture was centrifuged for 5 min at 4500 rpm (Megafuge) and the pellet was resuspended in 100  $\mu$ l of the remaining supernatant. The bacterial suspension was plated onto LB agar plates containing the relevant antibiotic. As a positive control, the competent cells were transformed with pUC18 (0.1 ng/ $\mu$ l), whereas competent cells with no DNA were used as a negative control. Finally, the plates were incubated overnight at  $37^{\circ}\text{C}$ .

### **2.13. Electroporation of *E. coli* DH5 $\alpha$**

Electroporation of the *E. coli* DH5 $\alpha$  was carried out if no *E. coli* JM109 transformants were obtained by heat shock transformation protocol. To prepare the electrocompetent *E. coli* DH5 $\alpha$ , 2  $\times$  750 ml TB medium in 2 liter baffled Erlenmeyer flasks were inoculated by cells of an overnight culture corresponding to 40 OD<sub>600</sub>. The culture media were incubated overnight at room temperature until the OD<sub>600</sub> of 0.5 to 1.5 was reached. Next, the cell were placed on ice for 15 min and then centrifuged for 15 min at  $4^{\circ}\text{C}$  at 3000 rpm in a GS-3 rotor (SORVALL). Each pellet was washed with 150 ml sterile H<sub>2</sub>O and subsequently resuspended in 2  $\times$  18 ml (2 tubes) 10% sterile glycerol. The cell suspension was centrifuged in a SS34 rotor (SORVALL) and the supernatant was discarded in a way that 2 ml of the supernatant remained in each tube. The final cell suspension (2  $\times$  2 ml) was divided into 50  $\mu$ l aliquots and stored at  $-70$ .

Prior to electroporation, the competent cells and the ligated DNA or plasmid DNA were mixed in an electroporation cuvette and placed on ice. Then, the cuvette was subjected to an electrical field in a Bio-Rad Gene Pulser II generating 2.5 kV, 25  $\mu$ F and 200  $\Omega$ . Upon electroporation, 1 ml LB medium was added to the electropermeabilized cells and the bacterial culture was incubated for 1 h at  $37^{\circ}\text{C}$  on a roller drum. Finally, the cells were plated on LB agar plates containing the relevant antibiotic (160).

#### **2.14. Transformation of *B. subtilis***

Transformation of the *Bacillus subtilis* strains was performed employing their natural transformation ability (86, 206). A single colony of *B. subtilis* was inoculated into 5 ml broth I and incubated overnight at 37°C. Competent cells were obtained by the inoculation of 1 ml of the overnight culture in 20 ml of broth I. The bacterial culture was incubated at 37°C for approximately 6 h. At the OD<sub>600</sub> of 1 – 2, the bacterial culture was centrifuged for 5 min at 10,000 rpm in a SS34 rotor (SORVALL). The pellet was subsequently resuspended in SMS broth and glycerol was added to a final concentration of 10% to store the cells at -70°C. 8 ml of broth II was inoculated by 1 ml of cell suspension and further incubated for 85 min at 37°C. The desired plasmid was added to 1 ml of the latter bacterial culture and the culture incubated on a roller drum for 30 min at 37°C. The culture was finally centrifuged for 5 min at 4500 rpm (Megafuge) and the resuspended pellet was plated on LB agar plates with relevant antibiotic.

#### **2.15. Electroporation of *B. subtilis***

The electroporation of the *B. subtilis* strains was carried out as described before (252). 5 ml of LB containing 0.5 M glucitol was inoculated by a single colony of *B. subtilis* and incubated overnight at 37°C. Subsequently, the overnight culture was diluted (1:16) by 75 ml of LB<sub>glucitol</sub> and incubated until an OD<sub>600</sub> of 0.85 – 0.95 was obtained. The cells were then centrifuged for 10 min at 4°C at 6500 rpm in a SS34 rotor (SORVALL) and the pellet was washed four times by ice-cooled EP buffer (1×10 ml and 3×5 ml). Finally, the cells were resuspended in 1 ml EP buffer to provide an OD<sub>600</sub> of 50 – 56 OD<sub>600</sub>/ml. Aliquots of 60 µl of the cell suspension were frozen at -70°C. Electroporation was performed using 60 µl of competent cells with approx. 50 ng of plasmid in a cooled electroporation cuvette. The cell-DNA mixture was subjected to an electrical field in a Bio-Rad Gene Pulser II generating 2 kV, 25 µF and 200 Ω. Finally, recovery broth (1 ml) was added to the electropermeabilized cells and the bacterial culture incubated for 3 h at 37°C followed by plating on the LB agar supplemented by an antibiotic.

## **2.16. Protein analysis methods**

### **2.16.1. Cell disruption**

#### **2.16.1.1. Cell disruption by sonication**

Cell density of the *E. coli* culture was determined by a spectrophotometer at 600 nm wavelength (OD<sub>600</sub>) prior to disruption. Unless otherwise specified, 10 OD<sub>600</sub> of the bacterial culture was centrifuged for 5 min at 4500 rpm (Megafuge). After washing the pellet by the desired resuspension buffer, the pellet was dissolved in the same resuspension buffer. The cell suspension was cooled on ice-water and the sonication was performed with 50% “Duty cycle” for 3 × 30 sec with 30 sec pause in between. The soluble as well as the insoluble fractions of the bacterial lysate were separated by centrifugation for 10 – 15 min at 4°C at 14,000 rpm (Biofuge). The supernatant was transferred into a new ice-cooled Eppendorf tube and the pellet dissolved in 1 ml of the resuspension buffer. 12 µl of the soluble and insoluble fractions were used to analyze the expressed protein on SDS-PAGE.

#### **2.16.1.2. Cell disruption by high pressure homogenizer**

Gene expression in *B. subtilis/E. coli* was followed by cell disruption using a high pressure homogenizer (EmulsiFlex-C5) in order to purify the desired protein. First of all, 200 ml of bacterial culture was centrifuged for 5 min at 8,500 rpm in a GSA rotor (SORVALL) and the bacterial pellet was washed once in resuspension buffer. Afterwards, the bacterial pellet was dissolved in 20 ml of resuspension buffer and poured into the ice-cooled chamber of the high pressure homogenizer. The bacterial suspension was then subjected to approx. 10,000 to 15,000 kPa pressure and the cells were completely ruptured after 2 – 3 min. The bacterial lysate was then centrifuged in the Biofuge for 15 – 30 min at 13,000 rpm at 4°C to separate the soluble and insoluble fractions. The supernatant (cleared lysate) was transferred into a new ice-cooled Eppendorf tube, while the pellet was dissolved in 1 ml of the same resuspension buffer. Both supernatant and the pellet fractions were loaded onto a SDS-PAGE to analyze the protein content.

The cleared lysate was then used for the protein purification by affinity chromatography or ion-exchange chromatography.

### 2.16.2. SDS-PAGE

The bacterial proteins were separated by a discontinuous SDS polyacrylamide gel electrophoresis (SDS-PAGE) (120). The discontinuous system is based on a stacking gel (Tris-glycine buffer pH 6.8; 4% acrylamide) which is poured on top of a running gel (Tris-glycine pH buffer 8.8; 8 to 12% acrylamide). In this study, 8% and 12% SDS-PAGE gels were used. The following table shows the amount of ingredients for two gels:

Components	Running gel (ml)		Stacking gel (ml)
	8%	12%	4%
30% acrylamide (37.5 acrylamide : 1 bisacrylamide)	5.3	8	0.67
Tris-HCl (1.5 M, pH 8.8)	5	5	-
Tris-HCl (0.5 M, pH 6.8)	-	-	1.25
SDS solution (10%)	0.2	0.2	0.05
APS solution (10%)	0.2	0.2	0.05
TEMED	0.012	0.008	0.005
H <sub>2</sub> O	9.3	6.6	3

In general, the length of the stacking gel was ¼ of the running gel. To separate the protein on SDS-PAGE, it was mixed with a 5x sample loading buffer followed by an incubation of the sample for 10 min at 98°C. After cooling, the denatured protein was loaded into the wells of gel and a current of 10 – 15 mA (per gel) applied. When the blue color of the sample passed the stacking gel, the current was increased to 20 mA (per gel). After electrophoresis, the gel was incubated for 30 – 60 min in Coomassie stain solution at room temperature. Then, the gel was covered by the destain solution to be destained by gentle agitation overnight.

### 2.16.3. Native PAGE electrophoresis

The native polyacrylamide gel electrophoresis (Native PAGE) was used to separate the intact proteins based on their charge to mass ratio. This method was used to study the binding of the regulatory proteins to their DNA binding sequence. For this purpose, the purified protein was mixed with the DNA (50 – 400 bp length) and the desired shift buffer. After the incubation, the mixture was loaded onto the 6% polyacrylamide gel. Preparation of two gels was performed according to the below table:

Components	Amount (ml)
30% acrylamide (37.5 acrylamide : 1 bisacrylamide)	4
5x TBE	4
APS solution (10%)	0.14
TEMED	0.007
H <sub>2</sub> O	11.9

The samples were directly loaded on to the gel and the gel was run at 15 – 20 mA.

### 2.16.4. Bradford assay

Concentration of the total protein was measured according to the Bradford method (16). The sample was diluted up to 800 µl in ddH<sub>2</sub>O and 200 µl of Bio-Rad reagent, containing Coomassie Brilliant Blue G-250, phosphoric acid, and methanol, was added. The mixture was incubated for at least 15 min at room temperature. Next, the absorbance of the samples was measured at 595 nm in a spectrophotometer. As a blank sample, 800 µl water was mixed with 200 µl of Bio-Rad reagent. The standard curve was depicted by the measurements of various BSA concentrations between 0 – 1.38 mg/ml. Finally, the concentration of the protein was calculated by the following equation:

$$\text{Protein conc. (mg/ml)} = (\text{Sample OD}_{595} - 0.6273)/0.0514$$



#### **2.16.5. Affinity chromatography by Ni-NTA agarose column**

The cleared lysate of *B. subtilis* producing the His<sub>6</sub>-tagged protein was prepared according to section 3.17.1.2. Two different buffers were used as listed in section 3.6 which were based on 50 mM sodium phosphate pH 8 and 50 mM HEPES pH 7.4. Purification of the His<sub>6</sub>-tag protein was performed by the addition of 1 ml of 50% Ni-NTA slurry (Qiagen) to 4 ml cleared lysate obtained from cells of approximately 56.5 OD<sub>600</sub>. PMSF was added to a final concentration of 2 mM and the mixture was gently shaken for 60 min at 4 °C. Next, the lysate-Ni-NTA mixture was loaded into a column with the bottom outlet cap. After dripping the flow-through, the column was washed twice with 4 ml wash buffer (20 mM imidazole). Finally, 500 µl elution buffer containing 250 mM imidazole was added four times to the column. 15 mM EDTA was added to the elution fraction in order to bind to the trace amount of the Ni<sup>2+</sup> washed from the column. The elution fractions were passed through a PD MidiTrap G-25 column to remove the imidazole. The whole procedure was performed at 4°C.

#### **2.16.6. Buffer exchange by PD MidiTrap G-25 column**

The buffer of the eluted His<sub>6</sub>-tagged protein was exchanged for the resuspension buffer with the same components to remove the imidazole. Therefore, PD MidiTrap G-25 columns (GE Healthcare), containing Sephadex<sup>®</sup> G-25 medium, were used to perform the buffer exchange. The 500 µl of the elution fraction was diluted to 1 ml by resuspension buffer. Next, the 1 ml was loaded onto the column. After dripping of excess liquid, 1.5 ml of the resuspension buffer was used to elute the protein. The procedure was performed at 4°C. The final elution fraction was used for the electrophoretic mobility shift studies.

#### **2.16.7. Ion-exchange chromatography (IEC)**

Purification of the native protein (with no tag) was carried out in order to perform the electrophoretic mobility shift assay. In this method, separation is based on the protein electrical charge. There are two different IECs: anion exchange chromatography and cation exchange

chromatography. Depending on the pH of the buffer, proteins retain positive or negative charges. Therefore, cation exchange is used for separation of positively charged proteins by a negative surface, while anion exchange acts reverse. In this study, anion exchange chromatography was attended using Pharmacia Liquid Chromatography Controller LCC-500 Plus, Fraction collector FRAC-200, and a Mono Q<sup>®</sup> HR 5/5 column (Pharmacia). Start buffer (Buffer A) had low ionic strength, whereas high ionic eluent buffer (Buffer B) contained 1M NaCl. The parameters of the chromatography are listed below:

Components	
Column capacity	20 – 50 mg/column
Sample	4 mg
Buffer A <sub>1</sub>	Tris-HCl (20 mM, pH 8)
Buffer B <sub>1</sub>	Tris-HCl (20 mM, pH 8), NaCl (1 M)
Buffer A <sub>2</sub>	HEPES (50 mM, pH 7.4), TCEP (1 mM)
Buffer B <sub>2</sub>	HEPES (50 mM, pH 7.4), NaCl (1 M), TCEP (1 mM)
Flow rate	1 ml/min
Gradient	0 – 50% B in 50 min, 50 – 100% B in 10 min
Detector	UV-M, 280 nm, 0.5 AUFS
Chart speed	0.5 cm/min

### 2.16.8. Electrophoretic mobility shift

The electrophoretic mobility shift assay (EMSA) was performed to identify the specific binding site of the MtlR activator protein on the corresponding promoter sequences. To show this interaction, the *P<sub>mtlA</sub>* promoter region was amplified from plasmid pKAM1 using the specific forward oligonucleotide and a reverse Cy5-labeled oligonucleotide (s5959 or s5960). 200 fmol of the purified PCR product was then used in a 50 µl shift reaction. In addition, 25 µl of 2x shift buffer (or 10 µl of 5x shift buffer) was added to the reaction. Finally, different amounts of the purified protein were added to the reaction (table 2.5). After incubation of the reaction on ice for 15 – 30 min, 10 µl of the reaction was loaded on the 6% native gel. The gel was run at 20 V at room temperature. Ultimately, the gel was scanned by a phosphorimager to detect the Cy5-labelled samples. The DNA-Protein complex migrates slower than the DNA alone.

**Table 2. 5.** The electrophoretic mobility shift reaction.

Components	Volume
Cy5-labeled DNA (50 fmol/ $\mu$ l)	4 $\mu$ l
2x/5x shift buffer	25/10 $\mu$ l
Purified protein	to 21 $\mu$ l
ddH <sub>2</sub> O	to 50 $\mu$ l

### 2.17. $\beta$ -galactosidase assay (Miller's assay)

Activity of  $\beta$ -galactosidase was measured according to Miller's assay (151) in a colorimetric way by using ortho-nitrophenyl- $\beta$ -galactoside (ONPG). The enzymatic reaction was performed by the addition of 100  $\mu$ l of bacterial culture to 900  $\mu$ l of Z buffer. Then, 10  $\mu$ l toluene was added to the suspension and incubated on a roller drum for 30 min at 37 °C. Next, the mixture was subjected to air flow in order to evaporate the residual toluene. Finally, ONPG was added to the mixture and the reaction was stopped by 500  $\mu$ l Na<sub>2</sub>CO<sub>3</sub> (1 M). The OD<sub>420</sub> and OD<sub>550</sub> of the enzymatic reaction were measured and the corresponding Miller units (M.U.) are calculated by the following equation:

$$1 \text{ Miller Unit} = 1000 \times \frac{\text{OD}_{420} - (1.75 \times \text{OD}_{550})}{t \times v \times \text{OD}_{600}}$$

t: reaction time in minute; v: sample volume in milliliters (0.1 in here); OD<sub>420</sub>: absorbance of yellow color which should be less than 0.65; OD<sub>550</sub>: scatter from cell debris, 1.75 is the constant in order to approximate the scatter observed at 420 nm; OD<sub>600</sub>: bacterial culture turbidity at 600 nm wavelength.

### 2.18. Fluorescence measurement

Fluorescence intensity of the recombinant eGFP was conducted by using a Spectrafluor microplate reader (Tecan Group Ltd) according to Wenzel *et al.* (242). At first, the bacterial culture was diluted to obtain an OD<sub>600</sub> of 0.3. Then, 100  $\mu$ l of the diluted cells were transferred into 96-well microplates (Greiner-Bio One GmbH, Frickenhausen, Germany). As a blank sample,

100  $\mu$ l of the same medium (uncultured) was applied. The measurements were performed using excitation filter at 485 nm, emission filter at 535 nm, gain [manual]: 60, 20  $\mu$ s integration time, 3 flashes, top read. For each sample, the measurement was carried out in triplet. Finally, the average of the blank was subtracted from the average of the samples to get the final value.

### **2.19. Bioinformatic**

Nucleotide alignment was performed using GENtle v.1.9.4 (University of Cologne, Germany). Clone manager basic version 8 (Sci-Ed software, USA) was used for cloning simulation and plasmid mapping. The genome sequence of *B. subtilis* 168 was firstly obtained from SubtiList World-Wide Web Server (<http://genolist.pasteur.fr/SubtiList/>) (117, 155-157), while GenoList World-Wide Web Server was used after the update of the genome sequence of *B. subtilis* (<http://genodb.pasteur.fr/cgi-bin/WebObjects/GenoList.woa>) (9).

### 3. Results

#### 3.1. Activity of the *mtlAFD* promoter ( $P_{mtlA}$ )

In order to identify the promoter of the *mtlAFD* operon ( $P_{mtlA}$ ), the region between the stop codon of *ycnL*, the upstream gene, and the start codon of *mtlA* on the *B. subtilis* 168 chromosomal DNA was amplified by oligonucleotides s5526 and s5527 in a PCR. The amplified fragment was then inserted upstream of the *lacZ* reporter gene, into vector pSUN279.2 via *NheI/AflIII* restriction sites and created pKAM1 (Fig. 3.2.A). By this means, the activity of  $P_{mtlA}$  was represented by the  $\beta$ -galactosidase activity. Plasmid pSUN279.2 is a derivative of pMTLBS72, which is a *B. subtilis/E. coli* shuttle vector, containing a pMB1 origin of replication originated from pUC18 for *E. coli* and pBS72 origin of replication for *B. subtilis*. Replicon pBS72, which has been isolated from *B. subtilis*, is a stable theta replicating plasmid with low copy number in *B. subtilis* (6 copies per chromosome). Afterwards, *B. subtilis* 3NA was transformed with pKAM1. Strain 3NA pKAM1 was cultivated in LB and induced by 0.2% mannitol at the OD<sub>600</sub> of 0.4. The growth of the bacteria and the production of  $\beta$ -galactosidase were determined at intervals of 1 h.

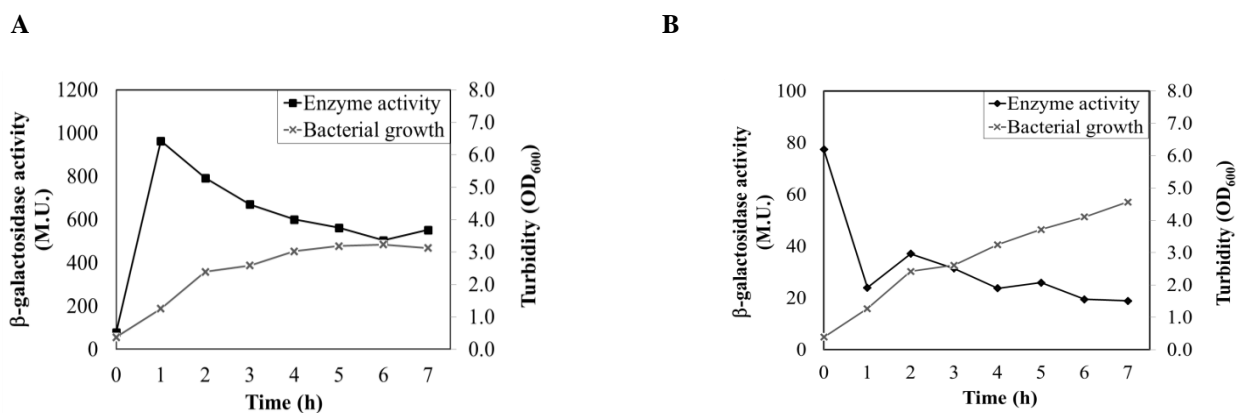


**Fig. 3. 1.** (A)  $\beta$ -galactosidase activity and growth curve of strain 3NA pKAM1 induced with 0.2% mannitol. (B)  $\beta$ -galactosidase activity and growth curve of the uninduced strain 3NA pKAM1 is shown. Mannitol was added at time 0 h.

As shown in Fig. 3.1.A, the maximal  $\beta$ -galactosidase activity was detected already 1 h after the addition of mannitol to the 3NA pKAM1 culture. This was likely due to the consumption of mannitol as a carbon source. In contrast, uninduced 3NA pKAM1 showed a low  $\beta$ -galactosidase activity (Fig. 3.1.B). Thereafter,  $\beta$ -galactosidase activity was determined 1 h after the addition of the sugars. Next, the influence of various sugars on the  $P_{m1A}$  activity in 3NA pKAM1 was investigated (Fig. 3.2.B). Mannitol and glucitol were added as the specific and non-specific inducers, respectively. To see the catabolite repression, glucose was added, while xylose, a non-PTS sugar, was a control.  $\beta$ -galactosidase activity was increased 27-fold by addition of mannitol. Moreover, no influence on  $P_{m1A}$  activity was observed by the addition of xylose alone or together with mannitol. In contrast, addition of the glucose repressed  $P_{m1A}$  by 2.7-fold. Likewise, addition of glucose to the bacterial culture reduced the basal activity in uninduced  $P_{m1A}$ . Finally, glucitol, as a non-specific inducer, induced  $P_{m1A}$  by 10.6-fold. Similar to mannitol-induced  $P_{m1A}$ , addition of glucose lowered the glucitol-induced  $P_{m1A}$  activity.

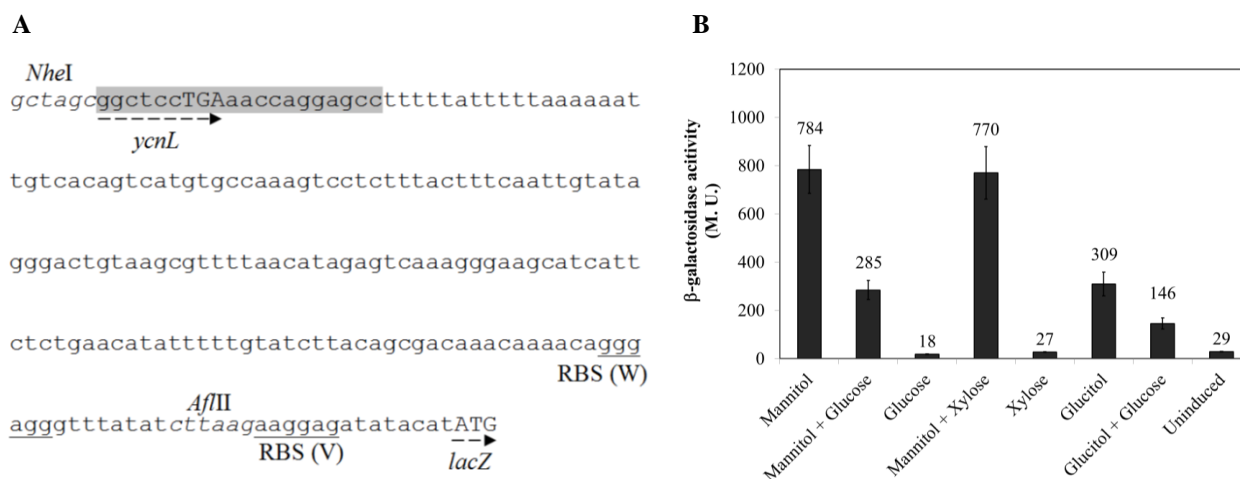


**Fig. 3. 2. (A)** Upstream sequence of *mtlAFD* containing  $P_{m1A}$  fused to *lacZ* on pKAM1. The  $P_{m1A}$  region is located between *NheI* and *AflIII* restriction sites. The region between *AflIII* and *lacZ* start codon is originated from bacteriophage T7 gene 10 (49). The putative transcriptional terminator of *ycnL* is highlighted in gray. Ribosomal binding sites (RBS) of  $P_{m1A}$  (W) and pSUN279.2 (V) are underlined. The stop codon of *ycnL* and start codon of *lacZ* are shown by capital letter. The end of *ycnL* and start codon of *lacZ* genes are shown by dashed arrows **(B)**  $\beta$ -galactosidase activity of 3NA pKAM1 in the presence of different sugars. Strain 3NA pKAM1 was induced at the  $OD_{600}$  of 0.4, and the  $\beta$ -galactosidase was measured after 1 h.

### 3.2. Identification of the $P_{m1A}$ transcription start site

To determine the  $P_{m1A}$  core elements, it was necessary to identify the transcription start site of  $P_{m1A}$ . To do so, primer extension method based on Cy5-labeled DNA was carried out. The Cy5-labeled oligonucleotides, s5959 and s5960, are reverse complementary of *lacZ* starting at 89 bp and 51 bp downstream of the *lacZ* start codon. At first, strain 3NA pKAM1 was cultivated in LB and induced by 0.8% mannitol, whereas uninduced 3NA pKAM1 was used as a control. Afterwards, total RNA of the cells was extracted 1 h after the addition of mannitol. Hybridization of the primer s5959 (or s5960) to mRNA and reverse transcription was carried out to generate the cDNA. In parallel, plasmid pKAM1 was sequenced with the same oligonucleotide in a dideoxy chain termination reaction method. Finally, the generated Cy5-labeled fragment band of cDNA was analysed in comparison to the fragment bands obtained in the sequencing reaction (Fig. 3.3.A). According to the primer extension experiment, the transcription starts at a C residue located 92 bp upstream of the *lacZ* start codon and 72 bp upstream of the *m1A* start codon in the *m1* operon (Fig. 3.3.B).

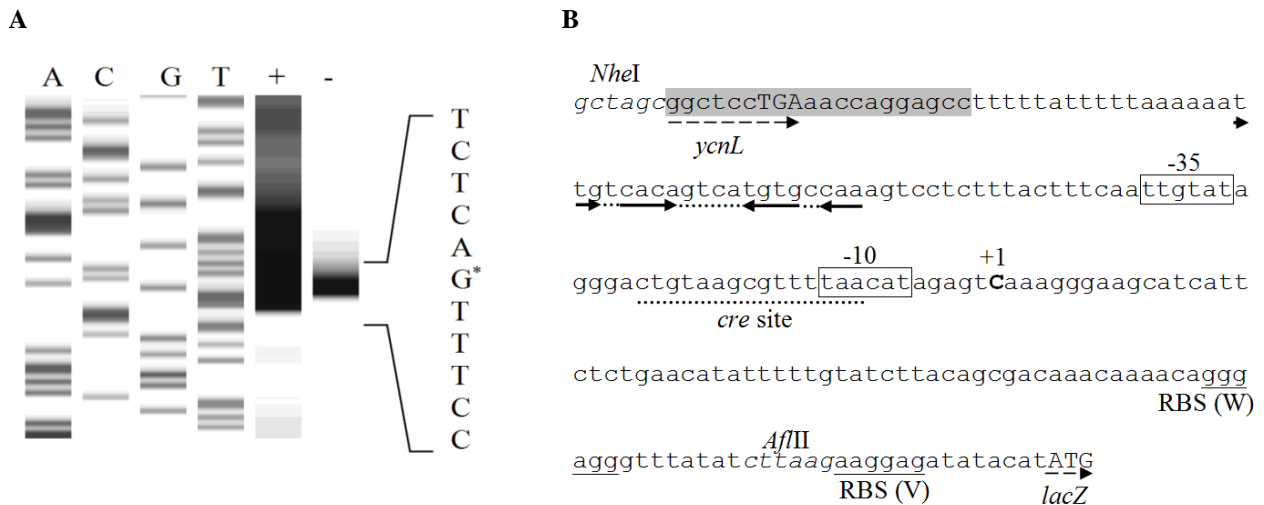


**Fig. 3.3.** (A) Primer extension of  $P_{m1A}$  on plasmid pKAM1. A, C, G, and T show the ddATP, ddCTP, ddGTP, and ddTTP used in the chain termination reaction. Total RNA of induced (+) and uninduced (-) 3NA pKAM1 were used for reverse transcription reaction. The transcription start site is shown by an asterisk. (B) Transcription start site of  $P_{m1A}$  is shown by bold capital letter.  $P_{m1A}$  core elements, namely -10 box and -35 box are enclosed by rectangles. An incomplete inverted repeat sequence is shown by the arrows and dashed lines located upstream of the -35 box. Putative catabolite responsive element (*cre*) is underlined by a dash.

The determination of the transcription start site allowed the identification of the -10 and -35 conserved boxes of  $P_{m1A}$ . The -10 box had the sequence TAACAT (consensus: TATAAT) and -35 box the sequence TTGTAT (consensus: TTGACA), respectively (mismatches to the consensus sequence are underlined). Moreover, a catabolite responsive element (*cre*) which had an overlap with the -10 box was found. The sequence of the *cre* box (CTGTAAAGCGTTTTAA) showed two mismatches (underlined) compared to the *cre* consensus sequence (WTGNAARCGNWWCA). Finally, an incomplete inverted repeat was detected upstream of the -35 box (TTGTCACAGTCATGTGCCAA) which could be the activator binding site (Fig. 3.3.B).

### 3.3. Shortening of the $P_{m1A}$ sequence

Identification of the transcription start site of  $P_{m1A}$  revealed the  $P_{m1A}$  core elements as well as the probable regulatory sequences. However, the complete length of the amplified  $P_{m1A}$  sequence on pKAM1 was 181 bp. It contained the terminator and stop codon of *ycnL* as well as the ribosomal binding site of  $P_{m1A}$  (Fig. 3.3.B). Hence, the 181 bp sequence was shortened in order to identify the essential parts of the  $P_{m1A}$  sequence (Fig. 3.4.A).

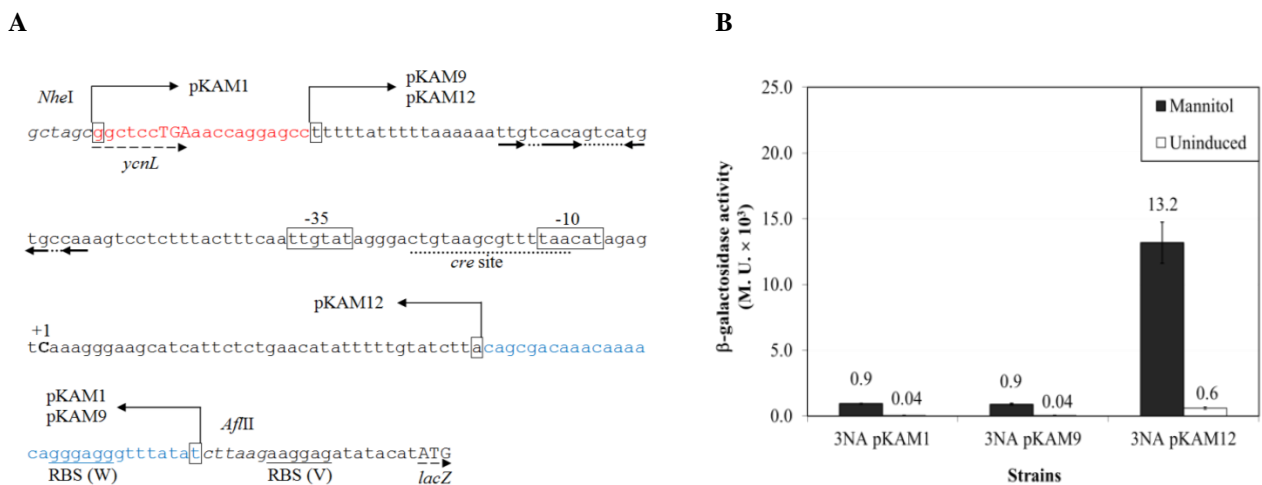


**Fig. 3.4.** (A) The sequence of  $P_{m1A}$  and the constructs thereof. The boundaries of the constructs are indicated by an arrow and a rectangle. The red sequence of pKAM1 was deleted to create pKAM9. The blue sequence in pKAM9 was deleted to construct pKAM12. (B)  $\beta$ -galactosidase activity of strain 3NA harboring pKAM1 and shortened  $P_{m1A}$  constructs on pKAM9 and pKAM12.



In the first step, 20 bp of the 5'-end of the *P<sub>mtlA</sub>* sequence including the terminator of *ycnL* was removed. The PCR was performed using oligonucleotides s6209/s5527 and *B. subtilis* 168 chromosomal DNA as the template. The PCR fragment was then digested by *NheI/AflIII* and inserted into pSUN279.2. Plasmid pKAM9 was created by the insertion of shortened *P<sub>mtlA</sub>* (Figure 3.4.A). After induction of strain 3NA pKAM9, it was observed that inducibility and maximal activity of *P<sub>mtlA</sub>* remained intact (Fig. 3.4.B). Next, the wild type ribosomal binding site, RBS (W), was removed from pKAM9 through a PCR using oligonucleotides s6209 and s6213. Digestion of the PCR product and insertion into pSUN279.2 resulted in pKAM12. Surprisingly, mannitol-induced strain 3NA pKAM12 showed a considerably higher  $\beta$ -galactosidase activity than strain 3NA pKAM9 (Fig. 3.4.B). Plasmid pKAM12 was used for further investigations.

### **3.4. *P<sub>mtlA</sub>* activity in minimal and rich medium**

Prior to further investigation of *P<sub>mtlA</sub>*, the  $\beta$ -galactosidase activity of 3NA pKAM12 in minimal and rich media were compared. Spizizen's minimal salt (SMS) and LB were chosen. SMS was supplemented by 1% glycerol as the main carbon source. Glucose (0.2%) and mannitol (0.2%) in combination or alone were added to the bacterial culture at the OD<sub>600</sub> of 0.4. The samples were collected 1 h after the addition of sugars to measure the  $\beta$ -galactosidase activity. The results indicated that the *P<sub>mtlA</sub>* activity was less inducible in LB compared to SMS caused by a higher basal activity, although the *P<sub>mtlA</sub>* activity was almost doubled in LB. Regardless of the inducibility and maximal activity, glucose repression ratio (mannitol/mannitol + glucose) was almost the same in both media (Fig. 3.5). Thus, all of the further measurements were performed in LB medium due to the higher activity of *P<sub>mtlA</sub>* as well as shorter lag phase of the growth of 3NA pKAM12.

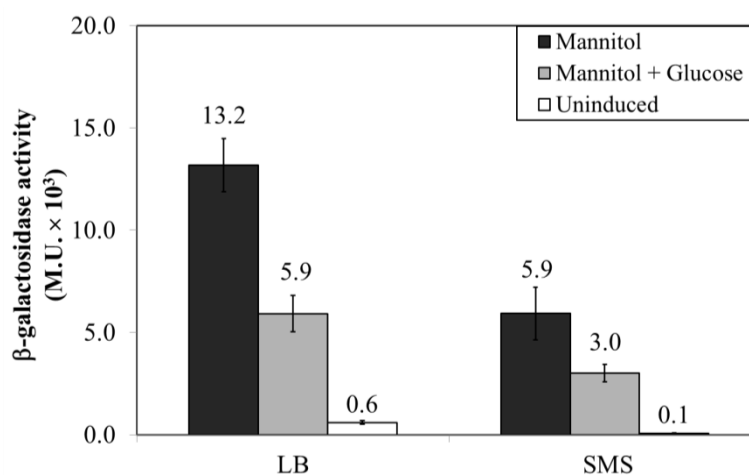


**Fig. 3. 5.**  $\beta$ -galactosidase activity of strain 3NA pKAM12 in LB compared to Spizizen's minimal salt (SMS) with or without 0.2% mannitol, as well as with 0.2% mannitol + 0.2% glucose.

### 3.5. Activity of the *mtlR* promoter ( $P_{mtlR}$ )

Regulation of the *mtlAFD* operon is controlled by an activator (MtlR) located 14.4 kbp downstream of the operon. Next, it was tested whether  $P_{mtlR}$  was regulated in the same way as  $P_{mtlA}$ . To investigate the regulation of the promoter of *mtlR* ( $P_{mtlR}$ ) the upstream region of *mtlR* between *ycaN* stop codon and the *mtlR* start codon was amplified from *B. subtilis* 168 genome by oligonucleotides s5799 and s5800 (Fig. 3.6.A). Similar to  $P_{mtlA}$ , the promoter fragment was inserted into pSUN279.2 via *NheI/AflIII* restriction sites creating pKAM3. Then, *B. subtilis* 3NA was transformed and the selected transformant, 3NA pKAM3, induced by different sugars. As shown in Fig. 3.6.B,  $P_{mtlR}$  was highly inducible by mannitol and glucitol similar to  $P_{mtlA}$ . The  $\beta$ -galactosidase activity of 3NA pKAM3, however, was drastically lower than of 3NA pKAM1 (172 Miller units compared to about 1,000 Miller units). Besides, glucose lowered the  $P_{mtlR}$  activity in the presence of either mannitol or glucitol. Altogether, the results indicated that  $P_{mtlR}$  is an autoinducible promoter with a 10-fold lower activity than  $P_{mtlA}$ .

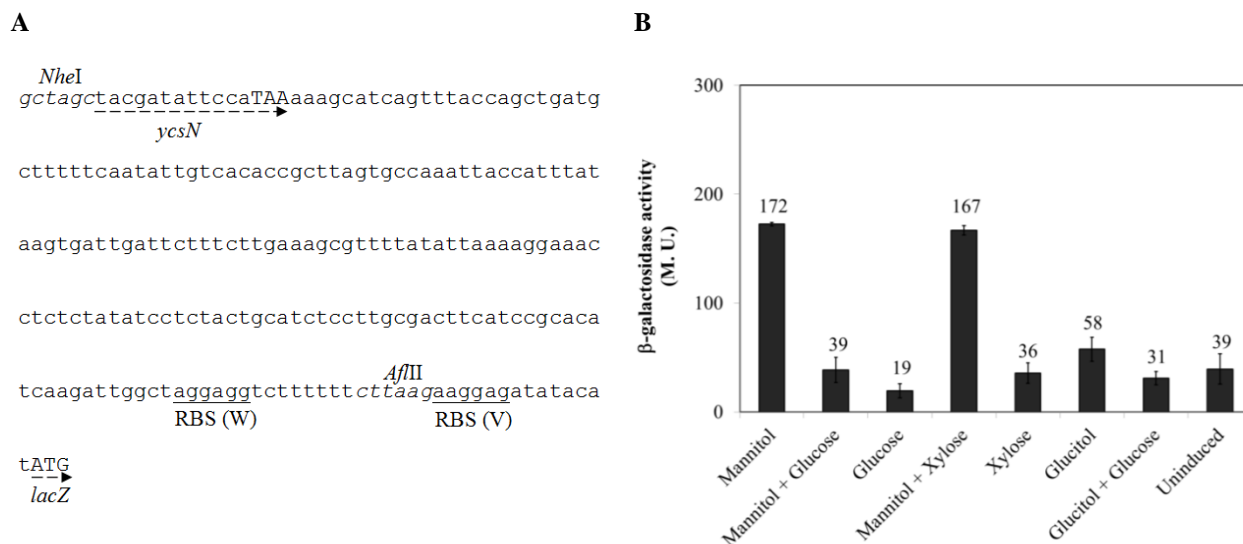


**Fig. 3. 6. (A)** The upstream region of *mtlR* is depicted between *NheI* and *AflIII* restriction sites. The stop codon of *ycsN* and start codon of *lacZ* are shown by capital letter. The end of *ycsN* is underlined by a dashed arrow. Ribosomal binding sites (RBS) of *P<sub>mtlR</sub>* (W) and pSUN79.2 (V) are underlined. **(B)** β-galactosidase activity of 3NA pKAM3 in the presence of mannitol, glucose, glucitol and xylose was monitored. The 3NA pKAM3 strain was induced at the OD<sub>600</sub> of 0.4 and the β-galactosidase activity was measured after 1 h.

### 3.6. Identification of the *P<sub>mtlR</sub>* transcription start site

The transcription start site of *P<sub>mtlR</sub>* was identified by primer extension method. A 3NA strain with plasmid pKAM3 harboring the intact promoter region of *P<sub>mtlR</sub>* was used as the source of mRNA. The total RNA of induced and uninduced 3NA pKAM3 were extracted and used for the reverse transcription with Cy5-labeled primer s5959 (or s5960). The obtained Cy5-labeled cDNA fragment was compared to the profile of the DNA sequencing reaction obtained from pKAM3 with the same primer. In this way, a single G residue was identified as the transcription start site of *P<sub>mtlR</sub>* (Fig. 3.7.A). The transcription start site was located 77 bp upstream of the *mtlR* start codon. Also, TATATT and TTGATT boxes were determined as Pribnow box and -35 box, respectively (Fig. 3.7.B). Additionally, a *cre* site was located at the spacer sequence overlapping the -10 box. The *cre* sequence of *P<sub>mtlR</sub>* (TTGAAAGCGTTTTAT) showed a 2 bp mismatch (underlined) with the consensus *cre* sequence (WTGNAARCGNWWCA). Ultimately, an incomplete inverted repeat upstream of the -35 box was found with similarity to the corresponding sequence detected in *P<sub>mtlA</sub>*.

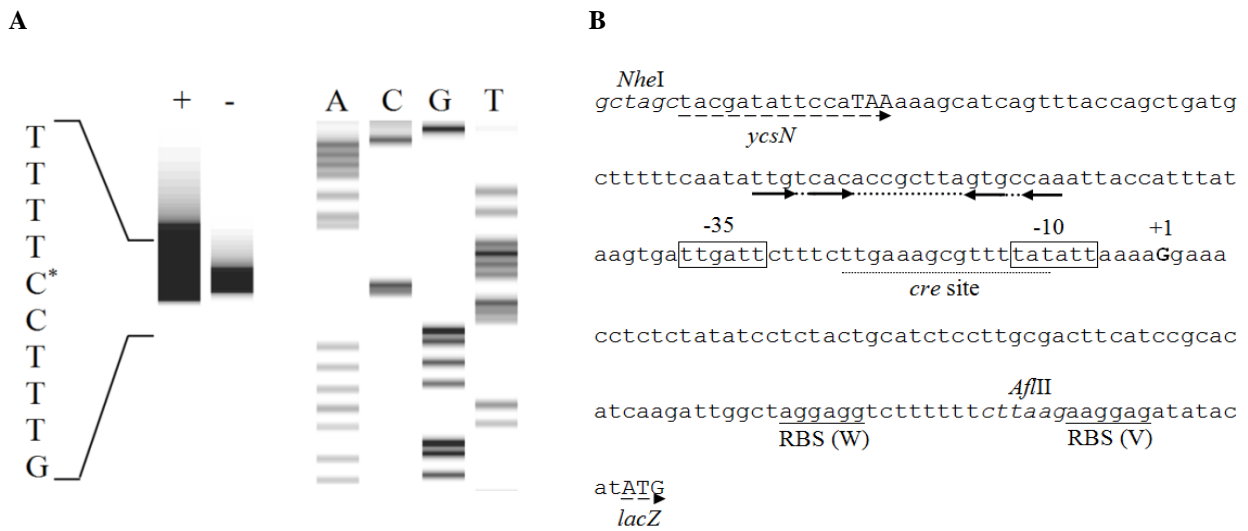


**Fig. 3. 7. (A)** Primer extension of  $P_{mtlR}$  on plasmid pKAM3. A, C, G, and T represent the ddATP, ddCTP, ddGTP, and ddTTP used for the chain termination reactions of the promoter sequencing. The cDNA band from the mRNA isolated from the induced and uninduced cultures are respectively shown in + and – lanes. **(B)** The sequence of  $P_{mtlR}$  on pKAM3 is shown. Transcription start site is indicated by bold capital letter. The -35 and -10 boxes are enclosed by rectangles. The *cre* site is underlined by a dash and the incomplete inverted repeat sequence is depicted by dashes and arrows. The end of *ycsN* and start of *lacZ* are depicted by dashed arrows.

### 3.7. Shortening of the 5' untranslated region of $P_{mtlR}$ -*lacZ* mRNA

The shortening of the  $P_{mtlA}$  3'-end resulted in a higher  $P_{mtlA}$  activity (section 3.3). Therefore, the  $P_{mtlR}$  sequence was also shortened at its 3'-end. In the first step, the Shine-Dalgarno sequence of  $P_{mtlR}$  was removed in order to test whether the presence of two ribosomal binding sites decreased the  $\beta$ -galactosidase activity. The 3'-end shortened  $P_{mtlR}$  was amplified by a PCR using oligonucleotides s5799/s6392 and *B. subtilis* 168 chromosomal DNA. Plasmid pKAM18 was constructed by the insertion of the resulting fragment into pSUN279.2 via *NheI*/*AflIII* (Fig. 3.8.A). Induction of strain 3NA pKAM18 indicated that the  $\beta$ -galactosidase activity in 3NA pKAM18 (having a single ribosomal binding site on  $P_{mtlA}$ -*lacZ* sequence) was half of 3NA pKAM3 (having two ribosomal binding site in  $P_{mtlR}$ -*lacZ* fusion) (Fig. 3.8.B). Previously, the shortening of the mRNA 5' UTR of  $P_{mtlA}$ -*lacZ* to 61 bp improved the transcription/translation. Hence, the length of the mRNA leader region of  $P_{mtlR}$ -*lacZ*, *i.e.* the region between the transcription start site and start codon of *lacZ*, was shortened to 51 and 61 bp. Constructs pKAM86 with 61 bp and pKAM87 with 51 bp 5' UTR were made in a PCR from *B. subtilis* 168

genome using s5799/s7066 and s5799/s7067 oligonucleotides, respectively. Unlike  $P_{mIa}$ , induction of 3NA pKAM86 and 3NA pKAM87 resulted in a low activity compared to 3NA pKAM3 and the loss of induction. Taken together, shortening of the mRNA leader region of  $P_{mIa}$ - $lacZ$  decreased the  $\beta$ -galactosidase activity. Nevertheless, pKAM18 having a single ribosomal binding site was used for further studies.

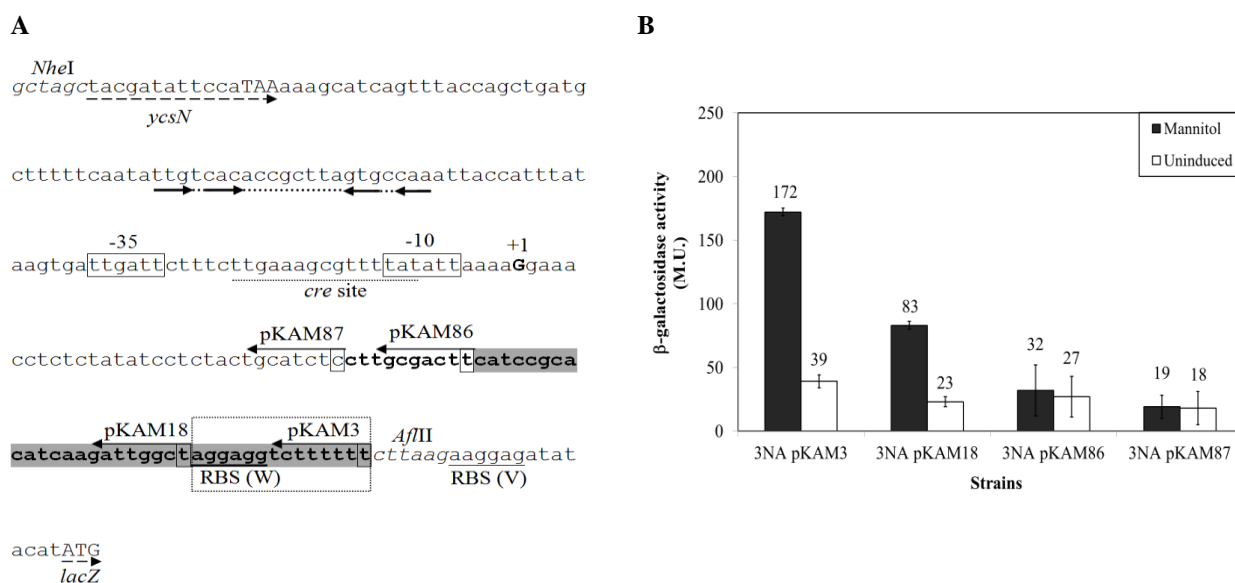


**Fig. 3. 8.** (A) The sequence of  $P_{mIa}$  on pKAM3 and the truncated versions thereof. The first base pair of each shortened construct is enclosed by a rectangle and an arrow. The dashed rectangle shows the region deleted in pKAM18. The gray highlighted nucleotides are deleted in pKAM86. The deleted nucleotides in pKAM87 are shown by bold letters. (B)  $\beta$ -galactosidase activity of strain 3NA harboring pKAM3, pKAM18, pKAM86, and pKAM87 in the presence and absence of 0.2% mannitol for 1 h is shown.

### 3.8. Comparison of $P_{mIa}$ and $P_{mIa}$

To compare  $P_{mIa}$  and  $P_{mIa}$  without having the influence of different 5' UTR,  $P_{mIa}$  was fused exactly at position +1 to the 5' UTR of  $mIa$  on pKAM12. Oligonucleotides s5799/s7149 and s7150/s6213 were used to amplify the primary fragments, *i.e.*  $P_{mIa}$  and UTR $_{mIa}$ , by PCR from *B. subtilis* genomic DNA. Fusion PCR was performed using the primary PCR products and oligonucleotides s5799/s6213. The final fragment was then inserted into pSUN279.1 via *NheI* and *AflIII* restriction sites (Fig. 3.9.A).

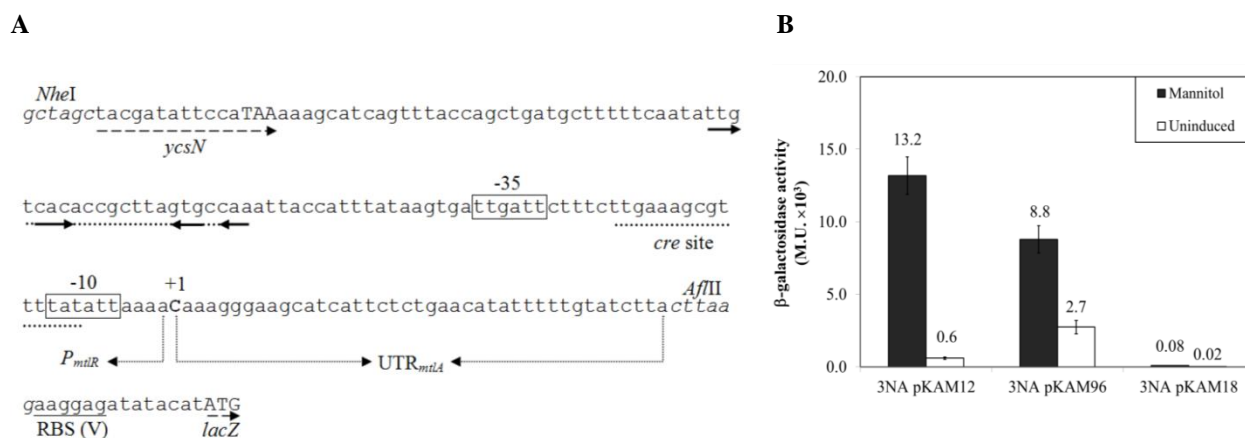


**Fig. 3. 9.** (A) The sequence of the  $P_{mtlR}$ - $UTR_{mtlA}$  fusion on pKAM96 is shown. (B)  $\beta$ -galactosidase activity of 3NA pKAM96 in the presence and absence of 0.2% mannitol compared to 3NA pKAM12 ( $P_{mtlA}$ ) and 3NA pKAM18 ( $P_{mtlR}$ ).

Transformation of *E. coli* JM109 by the ligation reaction showed no transformants. Therefore, *B. subtilis* 3NA was directly transformed with the ligation reaction and resulted in pKAM96. The  $\beta$ -galactosidase activity of induced and uninduced 3NA pKAM96 was compared to 3NA pKAM12 as well as to 3NA pKAM18 (Fig. 3.9.B). In comparison with 3NA pKAM18, changing the 5' UTR of *mtlR* by its counterpart from *mtlA* dramatically boosted the activity of  $P_{mtlR}$ ; however,  $P_{mtlR}$  still showed a weaker activity than  $P_{mtlA}$  (Fig. 3.9.B). Additionally, the basal activity of the  $P_{mtlR}$ - $UTR_{mtlA}$  was 4.5-fold higher than  $P_{mtlA}$ - $UTR_{mtlA}$ . This result indicated that the  $P_{mtlA}$  is stronger than  $P_{mtlR}$  as well as more tightly regulated.

### 3.9. HPr(H15~P)-dependent activity of $P_{mtlA}$

Principally, PRD-containing activators and antiterminators are phosphorylated by HPr(H15~P) in the presence of their sugar inducer. Supposing that MtlR is phosphorylated by HPr, the activity of  $P_{mtlA}$  was studied in *B. subtilis* strain TQ432, where the phosphoryl carrier histidine 15 of HPr was replaced with an alanine (mutant *ptsH*-H15A). Transformation of strain TQ432 by pKAM12 was performed in the minimal medium harboring glucitol instead of glucose as carbon source. In fact, TQ432 cannot grow on any PTS sugar due to the mutation of HPr-H15. Very low  $\beta$ -galactosidase activity was measured in the mannitol-induced and uninduced cultures.

Induction of  $P_{mtlA}$  in TQ432 pKAM12 by mannitol in LB showed that the  $P_{mtlA}$  activity was nearly abolished (Fig. 3.10).

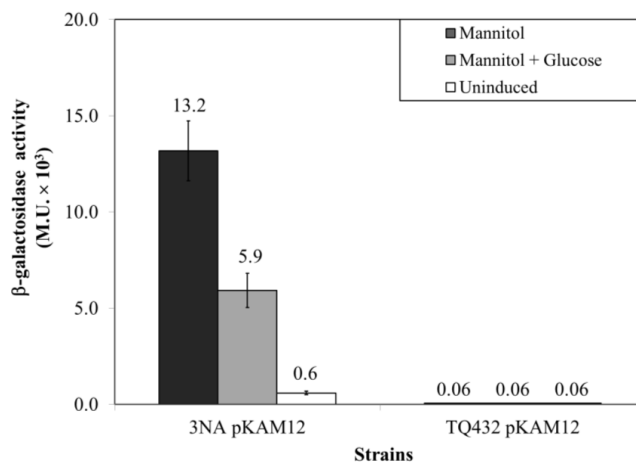


**Fig. 3. 10.**  $\beta$ -galactosidase activity of strains 3NA (wild type) and TQ432 (*ptsH*-H15A) harboring pKAM12 is shown. The sugars were added at  $OD_{600}$  of 0.4 and the  $\beta$ -galactosidase activity was measured after 1 h.

Besides, the presence of glucose had no effect on the  $P_{mtlA}$  activity in the mutant. This indicated that HPr-H15 plays an essential role in the activation of MtlR demonstrating that MtlR is a PRD-containing activator, which is likely regulated by other mannitol PTS components. Therefore the effect of other *mtl* components on  $P_{mtlA}$  activity was investigated.

### 3.10. Deletion of the mannitol utilization genes in *B. subtilis*

#### 3.10.1. Deletion of the activator encoding gene (*mtlR*)

The regulatory effect of MtlR on  $P_{mtlA}$  activity was investigated by the deletion of *mtlR* within the chromosome of *B. subtilis* 3NA. Plasmid pSUN308.3 (see appendices) was used for construction of integration vectors in this study. Three antibiotic resistance genes reside on this plasmid including erythromycin located inside the deletion cassette for *B. subtilis*, spectinomycin for selection of single cross-over mutants of *B. subtilis*, and finally ampicillin for selection of the plasmid inside the *E. coli*. Amplification of the downstream flanking gene, *ydaB*, was performed by oligonucleotides s5860 and s5812 in a PCR from *B. subtilis* 168 genomic DNA and the PCR

product was inserted into plasmid pSUN308.3 via *SpeI/StuI* restriction sites (pKAM05). Then, upstream gene of *mtlR*, namely *ycsN*, was amplified in a PCR from *B. subtilis* 168 chromosomal DNA by oligonucleotides s5809 and s5810. The PCR fragment was digested by *EcoRV* and *BglIII* and inserted into plasmid pKAM05. The resulting plasmid (pKAM4) harboring the cassette '*ycsN-ermC-ydaB*' was linearized by *PacI* and used for integration into the genome of *B. subtilis* 3NA. The transformants were selected on LB medium supplemented by erythromycin. In order to confirm the double cross-over, the transformants were streaked on LB<sub>Spc</sub> plates. Also, the deletion of *mtlR* was confirmed by PCR using oligonucleotides s5809/s5812 and the chromosomal DNA of the  $\Delta$ *mtlR* mutant (Fig. 3.11.A). The  $\Delta$ *mtlR* mutant (KM15) was unable to grow in mannitol minimal medium (Fig. 3.19). Subsequently, strain KM15 was transformed with pKAM12 and pKAM18 in order to study the effect of the MtlR on the  $P_{mtlA}$  and  $P_{mtlR}$  promoters. Deletion of the *mtlR* reduced the  $\beta$ -galactosidase activity of strain KM15 pKAM12 to 92 Miller units in the presence of mannitol. The same activity was observed in the absence of mannitol. This means that KM15 pKAM12 was no longer inducible by mannitol (Fig. 3.11.B). However, the presence of glucose still repressed the  $P_{mtlA}$  activity. Furthermore,  $\beta$ -galactosidase activity of KM15 pKAM18 was also declined. Besides,  $P_{mtlR}$  was no longer inducible in the  $\Delta$ *mtlR* mutant (Fig. 3.12). This shows that MtlR regulates its own promoter. Similar to  $P_{mtlA}$ ,  $P_{mtlR}$  activity was also repressed by glucose.

### 3.10.2. Deletion of the mannitol-specific enzyme II encoding genes (*mtlAF*)

The effect of the mannitol-specific enzyme II, *i.e.* EIICB<sup>Mtl</sup> and EIIA<sup>Mtl</sup>, on the  $P_{mtlA}$  and  $P_{mtlR}$  activities was studied by deletion of the *mtlAF* genes. The deletion cassette was constructed by the fusion of  $P_{mtlA}$  to *mtlD*. PCRs from the genome of *B. subtilis* 168 were performed using oligonucleotides s5918/s5919 and s5920/s5921. Final fusion PCR was accomplished by using oligonucleotides s5918/s5921 and the primary PCRs products. The ' $P_{mtlA}$ -*mtlD*' fragment was subsequently digested by *BglIII/EcoRV* and inserted into pSUN308.3 and created pKAM08. The upstream gene of *mtlAFD* operon, *ycnL*, was amplified in a PCR from *B. subtilis* 168 chromosome using oligonucleotides s6067 and s6079. The amplified *ycnL* was then digested by *StuI/SpeI* and inserted into pKAM08 to construct plasmid pKAM5.



## Results

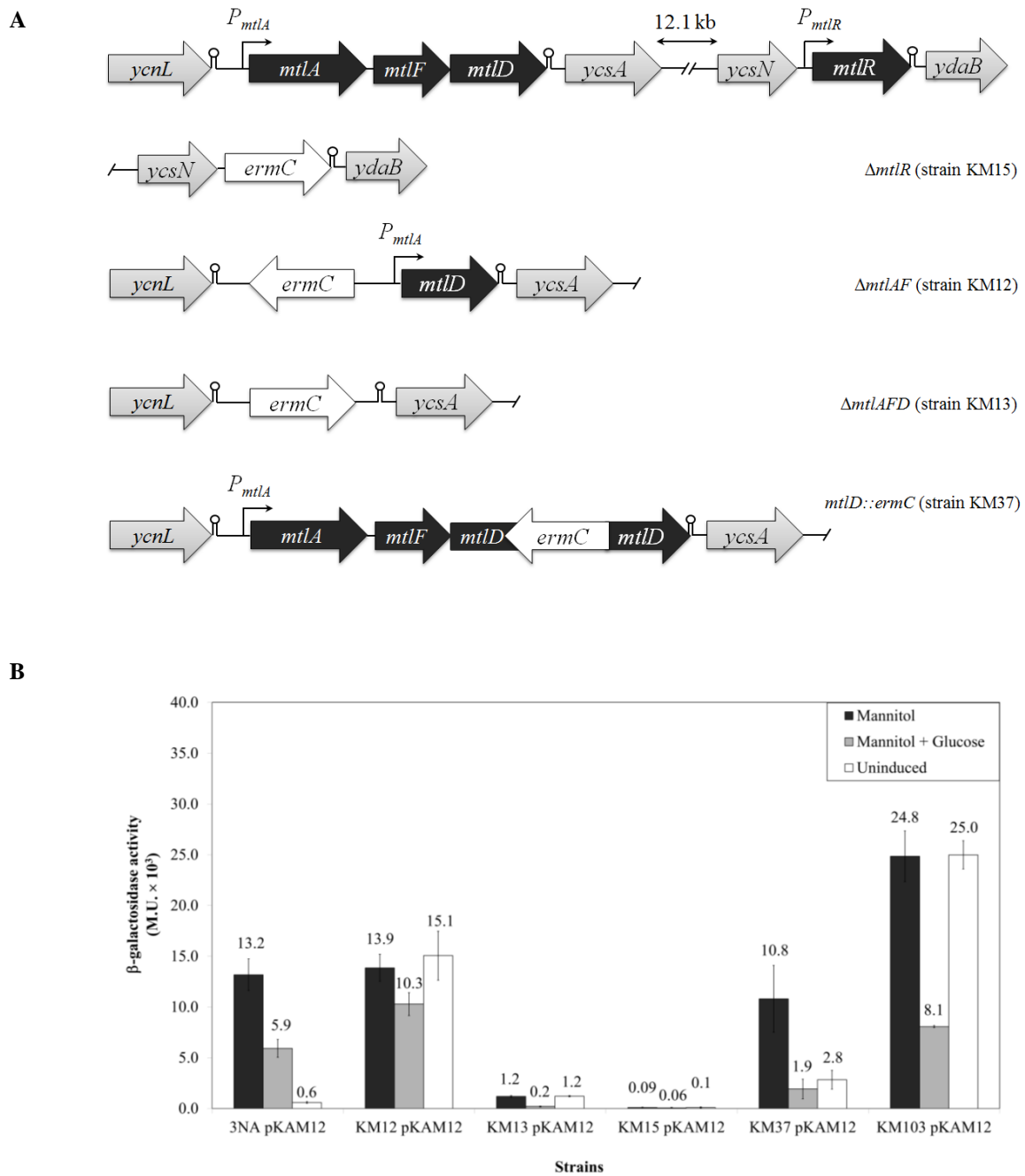


**Fig. 3. 11.** (A) The mannitol utilization genes and the mutations obtained by plasmids pKAM4 ( $\Delta mtlR$ ), pKAM5 ( $\Delta mtlAF$ ), pKAM6 ( $\Delta mtlAFD$ ), and pKAM14 ( $mtlD::ermC$ ). (B)  $\beta$ -galactosidase activity of the strains KM12 ( $\Delta mtlAF$ ), KM13 ( $\Delta mtlAFD$ ), KM15 ( $\Delta mtlR$ ), and KM37 ( $mtlD::ermC$ ) harboring pKAM12 is shown.

The strain 3NA was transformed with the deletion cassette '*ycnL-ermC-P<sub>mtlA</sub>-mtlD*' (pKAM5) and the transformants were selected on LB<sub>erm</sub> (Strain KM12; Fig. 3.11.A). Confirmation of the deletion of *mtlAF* was performed by PCR using oligonucleotides s6067/s5921 and the chromosomal DNA of  $\Delta$ *mtlAF* mutant. The strain was not able to grow on spectinomycin as expected for a double crossover event. Transformation of the strain KM12 ( $\Delta$ *mtlAF*::*ermC*) by pKAM12 and pKAM18 was carried out. The transformants were then used for induction studies and their  $\beta$ -galactosidase activities were measured (Fig. 3.11.B and Fig. 3.12). Both of the promoters, *P<sub>mtlA</sub>* and *P<sub>mtlR</sub>*, were constitutively active in strain KM12 showing approximately 13,900 and 243 Miller units  $\beta$ -galactosidase activity, respectively. In other words, the presence of mannitol as the inducer had no influence on the *P<sub>mtlA</sub>* or *P<sub>mtlR</sub>* activity. In contrast, the presence of glucose repressed the *P<sub>mtlA</sub>* and *P<sub>mtlR</sub>* activities as shown in Fig. 3.11.B and Fig. 3.12. This shows that the *P<sub>mtlA</sub>* and *P<sub>mtlR</sub>* activities were inhibited by the mannitol-specific EII if mannitol was absent in the medium. By deletion of the transporter, this inhibitory effect was removed and the *P<sub>mtlA</sub>* and *P<sub>mtlR</sub>* were constitutively active.

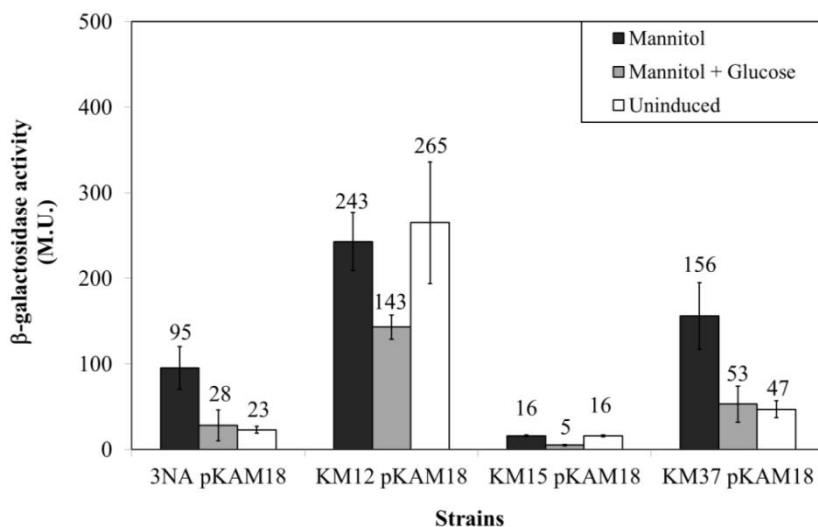


**Fig. 3. 12.** *P<sub>mtlR</sub>* activity in mannitol utilization deficient mutants.  $\beta$ -galactosidase activity of *B. subtilis* 3NA (wild type) and mannitol utilization deficient mutants, KM12 ( $\Delta$ *mtlAF*), KM15 ( $\Delta$ *mtlR*), and KM37 (*mtlD*::*ermC*), harboring pKAM18 (*P<sub>mtlR</sub>*) is represented.

### 3.10.3. Deletion of *mtlF* by a new markerless deletion system

In mannitol PTS, the separated cytoplasmic domain of the enzyme II complex, namely EIIA<sup>Mtl</sup>, transfers the phosphate from HPr(H15~P) to the membrane anchored domains EIICB<sup>Mtl</sup>. Therefore, the *mtlF* gene (encoding the phosphocarrier protein EIIA<sup>Mtl</sup>) was deleted within the chromosome of *B. subtilis* 3NA by a new markerless deletion system based on the site-specific recombination. A specific recombination sequence was designed according to a *mrpS* site (238) and a *loxP* site (95). The *mrpS* site is recognized by a tyrosine recombinase (MrpA) found in *Streptomyces coelicolor* A3(2), while *loxP* is recognized by the bacteriophage P1 recombinase Cre. The *mrpS* site contains a 30 bp inverted repeat sequence separated by a 6 bp spacer. Likewise, *loxP* contains a 26 bp inverted repeat sequence separated by a 8 bp spacer. In a recently designed sequence, half of the inverted repeat sequence of *mrpS* was replaced with the *loxP* in a way that the new sequence, denoted *mroxP*, was recognized by the Cre recombinase (Warth *et al.*, unpublished). The recombination between the two *mroxP* sequences by Cre recombinase resulted in the deletion of the desired gene located between the *mroxP* sites. Interestingly, a new recombination sequence was constructed by the recombined sequence which can be recognized by MrpA (Warth *et al.*, unpublished; Fig. 3.13). This deletion system was employed for a markerless deletion in *B. subtilis*. The deletion vector was constructed using pIC20HE as the parental vector (1). Two long oligonucleotides s6465/s6466 harboring the *mroxP* were used to amplify the chloramphenicol acetyl transferase of plasmid pMW363.1 originated from *Streptococcus pneumoniae*. Plasmid pMW363.1 is a derivative of pSUN308.3 harboring chloramphenicol resistance gene. The resulting fragment, *mroxP-cat-mroxP* was then inserted into pIC20HE via *XhoI* and *EcoRI* restriction sites (plasmid pKAM19; Fig. 3.14.A). Afterwards, deletion of the *mtlF* was performed using the 5'-truncated *mtlA* as the upstream flanking and the *mtlD* as the downstream flanking sequence of *cat* gene. Oligonucleotides s6759 and s6760 were used to amplify the truncated *mtlA* from *B. subtilis* 168 chromosome in a PCR. The PCR fragment was then inserted via *BamHI/XhoI* restriction sites into pKAM19 to create pKAM020. In another PCR, the truncated *mtlD* sequence was amplified by PCR from genomic DNA of *B. subtilis* 168 using oligonucleotides s6761/s6762. The amplified *mtlD* was inserted into the pKAM020 via *NheI/SacI* and constructed pKAM47.

## Results



**Fig. 3. 13.** The *mrpS* recombination site recognized by MrpA site-specific recombinase of *Streptomyces coelicolor* A3(2) and *loxP* recognized by Cre site-specific recombinase of bacteriophage P1 are depicted. The constructed sequence *mroxP* is a combination of *mrpS* and *loxP* sequences which is recognized by Cre recombinase. After recombination, the final emerged sequence is only recognized by MrpA.

To integrate plasmid pKAM47 into the chromosome of *B. subtilis* 3NA, pKAM47 DNA was digested by *ScaI* followed by the natural transformation of the strain 3NA. The transformants were then selected on LB<sub>cm</sub> and the integration of the DNA fragment was controlled by PCR. Next, the  $\Delta mtlF::mroxP$ -*cat*-*mroxP* strain was transformed with an unstable plasmid, namely pJOE6732.1 (see appendices). Plasmid pJOE6732.1, a derivative of pAM $\beta$ 1 plasmid, contains the *P*<sub>xyI</sub>-*cre*<sub>P1</sub> expressing the Cre recombinase. After selection of the transformants on LB<sub>spc</sub>, one of the transformants was cultivated at 37°C for 24 h. During the incubation, the Cre recombinase was expressed and recombined the *mroxP* sequences and resulted in the deletion of the *cat* gene from the  $\Delta mtlF::mroxP$ -*cat*-*mroxP* cassette. In addition, the bacteria lost pJOE6732.1 due to its instability. After 24 h incubation, dilutions of the bacterial culture were plated on LB agar and the

transformants were checked for the loss of chloramphenicol and spectinomycin resistance. The *mtlF* deficient strain, called KM103, was unable to grow on mannitol minimal medium. Also, strain KM103 was sensitive to chloramphenicol and spectinomycin (Fig. 3.14.B).

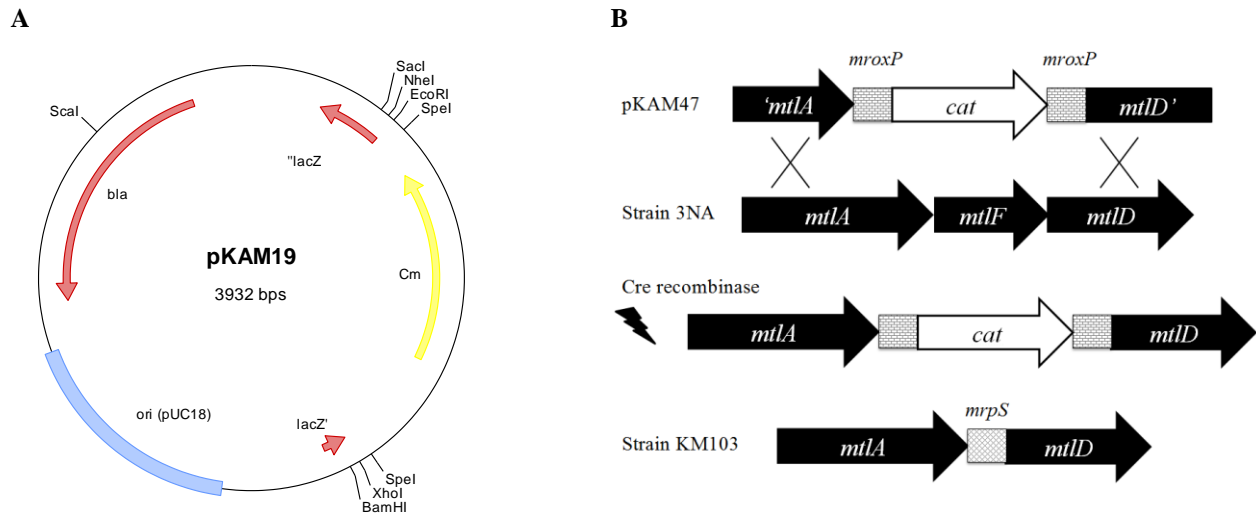


**Fig. 3. 14. (A)** Plasmid map of the plasmid pKAM19 used as the backbone for the markerless deletion of *mtlF*. **(B)** Deletion of the *mtlF* using *mroxP* recombination sites. In the first step, plasmid pKAM47 harboring the deletion cassette was integrated into the chromosome of *B. subtilis* 3NA. Afterwards, the expression of the Cre recombinase led to the site-specific recombination at the *mroxP* sites. The markerless  $\Delta$ *mtlF* strain KM103 was constructed by the deletion of the *cat* gene from the chromosome.

Finally,  $\beta$ -galactosidase activity of KM103 pKAM12 was measured in the presence of mannitol and glucose (Fig. 3.11.B.). Similar to KM12 pKAM12, the  $P_{mtlA}$  activity in KM103 pKAM12 was constitutive, but the strain grew slower than the wild type. Unlike the KM12 pKAM12,  $\beta$ -galactosidase activity surprisingly boosted up to 24,800 Miller units in KM103 pKAM12. This was almost double of the activity of the induced  $P_{mtlA}$  in the wild type strain. As expected, the addition of glucose reduced the  $\beta$ -galactosidase activity to 8,100 Miller units. Altogether, deletion of the  $EIIA^{Mtl}$  removed the  $P_{mtlA}$  inhibition in the absence of mannitol; however, the reason for the high activity of the  $P_{mtlA}$  is still unknown.

### 3.10.4. Disruption of the mannitol 1-phosphate dehydrogenase encoding gene (*mtlD*)

The effect of the mannitol 1-phosphate dehydrogenase on the  $P_{mtlA}$  and  $P_{mtlR}$  activities was investigated by the disruption of *mtlD*. To construct the integration cassette, a truncated version of *mtlD* was amplified in a PCR from *B. subtilis* 168 chromosome using oligonucleotides s6344/s6345. The resulting fragment was then inserted into pSUN308.3 via *EcoRV/NdeI* restriction sites (pKAM015). Afterwards, the erythromycin gene *ermC* was amplified by PCR from pSUN308.3 by oligonucleotides s5069/s5070. The blunt ends PCR product was then inserted into pKAM015 via *HincII* restriction site inside the *mtlD* (plasmid pKAM14). Integration of the cassette '*mtlD-ermC-mtlD*' into the chromosome of *B. subtilis* 3NA was performed and the transformants were selected on LB<sub>erm</sub>. The disruption of *mtlD* was confirmed by PCR using oligonucleotides s6344 and s6345. The *mtlD::ermC* mutant (strain KM37) was cultivated in LB supplemented by 1% glucose (as control), mannitol or glucitol. Incubation of the cell culture at 37°C revealed that the mannitol and glucitol retarded the growth of the cells in comparison to glucose (Fig. 3.15.A). In other words, the mannitol and glucitol are partially toxic for the cells and the cells were swollen and lysed after 4 h of incubation (Fig. 3.15.B).

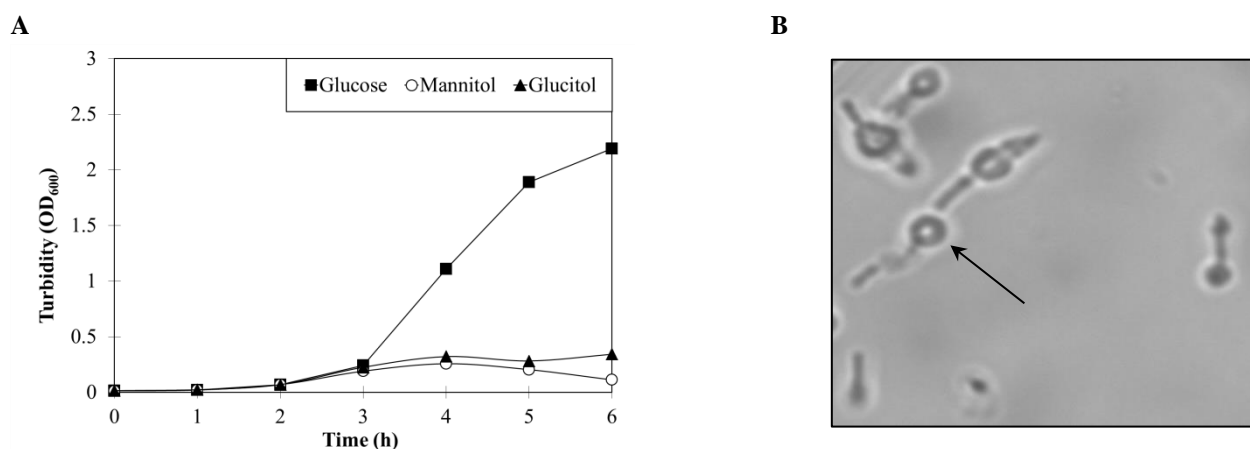


**Fig. 3. 15.** (A) Growth curve of the strain *mtlD::ermC* (strain KM37) in LB harboring 1% glucose, mannitol or glucitol as the main carbon source. (B) The swollen cells of *B. subtilis* KM37 in LB harboring mannitol as the main carbon source.

Likewise, the influence of the disruption of mannitol 1-phosphate dehydrogenase on the activity of  $P_{mnlA}$  was investigated. Strain KM37 pKAM12 was induced by different sugars (Fig. 3.11.B). Unexpectedly, the basal  $\beta$ -galactosidase activity of the KM37 pKAM12 was higher than the 3NA pKAM12 (4.7-fold). Due to the high basal  $\beta$ -galactosidase activity, the inducibility of the cells by mannitol were reduced. Besides, the presence of mannitol and glucitol resulted in partial lysis of the cells after 1 h. In contrast, addition of glucose prevented the lysis of the bacteria, although the  $P_{mnlA}$  activity was also repressed. In addition to pKAM12 harboring  $P_{mnlA}$ , KM37 was transformed with pKAM18 to monitor the  $P_{mnlR}$  activity in *mtlD::ermC* mutant. The results showed that the  $\beta$ -galactosidase activity of KM37 pKAM18 was higher than of 3NA pKAM18 in the presence and absence of mannitol (Fig. 3.12). Nonetheless, the catabolite repression remained effective. Overall,  $P_{mnlA}$  and  $P_{mnlR}$  were inducible in KM37, while glucose repressed their activities.

### 3.10.5. Deletion of the *mtlAFD* operon

The whole operon of the mannitol PTS, *mtlAFD*, was replaced with erythromycin resistance gene in order to investigate the  $P_{mnlA}$  activity in the absence of the EII<sup>Mtl</sup> components as well as mannitol 1-phosphate dehydrogenase. Construction of the *mtlAFD* deletion cassette was carried out by amplification of *ycsA* in the first step. The *ycsA* gene was amplified by PCR from *B. subtilis* 168 chromosome using oligonucleotides s5994/s5995. The amplified fragment was then inserted into pSUN308.3 by *SpeI/StuI* restriction sites (pKAM011). Next, oligonucleotides s6068 and s6080 were used for a PCR from genomic DNA of *B. subtilis* 168 to amplify *ycnL*. By insertion of the *ycnL* into pKAM011 via *EcoRV/BglIII* restriction sites, plasmid pKAM6 was constructed. Afterwards, the strain 3NA was transformed with pKAM6 and the erythromycin resistant transformants were selected (strain KM13). Subsequently, transformation of KM13 by pKAM12 was performed and the transformants were selected on spectinomycin. Induction of KM13 pKAM12 revealed an unexpected reduction in the  $\beta$ -galactosidase activity by 13-fold to about 1,000 Miller units compared to 3NA pKAM12. Nevertheless,  $P_{mnlA}$  in  $\Delta$ *mtlAFD* showed constitutive activity similar to *mtlAF* and *mtlF* mutants. Also, the catabolite repression was functional reducing the  $\beta$ -galactosidase activity to 200 Miller units (Fig. 3.11.B).

### 3.11. Regulation of $P_{mnlA}$ and $P_{mnlR}$ by glucitol

#### 3.11.1. $P_{mnlA}$ induction by glucitol

Glucitol is a sugar alcohol which is taken up by a non-PTS system in *B. subtilis*. Induction of the mannitol PTS by glucitol was reported before (239). To study the induction of  $P_{mnlA}$  by glucitol, wild type strain 3NA as well as KM12, KM13, KM15, KM37 and KM103 harboring pKAM12 (containing  $P_{mnlA-lacZ}$ ) were induced by glucitol (Fig 3.16). Induction of 3NA pKAM12 by glucitol gave about 8,000 Miller units  $\beta$ -galactosidase activity in comparison to the uninduced strain showing only 600 Miller units  $\beta$ -galactosidase activity. Besides, addition of glucose reduced the  $\beta$ -galactosidase activity by 1.7-fold. Deletion of  $mnlR$  lowered the  $\beta$ -galactosidase activity of KM15 pKAM12 in LB with glucitol to 81 Miller units and 100 Miller units without glucitol. In other words,  $P_{mnlA}$  was no longer inducible in KM15 pKAM12 and the  $P_{mnlA}$  activity was depleted. Likewise, the addition of glucose to KM15 pKAM12 culture decreased  $\beta$ -galactosidase activity to 61 Miller units. Moreover, deletion of  $mnlAF$  rendered  $P_{mnlA}$  constitutive in the presence and absence of glucitol. Besides, the presence of glucose reduced the  $\beta$ -galactosidase activity of KM12 pKAM12. This was similar to previous attempts where the influence of mannitol on  $P_{mnlA}$  in KM12 pKAM12 was investigated (section 3.10.2). Deletion of  $mnlF$  boosted the  $\beta$ -galactosidase activity to 18,000 – 25,000 Miller units. Also,  $P_{mnlA}$  was constitutive in KM103 pKAM12. Surprisingly, glucitol-induced KM37 pKAM12 culture expressed 11,800 Miller units  $\beta$ -galactosidase activity which was almost identical to mannitol-induced KM37 pKAM12. Indeed, the presence of mannitol 1-phosphate dehydrogenase in the cell made a significant difference between mannitol and glucitol as the inducers. Finally, deletion of the  $mnlAFD$  operon led to reduction of the  $P_{mnlA}$  constitutive activity. The  $\beta$ -galactosidase activity of KM13 pKAM12 in LB was about 1,000 Miller units in the presence and absence of glucitol which was the same as with KM13 pKAM12 in LB with or without mannitol.



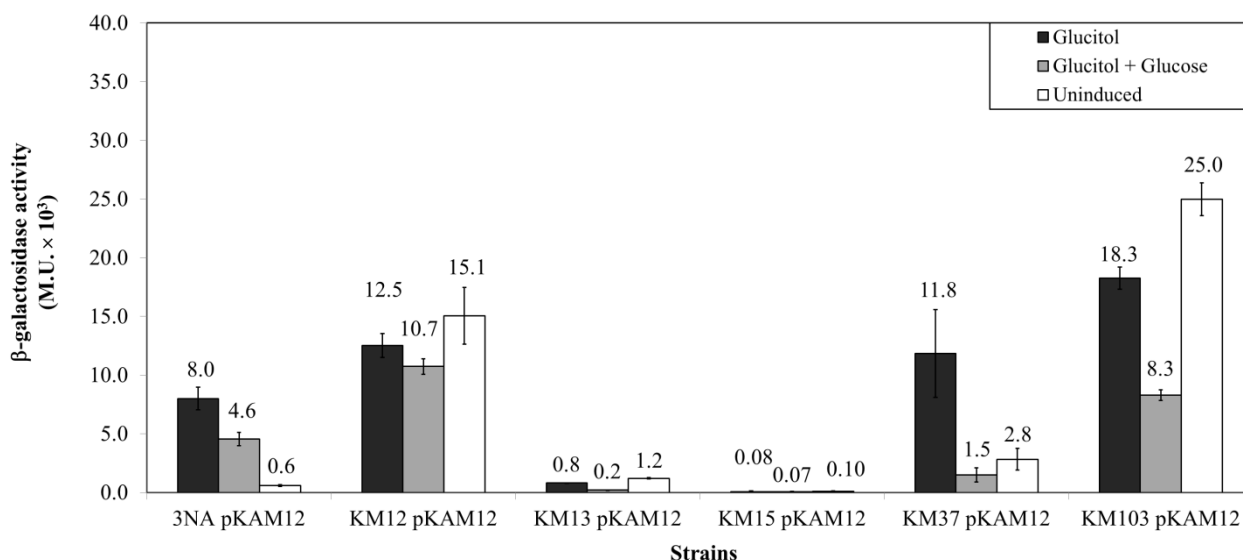


**Fig. 3. 16.** Induction of  $P_{mtA}$  by glucitol in strain 3NA and the mannitol utilization deficient mutants.  $\beta$ -galactosidase activity of the strains 3NA, KM12 ( $\Delta mtIAF$ ), KM13 ( $\Delta mtIAFD$ ), KM15 ( $\Delta mtIR$ ), KM37 ( $\Delta mtID$ ), KM103 ( $\Delta mtIF$ ) harboring pKAM12 ( $P_{mtA}$ ) is demonstrated. Glucitol (0.2%) and glucose (0.2%) were added at the OD<sub>600</sub> of 0.4 and the  $\beta$ -galactosidase activity was measured after 1 h.

### 3.11.2. Induction of $P_{mtIR}$ by glucitol

The activity of  $P_{mtIR}$  was investigated in the presence of glucitol in *B. subtilis* 3NA (wild type) as well as in mannitol utilization deficient mutants. For this purpose, *B. subtilis* 3NA, KM12 ( $\Delta mtIAF$ ), KM15 ( $\Delta mtIR$ ), and KM37 ( $mtID::ermC$ ) containing pKAM18 were induced by glucitol (Fig. 3.17). The  $\beta$ -galactosidase activity of the strains was measured 1 h after the addition of glucitol. Glucose was simultaneously added to the bacterial culture to test the carbon catabolite repression effect. The results showed that  $P_{mtIR}$  was less inducible by glucitol than mannitol in the 3NA pKAM18 strain with about 51 Miller units  $\beta$ -galactosidase activity. Additionally, presence of glucose repressed the  $P_{mtIR}$  activity in 3NA pKAM18. Deletion of the activator, MtlR, decreased the  $\beta$ -galactosidase activity to 10 – 16 Miller units in KM15 pKAM18. In this case,  $P_{mtIR}$  was no more inducible by glucitol. The presence and absence of glucitol had no influence on the  $\beta$ -galactosidase activity in KM12 pKAM18 where  $P_{mtIR}$  was constitutive. However, the addition of glucose decreased the  $\beta$ -galactosidase activity in KM12 pKAM18. Finally,  $\beta$ -galactosidase activity of KM37 pKAM18 in LB with or without glucitol was identical to KM37 pKAM18 with or without mannitol.

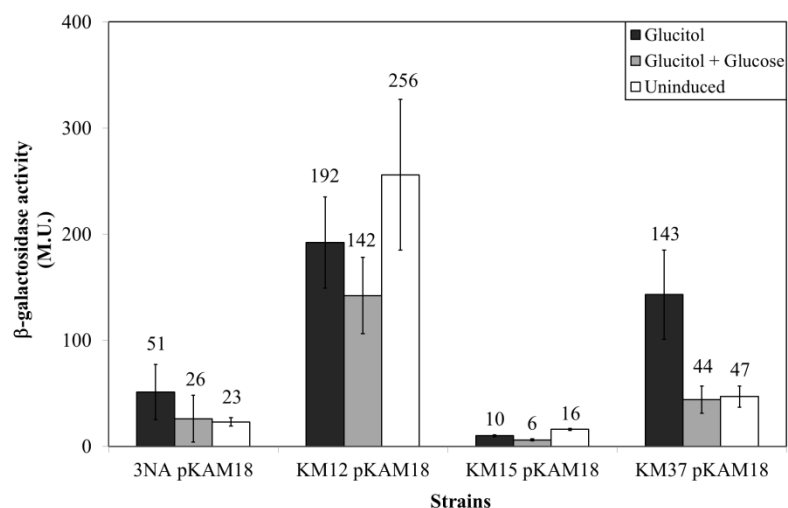


**Fig. 3. 17.** Induction of  $P_{mlR}$  by glucitol in strain 3NA and the mannitol utilization deficient mutants.  $\beta$ -galactosidase activity of *B. subtilis* 3NA, KM12 ( $\Delta mtlAF$ ), KM15 ( $\Delta mtlR$ ), and KM37 ( $\Delta mtlD$ ) harboring pKAM18 ( $P_{mlR}$ ) is shown. The bacterial strains were grown in LB at 37°C. Glucitol (0.2%) and glucose (0.2%) were added at the  $OD_{600}$  of 0.4 and the  $\beta$ -galactosidase activity was measured after 1 h.

### 3.11.3. Deletion of the *gutRBP* genes encoding glucitol utilization system

Assuming that the inducibility of  $P_{mtIA}$  and  $P_{mlR}$  by glucitol could be due to the interaction of the glucitol utilization system and mannitol PTS components, the complete *gutRBP* operon and its downstream gene, *ydjE* encoding a fructokinase, were replaced with a chloramphenicol acetyl transferase gene. The gene replacement cassette was constructed using oligonucleotides s6302/s6303 in a PCR with *B. subtilis* 168 for amplification of the upstream flanking gene, *ydjC*. The downstream flanking gene, *pspA*, was also amplified in a PCR by oligonucleotides s6304/s6305. The *ydjC* fragment was inserted into pMW363.1 via *EcoRI/NheI* (pKAM014). Next, the *pspA* fragment was inserted via *AflIII/NdeI* into pKAM014 to construct plasmid pKAM13. Strains 3NA and KM13 were transformed with pKAM13 harboring '*ydjC-cat-pspA*' in order to construct a  $\Delta gutRBP ydjE::cat$  strain (KM39) and a  $\Delta mtlAFD::ermC \Delta gutRBP ydjE::cat$  strain (KM40). Transformation of KM39 and KM40 by pKAM12 was carried out to construct strains KM39 pKAM12 and KM40 pKAM12. To both of the strains mannitol and glucitol were added to measure the  $\beta$ -galactosidase activity. Strain KM39 pKAM12 produced the same amount of  $\beta$ -galactosidase activity as 3NA pKAM12 (Fig. 3.18.A). KM39 pKAM12 showed 12,600

Miller units  $\beta$ -galactosidase activity in the presence of mannitol, 8,000 Miller units in the presence of glucitol, and about 600 Miller units in the uninduced strain. Strain KM40 pKAM12 showed the same  $\beta$ -galactosidase activity as KM13 pKAM12 having 1,200 Miller units (Fig. 3.18.B). Apparently, the results revealed that the deletion of the glucitol utilization components had no influence on the  $P_{mtlA}$  activity.

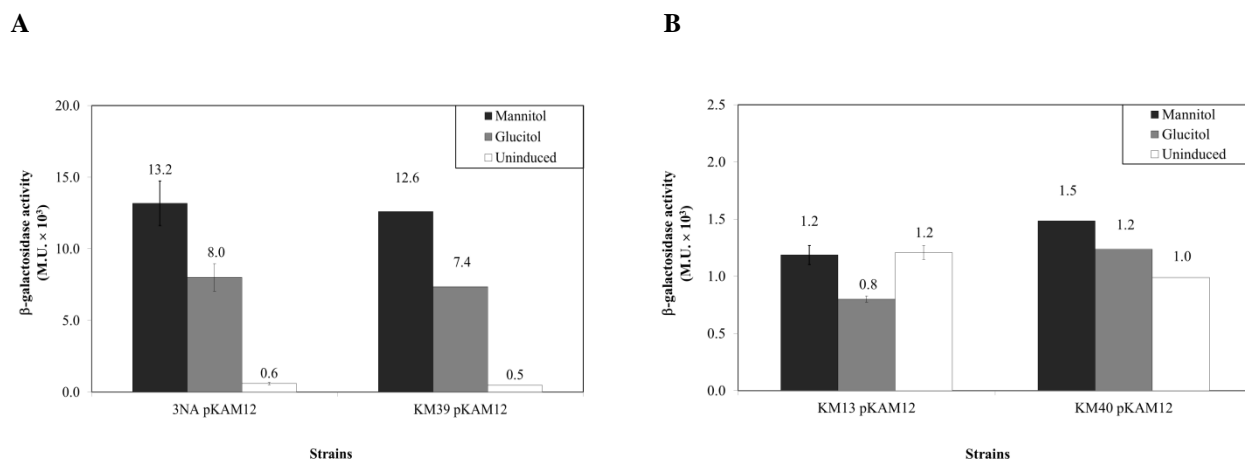


**Fig. 3. 18.** The activity of  $P_{mtlA}$  in deficient mutants of mannitol and glucitol utilization system. **(A)**  $\beta$ -galactosidase activity of the *B. subtilis* 3NA (wild type) and KM39 ( $\Delta gutRBPjdjE$ ) harboring pKAM12. **(B)** Production of  $\beta$ -galactosidase in the strains KM13 ( $\Delta mtlAFD$ ) and KM40 ( $\Delta mtlAFD \Delta gutRBPjdjE$ ) containing pKAM12. Measurements of KM39 pKAM12 and KM40 pKAM12 were performed once.

#### 3.11.4. Growth of the *mtl* and *gut* mutants in minimal medium

Deletion of the  $\Delta gutRBPjdjE$  genes revealed that the components of glucitol utilization system play no role in the induction of  $P_{mtlA}$  by glucitol. In addition to induction studies, the growth of the mannitol utilization deficient mutants was compared to deficient mutants of glucitol utilization system. The *mtl* and *gut* mutants were cultivated in minimal medium (broth I) harboring glucose, mannitol, or glucitol as the main carbon source, while the sodium citrate was removed from the bacterial culture. In this way, 1 OD<sub>600</sub> of the overnight culture was inoculated into 5 ml minimal medium in a 100 ml baffled Erlenmeyer flask and the growth was measured after 16 h incubation at 37°C (shaked at 200 rpm).

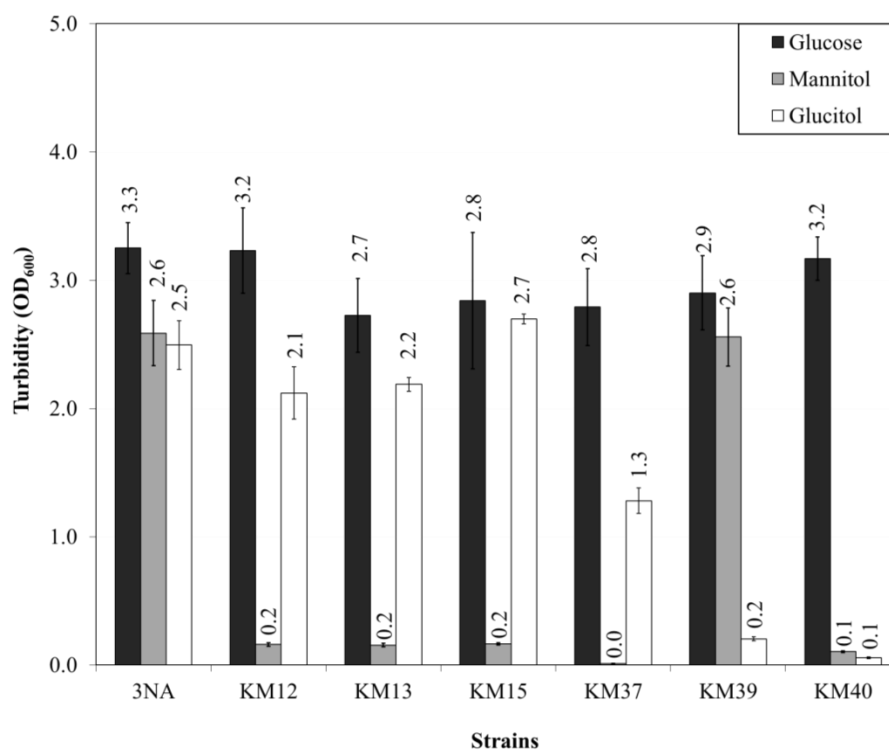


**Fig. 3. 19.** The growth of deficient mutants of mannitol and glucitol utilization system strains. *B. subtilis* 3NA, KM12 ( $\Delta mtlAF$ ), KM13 ( $\Delta mtlAFD$ ), KM15 ( $\Delta mtlR$ ), KM37 (*mtlD::cat*), KM39 ( $\Delta gutRBPjdjE$ ), and KM40 ( $\Delta mtlAFD \Delta gutRBPjdjE$ ) were cultivated in broth I harboring 1% glucose, mannitol, or glucitol as the main carbon source. The measurements were performed after 16 h of incubation at 37°C.

No growth was observed with the  $\Delta mtlAF$ ,  $\Delta mtlAFD$ , and  $\Delta mtlR$  mutants as well as with the  $\Delta mtlAFD \Delta gutRBPjdjE$  double mutant in the presence of mannitol as the main carbon source (Fig. 3.19). As mentioned before, the  $\Delta mtlD$  mutant was lysed in the presence of mannitol. However, glucitol as the main carbon source supported the growth of all of the mutants, except the  $\Delta gutRBPjdjE$  mutants, namely KM39 and KM40. Interestingly, the growth of the  $\Delta mtlD$  mutant was half of the wild type strain in the presence of the glucitol showing the necessity of mannitol 1-phosphate dehydrogenase for the glucitol assimilation.

### 3.12. Carbon catabolite repression of $P_{mtlA}$ and $P_{mtlR}$

#### 3.12.1. $P_{mtlA}$ activity in the presence of different PTS sugars

Primary studies showed that the presence of glucose reduced  $P_{mtlA}$  and  $P_{mtlR}$  activities. Thus, different PTS sugars such as fructose, glucose, mannose, and sucrose were used to study their probable influence on  $P_{mtlA}$  activity. To reduce the number of assays,  $P_{mtlA}$  activity was studied in strain KM12 ( $\Delta mtlAF$  mutant) harboring pKAM12. In this strain, the activity of  $P_{mtlA}$  was constitutive. Strain KM12 pKAM12 which was cultivated in LB with or without mannitol exhibited the same level of 13,900 – 15,100 Miller units  $\beta$ -galactosidase activity. Addition of glucose or fructose to the LB culture reduced  $\beta$ -galactosidase activity of KM12 pKAM12, while supplementation with mannose or sucrose had no influence on  $\beta$ -galactosidase activity (Fig. 3.20).

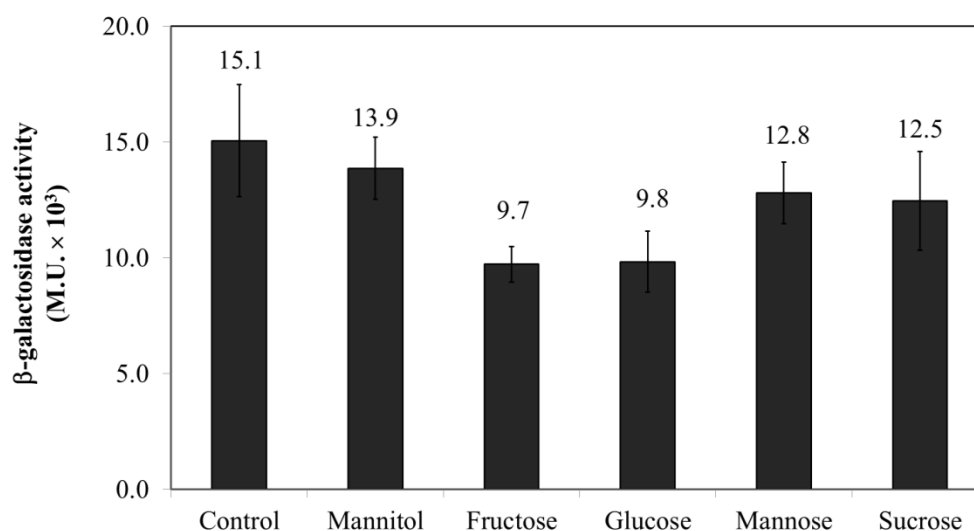


**Fig. 3. 20.** Carbon catabolite repression of  $P_{mtlA}$  by different PTS sugars.  $\beta$ -galactosidase activity of strain KM12 pKAM12 ( $\Delta mtlAF$ ) in LB supplemented by 0.2% of mannitol, fructose, glucose, mannose, or sucrose is represented. The desired sugar was added at the OD<sub>600</sub> of 0.4 and  $\beta$ -galactosidase activity was measured 1 h after induction. No sugar was added to the control.

#### 3.12.2. Activity of $P_{mtlA}$ in CcpA-dependent CCR mutants

Activity of  $P_{mtlA}$  in the presence of glucose was investigated in CcpA-dependent CCR deficient mutants. At first, glucose repression of  $P_{mtlA}$  was measured in *B. subtilis* QB5223, a

*ptsH*-S46A mutant. Replacement of serine 46 in HPr by an alanine prevents the formation of the CcpA-HPr(S46~P) complex. Strain QB5223 (*ptsH*-S46A) was transformed with plasmid pKAM12 and  $\beta$ -galactosidase activity was measured after growth in LB supplemented with mannitol or with mannitol and glucose. The presence of glucose slightly reduced the  $\beta$ -galactosidase activity of QB5223 pKAM12 from 13,700 to 10,300 Miller units (Fig. 3.21). This result shows a weaker glucose repression effect in comparison with 3NA pKAM12. However, *ptsH*-S46A mutation encoding HPr-S46A did not completely relieve  $P_{mtlA}$  from glucose repression. Thus, glucose repression of  $P_{mtlA}$  was measured in a  $\Delta crh$  mutant. For this purpose, strain TQ338 ( $\Delta crh$ ) was transformed with pKAM12. Addition of mannitol to the TQ338 pKAM12 culture showed a reduction of the  $\beta$ -galactosidase activity (about 8,100 Miller units) in comparison with 3NA pKAM12 (about 13,200 Miller units). Nevertheless, addition of glucose still reduced the  $P_{mtlA}$  activity by 2.4-fold which was the same as with 3NA pKAM12. Given that neither *ptsH*-S46A nor  $\Delta crh$  mutations in *B. subtilis* were able to abolish glucose repression, the  $P_{mtlA}$  activity was measured in a *ptsH*-S46A  $\Delta crh$  double mutant. Strain TQ338\_S46 harboring the *ptsH*-S46A  $\Delta crh$  double mutation was transformed with pKAM12. Comparing with 3NA pKAM12, induction of TQ338\_S46 pKAM12 by mannitol resulted in a lower  $\beta$ -galactosidase activity. However, the basal  $\beta$ -galactosidase activity of TQ338\_S46 pKAM12 culture was almost tripled in comparison with 3NA pKAM12 (Fig. 3.21). Similar to *ptsH*-S46A mutant, glucose repression was lower than in strain 3NA pKAM12 (about 1.3-fold). Apparently, deletion of *crh* or mutation of *ptsH*-S46A could not absolutely abolish the glucose repression of  $P_{mtlA}$ . Hence, *hprK* encoding the HPrK/P enzyme was deleted. Deletion of the *hprK* gene led to no phosphorylation of HPr-S46 (or Crh-S46), and thereby inhibits the formation of CcpA-HPr(S46~P) or CcpA-Crh(S46~P) complex. For this purpose, strain TQ308 ( $\Delta hprK$ ) was transformed with pKAM12. TQ308 pKAM12 exhibited a reduced growth rate in LB as compared to 3NA pKAM12. The former reached an OD<sub>600</sub> of 0.9 after 1 h of induction by mannitol, while 3NA pKAM12 reached an OD<sub>600</sub> of 1.6 – 1.7 under same conditions. TQ308 pKAM12 showed a  $\beta$ -galactosidase activity of about 8,600 Miller units after cultivation in LB supplemented with mannitol, while its basal  $\beta$ -galactosidase activity was 800 Miller units in LB without mannitol. Moreover, glucose repression was still functional in TQ308 pKAM12 reducing the  $P_{mtlA}$  activity by 1.65-fold. Therefore, glucose repression of  $P_{mtlA}$  was measured in a  $\Delta ccpA$  mutant. Strain

TQ303 which is the CcpA-deficient mutant was transformed with pKAM12 using minimal medium supplemented with succinate and glutamate. The  $P_{mtlA}$  activity in TQ303 pKAM12 was calculated from the cells grown in LB with or without mannitol.  $\beta$ -galactosidase activity of mannitol-induced TQ303 pKAM12 was lowered to 6,100 Miller units, whereas its basal  $\beta$ -galactosidase activity in LB remained of 500 Miller units (Fig. 3.21). Addition of the glucose strongly declined the  $\beta$ -galactosidase activity of TQ303 pKAM12 in LB with mannitol. Consequently, deletion of the CcpA-dependent CCR components did not completely abolish the glucose repression in  $P_{mtlA}$ . Hence, glucose repression in  $P_{mtlR}$  was studied by the CcpA-dependent CCR mutants.

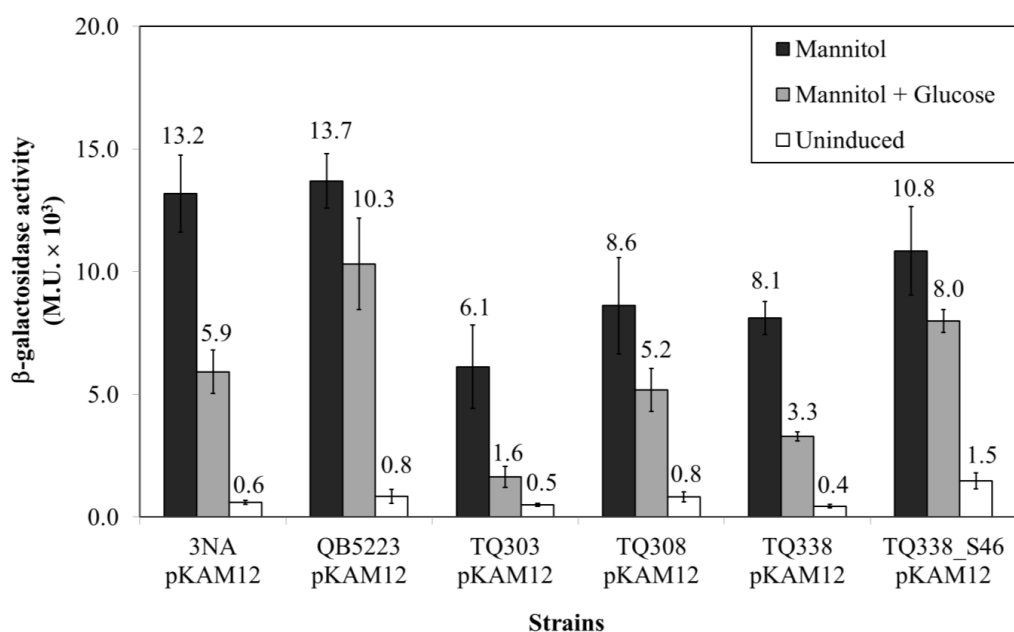


**Fig. 3. 21.** Catabolite repression of  $P_{mtlA}$  in CcpA-dependent CCR deficient mutants.  $\beta$ -galactosidase activity of strains 3NA, QB5223 (*ptsH-S46A*), TQ303 ( $\Delta$ *ccpA*), TQ308 ( $\Delta$ *hprK*), TQ338 ( $\Delta$ *crh*), and TQ338\_S46 (*ptsH-S46A*  $\Delta$ *crh*) harboring pKAM12 ( $P_{mtlA}$ ) in LB is shown. The desired sugar was added at the OD<sub>600</sub> of 0.4 and  $\beta$ -galactosidase activity was measured 1 h after induction. No sugar was added to the uninduced bacterial cultures.

### 3.12.3. $P_{mtlR}$ activity in CcpA-dependent CCR mutants

The *mtlAFD* operon is activated by MtlR; therefore, any variation of the MtlR amount in the cytoplasm could affect the  $P_{mtlA}$  activity. Since identification of  $P_{mtlR}$  indicated a *cre* site between -35 and -10 boxes of  $P_{mtlR}$ , the possibility of the binding of CcpA-HPr(S46~P) or CcpA-

Crh(S46~P) complex to  $P_{mtlR}$  was studied by the CcpA-dependent CCR deficient mutants. The strains TQ303 ( $\Delta ccpA$ ) and the double mutant TQ338\_S46 ( $\Delta crh ptsH-S46A$ ) were transformed with pKAM18 (containing  $P_{mtlR-lacZ}$ ).  $\beta$ -galactosidase activity of TQ303 pKAM18 was about the same as with 3NA pKAM18 in LB with or without mannitol (Fig. 3.22). The main difference was noticed when both mannitol and glucose were added to the culture medium. In this case,  $\beta$ -galactosidase activity of TQ303 pKAM18 was doubled. Similar to TQ303 pKAM18, glucose repression of  $P_{mtlR}$  in TQ338\_S46 pKAM18 was less than in 3NA pKAM18. However, the elevated basal  $\beta$ -galactosidase activity of TQ338\_S46 pKAM18 makes the interpretation difficult. Consequently, mutations of the CcpA-dependent CCR components showed slightly influence on the glucose repression of  $P_{mtlA}$  and  $P_{mtlR}$ .

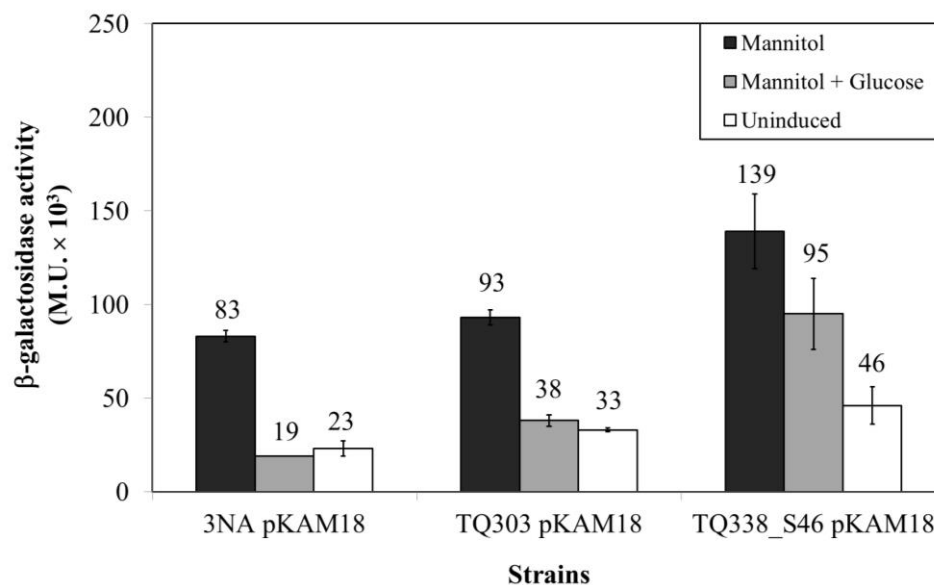


**Fig. 3. 22.** Catabolite repression of  $P_{mtlR}$  in CcpA-dependent CCR deficient mutants.  $\beta$ -galactosidase activity of strains 3NA, TQ303 ( $\Delta ccpA$ ), and TQ338\_S46 ( $ptsH-S46A \Delta crh$ ) harboring pKAM18 ( $P_{mtlR}$ ) is demonstrated. The strains were grown in LB and the desired sugar was added at the  $OD_{600}$  of 0.4 and  $\beta$ -galactosidase activity was measured 1 h after induction.

#### 3.12.4. Deletion of the glucose-PTS transporter

It was shown that deletion of the CcpA-dependent CCR components showed only a moderate reduction in the catabolite repression of  $P_{mtlA}$  and  $P_{mtlR}$ . Therefore, the probable



influence of the deletion of *ptsG*, encoding the EIICBA<sup>Glc</sup> (glucose-PTS transporter) on the *P<sub>mtlA</sub>* and *P<sub>mtlR</sub>* activities was considered. For this purpose, strain MW373 was used which lacks the glucose PTS transporter ( $\Delta$ *ptsG*). Transformation of MW373 by pKAM12 and pKAM18 was carried out and the resulting transformants were subjected to mannitol (for induction) and glucose (for repression). Interestingly,  $\beta$ -galactosidase activity of MW373 pKAM12 in LB with mannitol was similar in the presence and absence of glucose (about 11,300 Miller units), while the inducibility of *P<sub>mtlA</sub>* in  $\Delta$ *ptsG* mutant remained the same as in the wild type strain (Fig. 3.23.A). The presence of glucose did not alter the  $\beta$ -galactosidase activity of MW373 pKAM18 in LB supplemented with mannitol. The inducibility of *P<sub>mtlR</sub>* in MW373 pKAM18 also remained the same as in the wild type strain (Fig. 3.23.B).

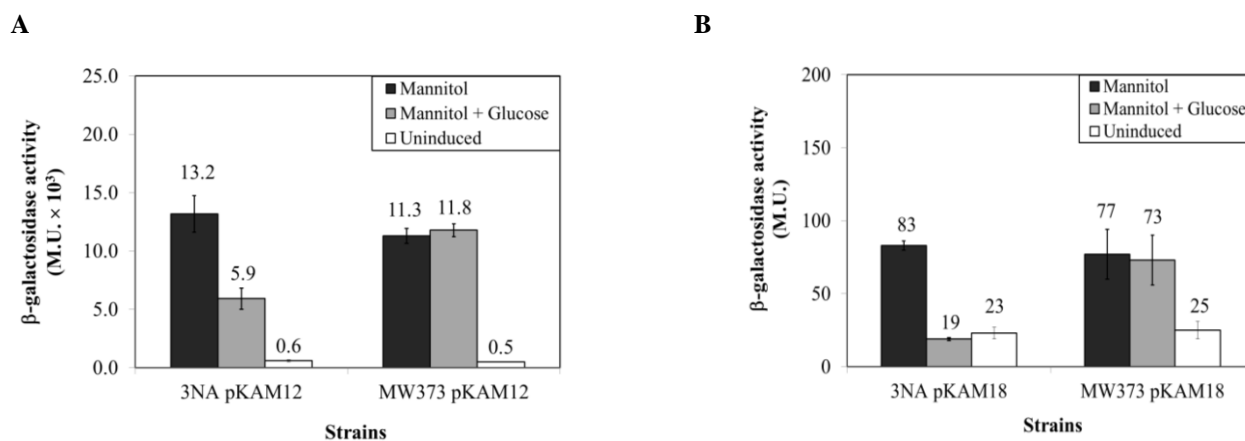


**Fig. 3. 23.** Catabolite repression of *P<sub>mtlA</sub>* and *P<sub>mtlR</sub>* in wild type and  $\Delta$ *ptsG* mutant. (A)  $\beta$ -galactosidase activity of strains 3NA and MW373 ( $\Delta$ *ptsG*) harboring pKAM12 (*P<sub>mtlA</sub>*) is demonstrated. (B)  $\beta$ -galactosidase activity of the strains 3NA and MW373 ( $\Delta$ *ptsG*) harboring pKAM18 (*P<sub>mtlR</sub>*) is represented. The desired sugar was added to the cells at the OD<sub>600</sub> of 0.4 and the  $\beta$ -galactosidase activity was measured 1 h after induction.

### 3.13. Regulation of the MtlR activity via phosphorylation of MtlR domains

#### 3.13.1. Integration of *P<sub>mtlA</sub>-lacZ* into the chromosome

Activity of MtlR was examined by mutation of the phosphorylation sites in the conserved domains of MtlR. To prevent a possible titration effect on the *P<sub>mtlA</sub>* activity, the *P<sub>mtlA</sub>-lacZ* fusion was integrated into the *amyE* gene encoding  $\alpha$ -amylase on the chromosome of *B. subtilis*. For this purpose, plasmid pDG1730 was used consisting of the *amyE* gene disrupted by

spectinomycin resistance gene. The *P<sub>mtlA</sub>-lacZ* fusion was amplified in a PCR by oligonucleotide s7455/s7481 using pKAM12 as a template. The PCR product was then inserted into pDG1730 DNA digested by *Hind*III and *Eco*RI and resulted in pKAM123. Afterwards, strain 3NA was transformed with plasmid pKAM123 harboring the *amyE-P<sub>mtlA</sub>-lacZ-spc-amyE* cassette. The transformants were then selected based on spectinomycin resistance. The disruption of the *amyE* gene was confirmed on LB agar plate containing starch. Strain KM176 harboring the *P<sub>mtlA</sub>-lacZ* fusion on the chromosome was subjected to mannitol (for induction) and glucose (for repression) in order to study the *P<sub>mtlA</sub>* activity. The basal  $\beta$ -galactosidase activity in uninduced KM176 was 69 Miller units. Addition of mannitol to LB induced the *P<sub>mtlA</sub>* activity in KM176 culture as indicated by the measurements of 776 Miller units  $\beta$ -galactosidase activity (Fig. 3.24). For this strain, simultaneous presence of mannitol and glucose in LB repressed the *P<sub>mtlA</sub>* activity about 3.6-fold.

### 3.13.2. Mutation of the PRDI domain

The influence of PRDI on the MtlR activity was studied by mutation of the putative phosphorylation sites at PRDI. At first, histidine 230 was mutated to alanine by a fusion PCR. PCRs from the chromosome of *B. subtilis* 168 were carried out using oligonucleotides s6949/s6868 and s6869/s6867. The fusion PCR was performed by oligonucleotides s6949/s6867 and the primary PCR products. The *P<sub>mtlR</sub>-mtlR-H230A* DNA fragment was then inserted into pJOE4786.1 digested by *Sma*I and resulted in pKAM025. Next, pKAM025 DNA was digested by *Xma*I/*Spe*I and the 2.3 kb fragment was inserted into pKAM4 via the same restriction sites to construct pKAM127. Finally, strain KM15 ( $\Delta$ *mtlR*) was transformed with plasmid pKAM127 and the transformants were selected on mannitol minimal plates. The correct integration of *P<sub>mtlR</sub>-mtlR-H230A* into the chromosome of *B. subtilis* led to the deletion of the erythromycin resistance gene. Strain KM210 (*mtlR*-H230A) was subsequently transformed with pKAM123 in order to integrate *P<sub>mtlA</sub>-lacZ* into the chromosome at the *amyE* gene (strain KM214). The  $\beta$ -galactosidase activity of the latter strain, namely KM214, was measured by the addition of mannitol in the presence and absence of glucose in the culture media. No significant difference was observed in the  $\beta$ -galactosidase activity of KM176 (*mtlR*) and KM214 (*mtlR*-H230A) (Fig.

3.24). Afterwards, the second phosphorylation site of PRDI, namely histidine 289, was mutated to alanine by a fusion PCR. PCRs were performed from *B. subtilis* 168 chromosome using oligonucleotides s6949/s6870 and s6871/s6867. Fusion PCR was accomplished using oligonucleotides s6949/s6867 and the primary PCR products. The *P<sub>mtlR</sub>-mtlR-H289A* fragment was then inserted into pJOE4786.1 via *Sma*I restriction sites and created plasmid pKAM026. Digestion of the pKAM026 DNA by *Xma*I/*Spe*I was carried out and the 2.3 kb fragment was inserted into pHM31 (see appendices) via the *Xma*I/*Nhe*I restriction sites and resulted in pKAM68. Integration of *P<sub>mtlR</sub>-mtlR-H289A* into the 3NA chromosome was accomplished in two steps based on histidine auxotrophy (158). First, plasmid pHM30 (see appendices) harboring a spectinomycin resistance gene was integrated into the chromosome of KM15. This integration disrupted the last gene of the *his* operon, *hisI*, in which the spectinomycin resistance gene was integrated into the chromosome. Selection of the transformants was performed on LB<sub>spc</sub> plates (strain KM162). Afterwards, the histidine auxotrophic mutant, *i.e.* strain KM162, was transformed with pKAM68 containing an intact *hisI* gene as well as *P<sub>mtlR</sub>-mtlR-H289A*. Selection of the transformants harboring the *mtlR-H289A* mutation was performed on Spizizen minimal medium plates lacking histidine. In this way, strain KM165 was constructed in which *P<sub>mtlR</sub>-mtlR-H289A* resided downstream of the *his* operon. Then, transformation of KM165 by pKAM123 was carried out in order to integrate the *P<sub>mtlA</sub>-lacZ* fusion into the *amyE* locus. The newly constructed strain was called KM179. Induction of the KM179 strain (*mtlR-H289A*) indicated a lower  $\beta$ -galactosidase activity, about 377 Miller units, compared to KM176 culture with a  $\beta$ -galactosidase activity of about 776 Miller units (wild type *mtlR*) (Fig. 3. 24). Interestingly, the glucose repression in KM179 culture with a  $\beta$ -galactosidase activity of about 16 Miller units  $\beta$ -galactosidase activity was stronger than in KM176 with 215 Miller units. Finally, the *P<sub>mtlA</sub>* activity was measured in the *mtlR-H230A H289A* double mutant. The *P<sub>mtlR</sub>-mtlR-H230A H289A* DNA fragment was amplified by using pKAM025 as a template and oligonucleotides s6949/s6870 and s6871/s6867 in PCRs. Next, fusion PCR was accomplished using oligonucleotides s6949/s6867 and the primary PCR products. The *P<sub>mtlR</sub>-mtlR-H230A H289A* PCR fragment was inserted into pJOE4786.1 digested by *Sma*I (pKAM027). Next, pKAM027 DNA was digested by *Xma*I/*Spe*I and the 2.3 kb fragment was inserted into pKAM4 via *Xma*I/*Spe*I restriction sites and created plasmid pKAM129. Strain KM212 was constructed by

transformation of strain KM15 ( $\Delta mtlR$ ) with pKAM129. Afterwards, the  $P_{mtlA}$ - $lacZ$  fusion on pKAM123 was integrated into the  $amyE$  locus of strain KM212 resulting in strain KM216. Induction of KM216 expressing  $mtlR$ -H230A H289A by mannitol indicated a similar  $\beta$ -galactosidase activity compared to KM179 ( $mtlR$ -H289A). The glucose repression in KM216 was also stronger than in KM176 (wild type  $mtlR$ ) (Fig. 3.24).

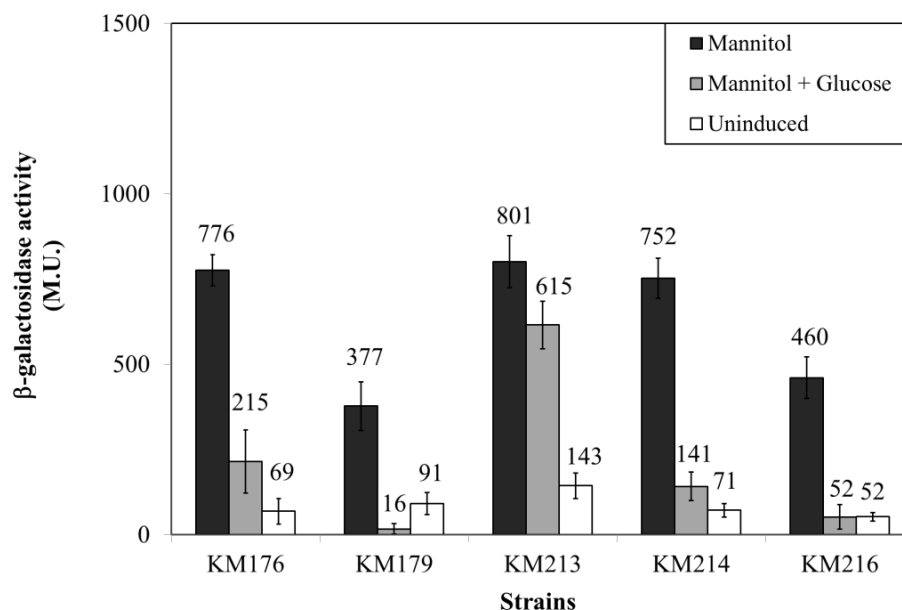


**Fig. 3. 24.** Activity of  $P_{mtlA}$  in the  $mtlR$  mutants.  $\beta$ -galactosidase activity of strains KM176 ( $mtlR$ ), KM179 ( $mtlR$ -H289A), KM213 ( $mtlR$ -H342D), KM214 ( $mtlR$ -H230A), and KM216 ( $mtlR$ -H230A H289A) in LB is shown. All of the strains contain an integrated  $P_{mtlA}$ - $lacZ$  fusion in their  $amyE$  locus. The desired sugar was added at the  $OD_{600}$  of 0.4 and  $\beta$ -galactosidase activity was measured 1 h after induction.

### 3.13.3. Mutation of the PRDII domain

Histidine 342 located at PRDII domain was exchanged by an aspartic acid in order to construct a mimic of a phosphorylated histidine. For this purpose,  $P_{mtlR}$ - $mtlR$ -H342D was amplified by oligonucleotides s6949/s6865 and s6866/s6867 in PCRs. Afterwards, a fusion PCR was carried out by oligonucleotides s6949/s6867 and the primary PCR products. The final  $P_{mtlR}$ - $mtlR$ -H342D fragment was blunt inserted into pJOE4786.1 which was already cut by *Sma*I. The resulting plasmid, pKAM024, was digested by *Xma*I and *Spe*I, and the 2.3 kb fragment was inserted into the pKAM4 via *Xma*I/*Spe*I restriction sites and led to construction of pKAM126.

Afterwards, strain KM15 ( $\Delta mtlR$ ) was transformed with pKAM126. The transformants expressing *mtlR*-H342D were selected on mannitol minimal plates. The newly constructed strain was named KM209. By integration of the  $P_{mtlA}$ -*lacZ* fusion into the *amyE* locus of KM209, strain KM213 was constructed. Induction of KM213 by mannitol in LB showed approximately 800 Miller units  $\beta$ -galactosidase activity resembling KM176. Besides, the basal  $\beta$ -galactosidase activity of KM213 expressing *mtlR*-H342D was doubled compared to KM176 (wild type *mtlR*). Finally, addition of glucose slightly reduced the  $\beta$ -galactosidase activity of KM213 (Fig. 3.24).

### 3.14. Operators of $P_{mtlA}$ and $P_{mtlR}$

#### 3.14.1. Alignment of the $P_{mtlA}$ and $P_{mtlR}$ putative activator binding sites

Induction of  $P_{mtlA}$  and  $P_{mtlR}$  showed that both of the promoters are activated by MtlR. Besides, sequence analyses revealed incomplete inverted repeats residing upstream of the -35 boxes in  $P_{mtlA}$  and  $P_{mtlR}$ . To find the exact MtlR binding site of  $P_{mtlA}$  and  $P_{mtlR}$ , the upstream sequences of the -35 boxes in  $P_{mtlA}$  and  $P_{mtlR}$  were aligned. As depicted in Fig. 3.25, 11 bp flanking sites of the incomplete inverted repeats were highly similar. This sequence was longer than the MtlR binding site so far predicted by Watanabe *et al.* (239).

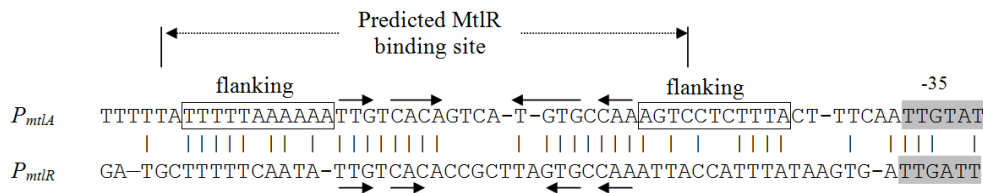


**Fig. 3. 25.** Alignment of the  $P_{mtlA}$  and  $P_{mtlR}$  -35 upstream sequences. The MtlR binding site is predicted by Watanabe *et al.* (239).

### 3.14.2. Fusion of the $P_{mtlA}$ upstream sequence to the $P_{mtlR}$ core elements

The putative MtlR binding sites of  $P_{mtlA}$  and  $P_{mtlR}$  were compared by the fusion of  $P_{mtlA}$  upstream sequence to  $P_{mtlR}$  core elements. For this purpose, PCRs from the chromosome of *B. subtilis* 168 were performed by oligonucleotides s6209/s6798 and s6799/s6392. The products of primary PCRs were then fused by a PCR using oligonucleotides s6209/s6392. The final  $P_{mtlA}$ - $P_{mtlR}$  fragment was then digested by *NheI* and *AflIII* and inserted into pSUN279.1 and created pKAM51. Fig. 3.26.A demonstrates the sequence of the hybrid promoter. Plasmid pKAM51 was used for transformation of *B. subtilis* 3NA, which was then induced by 0.2% mannitol in LB.  $\beta$ -galactosidase activity of 3NA pKAM51 was about 152 Miller units in LB supplemented with mannitol, whereas the basal  $\beta$ -galactosidase activity was only 47 Miller units after cultivation in LB (Fig. 3.26.B). In comparison with 3NA pKAM18 carrying  $P_{mtlR}$ , the  $\beta$ -galactosidase activity of 3NA pKAM51 was doubled in the both induced and uninduced cultures. This could be due to a higher affinity of MtlR to the  $P_{mtlA}$  operator.

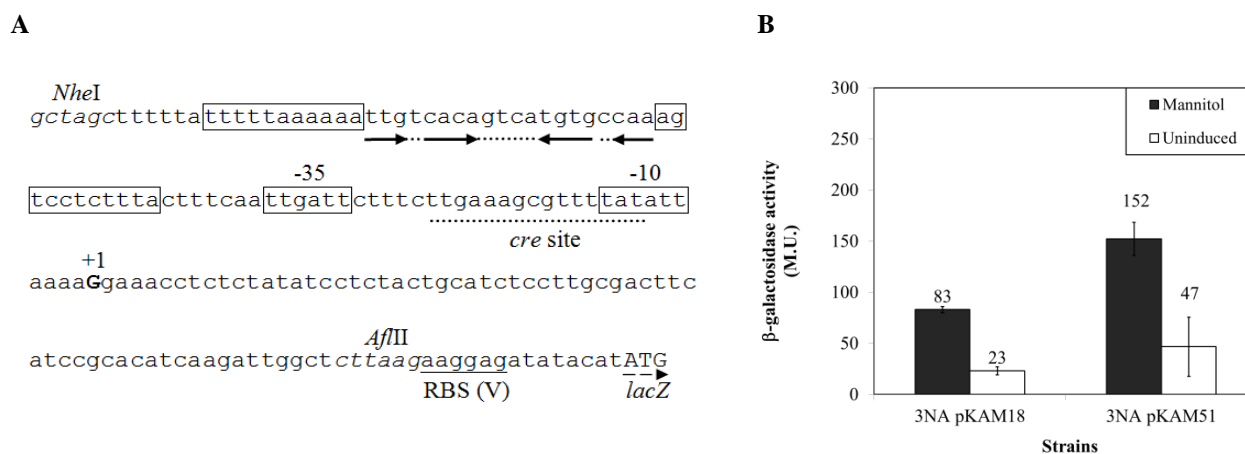


**Fig. 3. 26. (A)** The sequence of the  $P_{mtlA}$ - $P_{mtlR}$  fusion on pKAM51. **(B)**  $\beta$ -galactosidase activities of the induced and uninduced 3NA pKAM18 and 3NA pKAM51 strains.

### 3.14.3. Shortening of the 5'-end of $P_{mtlA}$

In section 3.3, it was shown that shortening of 20 bp from the  $P_{mtlA}$  5'-end had no effect on the  $P_{mtlA}$  activity on pKAM9. To identify the 5' boundary of  $P_{mtlA}$  *in vivo*, shortening of the 5'-end of  $P_{mtlA}$  was gradually performed in 2 bp blocks (Fig. 3.27.A). For these attempts, pKAM12

was chosen as a template and oligonucleotides s6726/s6213 (pKAM43), s6792/s6213 (pKAM48), s6793/s6213 (pKAM49), s6829/s6213 (pKAM57), s6830/s6213 (pKAM58), and s6210/s6213 (pKAM59) were used in PCRs. The obtained promoter fragments were then inserted into pSUN279.2 via *NheI/AflII*. The constructs are shown in Fig. 3.27.A. After transformation of 3NA by the resulting plasmids, induction of strain 3NA harboring pKAM43, pKAM48, or pKAM49 by mannitol showed no significant difference in  $\beta$ -galactosidase activity compared to 3NA pKAM12 culture (Fig. 3.27.B). Removal of additional 2 bp showed a reduction in  $\beta$ -galactosidase activity of 3NA pKAM57 and 3NA pKAM59. Nevertheless,  $P_{mtlA}$  was still inducible in 3NA pKAM57 and pKAM59 by 19-fold and 21-fold, respectively, which were similar to 3NA pKAM12 (22-fold induction) (Fig. 3.27.B). Finally, 3NA pKAM58 had a low  $\beta$ -galactosidase activity and indicated no inducibility. In fact, the results of the 5'-end shortening of  $P_{mtlA}$  were in line with the conserved -35 upstream sequence of  $P_{mtlA}$  and  $P_{mtlR}$  (section 3.14.1). Therefore, MtlR binding site likely begins at the position -83 with respect to the transcription start site.

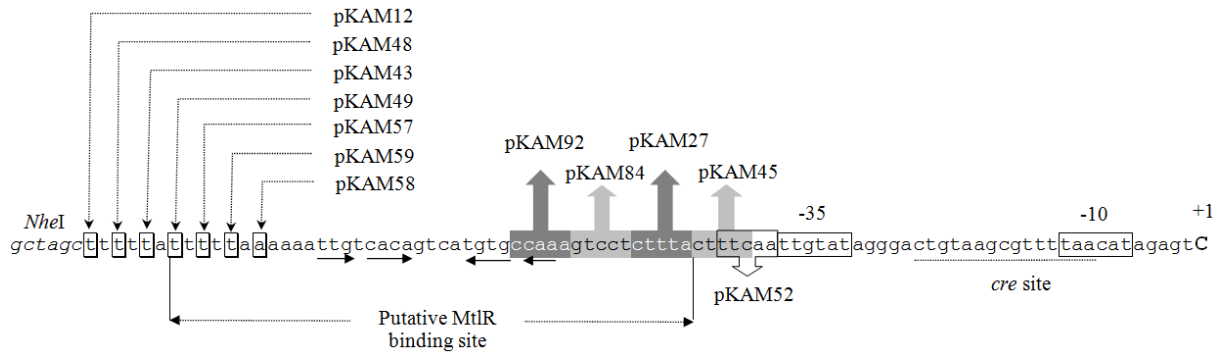
#### 3.14.4. Mutations between the MtlR binding site and -35 box of $P_{mtlA}$

Shortened  $P_{mtlA}$  constructs revealed the 5'-end of MtlR binding site. However, the 3'-end of the MtlR binding site remained unclear. Therefore, identification of the 3'-end of the MtlR binding site was started by exchanging 5 bp blocks to their complementary sequence (see Fig. 3.27.A). In this way, different  $P_{mtlA}$  constructs were generated by PCR from pKAM12 using oligonucleotides s6688/s6213 (pKAM27), s7065/s6213 (pKAM84), and s7091/s6213 (pKAM92). Also, fusion PCRs were carried out for construction of pKAM45 and pKAM52. PCRs were performed from pKAM12 using oligonucleotides s6209/s6728 and s6729/s6213. Fusion PCR was carried out using primary PCR products and oligonucleotides s6209/s6213 (pKAM45). For pKAM52, oligonucleotides s6209/s6800 and s6801/s6213 were applied in PCRs. These PCR products were then used as templates for the final PCR by s6209/s6213. Strain 3NA was then transformed with pKAM27, pKAM45, pKAM52, pKAM84, or pKAM92. In comparison with 3NA pKAM12, induced 3NA pKAM52 showed a reduced  $\beta$ -galactosidase activity with about 6,400 Miller units (Fig. 3.27.B). Also, the basal  $\beta$ -galactosidase activity of

## Results

3NA pKAM52 was 3-fold lower than of 3NA pKAM12. Strains 3NA pKAM45 and 3NA pKAM84 showed 8,500 and 7,400 Miller units  $\beta$ -galactosidase activity, respectively, whereas their basal  $\beta$ -galactosidase activity were 400 and 300 Miller units, respectively.

**A**



**B**

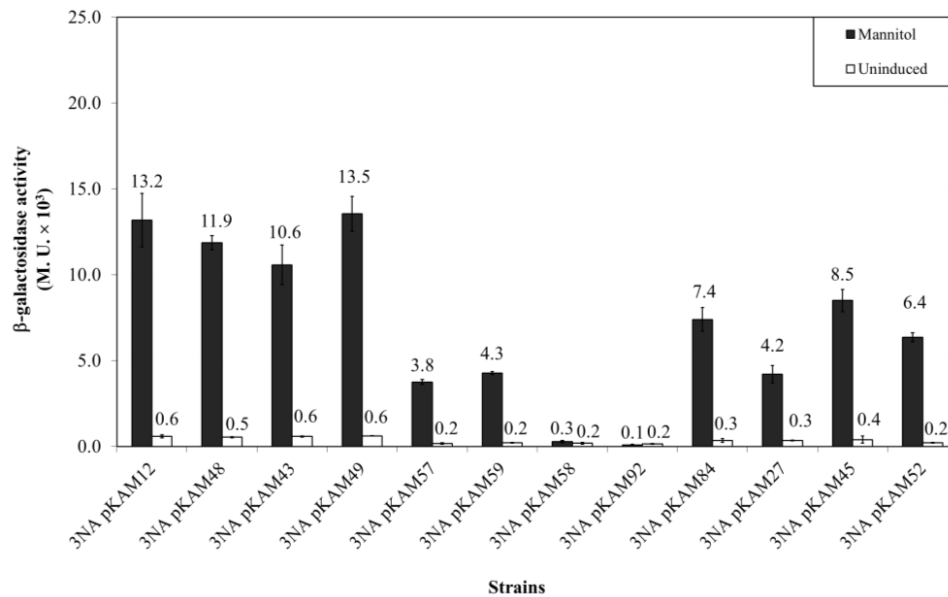


**Fig. 3. 27. (A)** Partial sequence of *P<sub>milA</sub>* on pKAM12 and the constructs thereof. The promoter -35 and -10 boxes are enclosed by rectangles, while a single C residue (bold capital letter) is the transcription start site. The putative *cre* site is underlined. The first base pair of each shortened promoter is shown by a box and an arrow. The base pair exchanges are highlighted in dark gray in pKAM27 and pKAM92, in light gray pKAM45 and pKAM84, or enclosed by a rectangle in pKAM52. **(B)**  $\beta$ -galactosidase activity of strain 3NA containing pKAM12, pKAM27, pKAM43, pKAM45, pKAM48, pKAM49, pKAM52, pKAM57, pKAM58, pKAM59, pKAM84, and pKAM92.



Induced 3NA pKAM27 showed a stronger  $\beta$ -galactosidase activity reduction (aprox. 4,200 Miller units) in comparison with 3NA containing pKAM52, pKAM45, and pKAM84. However, the basal  $\beta$ -galactosidase activity of 3NA pKAM27 remained at 300 Miller units (Fig. 3.27.B). Finally, the base pairs located at the inverted repeat upstream of -35 in  $P_{mItA}$  mutant were exchanged to their complementary sequence to create pKAM92. Addition of mannitol to 3NA pKAM92 indicated slight amount of  $\beta$ -galactosidase activity in which  $P_{mItA}$  was uninducible. Altogether, base pair exchanges between -35 box and the predicted MtlR binding site did not reveal a clear result. Thus, identification of the 3'-end of MtlR binding site in  $P_{mItA}$  was continued by construction of hybrid promoters (Fig. 3.27.B).

### 3.14.5. Construction of hybrid promoters

#### 3.14.5.1. Fusion of the putative ManR binding site of $P_{manP}$ to $P_{mItA}$ core elements

To identify the 3'-end of the MtlR binding site, different hybrid promoters were constructed. At first, it was necessary to have a well-known promoter in which the regulator binding site was well understood. Then, this promoter would be used as a platform for identification of the MtlR binding site. Therefore, the promoter of the mannose operon ( $P_{manP}$ ) in *B. subtilis* was exploited. Plasmids pKAM12 and pSUN284.1 (214), were used as the controls of  $P_{mItA}$  and  $P_{manP}$  activities, respectively. Plasmid pSUN284.1 is a plasmid similar to pKAM12 based on pBS72 replicon in *B. subtilis*, but it carries  $P_{manP}$  rather than  $P_{mItA}$ . Strain 3NA pSUN284.1 was induced by mannose, while 3NA pKAM12 was induced by mannitol. Induction of 3NA pSUN284.1 showed 15,000 Miller units  $\beta$ -galactosidase activity, while the basal  $\beta$ -galactosidase activity was only about 2,000 Miller units (Fig. 3.28.B). Subsequently, the activator binding site of  $P_{manP}$  was fused to the  $P_{mItA}$  core elements (Fig. 3.28.A). For this purpose, the upstream region of -35 box in  $P_{mItA}$  was replaced with the putative ManR binding site of  $P_{manP}$  to obtain the hybrid promoter 11 ( $P_{HP11}$ ). To fuse the  $P_{manP}$  fragment to the  $P_{mItA}$  core elements, oligonucleotides s6504/s6508 and s6509/s6507 were used in PCRs from *B. subtilis* 168 genomic DNA. Fusion PCR was performed by oligonucleotides s6504/s6507 using primary PCR products

## Results

as a template. By insertion of the  $P_{HP11}$  fragment via  $NheI/AflIII$  restriction sites into pSUN279.2, the precursor of pSUN284.1, plasmid pKAM25 was constructed.

A

Plasmid	Promoter		-35		-10		+1
pKAM12	<i>mtlA</i>	TTTTTATTTTAAAAAATGTCACAGTCATGTGCCAAAGTCCTCTTTACTTTCAA	TTGTAT	AGGGACTGTAAGCGTTT	TAACAT	AGAGT	C
pKAM25	$P_{HP11}$	<b>g</b> ttatagggaaaaatgcotttattacoggaacocatggtaaaaaaagcg	TTGTAT	AGGGACTGTAAGCGTTT	TAACAT	AGAGT	C
pKAM30	$P_{HP13}$	<b>a</b> ttatagggaaaaatgcotttattacoggaacocatggtaaaaaaagcg	aTGTAT	AGGGACTGTAAGCGTTT	TAACAT	AGAGT	C
pKAM29	$P_{HP12}$	<b>a</b> ttatagggaaaaatgcotttattacoggaacocatggtaaaaaaagcg	atTTAT	AGGGACTGTAAGCGTTT	TAACAT	AGAGT	C
pKAM62	$P_{HP20}$	<b>a</b> ttatagggaaaaatgcotttattacoggaacocatggtaaaaaaagcg	atTTTT	AGGGACTGTAAGCGTTT	TAACAT	AGAGT	C
pKAM23	$P_{HP9}$	<b>a</b> ttatagggaaaaatgcotttattacoggaacocatggtaaaaaaagcg	atTTTA	AGGGACTGTAAGCGTTT	TAACAT	AGAGT	C
pSUN284.1	<i>manP</i>	<b>a</b> ttatagggaaaaatgcotttattacoggaacocatggtaaaaaaagcg	atTTTA	atgagctgatttcggtat	tacagt	tgagac	a

B

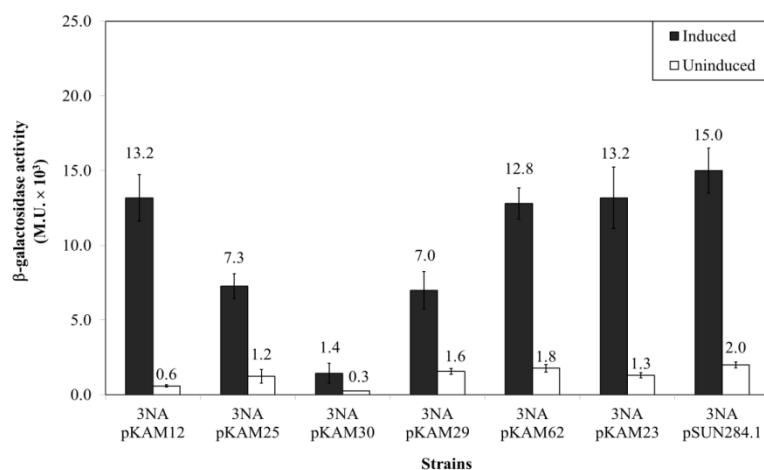


**Fig. 3.28.** (A) The sequences of the  $P_{manP}$ - $P_{mtlA}$  hybrid promoters. The  $P_{mtlA}$  sequence is shown by the capital letter, while  $P_{manP}$  by the bold small letter. (B)  $\beta$ -galactosidase activity of *B. subtilis* 3NA containing pKAM12 ( $P_{mtlA}$ ), pKAM23 ( $P_{HP9}$ ), pKAM25 ( $P_{HP11}$ ), pKAM29 ( $P_{HP12}$ ), pKAM30 ( $P_{HP13}$ ), pKAM62 ( $P_{HP20}$ ), and pSUN284.1 ( $P_{manP}$ ). All of the strains were induced by 0.2% mannose except strain 3NA pKAM12, which was induced by 0.2% mannitol.

After transformation of 3NA by pKAM25, the addition of 0.2% mannose to the 3NA pKAM25 culture showed that 3NA pKAM25 exhibited half of the  $\beta$ -galactosidase activity of 3NA pKAM12, although the basal  $\beta$ -galactosidase activity was doubled (1,200 Miller units). In the next step, the first base pair of the -35 box in  $P_{HP11}$  was replaced with its counterpart from  $P_{manP}$  resulting in promoter  $P_{HP13}$ . Construction of  $P_{HP13}$  was performed using oligonucleotides

s6504/s6652 and s6653/s6507 in PCRs from the chromosome of *B. subtilis* 168. The fusion PCR by using oligonucleotides s6504/s6507 and primary PCR products resulted in  $P_{HP13}$  which was next inserted into pSUN279.2 via *NheI/AflIII* and created pKAM30. Induction of 3NA pKAM30 with mannose showed a low  $\beta$ -galactosidase activity, although the  $P_{HP13}$  activity was inducible by 4-fold. Afterwards, additional base pairs of the -35 box of  $P_{HP13}$  were replaced with the  $P_{manP}$  counterparts by construction of  $P_{HP12}$ , and  $P_{HP20}$ . Plasmids pKAM29 ( $P_{HP12}$ ) and pKAM62 ( $P_{HP20}$ ) were constructed by fusion PCRs from the genomic DNA of *B. subtilis* 168. Oligonucleotides s6504/s6608 and s6609/s6507 (pKAM29) as well as s6504/s6855 and s6507/s6856 (pKAM62) were used for PCRs. Fusion PCRs were carried out using primary PCR products and oligonucleotides s6504/s6507 in both cases. The basal  $\beta$ -galactosidase activity of 3NA pKAM29 with 4 base pairs exchanged in the -35 box was about 1,600 Miller units, while the induced cells showed 7,000 Miller units  $\beta$ -galactosidase activity. Strain 3NA pKAM62 with 5 base pairs exchanged in the -35 box of hybrid promoter had a higher  $\beta$ -galactosidase activity than 3NA pKAM29. In 3NA pKAM62, 12,800 Miller units  $\beta$ -galactosidase activity was measured in the presence of mannose, whereas basal  $\beta$ -galactosidase activity was 1,800 Miller units. Finally,  $P_{HP9}$  was constructed in which the complete sequence of the -35 box was replaced with the  $P_{manP}$  sequence. To construct pKAM23 harboring  $P_{HP9}$ , oligonucleotides s6504/s6510 and s6511/s6507 were used for PCRs from *B. subtilis* 168 genome. The fusion PCR was performed by the primary PCR products, as template, and the s6504/s6507 oligonucleotides. Induction of 3NA pKAM23 indicated a similar  $\beta$ -galactosidase activity to pSUN284.1, although the basal  $\beta$ -galactosidase activity of 3NA pKAM23 was significantly lower (Fig. 3.28.A). Altogether, it is assumed that the ManR binding site overlaps the -35 hexamer. Comparison of the ATTTTA hexamer, the reported -35 box of  $P_{manP}$  (214), with the consensus  $\sigma^A$ -type -35 box (TTGACA) pointed out that  $P_{manP}$  probably has not a real -35 box. Indeed, different promoter structures of  $P_{manP}$  and  $P_{mtlA}$  makes it difficult to construct functional hybrid promoters. Thus, the promoter of *licBCAH* operon was exploited for construction of hybrid promoters.



## Results

A

Plasmid	Promoter		-35		-10	+1
pKAM 160	<i>licB</i>	cagcctgtatatacctttttccggtgctgcggaaaaaccctgag	tggtta	tgaaagcgatttcataa	tatgat	gatagc a
pKAM 161	<i>HP41</i>	TTTTTATTTTTAAAAAATTGTCACAGTCATGTGCCAAAGTCCTCTTTACTTTCAA	tggtta	tgaaagcgatttcataa	tatgat	gatagc a
pKAM 176	<i>HP43</i>	TTTTTATTTTTAAAAAATTGTCACAGTCATGTGCCAAAGTCCTCTTTACTTTgag	tggtta	tgaaagcgatttcataa	tatgat	gatagc a
pKAM 162	<i>HP42</i>	TTTTTATTTTTAAAAAATTGTCACAGTCATGTGCCAAAGTCCTCTTTAccctgag	tggtta	tgaaagcgatttcataa	tatgat	gatagc a

B

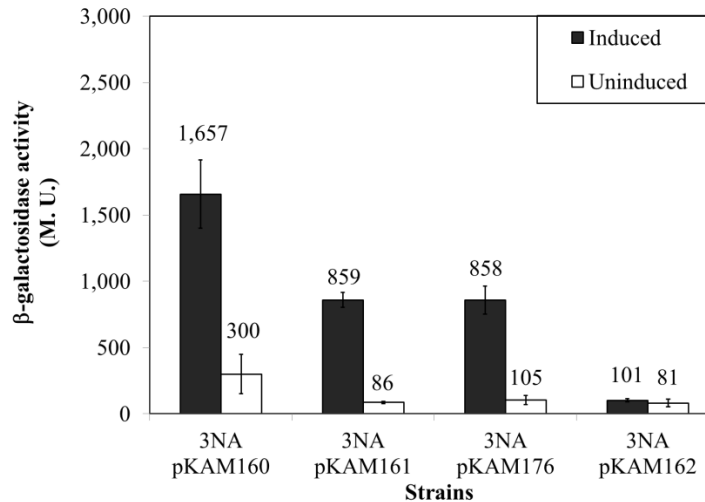


**Fig. 3. 30. (A)** The sequences of the  $P_{mlA}$ - $P_{licB}$  hybrid promoters. The  $P_{mlA}$  sequence is shown by capital letters, while the  $P_{licB}$  sequence by small letters. **(B)**  $\beta$ -galactosidase activity of *B. subtilis* 3NA harboring pKAM160 ( $P_{licB}$ ), pKAM161 ( $P_{HP41}$ ), pKAM162 ( $P_{HP42}$ ), pKAM176 ( $P_{HP43}$ ). Strain 3NA pKAM160 was induced by 0.2% cellobiose, while 3NA pKAM161, 3NA pKAM162, and 3NA pKAM176 were induced by 0.2% mannitol.

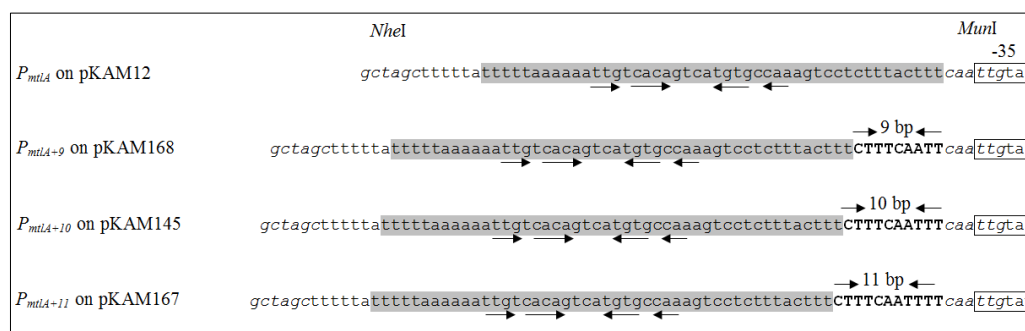
Next, the upstream region of  $P_{mlA}$  beginning exactly at the 5'-end of -35 box was fused to  $P_{licB}$  core elements. Oligonucleotides s6209/s7617 were used to amplify the  $P_{mlA}$  fragment from *B. subtilis* 168 genome, whereas oligonucleotides s7616/s7615 were used for amplification of  $P_{licB}$  fragment by PCR from the chromosome of *B. subtilis* 168. Digestion of the two fragments by *BsaI* was followed by a ligation reaction. Then, the ligated fragments were amplified by oligonucleotides s6209/s7615 in a PCR. Plasmid pKAM161 was constructed by the insertion of the  $P_{mlA}$ - $P_{licB}$  ( $P_{HP41}$ ) fragment into pSUN279.2 via *NheI*/*AflIII* restriction sites. The induced 3NA pKAM161 containing  $P_{HP41}$  showed half of the  $\beta$ -galactosidase activity of 3NA pKAM160 with approximately 860 Miller units. However, the  $P_{HP41}$  remained inducible by mannitol. Afterwards, a change of two base pairs in the heptamer (CAA to GAG) was carried out to construct the hybrid

$P_{HP43}$ . For this purpose, oligonucleotides s7714/s7615 were used in a PCR from the genome of *B. subtilis*. By insertion of the PCR fragment into pSUN279.2 via *NheI/AflIII*, the final vector, called pKAM176, was constructed. Induction of this strain showed no considerable changes to the strain containing  $P_{HP41}$ . Subsequently, next hybrid promoter, *i.e.*  $P_{HP42}$ , was constructed supposing that the heptamer spacer does not belong to the MtlR binding site. Thus, the -35 box and the upstream heptamer sequence of  $P_{licB}$  were fused to the putative MtlR binding site in  $P_{mtlA}$ . Construction of  $P_{HP42}$  was carried out by PCRs from the chromosome of *B. subtilis* 168 using oligonucleotides s6209/s7618 and s7619/s7615. The PCR products were then exploited in a fusion PCR using oligonucleotides s6209/s7615. Plasmid pKAM162 was constructed by the insertion of  $P_{HP42}$  into pSUN279.2 via *NheI* and *AflIII*. Surprisingly, addition of mannitol to the 3NA pKAM162 culture did not induce  $P_{HP42}$  and its  $\beta$ -galactosidase activity was about 80 to 100 Miller units (Fig. 3.30.B). Altogether, shortening of the  $P_{mtlA}$  5'-end and construction of hybrid promoters revealed the putative MtlR binding site (TTTTTAAAAAN<sub>20</sub>AGTCCTCTTTACTTT).

#### 3.14.5.4. Increasing the distance between putative MtlR binding site and -35 box in $P_{mtlA}$

To show whether the putative MtlR binding site overlaps the -35 box, as observed in  $P_{manP}$ , the distance between the -35 box and the putative MtlR binding site in  $P_{mtlA}$  was increased (Fig. 3.31.A). At first,  $P_{mtlA+10}$  was constructed in which the MtlR binding site was relocated 10 bp farther to -35 box than in  $P_{mtlA}$ . This distance corresponds to a complete turn of B-DNA double helix. Oligonucleotides s6209 and s7548 were used in a PCR from pKAM12 in order to amplify the  $P_{mtlA+10}$  fragment. The  $P_{mtlA+10}$  fragment was then inserted into pKAM12 via *NheI* and *MunI* restriction sites to construct pKAM145. Strain 3NA pKAM145 showed only about 800 Miller units  $\beta$ -galactosidase activity in LB with mannitol, while the basal  $\beta$ -galactosidase activity was about 100 Miller units in LB without mannitol (Fig. 3.31.B). Although the distance between MtlR and RNAP was increased,  $P_{mtlA+10}$  remained inducible by 8-fold. By addition of a single base pair, the inserted sequence between putative MtlR binding site and the -35 box increased to 11 bp ( $P_{mtlA+11}$ ).

A



B

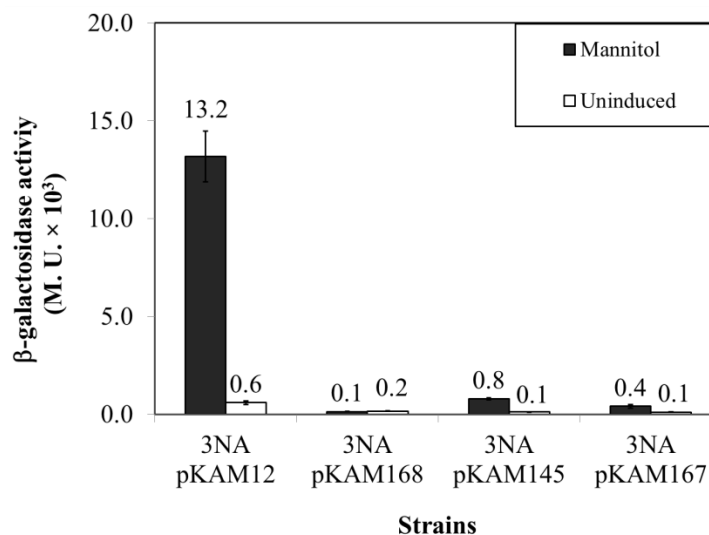


**Fig. 3. 31.** Increasing the distance between putative MtlR binding site and -35 box of  $P_{mtlA}$ . **(A)** Upstream sequence of the -35 box of  $P_{mtlA}$  on pKAM12 and the constructs thereof. **(B)**  $\beta$ -galactosidase activity of strain 3NA harboring pKAM12 ( $P_{mtlA}$ ), pKAM145 ( $P_{mtlA+10}$ ), pKAM167 ( $P_{mtlA+11}$ ), and pKAM168 ( $P_{mtlA+9}$ ).

Amplification of  $P_{mtlA+11}$  was performed by a PCR from pKAM12 using oligonucleotides s6209 and s7678. The  $P_{mtlA+11}$  fragment was inserted into pKAM12 via *NheI* and *MunI* restriction sites and created pKAM167. In the presence of mannitol in LB,  $\beta$ -galactosidase activity of 3NA pKAM167 was reduced to about 400 Miller units. Without mannitol, the basal  $\beta$ -galactosidase activity of 3NA pKAM167 was only about 100 Miller units. This indicated a 4-fold induction of  $P_{mtlA+11}$  activity. In contrast to  $P_{mtlA+11}$ , a single base pair was deleted in  $P_{mtlA+10}$  to construct  $P_{mtlA+9}$ . Amplification of  $P_{mtlA+9}$  was accomplished by a PCR from pKAM12 using

oligonucleotides s6209 and s7679. The  $P_{mrlA+9}$  fragment was then inserted into pKAM12 through *NheI* and *MunI* restriction sites resulting in pKAM168. Only about 150 Miller units  $\beta$ -galactosidase activity was measured when 3NA pKAM168 was cultivated in LB with or without mannitol (Fig. 3.31.B). In other words, by insertion of 9 bp between the -35 box and the putative MtlR binding site, the  $P_{mrlA+10}$  activity became constitutive at a very low level. Altogether, this study showed that  $P_{mrlA}$  remained inducible, even though MtlR binding site was relocated a complete DNA helix turn farther than the wild type locus. This shows that the MtlR binding site does not overlap the -35 box.

#### 3.14.5.5. Confirmation of MtlR binding site by $P_{mrlA}$ - $P_{manP}$ fusion

To confirm the 3'-end of MtlR binding site obtained by construction of  $P_{mrlA}$ - $P_{licB}$  hybrids, the MtlR binding site of  $P_{mrlA}$  was fused to the  $P_{manP}$  core elements (Fig. 3.32.A). As a control, the  $P_{mrlA}$  sequence containing MtlR binding site and the -35 box was fused in a PCR to the sequence between -35 and -10 boxes of  $P_{manP}$ . PCRs from *B. subtilis* 168 genome were performed using oligonucleotides s6209/s6861 and s6862/s6954. Next, primary PCR products were used in a fusion PCR by oligonucleotides s6209/s6954. The PCR product, denoted  $P_{HP23}$ , was then inserted into pSUN279.2 via *NheI/AflIII* restriction sites to create pKAM65. Addition of the mannitol to 3NA pKAM65 culture considerably activated  $P_{HP23}$  by leading to 11,000 Miller units  $\beta$ -galactosidase activity, whereas the basal  $\beta$ -galactosidase activity was only 1,200 Miller units (Fig. 3.32.B). Subsequently, the -35 box and 3 bp upstream of the -35 box in  $P_{HP23}$  were replaced with the  $P_{manP}$  counterparts (see  $P_{HP44}$ ; Fig. 3.32.A). Amplification of  $P_{HP44}$  was performed by oligonucleotides s7800 and s6954 in a PCR from *B. subtilis* 168 chromosome. The  $P_{HP44}$  fragment was then inserted into pSUN279.2 via *NheI/AflIII* (construct pKAM185). Induction of 3NA pKAM185 by mannitol showed 4,200 Miller units  $\beta$ -galactosidase activity in LB, while the basal  $\beta$ -galactosidase activity was only about 300 Miller units (Fig. 3.32.B). In other words,  $P_{HP44}$  was inducible by 14-fold which was even higher than  $P_{HP23}$  (9-fold). However, the weaker activity of  $P_{HP44}$  in comparison with  $P_{HP23}$  could be due to the absence of an optimal -35 box identical to the  $\sigma^A$ -type consensus sequence.



A

Plasmid	Promoter		-35		-10	+1
pKAM65	HP23	TTTTTATTTTTAAAAAATGTCACAGTCATGTGCCAAAGTCCTCTTTACTTTCAA	<b>TTGTAT</b>	atgagotgatttcgta	<b>taoagt</b>	tgagac a
pKAM185	HP44	TTTTTATTTTTAAAAAATGTCACAGTCATGTGCCAAAGTCCTCTTTACTTTgcg	<b>atttta</b>	atgagotgatttcgta	<b>taoagt</b>	tgagac a

B

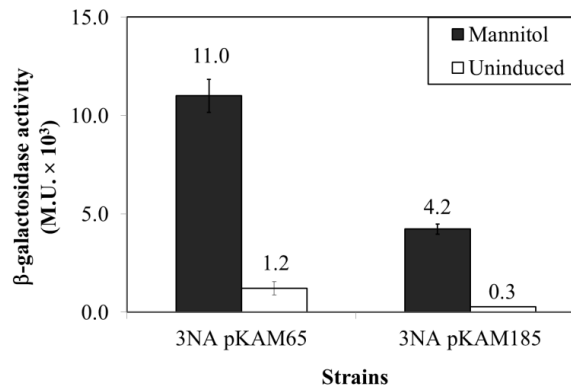


**Fig. 3.32.** (A) The sequences of the  $P_{manP}$ - $P_{mlA}$  hybrid promoters. The  $P_{mlA}$  sequence is shown by capital letters, while  $P_{manP}$  by bold small letters. (B)  $\beta$ -galactosidase activity of *B. subtilis* 3NA harboring pKAM65 ( $P_{HP23}$ ) and pKAM185 ( $P_{HP44}$ ).

### 3.14.6. *In vitro* activity of MtlR

The MtlR binding site located at  $P_{mlA}$  was characterized by the construction of hybrid promoters *in vivo*. Nevertheless, to confirm the identified MtlR binding site *in vitro*, it was necessary to carry out DNase I footprinting. Prior to perform the DNase I footprinting, the electrophoretic mobility shift assay was considered to find out the optimized *in vitro* conditions for the binding of MtlR to  $P_{mlA}$ . Briefly, in an electrophoretic mobility shift assay, the migration of the labeled DNA band is compared to the DNA-protein complex band by a non-denaturing polyacrylamide gel electrophoresis (native PAGE). Formation of the DNA-protein complex results in a slower migration of the complex; therefore, a shifted band appears compared with the labeled DNA without protein as a control. In this study, the Cy5-labeled  $P_{mlA}$  was mixed with the purified MtlR and loaded onto the native PAGE. To yield high amount of purified MtlR, different strategies were exploited for protein expression and purification.

### 3.14.6.1. Expression of *mtlR*-His<sub>6</sub> in *B. subtilis* KM12

To produce MtlR in *B. subtilis*, *mtlR* was inserted downstream of  $P_{mtlA}$  on pKAM12. Furthermore, a His<sub>6</sub>-tag was fused to the C-terminus of MtlR to facilitate the purification of the produced MtlR. The *mtlR*-His<sub>6</sub> fragment was amplified from the genome of *B. subtilis* 168 using oligonucleotides s6686 and s6687. Due to the presence of a *Nde*I restriction site inside the *mtlR* sequence, the forward oligonucleotide primer was extended towards the ribosomal binding site of *lacZ* on pKAM12 in order to insert the *mtlR*-His<sub>6</sub> via *Afl*II/*Xma*I into pKAM12 to construct plasmid pKAM39. As a host, *B. subtilis* KM12 ( $\Delta mtlAF$ ) was used in which  $P_{mtlA}$  was constitutive (section 3.10.2).

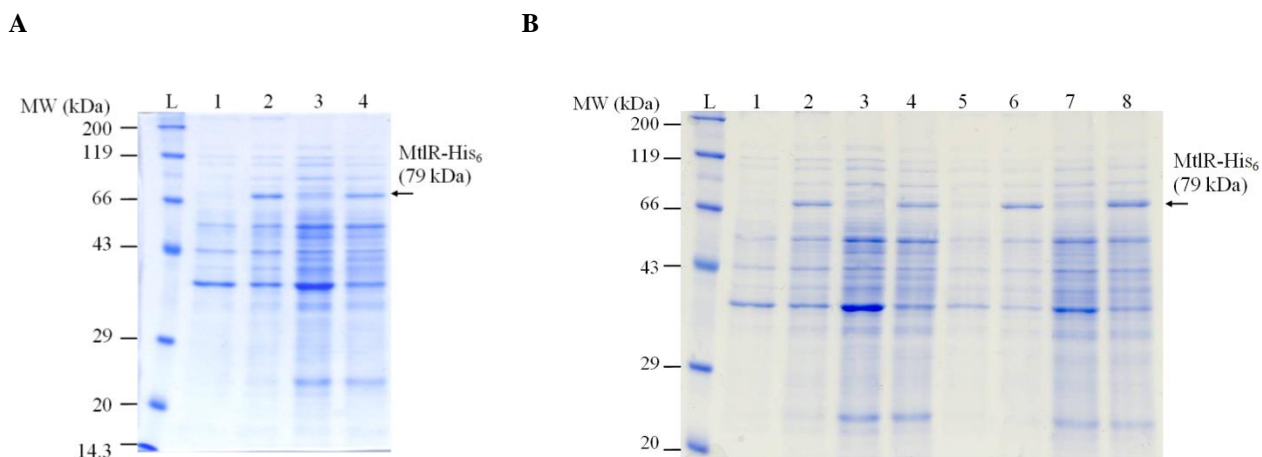


**Fig. 3.33.** The effect of the KM12 pKAM39 incubation temperature on MtlR-His<sub>6</sub> production (A) Expression of *mtlR*-His<sub>6</sub> in *B. subtilis* KM12 ( $\Delta mtlAF$ ) is demonstrated. Strain KM12 pKAM39 was incubated overnight at 37°C. Disruption of the cells was done by high pressure homogenizer. **Lane L:** Roti<sup>®</sup>-Mark Standard; **lane 1:** insoluble fraction of KM12 lysate; **lane 2:** insoluble fraction of KM12 pKAM39 lysate; **lane 3:** soluble fraction of crude extract of KM12; **lane 4:** soluble fraction of crude extract of KM12 pKAM39. (B) Strain KM12 pKAM39 was incubated at 30°C (Lanes 1 – 4) and 25°C (Lanes 5 – 8). **Lane L:** Roti<sup>®</sup>-Mark Standard, **lane 1:** insoluble fraction of KM12 lysate; **lane 2:** insoluble fraction of KM12 pKAM39 lysate; **lane 3:** soluble fraction of crude extract of KM12; **lane 4:** soluble fraction of crude extract of KM12 pKAM39; **lane 5:** insoluble fraction of KM12 lysate; **lane 6:** insoluble fraction of KM12 pKAM39 lysate; **lane 7:** soluble fraction of crude extract of KM12; **lane 8:** soluble fraction of crude extract of KM12 pKAM39.

For production of MtlR, the strain was grown overnight in LB at 37°C. After lysis of KM12 pKAM39 by high pressure homogenizer, soluble and insoluble fractions of the bacterial lysate were analyzed on SDS-PAGE which showed a high amount of MtlR-His<sub>6</sub> in the insoluble fraction (Fig. 3.33.A). This could be due to inclusion bodies formation. Therefore, the bacterial

culture was cultivated at 30°C and 25°C in order to reduce the formation of inclusion body. As shown in Fig. 3.33.B, MtlR-His<sub>6</sub> was produced in less amount of insoluble protein at 25°C. Therefore, KM12 pKAM39 was incubated at 25°C overnight and the bacterial culture harvested for purification of MtlR-His<sub>6</sub>. Purification of the MtlR-His<sub>6</sub> was carried out using Ni-NTA agarose. The flow-through and the wash fractions were analyzed on SDS-PAGE (Fig. 3.34). Elution fraction 2 contained the highest yield of purified MtlR-His<sub>6</sub> with about 4.9 mg/ml. For the electrophoretic mobility shift assay, the purified MtlR-His<sub>6</sub> (elution fraction 2) was diluted to 49 µg/ml using resuspension buffer I (NaH<sub>2</sub>PO<sub>4</sub> 50 mM, NaCl 300 mM, pH 8). The *P<sub>mtlA</sub>* DNA fragment was Cy5-labeled by PCR using oligonucleotides s6209 and 5'-Cy5 s5960 and pKAM12 as a template. Afterwards, the electrophoretic mobility shift reaction was performed by mixing MtlR-His<sub>6</sub> and Cy5-*P<sub>mtlA</sub>*. After incubation on ice for 15 min, the reactions were loaded onto a 6% native polyacrylamide gel. The results indicated a weak shifted band in the presence of MtlR-His<sub>6</sub> (Fig. 3.35). Next, the shift reaction was incubated at the room temperature and on ice. It is shown that the amount of shifted fragment was lower by increasing the temperature (Fig. 3.35). Thereafter, all of the reactions were incubated on ice for at least 15 min.

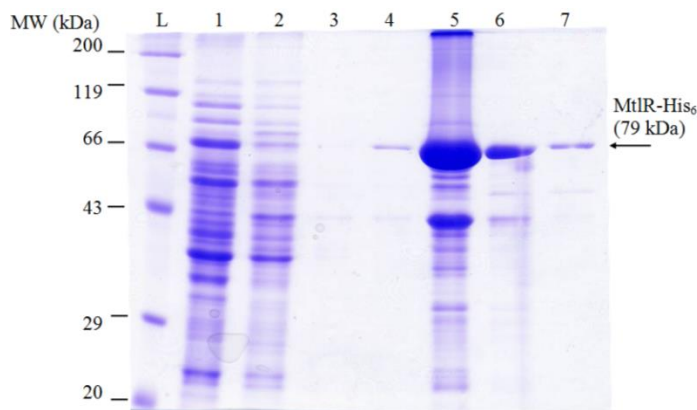


**Fig. 3. 34.** Purification of MtlR-His<sub>6</sub> using Ni-NTA agarose. KM12 pKAM39 was cultivated in LB overnight at 25°C. The cells were disrupted by high pressure homogenizer. Resuspension, washing and elution buffers I were used for affinity chromatography. **Lane L:** Roti<sup>®</sup>-Mark Standard; **lane 1:** flow-through; **lane 2:** wash fraction 1; **lane 3:** wash fraction 2; **lane 4:** elution fraction 1; **lane 5:** elution fraction 2; **lane 6:** elution fraction 3; **lane 7:** elution fraction 4.

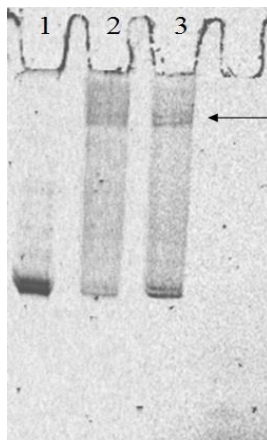


**Fig. 3. 35.** Electrophoretic mobility shift of Cy5-*P<sub>mlA</sub>* DNA fragment (33 fmol) by purified MtlR-His<sub>6</sub> (49 ng) at room temperature and on ice. The reaction was carried out using shift buffer A in a total volume of 10  $\mu$ l. After incubation on ice for 15 min, the Cy5-*P<sub>mlA</sub>* and MtlR-His<sub>6</sub> mixture was loaded on 6% native polyacrylamide gel. **Lane 1:** Cy5-*P<sub>mlA</sub>*; **lane 2:** Cy5-*P<sub>mlA</sub>* and MtlR-His<sub>6</sub> incubated on ice; **lane 3:** Cy5-*P<sub>mlA</sub>* and MtlR-His<sub>6</sub> incubated at RT.

To enhance the intensity of the Cy5-*P<sub>mlA</sub>* shifted band, electrophoretic mobility shift of Cy5-*P<sub>mlA</sub>* was repeated in shift buffer B (238) (Fig. 3.36.A). In comparison with shift buffer A, shift buffer B lacked EDTA and MgCl<sub>2</sub>. Moreover, the pH of the shift buffer B was also 7.5. The results indicated no significant difference between shift buffer A and B. Altogether, changing the shift buffer, incubation temperature and MtlR-His<sub>6</sub> concentration did not improve the mobility shift reaction. Therefore, the crude extract of strain KM12 pKAM39 was considered in order to investigate whether the MtlR-His<sub>6</sub> is inactivated during the purification process. For this purpose, the crude extract of strain KM12 pKAM39 was added to Cy5-*P<sub>mlA</sub>* DNA, rather than purified MtlR-His<sub>6</sub>. In this case, a weak Cy5-*P<sub>mlA</sub>* shifted band was obtained in the presence of KM12 pKAM39 crude extract (Fig. 3.36.B).

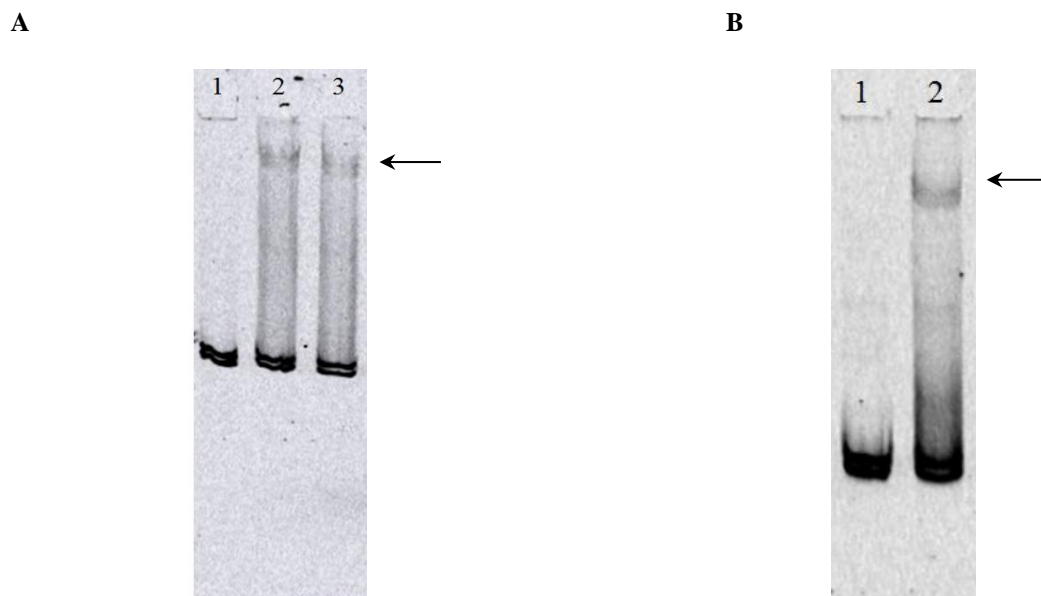


**Fig. 3. 36.** (A) Electrophoretic mobility shift of Cy5- $P_{mtlA}$  DNA fragment by the purified MtlR-His<sub>6</sub> using shift buffer B. **Lane 1:** Cy5- $P_{mtlA}$  (50 fmol); **lane 2:** Cy5- $P_{mtlA}$  (50 fmol) and MtlR-His<sub>6</sub> (25 ng); **lane 3:** Cy5- $P_{mtlA}$  (50 fmol) and MtlR-His<sub>6</sub> (51 ng). (B) Electrophoretic mobility shift of Cy5- $P_{mtlA}$  (50 fmol) by 2  $\mu$ l of KM12 pKAM39 crude extract. KM12 pKAM39 was incubated overnight at 25°C in LB. The cells were concentrated (OD<sub>600</sub> of 36) and disrupted by high pressure homogenizer as explained in methods. Shift buffer B was added in a total reaction volume of 10  $\mu$ l. **Lane 1:** Cy5- $P_{mtlA}$ ; **Lane 2:** Cy5- $P_{mtlA}$  and crude extract.

To confirm the specificity of the observed shifted band by the crude extract, a hybrid promoter was constructed in which the MtlR binding site of  $P_{mtlA}$  was replaced with ManR binding site of  $P_{manP}$ . Oligonucleotides s6504 and s6505 were used to amplify the ManR binding site of  $P_{manP}$  from the chromosomal DNA of *B. subtilis* 168 by PCR. Also, the  $P_{mtlA}$  core elements were amplified from the *B. subtilis* 168 chromosomal DNA by PCR using oligonucleotides s6506 and s6507. Next, oligonucleotides s6504/s6507 were applied in a fusion PCR using amplified ManR binding site and  $P_{mtlA}$  core elements as the templates. The final  $P_{manP}$ - $P_{mtlA}$  fragment (called  $P_{HP7}$ ) was inserted into pSUN279.2 via *NheI/AflIII* (pKAM21). Using pKAM21 as a template, the Cy5- $P_{HP7}$  fragment was amplified by oligonucleotides s6504 and 5'-Cy5-labeled s5959 in a PCR (Fig. 3.37.A). Electrophoretic mobility shift of Cy5- $P_{mtlA}$  DNA was carried out using the crude extract of KM12 pKAM39, while Cy5- $P_{HP7}$  DNA was a negative control. The addition of KM12 pKAM39 crude extract weakly shifted the Cy5- $P_{mtlA}$  band, whereas no Cy5- $P_{HP7}$  shifted band was observed (Fig. 3.37.B). Therefore, the reduced mobility of Cy5- $P_{mtlA}$  band was obviously due

to the presence of MtlR-His<sub>6</sub> in the crude extract. In summary, the expression of *mtlR*-His<sub>6</sub> in KM12 strain resulted in a weak shift of Cy5-*P<sub>mtlA</sub>* band using purified MtlR-His<sub>6</sub> or crude extract of KM12 pKAM39. Consequently, the overproduced MtlR-His<sub>6</sub> in KM12 was not fully active which could be due to the presence of a His<sub>6</sub>-tag at the C-terminus of MtlR. Alternatively, the phosphoryl bonds of the phosphorylated histidines in PRDII of MtlR could be labile. To overcome the latter obstacle, MtlR-H342D-His<sub>6</sub> mutant was overproduced in *B. subtilis* KM12.

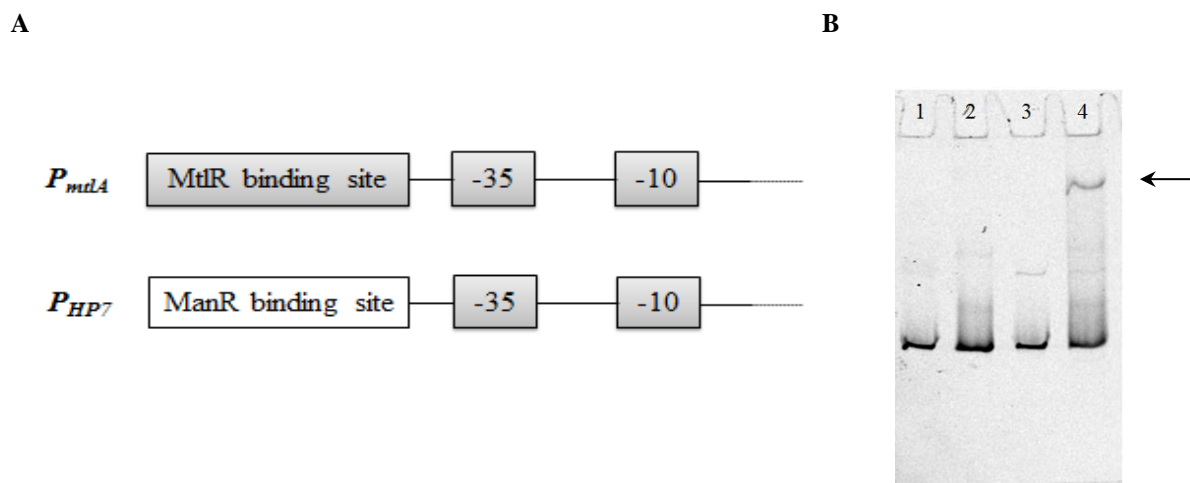


**Fig. 3.37.** (A) The schematic view of *P<sub>mtlA</sub>* and *P<sub>HP7</sub>*. (B) Electrophoretic mobility shift assay of Cy5-*P<sub>mtlA</sub>* (50 fmol) or Cy5-*P<sub>HP7</sub>* (50 fmol) DNA using 2  $\mu$ l of KM12 pKAM39 crude extract. The cells were concentrated to an OD<sub>600</sub> of 18 and disrupted by high pressure homogenizer as explained in methods. Shift buffer B was added in a total reaction volume of 10  $\mu$ l. **Lane 1:** Cy5-*P<sub>HP7</sub>*; **lane 2:** Cy5-*P<sub>HP7</sub>* and crude extract; **lane 3:** Cy5-*P<sub>mtlA</sub>*; **lane 4:** Cy5-*P<sub>mtlA</sub>* and crude extract.

#### 3.14.6.2. Expression of *mtlR*-H342D-His<sub>6</sub> in *B. subtilis* KM12

The low intensity of the shifted Cy5-*P<sub>mtlA</sub>* band in the presence of the purified MtlR-His<sub>6</sub> or crude extract of KM12 pKAM39 indicated a weak activity of the activator protein. It was assumed that the phosphate covalently bound to histidine 342 at PRDII of MtlR was labile. Therefore, the histidine 342 was mutated to an aspartic acid which is a phosphoryl histidine mimic as shown by *in vivo* studies (section 3.13.3). By this means, the probable inactivation of the MtlR due to dephosphorylation of PRDII during the purification process was prevented. His 342 was mutated to aspartic acid by oligonucleotides s6686/s6865 and s6866/s6687 in PCRs using the chromosomal DNA of *B. subtilis* 168 as a template. The primary PCR products were

then used in a fusion PCR by oligonucleotides s6686/s6687. The final PCR product, *mtlR*-H342D-His<sub>6</sub> DNA, was then inserted into pKAM12 using *Afl*III and *Xma*I restriction sites (plasmid pKAM93). After transformation of KM12 by pKAM93, the crude extract of the KM12 pKAM93 was used in an electrophoretic mobility shift assay. The Cy5-*P*<sub>*mtlA*</sub> DNA was clearly shifted in the presence of the KM12 pKAM93 crude extract, while Cy5-*P*<sub>*HP7*</sub> DNA was not shifted (Fig. 3.38).

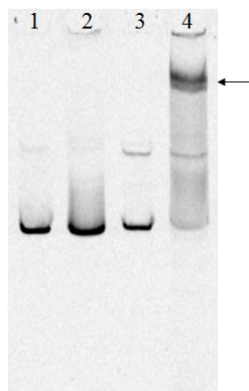


**Fig. 3. 38.** Electrophoretic mobility shift of 50 fmol of Cy5-*P*<sub>*HP7*</sub> DNA (negative control) and 50 fmol of Cy5-*P*<sub>*mtlA*</sub> DNA (sample) using cleared crude extract of KM12 pKAM93. The KM12 pKAM93 producing MtlR-H342D-His<sub>6</sub> was cultivated at 25°C and the bacterial culture was harvested after an overnight incubation. The disruption of KM12 pKAM93 (OD<sub>600</sub> of 17.5) was accomplished by the high pressure homogenizer and the cleared crude extract was used for electrophoretic shift studies. Shift buffer B was used in this study. **Lane 1:** Cy5-*P*<sub>*HP7*</sub>; **lane 2:** Cy5-*P*<sub>*HP7*</sub> and cleared crude extract; **lane 3:** Cy5-*P*<sub>*mtlA*</sub>; **lane 4:** Cy5-*P*<sub>*mtlA*</sub> and cleared crude extract.

Afterwards, the overexpressed MtlR-H342D-His<sub>6</sub> protein was purified by Ni-NTA column. Similar to the experiment with MtlR-His<sub>6</sub>, only a low amount of Cy5-*P*<sub>*mtlA*</sub> DNA was shifted by the purified MtlR-H342D-His<sub>6</sub> protein. Addition of MgCl<sub>2</sub> (shift buffer C), changing the purification buffer from NaH<sub>2</sub>PO<sub>4</sub> pH 8 (affinity chromatography buffer 1) to HEPES pH 7.4 (affinity chromatography buffer 2), as well as addition of the protease inhibitor and β-mercaptoethanol could not improve the binding of MtlR-H342D-His<sub>6</sub> to the DNA (data not shown). Obviously, the MtlR-H342D-His<sub>6</sub> protein was active in the crude extract, but not after purification. Hence, the fusion of His<sub>6</sub>-tag had no influence on the MtlR activity. It was assumed that the purification by Ni-NTA column damaged the MtlR-H342D-His<sub>6</sub> protein maybe due to the oxidation of MtlR, especially cysteine residues. Among them, cysteine 419 plays a vital role for

the MtlR activity. Therefore, MtlR mutants, *i.e.* MtlR-H342D and MtlR-H342D C419A, were purified using anion exchange chromatography. Further expression and purification strategies are summarized in table 3.1.

**Table 3. 1.** Expression of *mtlR* mutant genes with different promoters in different hosts and their purification.

Mutant	Expression promoter	Host	Purification
<i>mtlR</i> -H342D	<i>P<sub>mtlA</sub></i>	<i>B. subtilis</i> KM12	All mutant proteins were purified by anion exchange chromatography
<i>mtlR</i> -H342D	<i>rhaP<sub>BAD</sub></i>	<i>E. coli</i> JM109	
<i>mtlR</i> -H342D C419A	<i>P<sub>mtlA</sub></i>	<i>B. subtilis</i> 3NA	
<i>mtlR</i> -H342D C419A	<i>rhaP<sub>BAD</sub></i>	<i>E. coli</i> JM109	
<b><i>mtlR</i>-H342D C419A</b>	<b><i>rhaP<sub>BAD</sub></i></b>	<b><i>E. coli</i> JW2409-1</b>	

### 3.14.6.3. Expression of *mtlR*-H342D C419A in *E. coli* JW2409-1

In the presence of mannitol, the conserved cysteine 419 located at the EIIB<sup>Gat</sup> domain of MtlR is dephosphorylated by EIIA<sup>Mtl</sup>. *In vivo* studies showed that mutation of the cysteine 419 to alanine caused strong constitutive, but still CCR repressible MtlR activity (107). *In vivo*, H342D mutation significantly reduced the catabolite repression in MtlR (section 3.13.3). Therefore, both mutations were combined. Due to the mutations, the MtlR-H342D C419A activity should be independent from the phosphorylation. Thus, *mtlR*-H342D C419A was expressed in *E. coli*. The cysteine 419 was mutated to alanine in a fusion PCR. Oligonucleotides s7303/s7301 and s7302/s7304 were applied in PCRs using pKAM93 (*P<sub>mtlA</sub>-mtlR*-H342D) as a template. The fusion PCR was performed by oligonucleotides s7303/s7304 and the primary PCR products as the template. The amplified *mtlR*-H342D C419A fragment was then inserted into pJOE6089.4 (see appendices), a plasmid with moderate copy numbers based on pBR322 origin of replication, via *AflIII/XmaI* to construct pKAM182. In pKAM182, the expression of the *mtlR*-H342D C419A was under the control of *rhaP<sub>BAD</sub>*, a rhamnose-inducible promoter in *E. coli* (84). Next, *E. coli* JW2409-1 lacking the enzyme I (EI) of the PTS system was transformed with pKAM182. Strain JW2409-1 pKAM182 was cultivated in LB at 37°C, induced by 0.2% L-rhamnose, and incubated overnight. The cells were harvested and resuspended in 20 mM Tris-HCl (pH 8) and disrupted by sonication. Afterwards, crude extract of JW2409-1 pKAM182 was used for electrophoretic mobility shift assay. The results indicated that the crude extract of JW2409-1 pKAM182 is able to shift the Cy5-*P<sub>mtlA</sub>* DNA fragment, whereas *P<sub>HP7</sub>* DNA fragment (negative control) showed no



mobility shift (Fig. 3.39). Additionally, Cy5-labeled  $P_{mtlR}$  as well as  $'P_{mtlR}$  DNA were also tested.  $'P_{mtlR}$  was a 5'-shortened  $P_{mtlR}$  in which half of the MtlR binding site was removed. Oligonucleotides s5799/s5959 ( $P_{mtlR}$ ) and s6799/s5959 ( $'P_{mtlR}$ ) were used to amplify the Cy5-labeled DNA fragments by PCR from pKAM18 and pKAM51, respectively. Similar to Cy5- $P_{mtlA}$ , the Cy5- $P_{mtlR}$  band was also shifted in the presence of JW2409-1 pKAM182 crude extract. In contrast, the  $'P_{mtlR}$  fragment was not shifted (Fig. 3.39).

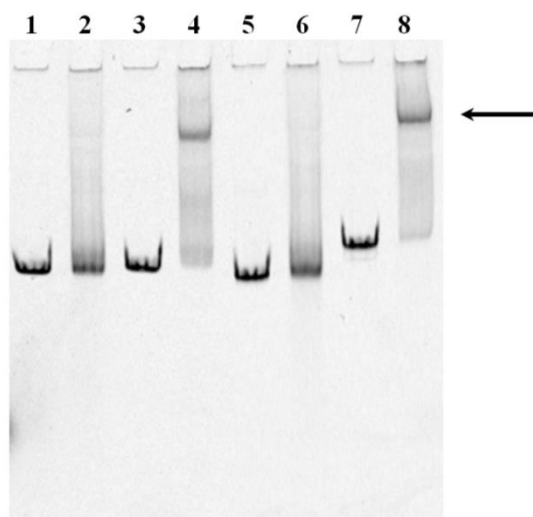


**Fig. 3. 39.** Electrophoretic mobility shift assay of Cy5- $P_{mtlA}$  DNA (150 fmol) and Cy5- $P_{mtlR}$  DNA (150 fmol) by 6  $\mu$ l crude extract of JW2409-1 pKAM182 (10 mg/ml) containing MtlR-H342D C419A. Shift reaction was performed in a total volume of 50  $\mu$ l harboring shift buffer D. As negative controls, DNA of Cy5- $P_{HP7}$  (150 fmol) and Cy5- $'P_{mtlR}$  (150 fmol) were applied. **Lane 1:** Cy5- $P_{HP7}$ ; **lane 2:** Cy5- $P_{HP7}$  and crude extract; **lane 3:** Cy5- $P_{mtlA}$ ; **lane 4:** Cy5- $P_{mtlA}$  and crude extract; **lane 5:** Cy5- $'P_{mtlR}$ ; **lane 6:** Cy5- $'P_{mtlR}$  and crude extract; **lane 7:** Cy5- $P_{mtlR}$ ; and **lane 8:** Cy5- $P_{mtlR}$  and crude extract.

Next, the crude extract of JW2409-1 pKAM182 was used for anion exchange chromatography. None of the collected fractions, however, shifted Cy5- $P_{mtlA}$  or Cy5- $P_{mtlR}$  bands. Mobility shift attempts by changing the purification buffer (Buffer A<sub>2</sub> and B<sub>2</sub> instead of A<sub>1</sub> and B<sub>1</sub>) and addition of 1 mM tris (2-carboxyethyl) phosphine (TCEP) as a reducing agent also failed. Finally, the expression of *mtlR*-H342D C419A was done at 30°C. In this case, a protein peak appeared in the flow-through fractions of the anion exchange chromatography diagram. This peak was not observed when the cells were cultivated and induced at 37°C. Next, all fractions obtained by

anion exchange chromatography were used in electrophoretic mobility shift assays using Cy5-*P<sub>mtlA</sub>* DNA (Fig. 3.40). Interestingly, the Cy5-*P<sub>mtlA</sub>* band was shifted by the flow-through fractions. SDS- PAGE analysis showed an almost purified band in the flow-through fractions corresponding to 78 kDa (Fig. 3.41.A). Fraction 3 was used for further studies.

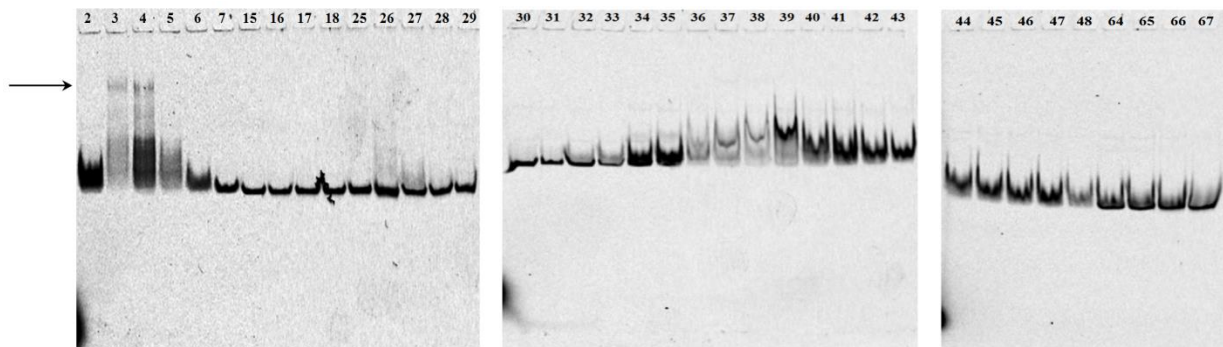


**Fig. 3. 40.** Electrophoretic mobility shift of Cy5-*P<sub>mtlA</sub>* DNA by the fractions obtained by anion exchange chromatography of JW2409-1 pAM182 crude extract. Strain JW2409-1 pKAM182 expressing *mtlR*-H342D C419A was induced by 0.2% L-rhamnose. The cells were incubated at 30°C overnight. Anion exchange chromatography was performed by buffers A<sub>2</sub> and B<sub>2</sub>. 20 µl of each fraction (fractions 2 – 67) was added to 200 fmol Cy5-*P<sub>mtlA</sub>* DNA fragment. The reaction was performed in a total volume of 50 µl using shift buffer D. The fractions 2 – 67 are represented by the numbers on top of each lane, while shifted band is demonstrated by an arrow.

Next, Cy5-labeled *P<sub>HP7</sub>*, *P<sub>mtlA</sub>*, *P<sub>mtlR</sub>*, and *P<sub>mtlR</sub>* DNA fragments were used in an electrophoretic mobility shift assay using purified MtlR-H342D C419A (fraction 3). The results indicated a clear shift of the Cy5-*P<sub>mtlA</sub>* and Cy5-*P<sub>mtlR</sub>* bands, whereas no shift was observed for the Cy5-*P<sub>HP7</sub>* and Cy5-*P<sub>mtlR</sub>* bands as negative controls (Fig. 3.41.B). Next, several concentrations of the purified MtlR-H342D C419A were used in order to determine the lowest amount of MtlR-H342D C419A necessary for the complete shift of Cy5-*P<sub>mtlA</sub>* band. It was shown that at least 390 ng of MtlR-H342D C419A corresponding to 4.95 pmol was necessary for a complete shift of 100 fmol Cy5-*P<sub>mtlA</sub>* fragment (Fig. 3.42.A). Likewise, non-labeled *P<sub>mtlA</sub>* was amplified by PCR using oligonucleotides s5526/s5527 from the genome of *B. subtilis* 168. Addition of the amplified unlabeled *P<sub>mtlA</sub>* DNA inhibited the shift of Cy5-*P<sub>mtlA</sub>* band (Fig. 3.42.B).

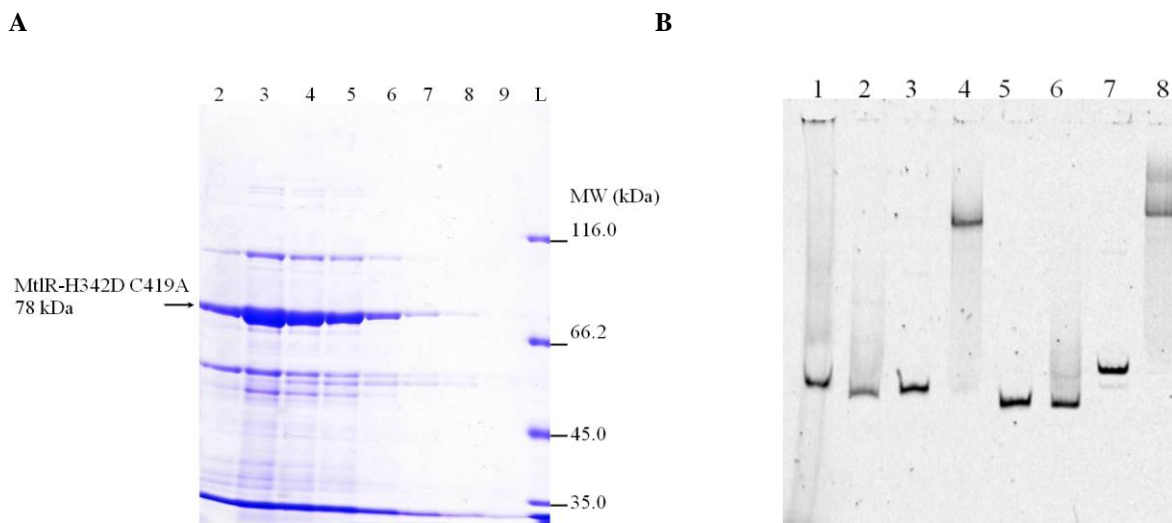


**Fig. 3. 41.** (A) SDS-PAGE analysis (8% gel) of the early fractions of anion exchange chromatography of crude extract of strain JW2409-1 pKAM182. Fractions 2 – 9 are represented on top of each lane, while L demonstrates the unstained protein molecular weight marker (Fermentas). (B) Electrophoretic mobility shift of DNA containing Cy5- $P_{HP7}$  (100 fmol), Cy5- $P_{mlA}$  (100 fmol), Cy5- $P_{mlR}$  (100 fmol), and Cy5- $P_{mlR}$  (100 fmol) by purified MtlR-H342D C419A (23  $\mu$ l, 130 ng/ml). The reaction was performed in a total volume of 50  $\mu$ l using shift buffer D. **Lane 1:** Cy5- $P_{HP7}$ ; **lane 2:** Cy5- $P_{HP7}$  and MtlR-H342D C419A; **lane 3:** Cy5- $P_{mlA}$ ; **lane 4:** Cy5- $P_{mlA}$  and MtlR-H342D C419A; **lane 5:** Cy5- $P_{mlR}$ ; **lane 6:** Cy5- $P_{mlR}$  and MtlR-H342D C419A; **lane 7:** Cy5- $P_{mlR}$ ; **lane 8:** Cy5- $P_{mlR}$  and MtlR-H342D C419A.

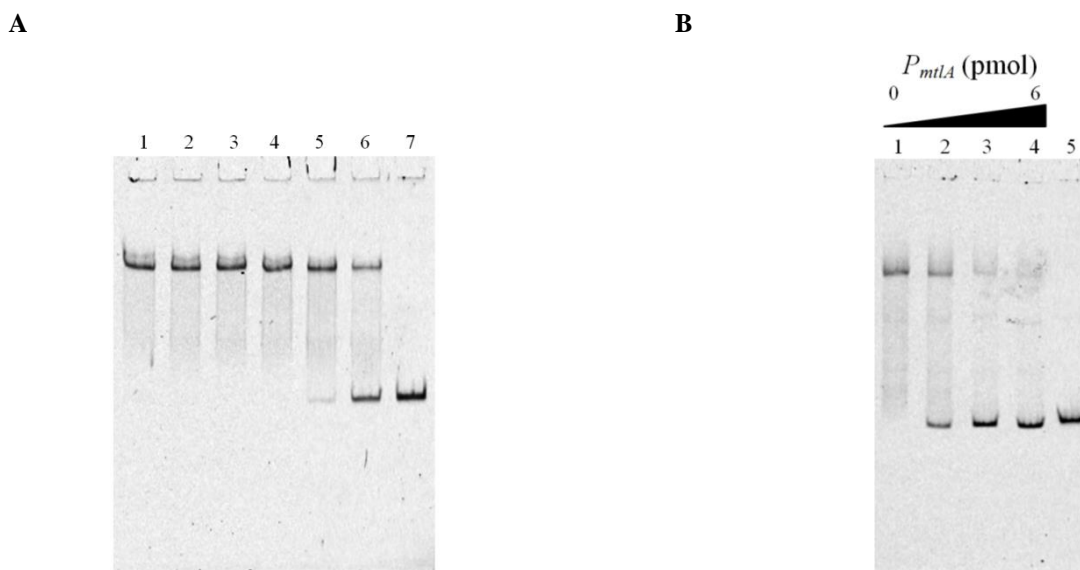


**Fig. 3. 42.** (A) Electrophoretic mobility shift of Cy5-labeled  $P_{mlA}$  DNA fragment by purified MtlR-H342D C419A. 100 fmol of Cy5- $P_{mlA}$  DNA was mixed with different concentrations of purified MtlR-H342D C419A, namely 780 ng (lane 1), 650 ng (lane 2), 520 ng (lane 3), 390 ng (lane 4), 260 ng (lane 5), 130 ng (lane 6), and without MtlR-H342D C419A (lane 7). (B) Electrophoretic mobility shift of Cy5- $P_{mlA}$  DNA (100 fmol) in the presence of unlabeled  $P_{mlA}$  fragment as a competitor. Unlabeled  $P_{mlA}$  DNA was added with the concentrations 0 pmol (lane 1), 2 pmol (lane 2), 4 pmol (lane 3), 6 pmol (lane 4). As a control, no MtlR-H342D C419A was added to the Cy5- $P_{mlA}$  fragment (lane 5). MtlR-H342D C419A was added to the reaction after mixing the Cy5-labeled  $P_{mlA}$  and unlabeled  $P_{mlA}$  DNA fragments. All of the reactions were carried out in a total volume of 50  $\mu$ l using shift buffer D.

### 3.14.7. Function of the $P_{mtlA}$ and $P_{mtlR}$ *cre* sites and their mutants

Catabolite responsive element (*cre*) is the binding site of the CcpA-HPr(S46~P) complex. Analyses of the  $P_{mtlA}$  and  $P_{mtlR}$  sequences revealed putative *cre* sites overlapping their -10 boxes. The function of these *cre* sites was investigated by mutation of their sequences. As demonstrated in Fig. 3.43, each of the *cre* sites of  $P_{mtlA}$  and  $P_{mtlR}$  comprise 3 mismatches compared with the consensus *cre* sequence. Thus, the *cre* sites of  $P_{mtlA}$  and  $P_{mtlR}$  were first of all mutated to repair the mismatches and construct perfect *cre* sites ( $P_{mtlA}^{cre+}$  and  $P_{mtlR}^{cre+}$ ; Fig. 3.43).  $P_{mtlA}^{cre+}$  was constructed by PCRs from *B. subtilis* 168 genome using oligonucleotides s6209/s6654 and s6655/s6213. Next, a fusion PCR was carried out by the primary PCR products and oligonucleotides s6209/s6213. The  $P_{mtlA}^{cre+}$  fragment was finally inserted into pSUN279.2 via *NheI/AflIII* (pKAM31). Similarly,  $P_{mtlR}^{cre+}$  was generated by PCRs from the chromosome of *B. subtilis* 168 using oligonucleotides s5799/s6664 and s6665/s6392. Afterwards, the primary PCR products were used in a fusion PCR by oligonucleotides s5799/s6392. The  $P_{mtlR}^{cre+}$  fragment was inserted into pSUN279.2 through *NheI/AflIII* restriction sites (pKAM33). Unexpectedly, strains 3NA pKAM31 ( $P_{mtlA}^{cre+}$ ) and 3NA pKAM33 ( $P_{mtlR}^{cre+}$ ) indicated low  $\beta$ -galactosidase activity. Strain 3NA pKAM31 showed about 21 Miller units, while strain 3NA pKAM33 produced only 4 Miller units  $\beta$ -galactosidase activity. Besides,  $P_{mtlA}^{cre+}$  and  $P_{mtlR}^{cre+}$  were not inducible. It was likely that the mutation of the mismatches located at the Pribnow box of  $P_{mtlA}$  and  $P_{mtlR}$  led to such a deficiency.

<i>cre</i> consensus		wWTGNAARCGNWWWCA <sub>w</sub> w
<i>cre</i> consensus sequence (Group A)		wWTGNAANCGNWWNCA <sub>w</sub> w
<i>cre</i> consensus sequence (Group B)		wWTGAAARCGYTTWNN <sub>w</sub> w
<i>P<sub>mtlA</sub></i>	pKAM12	a <b>CT</b> GTAAGCGTTTT <b>AA</b> ca
<i>P<sub>mtlA cre+</sub></i>	pKAM31	a[ <b>A</b> ]TGTAAGCGTTTT[ <b>CA</b> ]a
<i>P<sub>mtlA cre-</sub></i>	pKAM32	a <b>CAC</b> TAAG <b>GC</b> TTTT <b>AA</b> ca
<i>P<sub>mtlR</sub></i>	pKAM18	<b>c</b> TTGAAAGCGTTTT <b>AT</b> at
<i>P<sub>mtlR cre+</sub></i>	pKAM33	[ <b>t</b> ]TTGAAAGCGTTTT[ <b>CA</b> ]at
<i>P<sub>mtlR cre-</sub></i>	pKAM34	<b>c</b> T <b>AC</b> AAAG <b>GC</b> TTTT <b>AT</b> at

**Fig. 3. 43.** Consensus sequences of *cre* sites including group A and B, the *cre* sequences of *P<sub>mtlA</sub>* and *P<sub>mtlR</sub>*, and mutants thereof. Mismatches to consensus sequence are represented by bold letters. Mutations in the sequence of the promoters (-10 box and spacer sequence) are enclosed by rectangles. Improvements of the *cre* sites of *P<sub>mtlA</sub>* and *P<sub>mtlR</sub>* into the consensus query are *P<sub>mtlA cre+</sub>* (pKAM31) and *P<sub>mtlR cre+</sub>* (pKAM33), while the disruptions are *P<sub>mtlA cre-</sub>* (pKAM32) and *P<sub>mtlR cre-</sub>* (pKAM34). **N**: any base; **W**: A or T; **R**: A or G; **Y**: C or T.

Afterwards, the position of the mutated *cre* sites was changed in order to facilitate the base pair exchanges without affecting -10 boxes. At first, the *cre* sites of *P<sub>mtlA</sub>* and *P<sub>mtlR</sub>* were completely placed in the spacer sequence of *P<sub>mtlA</sub>* and *P<sub>mtlR</sub>* (Fig. 3.44). The new promoters, denoted *P<sub>mtlA cre</sub>*<sup>\*(-35 and -10)</sup> and *P<sub>mtlR cre</sub>*<sup>\*(-35 and -10)</sup>, were constructed by fusion PCRs. PCRs from *B. subtilis* 168 genomic DNA was carried out using oligonucleotides s6209/s6709 and s6710/s6213 (*P<sub>mtlA cre</sub>*<sup>\*(-35 and -10)</sup>). The final PCR was accomplished by primary PCR products and oligonucleotides s6209/s6213. Similarly, PCRs from the chromosome of *B. subtilis* 168 were performed by oligonucleotides s5799/s6711 and s6712/s6392. Next, *P<sub>mtlR cre</sub>*<sup>\*(-35 and -10)</sup> was generated by final PCR using primary PCR products and oligonucleotides s5799/s6392. Plasmids pKAM40 (*P<sub>mtlA cre</sub>*<sup>\*(-35 and -10)</sup>) and pKAM41 (*P<sub>mtlR cre</sub>*<sup>\*(-35 and -10)</sup>) were constructed by the insertion of the amplified fragments into pSUN279.2 via *NheI/AflIII*. Strain 3NA pKAM40 showed approximately 300 Miller units  $\beta$ -galactosidase activity, whereas 3NA pKAM41 had expressed only 20 Miller units  $\beta$ -galactosidase activity. Moreover, both of the promoters were no longer inducible.

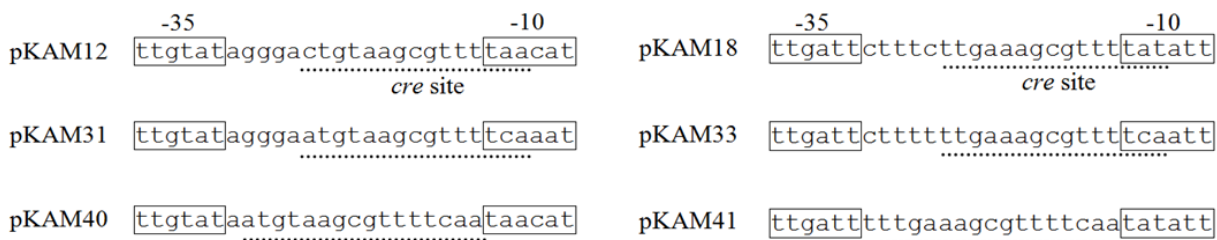


**Fig. 3. 44.** Adaptation of the spacer sequence between -35 and -10 in  $P_{mtlA}$  and  $P_{mtlR}$  to the *cre* consensus sequence and new positioning the newly generated *cre* sequence. The spacer sequence of  $P_{mtlA}$  (pKAM12),  $P_{mtlA}^{cre+}$  (pKAM31), and  $P_{mtlA}^{cre-(-35 \text{ and } -10)}$  (pKAM40), as well as the spacer sequence of  $P_{mtlR}$  (pKAM18),  $P_{mtlR}^{cre+}$  (pKAM33), and  $P_{mtlR}^{cre-(-35 \text{ and } -10)}$  (pKAM41) are demonstrated. Plasmids pKAM12 and pKAM18 showed the wild type *cre* sites, whereas pKAM31 and pKAM33 contained the improved *cre* sites. In pKAM40 and pKAM41, the improved *cre* sites were resided exactly between -35 and -10 boxes without overlapping -10 boxes in  $P_{mtlA}$  and  $P_{mtlR}$ .

In addition, the *cre* sites of  $P_{mtlA}$  and  $P_{mtlR}$  were mutated to disrupt the binding of the CcpA-HPr(S46~P) complex. Disruption of the *cre* site of  $P_{mtlA}$  was accomplished using oligonucleotides s6209/s6656 and s6657/s6213 in PCRs from the *B. subtilis* chromosomal DNA. The  $P_{mtlA}^{cre-}$  fragment was generated by a fusion PCR using the primary PCR products and oligonucleotides s6209/s6213. Likewise, the *cre* site of  $P_{mtlR}$  was mutated. Oligonucleotides s5799/s6666 and s6667/s6392 were used for PCRs from the genomic DNA of *B. subtilis* 168. By a fusion PCR using the primary PCR products and oligonucleotides s5799/s6392,  $P_{mtlR}^{cre-}$  was generated. Insertion of  $P_{mtlA}^{cre-}$  and  $P_{mtlR}^{cre-}$  into pSUN279.2 was performed via *NheI/AflII* to construct pKAM32 and pKAM34, respectively.  $\beta$ -galactosidase activities of 3NA pKAM32 and 3NA pKAM34 were measured after cultivation in LB (Fig. 3.45.A and Fig. 3.45.B). For induction, mannitol (0.2%) was added with or without 0.2% glucose to the bacterial culture. Interestingly,  $\beta$ -galactosidase activity of 3NA pKAM32 ( $P_{mtlA}^{cre-}$ ) was identical to 3NA pKAM12. Strain 3NA pKAM34 ( $P_{mtlR}^{cre-}$ ) exhibited a higher  $\beta$ -galactosidase activity (135 Miller units) in comparison to 3NA pKAM18. The addition of glucose to the induced 3NA pKAM34 culture reduced the  $\beta$ -galactosidase activity to 39 Miller units, while this amount was only about 19 Miller units in 3NA pKAM18. Due to a higher maximal activity of  $P_{mtlR}^{cre-}$ , it cannot be concluded that the  $P_{mtlR}$  *cre* site in the wild type strain is functional.

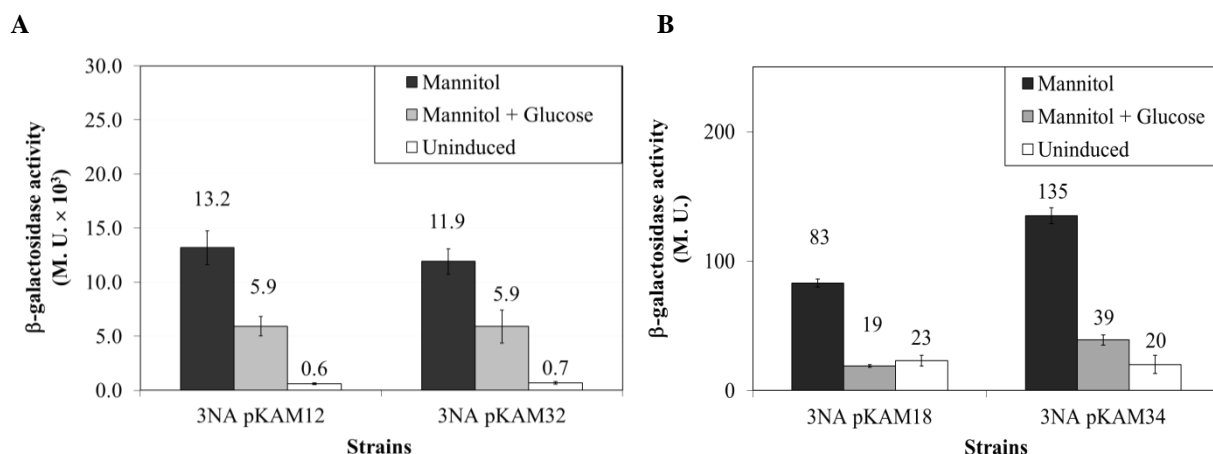
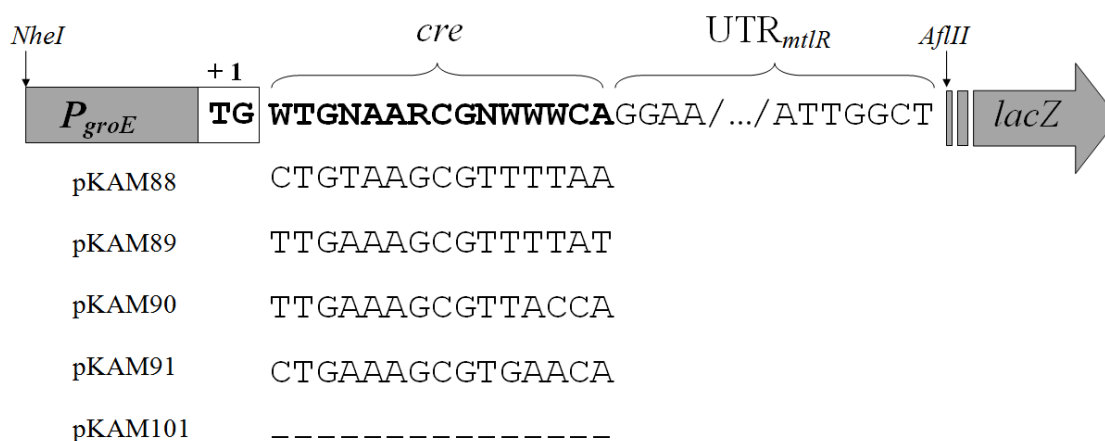


**Fig. 3.45.** Disruption of the *cre* sites of  $P_{mtlA}$  and  $P_{mtlR}$ . **(A)**  $\beta$ -galactosidase activity of 3NA pKAM12 ( $P_{mtlA}$ ) and 3NA pKAM32 ( $P_{mtlA}$  *cre*-) is shown. **(B)**  $\beta$ -galactosidase activity of 3NA pKAM18 ( $P_{mtlR}$ ) was compared to 3NA pKAM34 ( $P_{mtlR}$  *cre*-).

### 3.14.8. Fusion of $P_{groE}$ to *cre* sites

Mutation of the *cre* sites overlapping -10 box as well as new positioning of the *cre* sites significantly affected the  $P_{mtlA}$  and  $P_{mtlR}$  activities. Besides, expression of *mtlR* in the genome of *B. subtilis* could interfere with the obtained results due to the presence of a potential *cre* site in  $P_{mtlR}$ . Therefore, a constitutive promoter was used which was neither influenced by the CcpA-dependent CCR nor MtlR transcription activation. The promoter of the *groELS* operon ( $P_{groE}$ ) encoding the large and small subunits of GroEL chaperone is negatively regulated by a protein called HrcA (193, 197). The binding site of the HrcA is located at the UTR of the *groEL* mRNA; therefore, deletion of the mRNA leader sequence of  $P_{groE}$  resulted in a strong constitutive promoter activity. Therefore, this strong promoter activity might be blocked by the presence of a *cre* site located at the +1 of the UTR sequence in a road block mechanism. By using  $P_{groE}$  core elements, the function of the *cre* sites of  $P_{mtlA}$  and  $P_{mtlR}$  were compared to the already studied *cre* site of  $P_{acsA}$ . The *acsA* encoding an acetyl-CoA synthetase is regulated by the CcpA-dependent catabolite repression (80, 262). Additionally, there is another reported *cre* site located inside the coding frame of *mtlA* (44). This *cre* site, denoted  $cre_{mtlA}$ , was also studied. The UTR of  $P_{mtlR}$ -*lacZ* on pKAM18 was fused to  $P_{groE}$  core elements (Fig. 3.46.A).

A



B

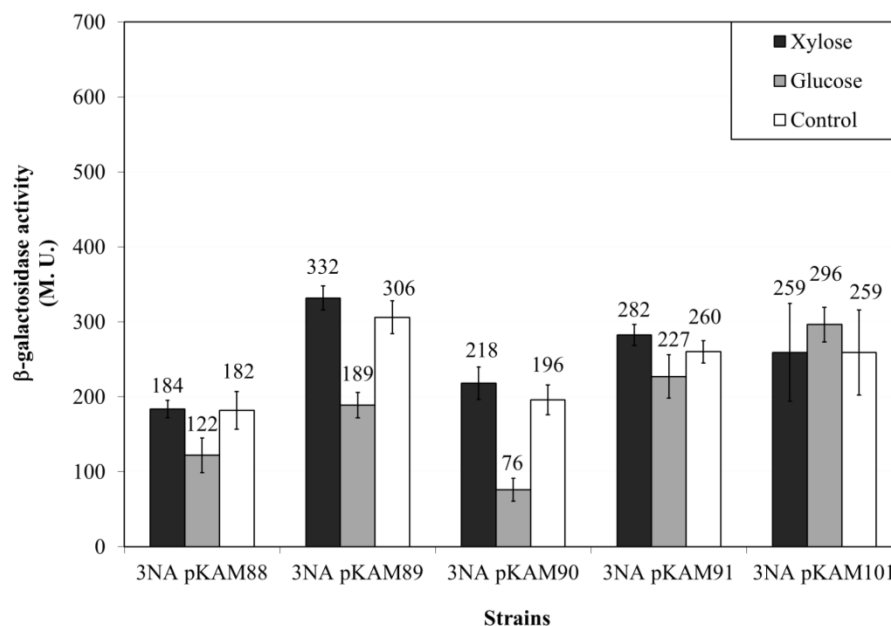


**Fig. 3. 46.** Function of the *cre* sites of *P<sub>mtlA</sub>*, *P<sub>mtlR</sub>*, *P<sub>acsA</sub>*, and *mtlA*. **(A)** Fusion of the *cre* sites of *P<sub>mtlA</sub>* (pKAM88), *P<sub>mtlR</sub>* (pKAM89), *P<sub>acsA</sub>* (pKAM90), and internal *cre* site of *mtlA* (pKAM91) to *P<sub>groE</sub>* and *UTR<sub>mtlR</sub>*. The construct pKAM101 shows the direct fusion of untranslated region of *P<sub>mtlR</sub>* (*UTR<sub>mtlR</sub>*) to the *P<sub>groE</sub>*. **(B)**  $\beta$ -galactosidase activity of strain 3NA harboring pKAM88, pKAM89, pKAM90, pKAM91, and pKAM101 in the presence of 0.2% glucose or 0.2% xylose. No sugar was added to the control. The cells were cultivated in LB at 37°C and the sugars were added at the  $OD_{600}$  of 0.4.  $\beta$ -galactosidase activity was measured 1 h after the addition of the sugars.

PCRs were performed by oligonucleotides s7098/s7189 and s7190/s6392 using genomic DNA of *B. subtilis* 168 as a template. *P<sub>groE</sub>-cre<sub>PmtlA</sub>* fragment was generated by fusion PCR using



oligonucleotides s7098/s6392 and the primary PCR product. Similarly, oligonucleotides s7098/s7191 and s7192/s6392 ( $P_{groE-cre_{PmtlR}}$ ), s7098/s7193 and s7194/s6392 ( $P_{groE-cre_{PacsA}}$ ), and s7098/s7195 and s7196/s6392 ( $P_{groE-cre_{mtlA}}$ ) were used for PCRs from the chromosome of *B. subtilis* 168. The final  $P_{groE-cre-UTR_{mtlR}}$  fusions were generated by oligonucleotides s7098/s6392 and the primary PCR products. As a negative control,  $P_{groE}$  was directly fused to the  $UTR_{mtlR}$ . Oligonucleotides s7098/s7237 and s7238/s6392 were used for PCRs from *B. subtilis* 168 chromosomal DNA. The  $P_{groE-UTR_{mtlR}}$  fragment was amplified in a fusion PCR by oligonucleotides s7098/s6392 and the primary PCR products. All of the  $P_{groE-cre-UTR_{mtlR}}$  fragments were then inserted into pSUN279.2 via *NheI/AflIII* (Fig. 3.46.A).  $\beta$ -galactosidase activity of strains 3NA pKAM88 ( $P_{groE-cre_{PmtlA}}$ ), 3NA pKAM89 ( $P_{groE-cre_{PmtlR}}$ ), 3NA pKAM90 ( $P_{groE-cre_{PacsA}}$ ), and 3NA pKAM91 ( $P_{groE-cre_{mtlA}}$ ) were compared to 3NA pKAM101 ( $P_{groE-UTR_{mtlR}}$ ) in the presence of xylose or glucose in LB (Fig. 3.46.B). The results indicated that  $cre_{PmtlA}$  on pKAM88 and  $cre_{PmtlR}$  on pKAM89 could reduce the  $P_{groE}$  activity by 1.5- and 1.7-fold in the presence of glucose, while this amount was about 2.8-fold in  $P_{acsA}$ . Strain 3NA pKAM101, the negative control, showed the same  $\beta$ -galactosidase activity in LB with or without glucose. Strain 3NA pKAM91 showed a 1.3-fold  $\beta$ -galactosidase activity reduction in LB with glucose. Therefore, it is assumed that the *mtlA* internal *cre* site has no biological function.

### 3.15. Expression system based on mannitol regulatory elements

#### 3.15.1. Optimization of -10 box in $P_{mtlA}$

The -10 box of  $P_{mtlA}$  was mutated to the  $\sigma^A$  consensus sequence (TATAAT) in order to increase the  $P_{mtlA}$  activity. Basically, isomerization of the dsDNA takes place at -10. Presence of a cytosine residue in the -10 box changes the stacking energies. As a consequence, unwinding of dsDNA and development of an open complex might be negatively affected in  $P_{mtlA}$ . Optimization of the Pribnow box of  $P_{mtlA}$  was carried out by using oligonucleotides s6209/s6713 and s6714/s6213 for PCRs from *B. subtilis* 168 chromosome. In the next step, fusion PCR was accomplished by using oligonucleotides s6209/s6213 and primary PCR products. The  $P_{mtlA}$  fragment comprising an optimized -10 box was then inserted into pSUN279.2 via *NheI/AflIII* to

construct pKAM42.  $\beta$ -galactosidase activity of 3NA pKAM42 was measured after cultivation in LB with or without mannitol (Fig. 3.47). Induced 3NA pKAM42 gave 11,700 Miller units  $\beta$ -galactosidase activity, whereas the basal  $\beta$ -galactosidase activity was about 2,100 Miller units. The intended optimization of the -10 box tripled the basal activity of  $P_{mtlA}$ , but maximal activity was about the same as with the induced  $P_{mtlA}$ . Hence,  $P_{mtlA}$  core elements were not altered for further studies.

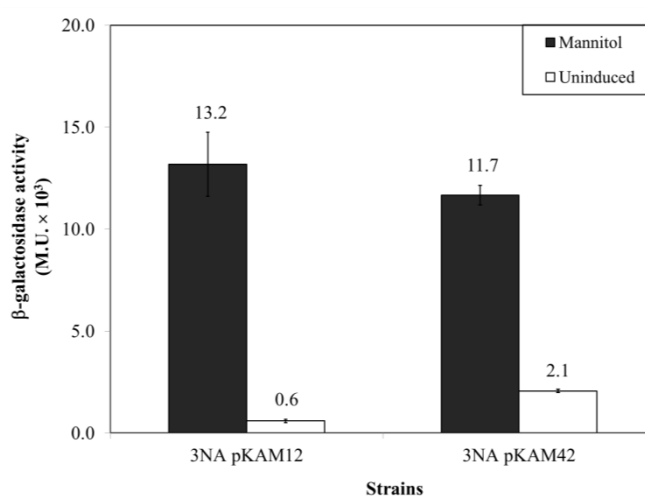


**Fig. 3. 47.** Intended optimization of -10 box of  $P_{mtlA}$ . The  $\beta$ -galactosidase activity of strain 3NA harboring pKAM12 ( $P_{mtlA}$  with wild type -10 box) and pKAM42 ( $P_{mtlA}$  with optimized -10 box).

### 3.15.2. Shortening the 5'UTR in $P_{mtlA}$ -*lacZ* mRNA

It was shown that shortening of the 5'UTR of  $P_{mtlA}$ -*lacZ* mRNA increased the  $\beta$ -galactosidase activity probably by enhancing the translational initiation efficiency (section 3.3). Further shortening of the 5'UTR of  $P_{mtlA}$ -*lacZ* mRNA on pKAM12 was carried out in order to enhance the  $\beta$ -galactosidase production. Interestingly, deletion of the first 10 bp from the 5'UTR of  $P_{mtlA}$ -*lacZ* mRNA on pKAM12 increased the  $\beta$ -galactosidase activity. Oligonucleotides s6209 and s6794 were used to amplify  $P_{mtlA}$  from *B. subtilis* 168 chromosome. The shortened  $P_{mtlA}$  was inserted into pSUN279.2 via *NheI/AflIII* to create pKAM50 (Fig. 3.48.A). After induction of the 3NA pKAM50, 16,000 Miller units  $\beta$ -galactosidase activity were achieved, while uninduced cells

showed about 800 Miller units (Fig. 3.48.B). Further deletion of the 5'UTR<sub>*P<sub>mtlA</sub>-lacZ*</sub> was accomplished by PCR with oligonucleotides s6209/s6727 and the chromosome of *B. subtilis* 168 as template. By insertion of the PCR fragment via *NheI/AflIII* into pSUN279.2, pKAM44 was constructed. Unlike 3NA pKAM12 and 3NA pKAM50, 3NA pKAM44 induced cells showed a reduction in  $\beta$ -galactosidase activity. Induced 3NA pKAM44 expressed only 3,500 Miller units  $\beta$ -galactosidase activity. Thus, shortened *P<sub>mtlA</sub>* on pKAM50 was used for further studies.

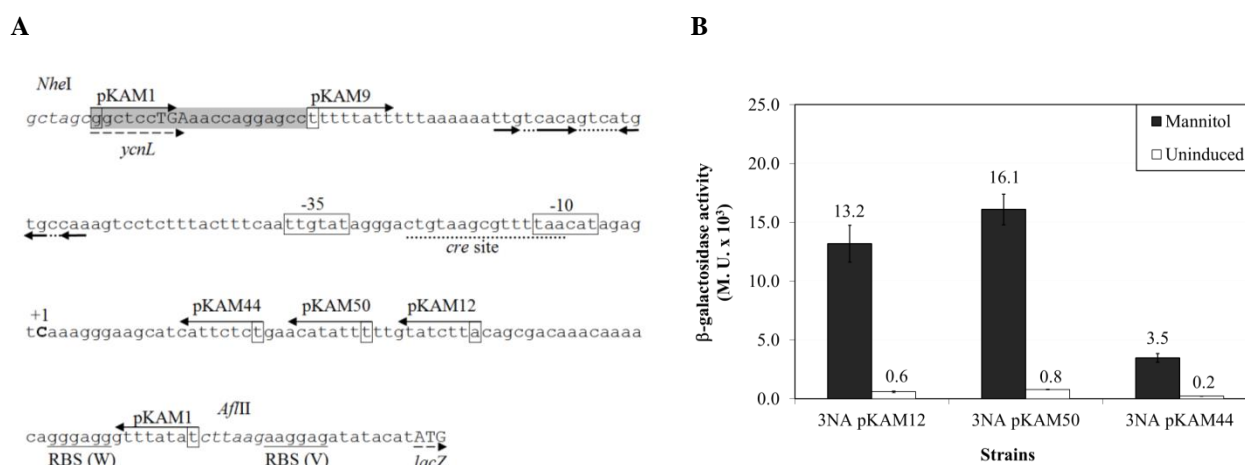


**Fig. 3. 48.** (A) *P<sub>mtlA</sub>* on pKAM12 and constructs thereof shortened at the UTR from 3'-end. The first base pair of each shortened *P<sub>mtlA</sub>* is enclosed by an arrow and a rectangle. (B)  $\beta$ -galactosidase activity of strain 3NA harboring pKAM12, pKAM44 and pKAM50.

### 3.15.3. Construction of expression vectors based on pUB110

So far, all of the studies on *P<sub>mtlA</sub>* and *P<sub>mtlR</sub>* were accomplished based on a low copy replicon, pBS72. In order to construct an expression vector with *P<sub>mtlA</sub>*, a high copy number vector was employed. Plasmid pMW168.1 was used as the vector backbone (242). This plasmid is a derivative of pUB110 (*ori<sub>pUB110</sub>*) originated from *Staphylococcus aureus* (119). Plasmid pMW168.1 contains a spectinomycin resistant gene originated from *Enterococcus faecalis*, an *ori<sup>+</sup>* of pUB110, and finally *gsiB* translational initiation region (*TIR<sub>gsiB</sub>*) fused to eGFP (Fig. 3.49; see appendices). By PCR from genomic DNA of *B. subtilis* 168, *P<sub>mtlA</sub>* was amplified using oligonucleotides s7355/s7620. Similarly, *P<sub>mtlR</sub>* was amplified employing oligonucleotides s7621/s7622. The PCR products were next inserted into pMW168.1 via *AgeI/BglIII*. In this way,



### 3.15.4. Improvement of the expression vector based on *P<sub>mtlA</sub>*

To optimize the activity of *P<sub>mtlA</sub>* on a pUB110 derivative, the *P<sub>mtlA</sub>* sequence on pKAM50 with its shortened 5'UTR originating from *mtlA* was inserted into the pMW168.1 to replace *P<sub>manP</sub>* and 5'UTR<sub>*gsiB*</sub>. The *P<sub>mtlA</sub>* fragment was amplified by PCR from pKAM50 using oligonucleotides s7355/s7356. The PCR fragment was inserted into pMW168.1 via *AgeI/AflIII* (pKAM144). Induced 3NA pKAM144 showed a 1.5-fold stronger fluorescence intensity than 3NA pKAM163 with about 1500 RFU (Fig. 3.50.A). Also, basal fluorescence intensity of 3NA pKAM144 was 3-fold higher than 3NA pKAM163. Plasmid pKAM144 lacked a *NdeI* restriction site at the start codon of the eGFP reporter gene. Therefore, plasmid pKAM114 was constructed in order to generate a *NdeI* restriction site at the start codon (Fig. 3.50.B).

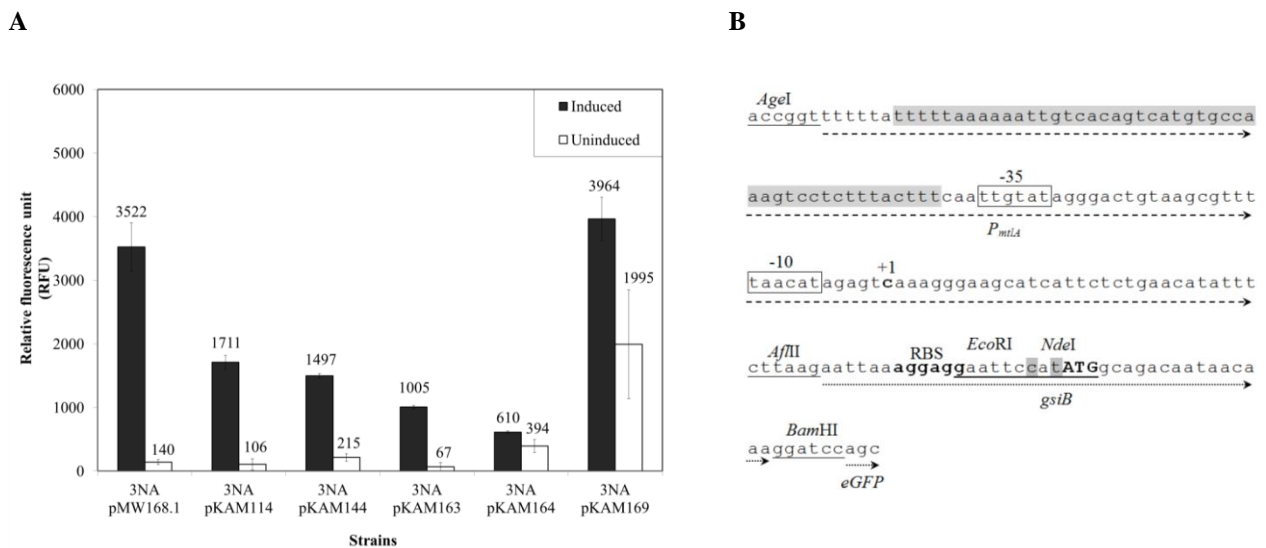


**Fig. 3. 50.** (A) Expression of eGFP in *B. subtilis* 3NA by *P<sub>manP</sub>* (pMW168.1), *P<sub>mtlA</sub>* (pKAM114, pKAM144, pKAM163, and pKAM169), or *P<sub>mtlR</sub>* (pKAM164). pKAM163 (contains *P<sub>mtlA</sub>*-UTR<sub>*manP*</sub>) and pKAM164 (contains *P<sub>mtlR</sub>*-UTR<sub>*manP*</sub>) were constructed by insertion of *P<sub>mtlA</sub>* and *P<sub>mtlR</sub>* core elements (without their UTR sequence) via *AgeI/BglIII* into pMW168.1. Insertion of *P<sub>mtlA</sub>* with its own UTR sequence (*P<sub>mtlA</sub>*-UTR<sub>*mtlA*</sub>) via *AgeI/AflIII* into pMW168.1 resulted in pKAM144. Construction of the *NdeI* site in pKAM144 led to creation of pKAM114. Insertion of *P<sub>mtlR</sub>*-*mtlR* into pKAM114 resulted in pKAM169. The bacterial culture was induced by mannose (*P<sub>manP</sub>*) or mannitol (*P<sub>mtlA</sub>*) at the OD<sub>600</sub> of 0.4 and the fluorescence intensity was measured after 6 h. (B) The *P<sub>mtlA</sub>* sequence on pKAM114. The restriction sites are underlined. The proposed MtlR binding site is gray highlighted. The Pribnow box and -35 box are enclosed by rectangles. The transcription start site (+1) and the ribosomal binding site (RBS) are shown by bold letters. The start codon of GsiB-eGFP hybrid protein is demonstrated by bold capital letter. The gene sequences are depicted by dashed arrows. Mutations for construction of *NdeI* restriction site are highlighted in gray.

Oligonucleotide s7355 and s7356 were used in a PCR from pKAM50 to amplify  $P_{mtlA}$ -TIR<sub>gsiB</sub> fragment. Oligonucleotide s7356 contained the *gsiB* ribosomal binding site and the initially translated codons of pMW168.1 as a tail (Fig. 3.49). The  $P_{mtlA}$ -TIR<sub>gsiB</sub> fragment was then inserted into pMW168.1 via *AgeI/BamHI* (Fig. 3.50.B). Strain 3NA pKAM114 produced about 1,711 RFU of eGFP in the presence of mannitol. The induction by mannitol was 16-fold compared to uninduced 3NA pKAM114. Despite the fact that eGFP production increased, the 3NA pKAM114 produced still half of the 3NA pMW168.1 fluorescence intensity (Fig. 3.50.A).

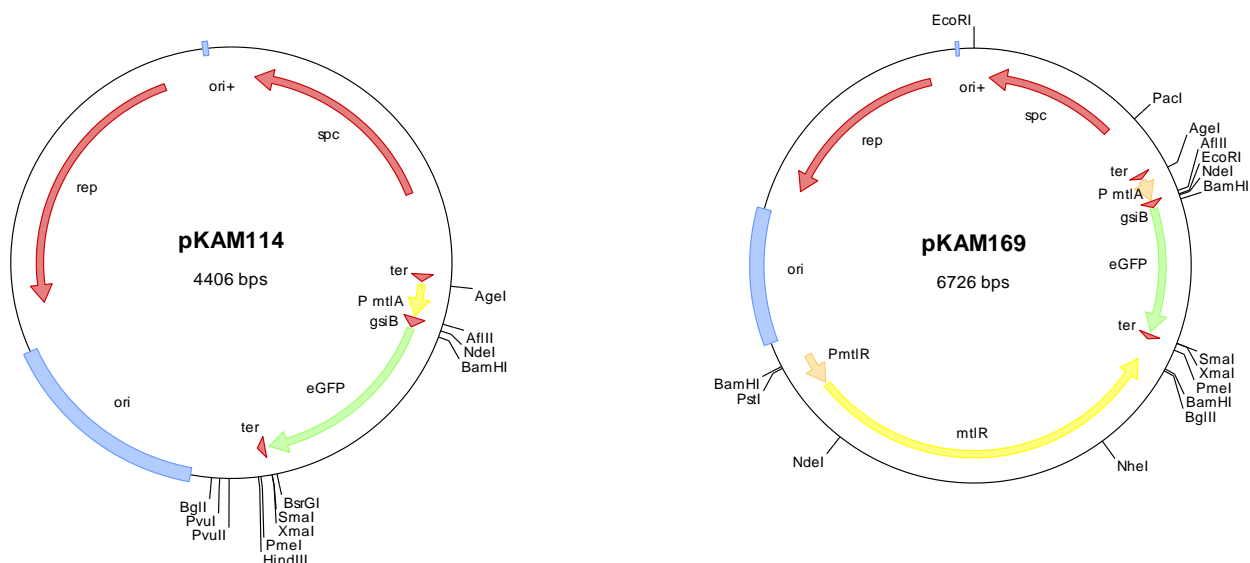


**Fig. 3. 51.** The plasmid map of pKAM114 harboring  $P_{mtlA}$  and its derivative pKAM169.

Lower activity of  $P_{mtlA}$  on pKAM114 in comparison with  $P_{manP}$  on pMW168.1 could be due to the lower amount of its activator in the cell. Comparison of the  $P_{manR}$  activity and  $P_{mtlR}$  activity on pBS72 derivatives expressing *lacZ* showed that  $P_{manR}$  on pSUN291 (214) was about 22 times stronger than  $P_{mtlR}$  on pKAM3. Thus, the single  $P_{mtlR}$ -*mtlR* copy on the chromosome might not express enough MtlR to activate  $P_{mtlA}$  in all of the pKAM114 copies. To increase the number of MtlR in the cell, the activator gene with its own promoter ( $P_{mtlR}$ -*mtlR*) was inserted into pKAM114. The  $P_{mtlR}$ -*mtlR* DNA cassette was amplified by PCR from *B. subtilis* 168 genome using oligonucleotides s5656/s5657. The fragment was then inserted into pJOE4786.1 which was

already cut by *Sma*I (pKAM01). Plasmid pKAM01 was then cut by *Bam*HI and the overhangs of the 2.3 kb fragment were filled in by Klenow polymerase. Next, pKAM114 was digested by *Pvu*II. By insertion of *P<sub>mtlR</sub>-mtlR* into pKAM114 DNA, plasmid pKAM169 was obtained. The plasmid map of pKAM114 and pKAM169 are depicted in Fig. 3.51. Induction of 3NA pKAM169 showed boosted fluorescence intensity in comparison with 3NA pKAM114. The fluorescence intensity of induced 3NA pKAM169 was about 3900 RFU which was slightly higher than of 3NA pMW168.1. However, the basal fluorescence intensity of the 3NA pKAM169 was considerably higher than of 3NA pMW168.1 (14-fold). Altogether, the results indicated that increasing the number of low copy MtlR in the cell, increased *P<sub>mtlA</sub>* activity. However, high basal activity of *P<sub>mtlA</sub>* on pKAM169 makes this expression system less suitable for industrial applications.

## 4. Discussion

### 4.1. Structure and transcription activation of $P_{mtlA}$ and $P_{mtlR}$

In this study, regulation of expression of the *mtlAFD* operon and its activator encoding gene (*mtlR*) in *B. subtilis* was investigated. For this purpose, the promoters of *mtlAFD* ( $P_{mtlA}$ ) and *mtlR* ( $P_{mtlR}$ ) were fused to *lacZ*. Both of these promoters were highly inducible by mannitol and glucitol. To clarify the structures of  $P_{mtlA}$  and  $P_{mtlR}$ , their transcription start sites were at first identified. Characterization of the transcription start sites of  $P_{mtlA}$  and  $P_{mtlR}$  indicated that both of these promoters contain conserved -10 and -35 boxes resembling  $\sigma^A$ -type promoter structure. Besides, a 17 bp spacer sequence was located between the -35 and -10 boxes in  $P_{mtlA}$  as well as in  $P_{mtlR}$ . Previously,  $P_{manP}$  and  $P_{manR}$  of mannose PTS and  $P_{licB}$  and  $P_{licR}$  of lichenan PTS, all of which are activated by PRD-containing activators, were also shown to have a  $\sigma^A$ -type structure (214, 221). Transcription initiation at  $P_{mtlA}$  and  $P_{mtlR}$  is activated by binding of MtlR to the promoters. Prior to this study, a 37 bp MtlR binding site in  $P_{mtlA}$  was proposed by Watanabe *et al.* (239) based on the MtlR binding site in *G. stearothermophilus*  $P_{mtlA}$  (Fig. 4.1) (94).

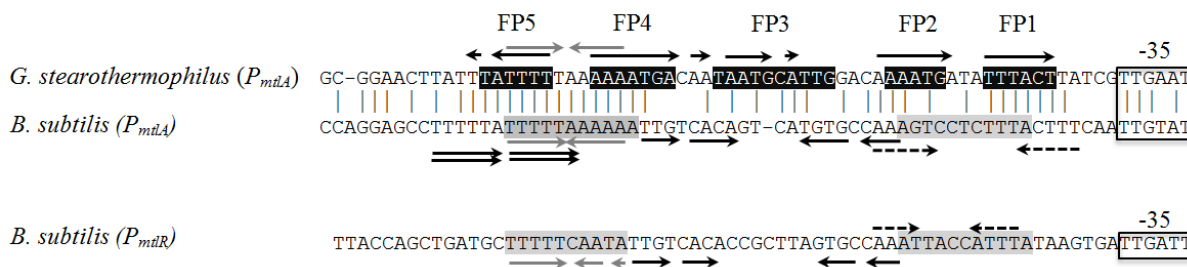


**Fig. 4. 1.** -35 box and its upstream sequence in *G. stearothermophilus*  $P_{mtlA}$  as well as in *B. subtilis*  $P_{mtlA}$  and  $P_{mtlR}$ . The regions identified by DNA footprint are shown by FP1 – FP5 and the sequences are highlighted in black. Similar flanking regions of  $P_{mtlA}$  and  $P_{mtlR}$  are highlighted in gray. The inverted repeats or direct repeats are shown by arrows.

Here, in order to find the probable MtlR binding site, the upstream sequences of -35 boxes of  $P_{mtlA}$  and  $P_{mtlR}$  were aligned. Comparison of the  $P_{mtlA}$  and  $P_{mtlR}$  sequences showed a similar incomplete inverted repeat (TTGNACAN<sub>4</sub>TGTGNCAA) upstream of their -35 boxes (Fig. 3.25). This inverted repeat was encompassed by 11 bp flanking sequences (called distal and



proximal flanking; highlighted in gray, Fig. 4.1) in  $P_{m1A}$  and  $P_{m1R}$ . Interestingly, *B. subtilis*  $P_{m1A}$  and *G. stearothermophilus*  $P_{m1A}$  shared a palindromic sequence (TTTTTAAAAA, denoted T<sub>5</sub>A<sub>5</sub>) at the distal flanking region of  $P_{m1A}$  (gray arrows; Fig. 4.1). Likewise, there is a similar sequence in  $P_{m1R}$ , albeit with two mismatches (TTTTTCAATA). In addition to the T<sub>5</sub>A<sub>5</sub> sequence, there is also a direct repeat (TTTTTA) at  $P_{m1A}$  shown by doubled arrows in Fig. 4.1. By shortening the  $P_{m1A}$  5'-end, half of this direct repeat was deleted with no significant influence on the  $P_{m1A}$  activity. In contrast, any deletion in the T<sub>5</sub>A<sub>5</sub> sequence reduced the  $P_{m1A}$  activity (Fig. 3.27). Construction of  $P_{m1A}$ - $P_{licB}$  as well as  $P_{m1A}$ - $P_{manP}$  hybrid promoters revealed the importance of another inverted repeat in  $P_{m1A}$  located adjacent to -35 box (AAAGTN<sub>7</sub>ACTTT; dashed arrows in Fig. 4.1). At first, it was thought that the palindromic T<sub>5</sub>A<sub>5</sub> sequence forms the boundary of the 5'-end, and the inverted repeat located adjacent to the  $P_{m1A}$  -35 box the boundary of the 3'-end of MtlR binding site (154). However, both of these inverted repeats are AT-rich sequences. Besides, these inverted repeats were similar to the UP element subsites including consensus proximal subsite (5'-AAAAARNR-3') and distal subsite (5'-AWWWWT TTTT-3') sequences (55). Practically, any deletion or disruption in these sequences only reduced the level of  $P_{m1A}$  activity, while  $P_{m1A}$  remained highly inducible (Fig. 3.27). Therefore, these repeats might be the distal and proximal subsites of an UP element, where  $\alpha$ CTDs of the RNA polymerase bind. Similar inverted repeats were found in  $P_{m1R}$ , albeit shorter or disrupted. Unlike the putative subsites of the UP element, any disruption in the incomplete inverted repeat (TTGNACAN<sub>4</sub>TGTGNCAA) located between flanking regions (highlighted in gray; Fig. 4.1) rendered  $P_{m1A}$  nearly inactive and no further inducible; therefore, this inverted repeat is likely the MtlR binding site (Fig. 3.27). The location of the MtlR binding site and its interaction with  $\alpha$ CTD is similar to the promoters activated by class I mechanism. Basically, location of the binding sites of class I activators is variable due to the flexibility of the linker between  $\alpha$ CTD and  $\alpha$ NTD. In contrast, the binding location of class II activators cannot be varied because of constraints in the location of  $\sigma$  domain 4 (10). Indeed, increasing the distance between MtlR binding site and -35 box considerably reduced the activity of  $P_{m1A}$ ; however, the  $P_{m1A}$  remained inducible (Fig. 3.31.A). This shows the flexibility of the location of MtlR binding site in  $P_{m1A}$ . Accordingly, a class I activation is proposed for  $P_{m1A}$  and  $P_{m1R}$ , where MtlR binds adjacent to the  $\alpha$ CTD monomers of RNA polymerase and its binding site has no overlap with -35 box. Unlike *B. subtilis* MtlR, it seems

that other DeoR-type PRD-containing activator, *B. subtilis* ManR, assemble a class II activation complex during the transcription initiation. The ManR binding site overlaps -35 box in  $P_{manP}$  as shown by construction of  $P_{manP}$ - $P_{mtlA}$  hybrid promoters (section 3.14.5.1). In this case,  $P_{manP}$  is activated by a class II mechanism.

*In vitro* studies were carried out to demonstrate the interaction between the putative MtlR binding site and MtlR. Previously, *B. subtilis* MtlR-His<sub>6</sub> and *G. stearothermophilus* MtlR-His<sub>6</sub> were produced and purified from *E. coli* and used for electrophoretic mobility shift (94, 239). However, only the MtlR binding site in *G. stearothermophilus* has been so far identified using DNase I footprinting assay (94). Unlike previous attempts, production of MtlR-His<sub>6</sub> or MtlR-H342D-His<sub>6</sub> in *B. subtilis* or *E. coli* failed in this study. Similar negative results were obtained producing ManR-His<sub>6</sub> in *E. coli* (213). It is assumed that the presence of Ni<sup>2+</sup> oxidizes the cysteine residues in MtlR, especially the one which is located at the EIIB<sup>Gal</sup>-like domain. This cysteine plays an important role in the activity of MtlR (see below). Therefore, a MtlR double mutant, MtlR-H342D C419A was produced in *E. coli* JM109 and purified using ion exchange chromatography. Surprisingly, the produced MtlR-H342D C419A in *E. coli* JM109 was inactive, even in the crude extract. An explanation would be that the PRDI domain of PRD-containing regulators might be phosphorylated by HPr(H15~P) in *E. coli*. Perhaps, this phosphorylation deactivates MtlR-H342D C419A in *E. coli*. Phosphorylation of PRDI was shown by Bahr *et al.* (8) when they expressed *licT* in *E. coli*. Thus, an *E. coli* strain was used in which the EI was deleted ( $\Delta ptsI$ ). The active form of purified MtlR-H342D C419A was obtained only by cultivation of *E. coli*  $\Delta ptsI$  at 30°C. Surprisingly, the functional protein did not bind to the matrix of an anion exchange chromatography column at pH 7.4, although the predicted pI of MtlR was about 5. Nevertheless, electrophoretic mobility shift assays showed that MtlR-H342D C419A interacts with  $P_{mtlA}$  and  $P_{mtlR}$  DNA fragments *in vitro*. Further experiments are necessary to optimize the DNase I footprinting assay.

Preliminary studies showed that  $P_{mtlA}$  has a higher maximal activity than  $P_{mtlR}$  (4.5-fold; sections 3.1 and 3.5). However, the  $P_{mtlR}$  core elements were more similar to the  $\sigma^A$ -type promoter consensus sequence than the corresponding elements of  $P_{mtlA}$ . This effect could be due to a different promoter strength or different translation initiation efficiency. To exclude the effect

of translation initiation efficiency on the promoter activity, the promoter core elements and -35 upstream sequence of  $P_{mtlA}$  and  $P_{mtlR}$  were fused to the same 5'UTR originating from *manP* (section 3.15.4). In this way, the maximal activity of  $P_{mtlA}$  (producing 1005 R.F.U.) was only 1.6-fold stronger than  $P_{mtlR}$  (producing 610 R.F.U.). Likewise, fusion of  $P_{mtlR}$  to the 5'UTR of *mtlA* dramatically increased the  $P_{mtlR}$  maximal activity (Fig. 3.9). Thus, it is assumed that the high level of difference between  $P_{mtlA}$  and  $P_{mtlR}$  activities in the preliminary studies was mainly due to the translational initiation efficiency. Likewise, the  $P_{mtlA}$ -UTR<sub>*manP*</sub> and  $P_{mtlR}$ -UTR<sub>*manP*</sub> fusions revealed that  $P_{mtlR}$  is only induced by 1.5-fold, while  $P_{mtlA}$  is inducible by 15-fold (compare 3NA pKAM163 to 3NA pKAM164; Fig. 3.50). Similar results were obtained by  $P_{mtlR}$ -UTR<sub>*mtlA*</sub> (Fig. 3.9). In fact, the higher induction rate of  $P_{mtlA}$  could be due to the upstream region of its -35 box containing MtlR binding site and putative UP elements. Experimentally, the  $P_{mtlR}$  activity was doubled by exchanging its upstream region of -35 box with the  $P_{mtlA}$  counterparts (Fig. 3.26.B). Accordingly, it is probable that  $P_{mtlR}$  has a good match to  $\sigma^A$ -type promoter core elements; therefore, this may make the transcription initiation of  $P_{mtlR}$  less dependent to the activator MtlR. This mechanism is vice versa in  $P_{mtlA}$ , where  $P_{mtlA}$  lacks a good match to  $\sigma^A$ -type promoter core elements and requires MtlR activator.

#### 4.2. Regulation of $P_{mtlA}$ and $P_{mtlR}$

The activities of  $P_{mtlA}$  and  $P_{mtlR}$  were studied in the *B. subtilis* mutants in which the *mtlAFD* operon structural genes or the *mtlR* gene were deleted or disrupted. First, the influence of the mannitol-specific PTS transporter was studied by deletion of the *mtlAF* genes. Loss of both EIICB<sup>Mtl</sup> and EIIA<sup>Mtl</sup> transporter components resulted in constitutive activities of  $P_{mtlA}$  and  $P_{mtlR}$ , although catabolite repression remained functional (Fig. 3.11 and Fig. 3.12). The activities of  $P_{levD}$ ,  $P_{manP}$  and  $P_{manR}$  are also constitutive when their cognate specific PTS transporter were disrupted or deleted in *B. subtilis* (145, 214). Similar to the  $\Delta$ *mtlAF* mutant,  $P_{mtlA}$  and  $P_{mtlR}$  activities were constitutive and glucose-repressible in the  $\Delta$ *mtlF* mutant (deletion of EIIA<sup>Mtl</sup>) as well as in the  $\Delta$ *mtlAFD* mutant. Thus, *B. subtilis* MtlR is negatively influenced by phosphorylation from EIICB<sup>Mtl</sup> and EIIA<sup>Mtl</sup> in the absence of mannitol similar to *G. stearothermophilus* MtlR (93). Unexpectedly, the maximal activities of  $P_{mtlA}$  and  $P_{mtlR}$  in

*B. subtilis*  $\Delta mtlF$ ,  $\Delta mtlAF$ , and  $\Delta mtlAFD$  were considerably different. The  $P_{mtlA}$  maximal activity in the  $\Delta mtlAF$  mutant was the same as with induced wild type strain (producing 13,000 – 14,000 Miller units  $\beta$ -galactosidase). In contrast, the  $P_{mtlA}$  maximal activity in the  $\Delta mtlF$  mutant (producing 24,000 Miller units  $\beta$ -galactosidase) was higher than in the  $\Delta mtlAF$  mutant. On the other hand,  $P_{mtlA}$  maximal activity in  $\Delta mtlAFD$  (producing 1,200 Miller units  $\beta$ -galactosidase) was considerably lower than in the  $\Delta mtlAF$  mutant. Similar results were obtained by Deutscher *et al.* (personal communication) when they integrated the  $P_{mtlA}$ -*lacZ* into the chromosome. The cytoplasmic phosphocarrier protein EIIA<sup>Mtl</sup> (encoded by *mtlF*) transfers the phosphoryl group from HPr(H15~P) to the domain B of membrane-bound EIICB<sup>Mtl</sup>. Therefore, in the absence of EIIA<sup>Mtl</sup>, the membrane-bound EIICB<sup>Mtl</sup> remains unphosphorylated. Maybe, the presence of the domain B of EIICB<sup>Mtl</sup> has a positive regulatory effect on MtlR activity when the cytoplasmic phosphocarrier EIIA<sup>Mtl</sup> is absent. This assumption was strengthened by the fact that expression of the domain B of EIICB<sup>Mtl</sup>, fused to another membrane protein, restored the high constitutive activity of  $P_{mtlA}$  in the mutant which lacks both EIIA<sup>Mtl</sup> and EIIB<sup>Mtl</sup> (Deutscher *et al.*; unpublished). Nevertheless, it does not explain the high activity of  $P_{mtlA}$  in the  $\Delta mtlF$  mutant, and its low activity in  $\Delta mtlAFD$ . The difference could also be due to the presence and absence of *mtlD*, encoding the mannitol 1-phosphate dehydrogenase. However, *mtlD* disruption or deletion (data not shown) led to the same  $P_{mtlA}$  maximal activity as in wild type strain, although the basal activity of  $P_{mtlA}$  was slightly increased. The  $P_{mtlR}$  activity obtained in the  $\Delta mtlD$  mutant was also comparable to  $P_{mtlA}$  in the  $\Delta mtlD$  mutant. Interestingly, by studying the genome of *B. subtilis*, an antisense RNA in the sequence of *mtlD* was predicted (103). The presence of an antisense RNA could also have a regulatory effect on expression of the *mtlAFD* and *mtlR* genes. But, deletion of the *mtlD* gene had no effect on the  $P_{mtlA}$  activity (data not shown). Thus, it is unlikely that the different  $P_{mtlA}$  activities in the *mtl* mutants are due to antisense RNA. Until now, there is no explanation for the different levels of  $P_{mtlA}$  activities in the  $\Delta mtlAF$ ,  $\Delta mtlF$ , and  $\Delta mtlAFD$  mutants.

Altogether, the results are in line with a recent publication revealing the phosphorylation of MtlR EII-like domains by EIICB<sup>Mtl</sup> and EIIA<sup>Mtl</sup> (107). *In vivo* and *in vitro* studies indicated that histidine 599, located at EIIA<sup>Mtl</sup>-like domain of MtlR, is phosphorylated by domain B of

EIICB<sup>Mtl</sup> in the absence of mannitol. Likewise, cysteine 419 in EIIB<sup>Gat</sup>-like domain of MtlR is phosphorylated by cytoplasmic phosphocarrier EIIA<sup>Mtl</sup>. Site-specific mutation of the histidine 599 to alanine of MtlR protein rendered  $P_{mtlA}$  partially constitutive with only 30% of the  $P_{mtlA}$  maximal activity in the wild type strain when mannitol was added to the bacterial culture. In contrast,  $P_{mtlA}$  indicated a strong constitutive activity in the *mtlR*-C419A mutant strain (107). Deletion of the EIIB<sup>Gat</sup>-like and EIIA<sup>Mtl</sup>-like domains of ManR likewise rendered  $P_{manP}$  constitutive (213). Therefore, phosphorylation of the domains EIIB<sup>Gat</sup>-like (containing C419) and EIIA<sup>Mtl</sup> (harboring H599) inactivates MtlR in the absence of mannitol. In the presence of mannitol, the dephosphorylation of these domains by the mannitol PTS transporter components results in a constitutive activity of MtlR (as also shown in this study) (107). Apparently, phosphorylation and dephosphorylation of MtlR cysteine 419 by EIIA<sup>Mtl</sup> plays a pivotal role in induction of the MtlR activity (107). Nevertheless, further experiments are necessary to clarify the interaction between the mannitol-specific PTS transporter components, MtlD and MtlR.

Deletion of the *mtlR* gene rendered  $P_{mtlA}$  and  $P_{mtlR}$  inactive. This shows that MtlR not only activates the *mtlAFD* operon which is reported by Watanabe *et al.* (239), but also acts as an activator for its own promoter. Similarly,  $P_{manR}$  is also activated by its own product (214). Mutation of the HPr histidine 15 to alanine strongly diminished the  $P_{mtlA}$  activity to about the same level than that of the deletion of *mtlR*. This was similar to  $P_{manP}$  whose activity was very poor in a *ptsH*-H15A mutant (214). Indeed, phosphorylation of MtlR by HPr(H15~P) stimulates the activity of MtlR as shown before for *B. subtilis* LicR (222), LevR (144), and *G. stearothermophilus* MtlR (93). Phosphorylation of the *B. subtilis* MtlR PRDII domain by HPr(H15~P) was recently shown *in vitro* (107). In addition, mutation of histidine 342 to aspartate which is located at PRDII of *B. subtilis* MtlR was phosphomimetic (see Fig. 3.24). Interestingly, the repression of the  $P_{mtlA}$  activity by glucose was significantly reduced in the *mtlR*-H342D mutant, while the induction of  $P_{mtlA}$  by mannitol remained unchanged (Fig. 3.24). This phenomenon was also reported by Joyet *et al.* (107). Therefore, dephosphorylation of *B. subtilis* MtlR PRDII acts as catabolite repression (CCR). This is comparable to *G. stearothermophilus* MtlR (93), LevR (144) and LicT in *B. subtilis* (135, 226). Such a CCR was firstly reported for the antiterminator BglG in *E. coli* (76). Finally, electrophoretic mobility shift studies showed that the double mutant MtlR-H342D C419A is active and independent from

phosphorylation by general and specific PTS proteins (Fig. 3.41.B). This confirms that a phosphorylated PRDII and a dephosphorylated EIIB<sup>Gat</sup>-like domain are essential for an active MtlR. Mutation of the histidine 289 to alanine which is located at the PRDI domain of MtlR significantly reduced the activity of MtlR. In contrast, mutation of the histidine 230 to alanine only slightly decreased the MtlR activity (Fig. 3.24). Similar results are reported by Joyet *et al.* (107). In addition to reduction of  $P_{mrlA}$  activity, carbon catabolite repression was slightly stronger in PRDI mutants. Apparently, PRDI might be important for the signal transfer from PRDII to the DNA binding domain of MtlR similar to LevR (45). On the other hand, phosphorylation of PRDII by HPr(H15~P) is not independent from PRDI, as reported for *G. stearothermophilus* MtlR (93). Also, it might be possible that mutation of the histidine to alanine affected the MtlR folding or caused structural changes. All in all, more experiments are needed to clarify the role of PRDI in the regulation of MtlR activity.

Glucitol, as a non-specific inducer, activates  $P_{mrlA}$  and  $P_{mrlR}$ . This effect was first reported by Horwitz and Kaplan when they were studying the mannitol 1-phosphate dehydrogenase activity of crude extracts of *B. subtilis*. They found an increase of mannitol 1-phosphate dehydrogenase activity when *B. subtilis* was cultivated on medium supplemented with glucitol (97). Later, microarray analysis confirmed the induction of *mtlAFD* expression by glucitol (239). Induction of  $P_{mrlA}$  and  $P_{mrlR}$  by glucitol was dependent on MtlR and in a  $\Delta mtlR$  mutant both of these promoters were inactive. On the other hand, deletion of the *gutRBP<sub>ydjE</sub>* had no influence on the induction of  $P_{mrlA}$  and  $P_{mrlR}$  by glucitol. Therefore, the activity of  $P_{mrlA}$  and  $P_{mrlR}$  caused by glucitol is MtlR-dependent and not GutR-dependent. Similar results were reported by Watanabe *et al.* (239). Besides, the  $\Delta mtlD$  mutant grew slower than the wild type strain in minimal medium containing glucitol as the major carbon source. Finally, addition of glucitol retarded the growth of the  $\Delta mtlD$  mutant in LB medium similar to mannitol. In fact, mannitol 1-phosphate dehydrogenase (MtlD) was essential for glucitol assimilation as reported before (239). The induction of the *mtlAFD* genes by glucitol was explained by the non-specific uptake of glucitol by mannitol-specific enzyme II shown by using D-[<sup>14</sup>C]glucitol (28). Glucitol is taken up by *B. subtilis* via GutP with no modification and is converted to fructose by glucitol dehydrogenase, GutB (42, 43). When glucitol is taken up by EIICB<sup>Mtl</sup>, glucitol 6-phosphate is generated. The latter product accumulates in the cell and is removed by mannitol 1-phosphate dehydrogenase

which has a low activity with glucitol 6-phosphate as substrate (97). Taken together, it is assumed that glucitol is taken up by the mannitol-specific EII due to its relaxed specificity in which the transporter can transport more than one sugar. Relaxed specificity of sugar transporters is well-known. For instance, the glucose permease (PtsG) takes up sucrose and salicin, and the  $\beta$ -glucoside permease (BglP) is capable of weak uptake of glucose (189). The uptake and phosphorylation of glucitol leads to activation of MtlR by dephosphorylation of EIIB<sup>Gat</sup>-like domain. Glucitol 6-phosphate accumulates in the cell and is catabolized slowly by mannitol 1-phosphate dehydrogenase, whereas in the  $\Delta mtlD$  strain, the accumulation of glucitol 6-phosphate inhibits the cell growth.

### 4.3. Carbon catabolite repression of $P_{mtlA}$ and $P_{mtlR}$

Addition of glucose represses the  $P_{mtlA}$  and  $P_{mtlR}$  activities in the presence of mannitol. Basically, the presence of glucose increases the level of FBP in the cell causing CcpA-dependent CCR. Therefore, the  $P_{mtlA}$  and  $P_{mtlR}$  activities were investigated in CcpA-dependent CCR-deficient mutants. CcpA forms a DNA binding complex with HPr(S46~P) as its coeffector. Mutation of the regulatory serine 46 of HPr to alanine (*ptsH*-S46A mutant) only partially relieved  $P_{mtlA}$  from CCR (Fig. 3.21). Similar to *mtlAFD* operon, the *ptsH*-S46A mutation partially or completely relieves many other catabolic operons from CCR, such as *xyLAB* (37), *bglPH* (116), *levDEFG* (146), *gntRKPZ* (181), *manPA* (214). Besides HPr(S46~P), Crh(S46~P) can also form a complex with CcpA inhibiting the catabolic operons. Deletion of Crh abolishes the residual CCR for many genes, such as *acsA* (262). Accordingly,  $P_{mtlA}$  activity was measured in a  $\Delta crh$  mutant as well as in a *ptsH*-S46A  $\Delta crh$  double mutant. Deletion of *crh* alone did not affect the CCR of  $P_{mtlA}$ , while CCR of  $P_{mtlA}$  in the *ptsH*-S46A  $\Delta crh$  double mutant was similar to the *ptsH*-S46A mutant in which  $P_{mtlA}$  activity was reduced (Fig. 3.21). In fact, Crh plays a minor role as the CcpA effector for CCR (202). Recently, it is found out that unphosphorylated Crh mainly inhibits methylglyoxal synthase (MgsA) activity. In this way, the cell prevents the accumulation of phosphosugars under carbon overflow condition (122). This could explain the lower  $P_{mtlA}$  activity in both the  $\Delta crh$  *ptsH*-S46A and  $\Delta crh$  mutants (Fig. 3.21). In the absence of Crh, MgsA constantly converts dihydroxyacetone phosphate to methylglyoxal. Methylglyoxal is afterwards

excreted into the extracellular milieu or further converted to pyruvate. Altogether, the PEP production is reduced due to the loss of DHAP causing a lower amount of HPr(H15~P). In addition, methylglyoxal seems to be toxic for the cells. Coeffectors Crh and HPr are both phosphorylated by HPrK/P as a result of high FBP concentration in the cell. Transcriptome analyses of *B. subtilis* indicated that deletion of *hprK* (encoding HPrK/P) resulted in a loss of CcpA-dependent CCR (139). Deletion of *hprK*, however, did not significantly affect the CCR of  $P_{mtlA}$ . Besides, the  $\Delta hprK$  mutant grew significantly slower than the wild type strain. Finally, *ccpA*, encoding the master regulator of CCR, was deleted. Unexpectedly, the  $P_{mtlA}$  activity in a  $\Delta ccpA$  was strongly repressed by glucose, although the  $P_{mtlA}$  activity in the  $\Delta ccpA$  mutant was significantly lower than in wild type strain. The observed high CCR of  $P_{mtlA}$  in the  $\Delta ccpA$  mutant could be due to an alteration of the cell physiology. In fact, CcpA is a pleiotropic regulator controlling important metabolic pathways, such as glycolysis (112, 141, 223), ammonium assimilation (34, 56, 234), excretion of excess carbon source, and fermentation (210). In addition,  $P_{mtlA}$  could be also indirectly subjected to CCR via *mtlR* expression. Production of MtlR is prerequisite for induction of  $P_{mtlR}$ . Any depletion in the MtlR amount in the cytoplasm is supposed to change the transcription of  $P_{mtlA}$  drastically. Accordingly, it is assumed that CCR could mainly alter the transcription of  $P_{mtlR}$ , thereby controls the  $P_{mtlA}$  activity. Indeed,  $P_{mtlR}$  has relieved from CCR in the  $\Delta ccpA$  mutant, albeit partially. Reduction of CCR in  $P_{mtlR}$  has also occurred in the *ptsH*-S46A  $\Delta crh$  double mutant, although the basal activity was doubled in the latter mutant. In summary, any disruption of *trans* elements of the CcpA-dependent CCR only partially relieved  $P_{mtlR}$  and  $P_{mtlA}$  activities from CCR. On the other hand, analyses of  $P_{mtlA}$  and  $P_{mtlR}$  sequences revealed putative *cre* sites resembling *cre* consensus sequence (WTGAARCGNWWCA). These putative *cre* sites of  $P_{mtlA}$  and  $P_{mtlR}$  overlapped the -10 boxes. By these means, binding of the CcpA-HPr(S46~P) complex to the *cre* site prevents the binding of RNAP by a steric hindrance mechanism. Interestingly, the *cre* sites of  $P_{mtlA}$  and  $P_{mtlR}$  lack the conserved cytosine at the end of *cre* sequence. It is likely that the left-side TG bases in WTGAARCGNWWCA sequence are required for pairing with the right-side CA bases resulting in the proper binding of CcpA-HPr(S46~P) complex (61). This cytosine plays an essential role in the operation of *cre* sites of *amyE*, *gntR*, and *hutP* (62, 240, 248). In order to repair the *cre* sites of  $P_{mtlA}$  and  $P_{mtlR}$ , the conserved right-side CA bases were introduced in  $P_{mtlA}$



and  $P_{mIIR}$  putative *cre* sites (Fig. 3.44). Alteration of the *cre* sites rendered  $P_{mIIA}$  and  $P_{mIIR}$  inactive. Perhaps, mutation in the second position (underlined) of the -10 box (TATAAAT) in  $P_{mIIA}$  and  $P_{mIIR}$  and addition of a cytosine to this AT-rich hexamer deactivated the promoters. On the contrary, mutation of the conserved left-side TG for further disruption of the putative *cre* site of  $P_{mIIA}$  did not alter the CCR of  $P_{mIIA}$  (Fig. 3.43 and Fig. 3.45). Disruption of  $P_{mIIR}$  *cre* site, however, partially reduced the  $P_{mIIR}$  CCR. First interpretation may point out that the  $P_{mIIR}$  *cre* site was functional, whereas the  $P_{mIIA}$  *cre* site was inefficient. However, in all of the undertaken experiments, the CCR of  $P_{mIIR}$  affects the  $P_{mIIA}$  CCR. To remove the influence of  $P_{mIIR}$  *cre* on  $P_{mIIA}$  CCR, the *cre* sites of  $P_{mIIA}$  and  $P_{mIIR}$  were fused to a constitutive promoter whose activation is independent from mannitol induction. In this way, it was shown that the *cre* sites of  $P_{mIIA}$  and  $P_{mIIR}$  are partially able to block the transcription initiation of  $P_{groE}$ . Besides, the *cre* site of  $P_{mIIR}$  was more efficient than  $P_{mIIA}$ . Fujita analysed 50 reported *cre* sites of *B. subtilis*. This analysis revealed two groups of *cre* sites including: WTGNAANCGNWWNCA (group A) and WTGAAARCGYTTWNN (group B) (61). In group A, pairing the TG and CA (underlined) is essential for an operational *cre* site. In the group B, this pairing is compensated by A and T pairs (underlined), as shown for *iolA* *cre* site (153). Altogether, it seems that the sequences in  $P_{mIIA}$  and  $P_{mIIR}$  belong to the group B *cre* sites where palindromic A's and T's are necessary for binding the CcpA-HPr(S46~P) complex. In this way,  $P_{mIIA}$  has a weak *cre* site, as experimentally shown, due to the presence of two mismatches (underlined) to the group B consensus sequence (CTGTAAGCGTTTTAA). Unlike the  $P_{mIIA}$  *cre* site, the *cre* site of  $P_{mIIR}$  contains no mismatches compared to the group B *cre* consensus sequence. These *cre* sites are likely weaker than the group A *cre* sites as indicated by comparison of *cre* sites of *acsA*,  $P_{mIIA}$  and  $P_{mIIR}$ . Consequently, the CcpA-dependent CCR is mediated by two weak *cre* sites located at  $P_{mIIA}$  and  $P_{mIIR}$  at the transcription initiation level.

In addition to CcpA-dependent CCR, CcpA-independent CCR mediated by HPr (a.k.a. induction prevention) was also studied. Uptake of glucose reduces the concentration of HPr(H15~P), thereby reduces the activity of the regulators by induction prevention (61, 75). To prevent the uptake of glucose, the glucose-specific PTS transporter encoded by *ptsG* was deleted. Here, it is shown that  $P_{mIIA}$  and  $P_{mIIR}$  in a  $\Delta ptsG$  mutant were fully active in the simultaneous presence of mannitol and glucose. In other words, glucose repression was completely abolished

in the  $\Delta ptsG$  mutant. This phenomenon was previously shown for the *bglPH* operon by the mutation of EIICBA<sup>Glc</sup> residues (6) and in *gntRKPZ* operon by insertional mutagenesis of *ptsG* (171). Apart from EIICBA<sup>Glc</sup>, there are two other glucose transporters in *B. subtilis*, namely GlcP and GlcU. However, both of these transporters are not expressed during the exponential phase (58, 159, 171). Recently, it was shown that the uptake of D-[<sup>14</sup>C]glucose did not occur only in a  $\Delta ptsG$  mutant (100). Thus, in addition to HPr-mediated CCR, the CcpA-dependent CCR is also not functional in a  $\Delta ptsG$  mutant due to low level of FBP pool in the cell. Previous experiments (see above) showed that disruption of CcpA-dependent CCR components causes only a partial reduction in  $P_{m1A}$  or  $P_{m1R}$  CCR. Thus, it seems that depletion of HPr(H15~P) and induction prevention mainly causes CCR of the *m1AFD* operon. This is in line with our previous observations with the MtlR-H342D mutant, where MtlR was highly active in the presence of glucose (strain KM213; Fig. 3.24). Likewise, the activity of  $P_{m1A}$  was repressed in the presence of fructose. In contrast, sucrose and mannose had no significant influence on the  $P_{m1A}$  activity. Glucose, fructose, mannitol, and sucrose are the preferred carbon sources of *B. subtilis*. All of these sugars are taken up by PTS and exert strong CCR in other catabolic operons, such as in *xynPB* operon encoding the  $\beta$ -xyloside utilization system (202). Taken together, it is probable that HPr-mediated CCR of  $P_{m1A}$  and  $P_{m1R}$  is caused by the dephosphorylation of HPr(H15~P) by glucose- and fructose-specific transporters. Apparently, there is also a hierarchy between the preferred carbon sources in *B. subtilis*. Perhaps, HPr(H15~P) has a higher affinity towards glucose and fructose PTS permeases than mannitol-, mannose- and sucrose-specific EII. Besides, it might be possible that the PRDII domain of MtlR is directly dephosphorylated by glucose and fructose PTS permeases. Both of these assumptions need more experimental evidence. In conclusion, the carbon catabolite repression acts at two levels in mannitol PTS: the transcriptional level caused by CcpA-dependent CCR and posttranslational level caused by HPr (or likely PtsG) modulating the MtlR activity via PRDII domain phosphorylation.

#### **4.4. Translation initiation and construction of an expression system**

A mannitol-inducible expression system in *B. subtilis* was constructed based on  $P_{m1A}$  due to its stronger activity than  $P_{m1R}$  (discussed in section 4.1). In order to enhance the  $P_{m1A}$  activity,

the transcriptional and translational initiation regions were manipulated. At first, the  $P_{mtlA}$  -10 box was replaced with the consensus -10 hexamer (TATAAT) of the  $\sigma^A$ -type promoters. This replacement only increased the basal activity, but not the  $P_{mtlA}$  maximal activity. Presumably, the similarity of  $P_{mtlA}$  core elements to the consensus  $\sigma^A$ -type promoter core elements reduces  $P_{mtlA}$  dependency to an activator. Another key factor for controlling the protein synthesis is the abundance of mRNA. Accordingly, instead of changing the  $P_{mtlA}$  core elements, the translation initiation was studied by shortening of the 5' leader sequence of *mtlA* mRNA in the  $P_{mtlA}$ -*lacZ* cassette on pKAM1 (Fig. 3.48.A). Also, the 5'UTR of *mtlR* mRNA on pKAM3 was shortened (Fig. 3.8.A). Basically, cellular mRNA concentration depends upon the rates of its synthesis and degradation. The mechanism of mRNA degradation and the half-life of mRNA are not clear for the *mtlA* and *mtlR* mRNAs. Nevertheless, having an optimal ribosomal binding site at the 5'-end of an mRNA, and in a consequence a high translation rate, appears to protect the mRNA against 5' to 3' exonuclease activity, as shown in *gsiB* mRNA (108). In addition to an optimized ribosomal binding site, thermo-responsive RNA structures also modulate the translation initiation (109). Characterization of the  $P_{mtlA}$  and  $P_{mtlR}$  transcription start sites showed long 5' leader sequences in *mtlA* mRNA and *mtlR* mRNA. The length of 5'-UTR of *mtlA* mRNA was 72 bp, whereas 5'-UTR of *mtlR* mRNA is 77 bp long. After construction of pKAM1 harboring the  $P_{mtlA}$ -*lacZ* cassette, two ribosomal binding sites were placed upstream of the *lacZ* (Fig. 3.2.A). This first one was originated from *mtlA* (shown by RBS W) and the second one from bacteriophage T7 (shown by RBS V). Interestingly, shortening of the 5' leader sequence of *mtlA* mRNA in pKAM12 and pKAM50 dramatically increased the expression of *lacZ* compared with pKAM1. This increase of the  $P_{mtlA}$  activity could be presumably because of the deletion of one of the ribosomal binding sites, namely the *mtlA* RBS. On the other hand, analysis of the deleted region in 5'UTR of the *mtlA* mRNA revealed an incomplete inverted repeat adjacent to the ribosomal binding site (Fig. 4.2). This incomplete inverted repeat could cause a secondary structure near the ribosomal binding site, thereby creating a spatial hindrance for binding the ribosome. Likewise, it could form a loop which inhibits the mRNA decay by the RNase J1 as reported for *gapA* mRNA (131). Altogether, partial deletion or complete deletion of this inverted repeat increases the activity of  $P_{mtlA}$ .

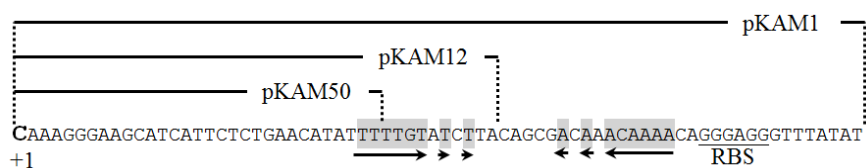


**Fig. 4. 2.** The 5' leader sequence of *mtlA* mRNA on pKAM1. Transcription start site of  $P_{mtlA}$  is shown by +1. The RBS demonstrates the ribosomal binding site of *mtlA*. The 5' leader sequence of *mtlA* mRNA fused to  $P_{mtlA}$  core elements in pKAM1, pKAM12 and pKAM50 are represented by solid and dashed lines. The incomplete inverted repeat is shown by arrows and highlighted in gray.

Unlike 5' UTR of *mtlA* mRNA, shortening of 5'UTR of the *mtlR* mRNA gradually decreased the expression of *lacZ*. The  $P_{mtlR}$ -*lacZ* fusion on pKAM3 contained two simultaneous ribosomal binding sites (Fig. 3.6.A). However, deletion of the second ribosomal binding site, RBS of *mtlR* decreased the activity of  $P_{mtlR}$ . By viewing the sequence of 5'UTR of *mtlR* mRNA, two repeats, *i.e.* ACCTC and CTCCT, were found complementary to the ribosomal binding site (Fig. 4.3).

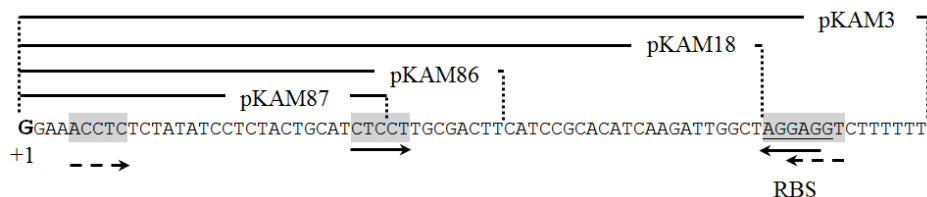


**Fig. 4. 3.** The 5' mRNA leader sequence of *mtlR* on pKAM3. Transcription start site of  $P_{mtlR}$  is shown by +1. The RBS demonstrates the ribosomal binding site of *mtlR*. The 5' mRNA leader sequence of *mtlR* fused to  $P_{mtlR}$  core elements in pKAM3, pKAM18, pKAM86, and pKAM87 are represented by solid and dashed lines. The incomplete inverted repeat is shown by arrows and highlighted in gray.

It is likely that these repeats form stable secondary structures with ribosomal binding sites. Therefore, the presence of the second RBS from *mtlR* may prevent the formation of a secondary structure between the vector RBS and the found repeats. It must be noted that in the pKAM86 and pKAM87 constructs two longer palindromic sequences were formed overlapping the ribosomal binding site (data not shown). Further experiments are necessary to analyze the stability of the *mtlA* and *mtlR* mRNAs.

Ultimately, a mannitol expression vector system was constructed by changing the parental vector (pBS72 which is a low copy vector) to a pUB110 derivative with high copy number. Similar to Wenzel *et al.* (242), the translational initiation region of *gsiB* which has a stable mRNA due to an optimized RBS was used (108). Comparison of the mannitol-inducible expression system with the already described mannose-inducible system (242) showed that the expression of eGFP was half of the mannose-induced system. One of the major problems by increasing the copy number of a gene is the regulator copy number and titration of the regulator and the binding site. In comparison with  $P_{mtlR}$ , the activity of  $P_{manR}$  is about 10-fold higher (214). Therefore, a single copy of  $P_{manR}$ -*manR* on the chromosome supports the activity of  $P_{manP}$  on a high copy number vector. Increasing the copy number of *mtlR* by insertion of  $P_{mtlR}$ -*mtlR* on the expression vector increased the  $P_{mtlA}$  activity to the level of mannose-inducible system. However, the basal activity was increased. In fact, a delicate balance between the expression of MtlR and the copy number of  $P_{mtlA}$  is necessary.

## 5. Conclusion and perspectives

The aim of this study was to analyze the regulation of the mannitol utilization system in *B. subtilis*. Phosphorylation and dephosphorylation of the MtlR domains by specific and general proteins of the PTS plays the pivotal role in the regulation of mannitol utilization system. The observed carbon catabolite repression for the  $P_{mtlA}$  and  $P_{mtlR}$  activities is also mainly functional at post translational level in the mannitol utilization system by affecting the phosphorylation status of MtlR. The CcpA-dependent pathway affected the transcription of the *mtlAFD* operon as well as the *mtlR* gene to a less content. Finally, an expression vector system has been constructed by using the  $P_{mtlA}$  sequence, which is highly inducible by mannitol. However, further characterization and optimization of this system must be done. Some further perspectives of this work are listed below:

- Confirmation of the MtlR and  $\alpha$ CTD binding sites located on  $P_{mtlA}$  and  $P_{mtlR}$  *in vitro*.
- Analyze the structures of *mtlAFD* and *mtlR* mRNAs and its mRNA stability.
- Characterization of the possible antisense RNAs resided within *mtlAFD* operon and their influence on the *mtlAFD* operon and *mtlR* regulation.
- Characterization of the role of PRDI in the regulation of MtlR as a PRD-containing activator and studying the probable interaction of the MtlR domains with each other and probably with PtsG.
- Improvement of the *mtl* expression system by increasing the stability of the pUB110 derivative plasmid pKAM114.

## 6. References

1. **Altenbuchner, J., P. Viell, and I. Pelletier.** 1992. Positive selection vectors based on palindromic DNA sequences. *Methods in Enzymology* **216**:457-466.
2. **Anna, D. F., M. Rosa, P. Emilia, B. Simonetta, and R. Mose.** 2003. High-level expression of *Alicyclobacillus acidocaldarius* thioredoxin in *Pichia pastoris* and *Bacillus subtilis*. *Protein Expression and Purification* **30**:179-184.
3. **Arnaud, M., M. Debarbouille, G. Rapoport, M. H. Saier, and J. Reizer.** 1996. In vitro reconstitution of transcriptional antitermination by the SacT and SacY proteins of *Bacillus subtilis*. *Journal of Biological Chemistry* **271**:18966-18972.
4. **Arnaud, M., P. Vary, M. Zagorec, A. Klier, M. Debarbouille, P. Postma, and G. Rapoport.** 1992. Regulation of the *sacPA* operon of *Bacillus subtilis*: identification of phosphotransferase system components involved in SacT activity. *Journal of Bacteriology* **174**:3161-3170.
5. **Baba, T., T. Ara, M. Hasegawa, Y. Takai, Y. Okumura, M. Baba, K. A. Datsenko, M. Tomita, B. L. Wanner, and H. Mori.** 2006. Construction of *Escherichia coli* K-12 in-frame, single-gene knockout mutants: the Keio collection. *Molecular Systems Biology* **2**.
6. **Bachem, S., N. Faires, and J. Stülke.** 1997. Characterization of the presumptive phosphorylation sites of the *Bacillus subtilis* glucose permease by site-directed mutagenesis: implication in glucose transport and catabolite repression. *FEMS Microbiology Letters* **156**:233-238.
7. **Bachem, S. and J. Stülke.** 1998. Regulation of the *Bacillus subtilis* GlcT antiterminator protein by components of the phosphotransferase system. *Journal of Bacteriology* **180**:5319-5326.
8. **Bahr, T., D. Lüttmann, W. März, B. Rak, and B. Görke.** 2011. Insight into bacterial phosphotransferase system-mediated signaling by interspecies transplantation of a transcriptional regulator. *Journal of Bacteriology* **193**:2013-2026.
9. **Barbe, V., S. Cruveiller, F. Kunst, P. Lenoble, G. Meurice, A. Sekowska, D. Vallenet, T. Z. Wang, I. Moszer, C. Medigue, and A. Danchin.** 2009. From a consortium sequence to a unified sequence: the *Bacillus subtilis* 168 reference genome a decade later. *Microbiology* **155**:1758-1775.
10. **Barnard, A., A. Wolfe, and S. Busby.** 2004. Regulation at complex bacterial promoters: how bacteria use different promoter organizations to produce different regulatory outcomes. *Current Opinion in Microbiology* **7**:102-108.
11. **Bertram, R., S. Rigali, N. Wood, A. T. Lulko, O. P. Kuipers, and F. Titgemeyer.** 2011. Regulon of the N-acetylglucosamine utilization regulator NagR in *Bacillus subtilis*. *Journal of Bacteriology* **193**:3525-3536.
12. **Bethesda Research Labs.** 1986. BRL pUC host: *E. coli* DH5 $\alpha$  competent cells. *Focus* **8**:9.
13. **Bhavsar, A. P., X. M. Zhao, and E. D. Brown.** 2001. Development and characterization of a xylose-dependent system for expression of cloned genes in *Bacillus subtilis*:

- Conditional complementation of a teichoic acid mutant. *Applied and Environmental Microbiology* **67**:403-410.
14. **Bongers, R. S., J. W. Veening, M. Van Wieringen, O. P. Kuipers, and M. Kleerebezem.** 2005. Development and characterization of a subtilin-regulated expression system in *Bacillus subtilis*: Strict control of gene expression by addition of subtilin. *Applied and Environmental Microbiology* **71**:8818-8824.
  15. **Braaz, R., S. L. Wong, and D. Jendrossek.** 2002. Production of PHA depolymerase a (PhaZ5) from *Paucimonas lemoignei* in *Bacillus subtilis*. *FEMS Microbiology Letters* **209**:237-241.
  16. **Bradford, M. M.** 1976. Rapid and sensitive method for quantitation of microgram quantities of protein utilizing principle of protein dye binding. *Analytical Biochemistry* **72**:248-254.
  17. **Brefort, G., M. Magot, H. Ionesco, and M. Sebald.** 1977. Characterization and transferability of *Clostridium perfringens* plasmids. *Plasmid* **1**:52-66.
  18. **Brockmeier, U., M. Wendorff, and T. Eggert.** 2006. Versatile expression and secretion vectors for *Bacillus subtilis*. *Current Microbiology* **52**:143-148.
  19. **Bron, S.** 1989. Plasmids, p. 75-138. In Harwood C.R. (ed.), *Bacillus* (Biotechnology Handbooks vol. 2). Plenum Press, New York.
  20. **Bron, S.** 1990. Plasmids, p. 75-138. In Harwood C.R. and Cutting S.M. (eds.), *Molecular biological methods for Bacillus*. John Wiley and Sons, Chichester, United Kingdom.
  21. **Bron, S., W. Meijer, S. Holsappel, and P. Haima.** 1991. Plasmid instability and molecular cloning in *Bacillus subtilis*. *Research in Microbiology* **142**:875-883.
  22. **Brown, N. L., J. V. Stoyanov, S. P. Kidd, and J. L. Hobman.** 2003. The MerR family of transcriptional regulators. *FEMS Microbiology Reviews* **27**:145-163.
  23. **Browning, D. F. and S. J. W. Busby.** 2004. The regulation of bacterial transcription initiation. *Nature reviews.Microbiology*. **2**:57-65.
  24. **Bruand, C., S. D. Ehrlich, and L. Janniere.** 1991. Unidirectional theta replication of the structurally stable *Enterococcus faecalis* plasmid pAM $\beta$ 1. *The EMBO journal* **10**:2171-2177.
  25. **Burkholder, P. R. and N. H. Giles.** 1947. Induced biochemical mutations in *Bacillus subtilis*. *American Journal of Botany* **34**:345-348.
  26. **Bürklen, L., F. Schöck, and M. K. Dahl.** 1998. Molecular analysis of the interaction between the *Bacillus subtilis* trehalose repressor TreR and the *tre* operator. *Molecular and General Genetics* **260**:48-55.
  27. **Ceglowski, P., A. Boitsov, N. Karamyan, S. H. Chai, and J. C. Alonso.** 1993. Characterization of the effectors required for stable inheritance of *Streptococcus pyogenes* pSM19035-derived plasmids in *Bacillus subtilis*. *Molecular & General Genetics* **241**:579-585.
  28. **Chalumeau, H., A. Delobbe, and P. Gay.** 1978. Biochemical and genetic study of D-glucitol transport and catabolism in *Bacillus subtilis*. *Journal of Bacteriology* **134**:920-928.
  29. **Charrier, V., J. Deutscher, A. Galinier, and I. Martin-Verstraete.** 1997. Protein phosphorylation chain of a *Bacillus subtilis* fructose-specific phosphotransferase system and its participation in regulation of the expression of the *lev* operon. *Biochemistry* **36**:1163-1172.



30. **Chauvaux, S., I. T. Paulsen, and M. H. Saier.** 1998. CcpB, a novel transcription factor implicated in catabolite repression in *Bacillus subtilis*. *Journal of Bacteriology* **180**:491-497.
31. **Claus D. and Fritze D.** 1989. Taxonomy of *Bacillus*, p. 5-26. In Harwood C.R. (ed.), *Bacillus* (Biotechnology Handbooks vol. 2). Plenum Press, New York.
32. **Clewell, D. B., Y. Yagi, G. M. Dunny, and S. K. Schultz.** 1974. Characterization of 3 plasmid deoxyribonucleic acid molecules in a strain of *Streptococcus faecalis*: Identification of a plasmid determining erythromycin resistance. *Journal of Bacteriology* **117**:283-289.
33. **Cohn F.** 1872. Untersuchungen über Bakterien. *Beitr.Biol.Pflanz* **1**:124-224.
34. **Commichau, F. M., K. Forchhammer, and J. Stülke.** 2006. Regulatory links between carbon and nitrogen metabolism. *Current Opinion in Microbiology* **9**:167-172.
35. **Conrad, B., R. S. Savchenko, R. Breves, and J. Hofemeister.** 1996. A T7 promoter-specific, inducible protein expression system for *Bacillus subtilis*. *Molecular & General Genetics* **250**:230-236.
36. **Crutz, A. M., M. Steinmetz, S. Aymerich, R. Richter, and D. Lecoq.** 1990. Induction of levansucrase in *Bacillus subtilis*: an antitermination mechanism negatively controlled by the phosphotransferase system. *Journal of Bacteriology* **172**:1043-1050.
37. **Dahl, M. K. and W. Hillen.** 1995. Contributions of XylR, CcpA and HPr to catabolite repression of the *xyl* operon in *Bacillus subtilis*. *FEMS Microbiology Letters* **132**:79-83.
38. **Darbon, E., P. Servant, S. Poncet, and J. Deutscher.** 2002. Antitermination by GlpP, catabolite repression via CcpA and inducer exclusion triggered by P~GlpK dephosphorylation control *Bacillus subtilis glpFK* expression. *Molecular Microbiology* **43**:1039-1052.
39. **De Lencastre, H. and De Sa-Nogueira, I.** 2000. Highly regulable promoter for heterologous gene expression. U.S. Patent 6,030,807, filed September 10, 1997, and issued February 29, 2000.
40. **Débarbouillé, M., M. Arnaud, A. Fouet, A. Klier, and G. Rapoport.** 1990. The *sacT* gene regulating the *sacPA* operon in *Bacillus subtilis* shares strong homology with transcriptional antiterminators. *Journal of Bacteriology* **172**:3966-3973.
41. **Débarbouillé, M., I. Martin-Verstraete, A. Klier, and G. Rapoport.** 1991. The transcriptional regulator LevR of *Bacillus subtilis* has domains homologous to both sigma 54- and phosphotransferase system-dependent regulators. *Proceedings of the National Academy of Sciences* **88**:2212-2216.
42. **Delobbe, A., H. Chalumeau, J. M. CLAVERIE, and P. GAY.** 1976. Phosphorylation of intracellular fructose in *Bacillus subtilis* mediated by phosphoenolpyruvate-l-Fructose phosphotransferase. *European Journal of Biochemistry* **66**:485-491.
43. **Delobbe, A., H. Chalumeau, and P. GAY.** 1975. Existence of two alternative pathways for fructose and sorbitol metabolism in *Bacillus subtilis* Marburg. *European Journal of Biochemistry* **51**:503-510.
44. **Deutscher, J., A. Galinier, and S. Masuda.** 2002. Carbohydrate uptake and metabolism, p. 129-150. In Sonenshein A.L., Hoch J.A., and Losick R. (eds.), *Bacillus subtilis* and its closest relatives: from genes to cells. ASM Press, Washington, D.C.
45. **Deutscher, J., C. Francke, and P. W. Postma.** 2006. How phosphotransferase system-related protein phosphorylation regulates carbohydrate metabolism in bacteria. *Microbiology and Molecular Biology Reviews* **70**:939-1031.

46. **Doan, T. and S. p. Aymerich.** 2003. Regulation of the central glycolytic genes in *Bacillus subtilis*: binding of the repressor CggR to its single DNA target sequence is modulated by fructose-1,6-bisphosphate. *Molecular Microbiology* **47**:1709-1721.
47. **Doherty, G. P., M. J. Fogg, A. J. Wilkinson, and P. J. Lewis.** 2010. Small subunits of RNA polymerase: localization, levels and implications for core enzyme composition. *Microbiology-Sgm* **156**:3532-3543.
48. **Dove, S. L., S. A. Darst, and A. Hochschild.** 2003. Region 4 of sigma as a target for transcription regulation. *Molecular Microbiology* **48**:863-874.
49. **Dunn, J. J. and F. W. Studier.** 1983. Complete nucleotide sequence of bacteriophage T7 DNA and the locations of T7 genetic elements. *Journal of Molecular Biology* **166**:477-535.
50. **Earl, A. M., R. Losick, and R. Kolter.** 2008. Ecology and genomics of *Bacillus subtilis*. *Trends in Microbiology* **16**:269-275.
51. **Ebright, R. H.** 1993. Transcription activation at Class I CAP-dependent promoters. *Molecular Microbiology* **8**:797-802.
52. **Eder, S., L. Shi, K. Jensen, K. Yamane, and F. M. Hulett.** 1996. A *Bacillus subtilis* secreted phosphodiesterase alkaline phosphatase is the product of a Pho regulon gene, *phoD*. *Microbiology-Uk* **142**:2041-2047.
53. **Ehenberg R.C.** 1835. Dritter Beitrag zur Erkenntniss grosser Organisation in der Richtung des kleinsten Raumes. *Abh.Preuss.Akad.Wiss.Phys.Kl.Baelin aus der Jahre 1833-1835* 143-336.
54. **Estrem, S. T., W. Ross, T. Gaal, Z. W. S. Chen, W. Niu, R. H. Ebright, and R. L. Gourse.** 1999. Bacterial promoter architecture: subsite structure of UP elements and interactions with the carboxy-terminal domain of the RNA polymerase  $\alpha$  subunit. *Genes & Development* **13**:2134-2147.
55. **Estrem, S. T., W. Ross, T. Gaal, Z. W. S. Chen, W. Niu, R. H. Ebright, and R. L. Gourse.** 1999. Bacterial promoter architecture: subsite structure of UP elements and interactions with the carboxy-terminal domain of the RNA polymerase  $\alpha$  subunit. *Genes & Development* **13**:2134-2147.
56. **Faires, N., S. Tobisch, S. Bachem, I. Martin-Verstraete, M. Hecker, and J. Stülke.** 1999. The catabolite control protein CcpA controls ammonium assimilation in *Bacillus subtilis*. *Journal of Molecular Microbiology and Biotechnology* **1**:141-148.
57. **Ferreira, L. C. S., R. C. C. Ferreira, and W. Schumann.** 2005. *Bacillus subtilis* as a tool for vaccine development: from antigen factories to delivery vectors. *Anais da Academia Brasileira de Ciencias* **77**:113-124.
58. **Fiegler, H., J. Bassias, I. Jankovic, and R. Brückner.** 1999. Identification of a gene in *Staphylococcus xylosus* encoding a novel glucose uptake protein. *Journal of Bacteriology* **181**:4929-4936.
59. **Fouet, A., M. Arnaud, A. Klier, and G. Rapoport.** 1987. *Bacillus subtilis* sucrose-specific enzyme II of the phosphotransferase system: expression in *Escherichia coli* and homology to enzymes II from enteric bacteria. *Proceedings of the National Academy of Sciences of the United States of America* **84**:8773-8777.
60. **Fu, L. L., Z. R. Xu, W. F. Li, J. B. Shuai, P. Lu, and C. X. H. hu.** 2007. Protein secretion pathways in *Bacillus subtilis*: implication for optimization of heterologous protein secretion. *Biotechnology Advances* **25**:1-12.

61. **Fujita, Y.** 2009. Carbon catabolite control of the metabolic network in *Bacillus subtilis*. *Bioscience, biotechnology, and biochemistry* **73**:245-259.
62. **Fujita, Y., Y. Miwa, A. Galinier, and J. Deutscher.** 1995. Specific recognition of the *Bacillus subtilis gnt cis*-acting catabolite-responsive element by a protein complex formed between CcpA and seryl-phosphorylated HPr. *Molecular Microbiology* **17**:953-960.
63. **Fukushima, T., H. Yamamoto, A. Atrih, S. J. Foster, and J. Sekiguchi.** 2002. A polysaccharide deacetylase gene (*pdaA*) is required for germination and for production of muramic delta-lactam residues in the spore cortex of *Bacillus subtilis*. *Journal of Bacteriology* **184**:6007-6015.
64. **Galinier, A., J. Haiech, M. C. Kilhoffer, M. Jaquinod, J. Stülke, J. Deutscher, and I. Martin-Verstraete.** 1997. The *Bacillus subtilis crh* gene encodes a HPr-like protein involved in carbon catabolite repression. *Proceedings of the National Academy of Sciences* **94**:8439-8444.
65. **Galinier, A., M. Kravanja, R. Engelmann, W. Hengstenberg, M. C. Kilhoffer, J. Deutscher, and J. Haiech.** 1998. New protein kinase and protein phosphatase families mediate signal transduction in bacterial catabolite repression. *Proceedings of the National Academy of Sciences* **95**:1823-1828.
66. **Gärtner, D., J. Degenkolb, J. A. E. Ripperger, R. Allmansberger, and W. Hillen.** 1992. Regulation of the *Bacillus subtilis* W23 xylose utilization operon: Interaction of the *xyl* repressor with the *xyl* operator and the inducer xylose. *Molecular & General Genetics* **232**:415-422.
67. **Gay, P. and A. DELOBBE.** 1977. Fructose transport in *Bacillus subtilis*. *European Journal of Biochemistry* **79**:363-373.
68. **Geanacopoulos, M., G. Vasmatazis, V. B. Zhurkin, and S. Adhya.** 2001. Gal repressosome contains an antiparallel DNA loop. *Nature Structural Biology* **8**:432-436.
69. **Geissendorfer, M. and W. Hillen.** 1990. Regulated expression of heterologous genes in *Bacillus subtilis* using the *Tn10* encoded *tet* regulatory elements. *Applied Microbiology and Biotechnology* **33**:657-663.
70. **Ghosh, T., D. Bose, and X. Zhang.** 2010. Mechanisms for activating bacterial RNA polymerase. *FEMS Microbiology Reviews* **34**:611-627.
71. **Gilbert, W. and B. Müller-Hill.** 1966. Isolation of the *lac* repressor. *Proceedings of the National Academy of Sciences of the United States of America* **56**:1891-1898.
72. **Gonzy-Tréboul, G., J. H. de Waard, M. Zagorec, and P. W. Postma.** 1991. The glucose permease of the phosphotransferase system of *Bacillus subtilis*: evidence for II<sup>Glc</sup> and III<sup>Glc</sup> domains. *Molecular Microbiology* **5**:1241-1249.
73. **Gonzy-Tréboul, G. and M. Steinmetz.** 1987. Phosphoenolpyruvate:sugar phosphotransferase system of *Bacillus subtilis*: Cloning of the region containing the *ptsH* and *ptsI* genes and evidence for a *crr*-like gene. *Journal of Bacteriology* **169**:2287-2290.
74. **Gonzy-Tréboul, G., M. Zagorec, M. C. Rainuion, and M. Steinmetz.** 1989. Phosphoenolpyruvate:sugar phosphotransferase system of *Bacillus subtilis*: nucleotide sequence of *ptsX*, *ptsH* and the 5'-end of *ptsI* and evidence for a *ptsHI* operon. *Molecular Microbiology* **3**:103-112.
75. **Görke, B. and J. Stülke.** 2008. Carbon catabolite repression in bacteria: many ways to make the most out of nutrients. *Nature reviews.Microbiology* **6**:613-624.

76. **Görke, B. and B. Rak.** 1999. Catabolite control of *Escherichia coli* regulatory protein BglG activity by antagonistically acting phosphorylations. *The EMBO journal* **18**:3370-3379.
77. **Grainger, D. C. and S. J. Busby.** 2008. Global regulators of transcription in *Escherichia coli*: Mechanisms of action and methods for study, p. 93-113.
78. **Graumann P.** 2012. *Bacillus*: cellular and molecular biology. Caister Academic Press, Norfolk.
79. **Greenberg, D. B., J. Stülke, and M. H. Saier.** 2002. Domain analysis of transcriptional regulators bearing PTS regulatory domains. *Research in Microbiology* **153**:519-526.
80. **Grundy, F. J., A. J. Turinsky, and T. M. Henkin.** 1994. Catabolite regulation of *Bacillus subtilis* acetate and acetoin utilization genes by CcpA. *Journal of Bacteriology* **176**:4527-4533.
81. **Gruss, A. and S. D. Ehrlich.** 1989. The family of highly interrelated single-stranded deoxyribonucleic acid plasmids. *Microbiological Reviews* **53**:231-241.
82. **Guérout-Fleury, A. M., N. Frandsen, and P. Stragier.** 1996. Plasmids for ectopic integration in *Bacillus subtilis*. *Gene* **180**:57-61.
83. **Haldenwang, W. G.** 1995. The sigma factors of *Bacillus subtilis*. *Microbiological Reviews* **59**:1-30.
84. **Haldimann, A., L. L. Daniels, and B. L. Wanner.** 1998. Use of new methods for construction of tightly regulated arabinose and rhamnose promoter fusions in studies of the *Escherichia coli* phosphate regulon. *Journal of Bacteriology* **180**:1277-1286.
85. **Harwood C.R.** 1989. Introduction to the Biotechnology of *Bacillus*, p. 1-4. *In* Harwood C.R. (ed.), *Bacillus* (Biotechnology Handbooks vol. 2). Plenum Press, New York.
86. **Harwood C.R. and Cutting S.M.** 1990. *Molecular biological methods for Bacillus*. John Wiley and Sons, Chichester, United Kingdom.
87. **Harwood, C. R.** 1992. *Bacillus subtilis* and its relatives: molecular biological and industrial workhorses. *Trends in Biotechnology* **10**:247-256.
88. **Haugen, S. P., W. Ross, and R. L. Gourse.** 2008. Advances in bacterial promoter recognition and its control by factors that do not bind DNA. *Nature Reviews Microbiology* **6**:507-519.
89. **Hawley, D. K. and W. R. McClure.** 1983. Compilation and analysis of *Escherichia coli* promoter DNA sequences. *Nucleic Acids Research* **11**:2237-2255.
90. **Heldwein, E. E. Z. and R. G. Brennan.** 2001. Crystal structure of the transcription activator BmrR bound to DNA and a drug. *Nature* **409**:378-382.
91. **Helfert, C., S. Gotsche, and M. K. Dahl.** 1995. Cleavage of trehalose-phosphate in *Bacillus subtilis* is catalyzed by a phospho- $\alpha$ -(1-1)-glucosidase encoded by the *treA* gene. *Molecular Microbiology* **16**:111-120.
92. **Heng, C., Z. J. Chen, L. X. Du, and F. P. Lu.** 2005. Expression and secretion of an acid-stable  $\alpha$ -amylase gene in *Bacillus subtilis* by SacB promoter and signal peptide. *Biotechnology Letters* **27**:1731-1736.
93. **Henstra, S. A., R. H. Duurkens, and G. T. Robillard.** 2000. Multiple phosphorylation events regulate the activity of the mannitol transcriptional regulator MtlR of the *Bacillus stearothermophilus* phosphoenolpyruvate-dependent mannitol phosphotransferase system. *The Journal of biological chemistry* **275**:7037-7044.

94. **Henstra, S. A., M. Tuinhof, R. H. Duurkens, and G. T. Robillard.** 1999. The *Bacillus stearothermophilus* mannitol regulator, MtlR, of the phosphotransferase system - A DNA-binding protein, regulated by HPr and IICB<sup>mtl</sup>-dependent phosphorylation. The Journal of biological chemistry **274**:4754-4763.
95. **Hoess, R. H. and K. Abremski.** 1984. Interaction of the bacteriophage P1 recombinase Cre with the recombining site *loxP*. Proceedings of the National Academy of Sciences of the United States of America-Biological Sciences **81**:1026-1029.
96. **Horodniceanu, T., D. H. Bouanchaud, G. Bieth, and Y. A. Chabbert.** 1976. R plasmids in *Streptococcus agalactiae* (group B). Antimicrobial Agents and Chemotherapy **10**:795-801.
97. **Horwitz, S. B. and N. O. Kaplan.** 1964. Hexitol dehydrogenases of *Bacillus Subtilis*. The Journal of biological chemistry **239**:830-838.
98. **Hyde, E. I., M. D. Hilton, and H. R. Whiteley.** 1986. Interactions of *Bacillus subtilis* RNA polymerase with subunits determining the specificity of initiation: sigma and delta peptides can bind simultaneously to core. Journal of Biological Chemistry **261**:6565-6570.
99. **Imanaka, T., M. Fujii, and S. Aiba.** 1981. Isolation and characterization of antibiotic resistance plasmids from thermophilic bacilli and construction of deletion plasmids. Journal of Bacteriology **146**:1091-1097.
100. **Inaoka, T., T. Satomura, Y. Fujita, and K. Ochi.** 2009. Novel gene regulation mediated by overproduction of secondary metabolite neotrehalosadamine in *Bacillus subtilis*. FEMS Microbiology Letters **291**:151-156.
101. **Iordanescu S.** 1976. Three distinct plasmids originating in the same *Staphylococcus aureus* strain. Archives roumaines de pathologi **35**:111-118.
102. **Iordanescu, S., M. Surdeanu, P. D. Latta, and R. Novick.** 1978. Incompatibility and molecular relationships between small staphylococcal plasmids carrying same resistance marker. Plasmid **1**:468-479.
103. **Irnov, I., C. M. Sharma, J. Vogel, and W. C. Winkler.** 2010. Identification of regulatory RNAs in *Bacillus subtilis*. Nucleic Acids Research **38**:6637-6651.
104. **Jan, J., F. Valle, F. Bolivar, and E. Merino.** 2001. Construction of protein overproducer strains in *Bacillus subtilis* by an integrative approach. Applied Microbiology and Biotechnology **55**:69-75.
105. **Jeske, M. and J. Altenbuchner.** 2010. The *Escherichia coli* rhamnose promoter *rhaP<sub>BAD</sub>* is in *Pseudomonas putida* KT2440 independent of Crp-cAMP activation. Applied Microbiology and Biotechnology **85**:1923-1933.
106. **Jourlin-Castelli, C., N. Mani, M. M. Nakano, and A. L. Sonenshein.** 2000. CcpC, a novel regulator of the LysR family required for glucose repression of the *citB* gene in *Bacillus subtilis*. Journal of Molecular Biology **295**:865-878.
107. **Joyet, P., M. Derkaoui, S. Poncet, and J. Deutscher.** 2010. Control of *Bacillus subtilis* *mtl* operon expression by complex phosphorylation-dependent regulation of the transcriptional activator MtlR. Molecular Microbiology **76**:1279-1294.
108. **Jürgen, B., T. Schweder, and M. Hecker.** 1998. The stability of mRNA from the *gsiB* gene of *Bacillus subtilis* is dependent on the presence of a strong ribosome binding site. Molecular and General Genetics MGG **258**:538-545.
109. **Kaberdin, V. R. and U. Bläsi.** 2006. Translation initiation and the fate of bacterial mRNAs. FEMS Microbiology Reviews **30**:967-979.

110. **Kawamura, F. and R. H. Doi.** 1984. Construction of a *Bacillus subtilis* double mutant deficient in extracellular alkaline and neutral proteases. *Journal of Bacteriology* **160**:442-444.
111. **Kerovuoto, J., N. von Weymarn, M. Povelainen, S. Auer, and A. Miasnikov.** 2000. A new efficient expression system for *Bacillus* and its application to production of recombinant phytase. *Biotechnology Letters* **22**:1311-1317.
112. **Kim, H. J., A. Roux, and A. L. Sonenshein.** 2002. Direct and indirect roles of CcpA in regulation of *Bacillus subtilis* Krebs cycle genes. *Molecular Microbiology* **45**:179-190.
113. **Klier, A. F. and G. Rapoport.** 1988. Genetics and regulation of carbohydrate catabolism in *Bacillus*. *Annual Review of Microbiology* **42**:65-95.
114. **Kotrba, P., M. Inui, and H. Yukawa.** 2001. Bacterial phosphotransferase system (PTS) in carbohydrate uptake and control of carbon metabolism. *Journal of Bioscience and Bioengineering* **92**:502-517.
115. **Krüger, S., S. Gertz, and M. Hecker.** 1996. Transcriptional analysis of *bglPH* expression in *Bacillus subtilis*: evidence for two distinct pathways mediating carbon catabolite repression. *Journal of Bacteriology* **178**:2637-2644.
116. **Krüger, S. and M. Hecker.** 1995. Regulation of the putative *bglPH* operon for aryl-beta-glucoside utilization in *Bacillus subtilis*. *Journal of Bacteriology* **177**:5590-5597.
117. **Kunst, F., N. Ogasawara, I. Moszer, A. M. Albertini, G. Alloni, V. Azevedo, M. G. Bertero, P. Bessieres, A. Bolotin, S. Borchert, R. Borriss, L. Boursier, A. Brans, M. Braun, S. C. Brignell, S. Bron, S. Brouillet, C. V. Bruschi, B. Caldwell, V. Capuano, N. M. Carter, S. K. Choi, J. J. Codani, I. F. Connerton, A. Danchin, and et al.** 1997. The complete genome sequence of the Gram-positive bacterium *Bacillus subtilis*. *Nature* **390**:249-256.
118. **Kunst, F., M. Steinmetz, J. A. Lepesant, and R. Dedonder.** 1977. Presence of a third sucrose hydrolyzing enzyme in *Bacillus subtilis*: constitutive levanase synthesis by mutants of *Bacillus subtilis* Marburg 168. *Biochimie* **59**:287-292.
119. **Lacey, R. W. and I. Chopra.** 1974. Genetic studies of a multi-resistant strain of *Staphylococcus aureus*. *Journal of Medical Microbiology* **7**:285-297.
120. **Laemmli, U. K.** 1970. Cleavage of structural proteins during assembly of head of bacteriophage-T4. *Nature* **227**:680-685.
121. **Lam, K. H. E., K. C. Chow, and W. K. R. Wong.** 1998. Construction of an efficient *Bacillus subtilis* system for extracellular production of heterologous proteins. *Journal of Biotechnology* **63**:167-177.
122. **Landmann, J. J., R. A. Busse, J. H. Latz, K. D. Singh, J. Stülke, and B. Görke.** 2011. Crh, the paralogue of the phosphocarrier protein HPr, controls the methylglyoxal bypass of glycolysis in *Bacillus subtilis*. *Molecular Microbiology* **82**:770-787.
123. **Langbein, I., S. Bachem, and J. Stülke.** 1999. Specific interaction of the RNA-binding domain of the *Bacillus subtilis* transcriptional antiterminator GlcT with its RNA target, RAT. *Journal of Molecular Biology* **293**:795-805.
124. **Le Coq, D., C. Lindner, S. Krüger, M. Steinmetz, and J. Stülke.** 1995. New  $\beta$ -glucoside (*bgl*) genes in *Bacillus subtilis*: the *bglP* gene product has both transport and regulatory functions similar to those of *BglF*, its *Escherichia coli* homolog. *Journal of Bacteriology* **177**:1527-1535.
125. **Le Grice, S. F. J.** 1990. Regulated promoter for high-level expression of heterologous genes in *Bacillus subtilis*. *Methods in Enzymology* **185**:201-214.

126. **Le, A. T. T. and W. Schumann.** 2007. A novel cold-inducible expression system for *Bacillus subtilis*. *Protein Expression and Purification* **53**:264-269.
127. **Leblanc, D. J. and L. N. Lee.** 1984. Physical and genetic analyses of *Streptococcal plasmid* pAM $\beta$ 1 and cloning of its replication region. *Journal of Bacteriology* **157**:445-453.
128. **Lee, J. W. K., C. W. Edwards, and F. M. Hulett.** 1991. *Bacillus licheniformis* Apase I gene promoter: A strong well-regulated promoter in *Bacillus subtilis*. *Journal of General Microbiology* **137**:1127-1133.
129. **Lee, S. J., D. M. Kim, K. H. Bae, S. M. Byun, and J. H. Chung.** 2000. Enhancement of secretion and extracellular stability of staphylokinase in *Bacillus subtilis* by wprA gene disruption. *Applied and Environmental Microbiology* **66**:476-480.
130. **Lee, S. Y. and S. Rasheed.** 1990. A simple procedure for maximum yield of high-quality plasmid DNA. *Biotechniques* **9**:676-679.
131. **Lehnik-Habrink, M., R. J. Lewis, U. Mäder, and J. Stülke.** 2012. RNA degradation in *Bacillus subtilis*: an interplay of essential endo- and exoribonucleases. *Molecular Microbiology* **84**:1005-1017.
132. **Lepesant, J.-A., J. Lepesant-Kejzlarová, M. Pascal, F. Kunst, A. Billault, and R. Dedonder.** 1974. Identification of the structural gene of levansucrase in *Bacillus subtilis* Marburg. *Molecular and General Genetics MGG* **128**:213-221.
133. **Lesuisse, E., K. Schanck, and C. Colson.** 1993. Purification and preliminary characterization of the extracellular lipase of *Bacillus subtilis* 168, an extremely basic pH-tolerant enzyme. *European Journal of Biochemistry* **216**:155-160.
134. **Li, W. F., X. X. Zhou, and P. Lu.** 2004. Bottlenecks in the expression and secretion of heterologous proteins in *Bacillus subtilis*. *Research in microbiology*. **155**:605-610.
135. **Lindner, C., A. Galinier, M. Hecker, and J. Deutscher.** 1999. Regulation of the activity of the *Bacillus subtilis* antiterminator LicT by multiple PEP-dependent, enzyme I- and HPr-catalysed phosphorylation. *Molecular Microbiology* **31**:995-1006.
136. **Lindner, C., M. Hecker, D. Le Coq, and J. Deutscher.** 2002. *Bacillus subtilis* mutant LicT antiterminators exhibiting enzyme I- and HPr-independent antitermination affect catabolite repression of the *bgIPH* operon. *Journal of Bacteriology* **184**:4819-4828.
137. **Lloyd, G., P. Landini, and S. Busby.** 2001. Activation and repression of transcription initiation in bacteria. *Regulation of Gene Expression* **37**:17-31.
138. **López, D. and R. Kolter.** 2010. Extracellular signals that define distinct and coexisting cell fates in *Bacillus subtilis*. *FEMS Microbiology Reviews* **34**:134-149.
139. **Lorca, G. L., Y. J. Chung, R. D. Barabote, W. Weyler, C. H. Schilling, and M. H. Saier.** 2005. Catabolite repression and activation in *Bacillus subtilis*: Dependency on CcpA, HPr, and HprK. *Journal of Bacteriology* **187**:7826-7839.
140. **Ludwig, H., G. Homuth, M. Schmalisch, F. M. Dyka, M. Hecker, and J. Stülke.** 2001. Transcription of glycolytic genes and operons in *Bacillus subtilis*: evidence for the presence of multiple levels of control of the *gapA* operon. *Molecular Microbiology* **41**:409-422.
141. **Ludwig, H., N. Rebhan, H. M. Blencke, M. Merzbacher, and J. Stülke.** 2002. Control of the glycolytic *gapA* operon by the catabolite control protein A in *Bacillus subtilis*: a novel mechanism of CcpA-mediated regulation. *Molecular Microbiology* **45**:543-553.

142. **Luria, S. E., J. N. Adams, and R. C. Ting.** 1960. Transduction of lactose-utilizing ability among strains of *E. coli* and *S. dysenteriae* and the properties of the transducing phage particles. *Virology* **12**:348-390.
143. **Manival, X., Y. S. Yang, M. P. Strub, M. Kochoyan, M. Steinmetz, and S. Aymerich.** 1997. From genetic to structural characterization of a new class of RNA-binding domain within the SacY/BglG family of antiterminator proteins. *The EMBO journal* **16**:5019-5029.
144. **Martin-Verstraete, I., V. Charrier, J. Stülke, A. Galinier, B. Erni, G. Rapoport, and J. Deutscher.** 1998. Antagonistic effects of dual PTS-catalysed phosphorylation on the *Bacillus subtilis* transcriptional activator LevR. *Molecular Microbiology* **28**:293-303.
145. **Martin-Verstraete, I., M. Debarbouille, A. Klier, and G. Rapoport.** 1990. Levanase operon of *Bacillus subtilis* includes a fructose-specific phosphotransferase system regulating the expression of the operon. *Journal of Molecular Biology* **214**:657-671.
146. **Martin-Verstraete, I., J. Stülke, A. Klier, and G. Rapoport.** 1995. Two different mechanisms mediate catabolite repression of the *Bacillus subtilis* levanase operon. *Journal of Bacteriology* **177**:6919-6927.
147. **Martin-Verstraete, I., M. Débarbouillé, A. Klier, and G. Rapoport.** 1994. Interactions of wild-type and truncated LevR of *Bacillus subtilis* with the upstream activating sequence of the levanase operon. *Journal of Molecular Biology* **241**:178-192.
148. **Martin-Verstraete, I., A. Galinier, E. Darbon, Y. Quentin, M. C. Kilhoffer, V. Charrier, J. Haiech, G. Rapoport, and J. Deutscher.** 1999. The Q15H mutation enables Crh, a *Bacillus subtilis* HPr-like protein, to carry out some regulatory HPr functions, but does not make it an effective phosphocarrier for sugar transport. *Microbiology* **145**:3195-3204.
149. **Meijer, W. J. J., G. B. A. Wisman, P. Terpstra, P. B. Thorsted, C. M. Thomas, S. Holsappel, G. Venema, and S. Bron.** 1998. Rolling-circle plasmids from *Bacillus subtilis*: complete nucleotide sequences and analyses of genes of pTA1015, pTA1040, pTA1050 and pTA1060, and comparisons with related plasmids from Gram-positive bacteria. *FEMS Microbiology Reviews* **21**:337-368.
150. **Michel, J. F. and J. Millet.** 1970. Physiological studies on early-blocked sporulation mutants of *Bacillus subtilis*. *The Journal of applied bacteriology* **33**:220-227.
151. **Miller J.H.** 1972. *Experiments in molecular genetics*. Cold Spring Harbor Laboratory Press, New York.
152. **Miwa, Y., A. Nakata, A. Ogiwara, M. Yamamoto, and Y. Fujita.** 2000. Evaluation and characterization of catabolite-responsive elements (*cre*) of *Bacillus subtilis*. *Nucleic Acids Research* **28**:1206-1210.
153. **Miwa, Y. and Y. Fujita.** 2001. Involvement of two distinct catabolite-responsive elements in catabolite repression of the *Bacillus subtilis* myo-inositol (*iol*) Operon. *Journal of Bacteriology* **183**:5877-5884.
154. **Morabbi Heravi, K., M. Wenzel, and J. Altenbuchner.** 2011. Regulation of *mtl* operon promoter of *Bacillus subtilis*: Requirements of its use in expression vectors. *Microbial Cell Factories* **10**.
155. **Moszer Vvan, P. G. and A. Danchin.** 1995. SubtiList: A relational database for the *Bacillus subtilis* genome. *Microbiology (Reading)* **141**:261-268.
156. **Moszer, I.** 1998. The complete genome of *Bacillus subtilis*: from sequence annotation to data management and analysis. *FEBS Letters* **430**:28-36.



157. **Moszer, I., L. M. Jones, S. Moreira, C. Fabry, and A. Danchin.** 2002. SubtiList: the reference database for the *Bacillus subtilis* genome. *Nucleic Acids Research* **30**:62-65.
158. **Motejadded, H. and J. Altenbuchner.** 2007. Integration of a lipase gene into the *Bacillus subtilis* chromosome: Recombinant strains without antibiotic resistance marker. *Iranian Journal of Biotechnology* **5**:105-109.
159. **Nakatani, Y., W. L. Nicholson, K. D. Neitzke, P. Setlow, and E. Freese.** 1989. Sigma-G RNA polymerase controls forespore-specific expression of the glucose dehydrogenase operon in *Bacillus subtilis*. *Nucleic Acids Research* **17**:999-1017.
160. **Neutzner M.** 2003. Institut für Industrielle Genetik. Regulatoren des Zellteilungszyklus der Hefe *Saccharomyces cerevisiae*: die Polo-Kinase Cdc5 und der Ubiquitinierungsfaktor Hct1.
161. **Nguyen, H. D., Q. A. Nguyen, R. C. Ferreira, L. C. S. Ferreira, L. T. Tran, and W. Schumann.** 2005. Construction of plasmid-based expression vectors for *Bacillus subtilis* exhibiting full structural stability. *Plasmid* **54**:241-248.
162. **Nickels, B. E., S. L. Dove, K. S. Murakami, S. A. Darst, and A. Hochschild.** 2002. Protein-protein and protein-DNA interactions of  $\sigma^{70}$  region 4 involved in transcription activation by  $\lambda$ cl. *Journal of Molecular Biology* **324**:17-34.
163. **Nijland, R., C. Lindner, M. van Hartskamp, L. W. Hamoen, and O. P. Kuipers.** 2007. Heterologous production and secretion of *Clostridium perfringens*  $\beta$ -toxin in closely related Gram-positive hosts. *Journal of Biotechnology* **127**:361-372.
164. **Novick, R. P.** 1989. Staphylococcal plasmids and their replication. *Annual Review of Microbiology* **43**:537-565.
165. **Oberholzer, A. E., M. Bumann, P. Schneider, C. B+ñchler, C. Siebold, U. Baumann, and B. Erni.** 2005. Crystal structure of the phosphoenolpyruvate-binding enzyme I-domain from the *Thermoanaerobacter tengcongensis* PEP: sugar phosphotransferase system (PTS). *Journal of Molecular Biology* **346**:521-532.
166. **Olmos-Soto, J. and R. Contreras-Flores.** 2003. Genetic system constructed to overproduce and secrete proinsulin in *Bacillus subtilis*. *Applied Microbiology and Biotechnology* **62**:369-373.
167. **Österberg, S., T. Peso-Santos, and V. Shingler.** 2011. Regulation of alternative sigma factor use, p. 37-55.
168. **Palva, I.** 1982. Molecular cloning of  $\alpha$ -amylase gene from *Bacillus amyloliquefaciens* and its expression in *B. subtilis*. *Gene* **19**:81-87.
169. **Palva, I., P. Lehtovaara, L. Kaariainen, M. Sibakov, K. Cantell, C. H. Schein, K. Kashiwagi, and C. Weissmann.** 1983. Secretion of Interferon by *Bacillus subtilis*. *Gene* **22**:229-235.
170. **Palva, I., M. Sarvas, P. Lehtovaara, M. Sibakov, and L. Kaariainen.** 1982. Secretion of *Escherichia coli*  $\beta$ -lactamase from *Bacillus subtilis* by the aid of  $\alpha$ -amylase signal sequence. *Proceedings of the National Academy of Sciences of the United States of America-Biological Sciences* **79**:5582-5586.
171. **Paulsen, I. T., S. Chauvaux, P. Choi, and M. H. Saier.** 1998. Characterization of glucose-specific catabolite repression-resistant mutants of *Bacillus subtilis*: Identification of a novel hexose:H<sup>+</sup> symporter. *J. Bacteriol.* **180**:498-504.
172. **Pero, J., J. Nelson, and T. D. Fox.** 1975. Highly asymmetric transcription by RNA polymerase containing phage-SP01-induced polypeptides and a new host protein.

- Proceedings of the National Academy of Sciences of the United States of America **72**:1589-1593.
173. **Perret, J. and P. GAY.** 1979. Kinetic study of a phosphoryl exchange reaction between fructose and fructose 1-phosphate catalyzed by the membrane-bound enzyme II of the phosphoenolpyruvate-fructose 1-phosphotransferase system of *Bacillus subtilis*. European Journal of Biochemistry **102**:237-246.
  174. **Phan, T. T. P., H. D. Nguyen, and W. Schumann.** 2006. Novel plasmid-based expression vectors for intra- and extracellular production of recombinant proteins in *Bacillus subtilis*. Protein Expression and Purification **46**:189-195.
  175. **Phan, T. T. P. and W. Schumann.** 2007. Development of a glycine-inducible expression system for *Bacillus subtilis*. Journal of Biotechnology **128**:486-499.
  176. **Postma, P. W. and S. Roseman.** 1976. Bacterial phosphoenolpyruvate:sugar phosphotransferase system. Biochimica et Biophysica Acta **457**:213-257.
  177. **Presecan, E., I. Moszer, L. Boursier, H. C. Ramos, V. de la Fuente, M. F. Hullo, C. Lelong, S. Schleich, A. Sekowska, B. H. Song, G. Villani, F. Kunst, A. Danchin, and P. Glaser.** 1997. The *Bacillus subtilis* genome from *gerBC* (311°) to *licR* (334°). Microbiology **143**:3313-3328.
  178. **Presecan-Siedel, E., A. Galinier, R. Longin, J. Deutscher, A. Danchin, P. Glaser, and I. Martin-Verstraete.** 1999. Catabolite Regulation of the *pta* gene as part of carbon flow pathways in *Bacillus subtilis*. Journal of Bacteriology **181**:6889-6897.
  179. **Quisel, J. D., W. F. Burkholder, and A. D. Grossman.** 2001. *In vivo* effects of sporulation kinases on mutant Spo0A proteins in *Bacillus subtilis*. Journal of Bacteriology **183**:6573-6578.
  180. **Reizer, J., S. Bachem, A. Reizer, M. Arnaud, M. H. Saier, and J. Stülke.** 1999. Novel phosphotransferase system genes revealed by genome analysis - the complete complement of PTS proteins encoded within the genome of *Bacillus subtilis*. Microbiology **145**:3419-3429.
  181. **Reizer, J., U. Bergstedt, A. Galinier, E. Küster, M. H. Saier, W. Hillen, M. Steinmetz, and J. Deutscher.** 1996. Catabolite repression resistance of *gnt* operon expression in *Bacillus subtilis* conferred by mutation of His-15, the site of phosphoenolpyruvate-dependent phosphorylation of the phosphocarrier protein HPr. Journal of Bacteriology **178**:5480-5486.
  182. **Reizer, J., C. Hoischen, F. Titgemeyer, C. Rivolta, R. Rabus, J. Stulke, D. Karamata, M. H. Saier, and W. Hillen.** 1998. A novel protein kinase that controls carbon catabolite repression in bacteria. Molecular Microbiology **27**:1157-1169.
  183. **Rojo, F.** 1999. Repression of transcription initiation in bacteria. Journal of Bacteriology **181**:2987-2991.
  184. **Ross, W., K. K. Gosink, J. Salomon, K. Igarashi, C. Zou, A. Ishihama, K. Severinov, and R. L. Gourse.** 1993. A third recognition element in bacterial promoters: DNA binding by the alpha subunit of RNA polymerase. Science **262**:1407-1413.
  185. **Sadaie, Y., H. Nakadate, R. Fukui, L. M. Yee, and K. Asai.** 2008. Glucomannan utilization operon of *Bacillus subtilis*. FEMS Microbiology Letters **279**:103-109.
  186. **Sambrook, J., E. F. Fritsch, and Maniatis T.** 1989. Molecular cloning: a laboratory manual. Cold spring Harbor Laboratory, NY.

187. **Sanger, F., S. Nicklen, and A. R. Coulson.** 1977. DNA sequencing with chain-terminating inhibitors. *Proceedings of the National Academy of Sciences of the United States of America* **74**:5463-5467.
188. **Schallmeyer, M., A. Singh, and O. P. Ward.** 2004. Developments in the use of *Bacillus* species for industrial production. *Canadian Journal of Microbiology* **50**:1-17.
189. **Schilling, O., C. Herzberg, T. Hertrich, H. Vorsmann, D. Jessen, S. Hubner, F. Titgemeyer, and J. Stülke.** 2006. Keeping signals straight in transcription regulation: specificity determinants for the interaction of a family of conserved bacterial RNA-protein couples. *Nucleic Acids Research* **34**:6102-6115.
190. **Schilling, O., I. Langbein, M. Müller, M. H. Schmalisch, and J. Stülke.** 2004. A protein-dependent riboswitch controlling *ptsGHI* operon expression in *Bacillus subtilis*: RNA structure rather than sequence provides interaction specificity. *Nucleic Acids Research* **32**:2853-2864.
191. **Schlx, P. J., M. W. Capp, and M. T. Record.** 1995. Inhibition of transcription initiation by *lac* repressor. *Journal of Molecular Biology* **245**:331-350.
192. **Schmalisch, M. H., S. Bachem, and J. Stülke.** 2003. Control of the *Bacillus subtilis* antiterminator protein GlcT by phosphorylation. Elucidation of the phosphorylation chain leading to inactivation of GlcT. *The Journal of biological chemistry* **278**:51108-51115.
193. **Schmidt, A., M. Schiesswohl, U. Volker, M. Hecker, and W. Schumann.** 1992. Cloning, sequencing, mapping, and transcriptional analysis of the *groESL* operon from *Bacillus subtilis*. *Journal of Bacteriology* **174**:3993-3999.
194. **Schnetzer, K., J. Stülke, S. Gertz, S. Krüger, M. Krieg, M. Hecker, and B. Rak.** 1996. LicT, a *Bacillus subtilis* transcriptional antiterminator protein of the BglG family. *Journal of Bacteriology* **178**:1971-1979.
195. **Schöck, F. and M. K. Dahl.** 1996. Analysis of DNA flanking the *treA* gene of *Bacillus subtilis* reveals genes encoding a putative specific enzyme II<sup>Tre</sup> and a potential regulator of the trehalose operon. *Gene* **175**:59-63.
196. **Schönert, S., S. Seitz, H. Krafft, E. A. Feuerbaum, I. Andernach, G. Witz, and M. K. Dahl.** 2006. Maltose and maltodextrin utilization by *Bacillus subtilis*. *Journal of Bacteriology* **188**:3911-3922.
197. **Schulz, A. and W. Schumann.** 1996. *hrcA*, the first gene of the *Bacillus subtilis dnaK* operon encodes a negative regulator of class I heat shock genes. *Journal of Bacteriology* **178**:1088-1093.
198. **Schumann, W.** 2007. Production of recombinant proteins in *Bacillus subtilis*. *Advances in applied microbiology* **62**:137-189.
199. **Servant, P., D. Le Coq, and S. Aymerich.** 2005. CcpN (YqzB), a novel regulator for CcpA-independent catabolite repression of *Bacillus subtilis* gluconeogenic genes. *Molecular Microbiology* **55**:1435-1451.
200. **Shivers, R. P. and A. L. Sonenshein.** 2005. *Bacillus subtilis ilvB* operon: an intersection of global regulons. *Molecular Microbiology* **56**:1549-1559.
201. **Simonen, M. and I. Palva.** 1993. Protein secretion in *Bacillus* species. *Microbiological Reviews* **57**:109-137.
202. **Singh, K. D., M. H. Schmalisch, J. Stülke, and B. Görke.** 2008. Carbon catabolite repression in *Bacillus subtilis*: Quantitative analysis of repression exerted by different carbon sources. *Journal of Bacteriology* **190**:7275-7284.

203. **Smits, W. K., T. T. Hoa, L. W. Hamoen, O. P. Kuipers, and D. Dubnau.** 2007. Antirepression as a second mechanism of transcriptional activation by a minor groove binding protein. *Molecular Microbiology* **64**:368-381.
204. **Sonenshein, A. L.** 2007. Control of key metabolic intersections in *Bacillus subtilis*. *Nature reviews.Microbiology* **5**:917-927.
205. **Sonenshein, A. L., Hoch J.A., and Losick R.** 2001. *Bacillus subtilis* and Its Closest Relatives: from Genes to Cells. ASM Press.
206. **Spizizen, J.** 1958. Transformation of biochemically deficient strains of *Bacillus subtilis* by deoxyribonucleate. *Proceedings of the National Academy of Sciences of the United States of America* **44**:1072-1078.
207. **Steinmetz, M., D. Lecoq, and S. Aymerich.** 1989. Induction of saccharolytic enzymes by sucrose in *Bacillus subtilis*: evidence for 2 partially interchangeable regulatory pathways. *Journal of Bacteriology* **171**:1519-1523.
208. **Stülke, J., M. Arnaud, G. Rapoport, and I. Martin-Verstraete.** 1998. PRD - a protein domain involved in PTS-dependent induction and carbon catabolite repression of catabolic operons in bacteria. *Molecular Microbiology* **28**:865-874.
209. **Stülke, J. and W. Hillen.** 1999. Carbon catabolite repression in bacteria. *Current Opinion in Microbiology* **2**:195-201.
210. **Stülke, J. and W. Hillen.** 2000. Regulation of carbon catabolism in *Bacillus* species. *Annual Review of Microbiology* **54**:849-880.
211. **Stülke, J., I. Martin-Verstraete, V. Charrier, A. Klier, J. Deutscher, and G. Rapoport.** 1995. The HPr protein of the phosphotransferase system links induction and catabolite repression of the *Bacillus subtilis* levanase operon. *Journal of Bacteriology* **177**:6928-6936.
212. **Stülke, J., I. Martin-Verstraete, M. Zagorec, M. Rose, A. Klier, and G. Rapoport.** 1997. Induction of the *Bacillus subtilis ptsGHI* operon by glucose is controlled by a novel antiterminator, GlcT. *Molecular Microbiology* **25**:65-78.
213. **Sun, T.** 2010. Institut für Industrielle Genetik. Regulation des Mannose-Operons in *Bacillus subtilis*.
214. **Sun, T. and J. Altenbuchner.** 2010. Characterization of a mannose utilization system in *Bacillus subtilis*. *Journal of Bacteriology* **192**:2128-2139.
215. **Sutrina, S. L., P. Reddy, M. H. Saier, and J. Reizer.** 1990. The glucose permease of *Bacillus subtilis* is a single polypeptide chain that functions to energize the sucrose permease. *The Journal of biological chemistry* **265**:18581-18589.
216. **Tachibana, K. I., K. Yoda, S. Watanabe, H. Kadokura, Y. Katayama, K. Yamane, M. Yamasaki, and G. Tamura.** 1987. Secretion of *Bacillus subtilis*  $\alpha$ -amylase in the periplasmic space of *Escherichia coli*. *Journal of General Microbiology* **133**:1775-1782.
217. **Tanaka, T. and T. Koshikawa.** 1977. Isolation and characterization of 4 types of plasmids from *Bacillus subtilis* (natto). *Journal of Bacteriology* **131**:699-701.
218. **Tanaka, T. and M. Ogura.** 1998. A novel *Bacillus natto* plasmid pLS32 capable of replication in *Bacillus subtilis*. *FEBS Letters* **422**:243-246.
219. **Terpe, K.** 2006. Overview of bacterial expression systems for heterologous protein production: from molecular and biochemical fundamentals to commercial systems. *Applied Microbiology and Biotechnology* **72**:211-222.

220. **Titok, M. A., J. Chapuis, Y. V. Selezneva, A. V. Lagodich, V. A. Prokulevich, S. D. Ehrlich, and L. Janniere.** 2003. *Bacillus subtilis* soil isolates: plasmid replicon analysis and construction of a new theta-replicating vector. *Plasmid* **49**:53-62.
221. **Tobisch, S., P. Glaser, S. Kruger, and M. Hecker.** 1997. Identification and characterization of a new beta-glucoside utilization system in *Bacillus subtilis*. *Journal of Bacteriology* **179**:496-506.
222. **Tobisch, S., J. Stülke, and M. Hecker.** 1999. Regulation of the *lic* operon of *Bacillus subtilis* and characterization of potential phosphorylation sites of the LicR regulator protein by site-directed mutagenesis. *Journal of Bacteriology* **181**:4995-5003.
223. **Tobisch, S., D. Zühlke, J. Bernhardt, J. Stülke, and M. Hecker.** 1999. Role of CcpA in regulation of the central pathways of carbon catabolism in *Bacillus subtilis*. *Journal of Bacteriology* **181**:6996-7004.
224. **Tojo, S., T. Satomura, K. Morisaki, J. Deutscher, K. Hirooka, and Y. Fujita.** 2005. Elaborate transcription regulation of the *Bacillus subtilis* *ilv-leu* operon involved in the biosynthesis of branched-chain amino acids through global regulators of CcpA, CodY and TnrA. *Molecular Microbiology* **56**:1560-1573.
225. **Tortosa, P., S. Aymerich, C. Lindner, M. H. Saier, J. Reizer, and D. Lecoq.** 1997. Multiple phosphorylation of SacY, a *Bacillus subtilis* transcriptional antiterminator negatively controlled by the phosphotransferase system. *Journal of Biological Chemistry* **272**:17230-17237.
226. **Tortosa, P., N. Declerck, H. Dutartre, C. Lindner, J. Deutscher, and D. Le Coq.** 2001. Sites of positive and negative regulation in the *Bacillus subtilis* antiterminators LicT and SacY. *Molecular Microbiology* **41**:1381-1393.
227. **Turinsky, A. J., F. J. Grundy, J. H. Kim, G. H. Chambliss, and T. M. Henkin.** 1998. Transcriptional activation of the *Bacillus subtilis* *ackA* gene requires sequences upstream of the promoter. *Journal of Bacteriology* **180**:5961-5967.
228. **Uozumi, T., A. Ozaki, T. Beppu, and K. Arima.** 1980. New cryptic plasmid of *Bacillus subtilis* and restriction analysis of other plasmids found by general screening. *Journal of Bacteriology* **142**:315-318.
229. **Valentin-Hansen, P., L. SogaardAndersen, and H. Pedersen.** 1996. A flexible partnership: The CytR anti-activator and the cAMP-CRP activator protein, comrades in transcription control. *Molecular Microbiology* **20**:461-466.
230. **van Hijum, S. A. F. T., M. H. Medema, and O. P. Kuipers.** 2009. Mechanisms and evolution of control logic in prokaryotic transcriptional regulation. *Microbiology and Molecular Biology Reviews* **73**:481-509.
231. **van Tilbeurgh, H. and N. Declerck.** 2001. Structural insights into the regulation of bacterial signalling proteins containing PRDs. *Current Opinion in Structural Biology* **11**:685-693.
232. **van Tilbeurgh, H., D. Le Coq, and N. Declerck.** 2001. Crystal structure of an activated form of the PTS regulation domain from the LicT transcriptional antiterminator. *The EMBO journal* **20**:3789-3799.
233. **Vitikainen, M., H. L. Hyyrylainen, A. Kivimaki, V. P. Kontinen, and M. Sarvas.** 2005. Secretion of heterologous proteins in *Bacillus subtilis* can be improved by engineering cell components affecting post-translocational protein folding and degradation. *Journal of Applied Microbiology* **99**:363-375.

234. **Wacker, I., H. Ludwig, I. Reif, H. M. Blencke, C. Detsch, and J. Stülke.** 2003. The regulatory link between carbon and nitrogen metabolism in *Bacillus subtilis*: regulation of the *gltAB* operon by the catabolite control protein CcpA. *Microbiology* **149**:3001-3009.
235. **Wade, J. T. and K. Struhl.** 2008. The transition from transcriptional initiation to elongation. *Current Opinion in Genetics & Development* **18**:130-136.
236. **Wanker, E., A. Huber, and H. Schwab.** 1995. Purification and characterization of the *Bacillus subtilis* levanase produced in *Escherichia coli*. *Applied and Environmental Microbiology* **61**:1953-1958.
237. **Warner, J. B. and J. S. Lolkema.** 2003. CcpA-dependent carbon catabolite repression in bacteria. *Microbiology and molecular biology reviews* : MMBR **67**:475-490.
238. **Warth, L., I. Haug, and J. Altenbuchner.** 2011. Characterization of the tyrosine recombinase MrpA encoded by the *Streptomyces coelicolor* A3(2) plasmid SCP2\*. *Archives of Microbiology* **193**:187-200.
239. **Watanabe, S., M. Hamano, H. Kakeshita, K. Bunai, S. Tojo, H. Yamaguchi, Y. Fujita, S. L. Wong, and K. Yamane.** 2003. Mannitol-1-phosphate dehydrogenase (MtlD) is required for mannitol and glucitol assimilation in *Bacillus subtilis*: Possible cooperation of *mtl* and *gut* operons. *Journal of Bacteriology* **185**:4816-4824.
240. **Weickert, M. J. and G. H. Chambliss.** 1990. Site-directed mutagenesis of a catabolite repression operator sequence in *Bacillus subtilis*. *Proceedings of the National Academy of Sciences* **87**:6238-6242.
241. **Weisblum, B., M. Y. Graham, T. Gryczan, and D. Dubnau.** 1979. Plasmid copy number control: Isolation and characterization of high-copy-number mutants of plasmid pE194. *Journal of Bacteriology* **137**:635-643.
242. **Wenzel, M., A. Müller, M. Siemann-Herzberg, and J. Altenbuchner.** 2011. Self-inducible *Bacillus subtilis* expression system for reliable and inexpensive protein production by high-cell-density fermentation. *Applied and Environmental Microbiology* **77**:6419-6425.
243. **Westers, L., D. S. Dijkstra, H. Westers, J. M. van Dijl, and W. J. Quax.** 2006. Secretion of functional human interleukin-3 from *Bacillus subtilis*. *Journal of Biotechnology* **123**:211-224.
244. **Westers, L., H. Westers, and W. J. Quax.** 2004. *Bacillus subtilis* as cell factory for pharmaceutical proteins: a biotechnological approach to optimize the host organism. *Biochimica et Biophysica Acta-Molecular Cell Research* **1694**:299-310.
245. **Wilms, B., A. Hauck, M. Reuss, C. Syldatk, R. Mattes, M. Siemann, and J. Altenbuchner.** 2001. High-cell-density fermentation for production of L-N-carbamoylase using an expression system based on the *Escherichia coli rhaBAD* promoter. *Biotechnology and Bioengineering* **73**:95-103.
246. **Wosten, M. M. S. M.** 1998. Eubacterial sigma-factors. *Fems Microbiology Reviews* **22**:127-150.
247. **Wösten, M. M. S. M.** 1998. Eubacterial sigma-factors. *FEMS Microbiology Reviews* **22**:127-150.
248. **Wray, L. V., F. K. Pettengill, and S. H. Fisher.** 1994. Catabolite repression of the *Bacillus subtilis hut* operon requires a *cis*-acting site located downstream of the transcription initiation site. *Journal of Bacteriology* **176**:1894-1902.

249. **Wu, S. C. and S. L. Wong.** 2002. Engineering of a *Bacillus subtilis* strain with adjustable levels of intracellular biotin for secretory production of functional streptavidin. *Applied and Environmental Microbiology* **68**:1102-1108.
250. **Wu, S. C., J. C. Yeung, Y. J. Duan, R. Q. Ye, S. J. Szarka, H. R. Habibi, and S. L. Wong.** 2002. Functional production and characterization of a fibrin-specific single-chain antibody fragment from *Bacillus subtilis*: effects of molecular chaperones and a wall-bound protease on antibody fragment production. *Applied and Environmental Microbiology* **68**:3261-3269.
251. **Wu, X. C., W. Lee, L. Tran, and S. L. Wong.** 1991. Engineering a *Bacillus subtilis* expression-secretion system with a strain deficient in 6 extracellular proteases. *Journal of Bacteriology* **173**:4952-4958.
252. **Xue, G. P., J. S. Johnson, and B. P. Dalrymple.** 1999. High osmolarity improves the electro-transformation efficiency of the gram-positive bacteria *Bacillus subtilis* and *Bacillus licheniformis*. *Journal of Microbiological Methods* **34**:183-191.
253. **Yamamoto, H., M. Serizawa, J. Thompson, and J. Sekiguchi.** 2001. Regulation of the *glv* operon in *Bacillus subtilis*: YfiA (GlvR) is a positive regulator of the operon that is repressed through CcpA and *cre*. *Journal of Bacteriology* **183**:5110-5121.
254. **Yang, M. Y., E. Ferrari, and D. J. Henner.** 1984. Cloning of the neutral protease gene of *Bacillus subtilis* and the use of the cloned gene to create an *in vitro*-derived deletion mutation. *Journal of Bacteriology* **160**:15-21.
255. **Yang, M., W. Zhang, X. Zhang, and P. Cen.** 2006. Construction and characterization of a novel maltose inducible expression vector in *Bacillus subtilis*. *Biotechnology Letters* **28**:1713-1718.
256. **Yang, S., H. Huang, R. A. Zhang, X. D. Huang, S. Y. Li, and Z. Y. Yuan.** 2001. Expression and purification of extracellular penicillin G acylase in *Bacillus subtilis*. *Protein Expression and Purification* **21**:60-64.
257. **Yanisch-Perron, C., J. Vieira, and J. Messing.** 1985. Improved M13 phage cloning vectors and host strains: nucleotide sequences of the M13mp18 and pUC19 Vectors. *Gene* **33**:103-119.
258. **Yansura, D. G. and D. J. Henner.** 1984. Use of the *Escherichia coli lac* repressor and operator to control gene expression in *Bacillus subtilis*. *Proceedings of the National Academy of Sciences of the United States of America* **81**:439-443.
259. **Yansura, D. G. and D. J. Henner.** 1984. Use of the *Escherichia coli lac* repressor and operator to control gene expression in *Bacillus subtilis*. *Proceedings of the National Academy of Sciences of the United States of America-Biological Sciences* **81**:439-443.
260. **Ye R., Yang L.P., and Wong S.L.** Construction of protease deficient *Bacillus subtilis* strains for expression studies: inactivation of seven extracellular proteases and the intracellular LonA protease. 160-169. 1996. Seoul, Korea, The Korean Society for Applied Microbiology. *Proceedings of the International Symposium on Recent Advances in Bioindustry*. 1996.
261. **Ye, R. Q., J. H. Kim, B. G. Kim, S. Szarka, E. Sihota, and S. L. Wong.** 1999. High-level secretory production of intact, biologically active staphylokinase from *Bacillus subtilis*. *Biotechnology and Bioengineering* **62**:87-96.
262. **Zalieskas, J. M., L. V. Wray, and S. H. Fisher.** 1998. Expression of the *Bacillus subtilis acsA* gene: Position and sequence context affect *cre*-mediated carbon catabolite repression. *Journal of Bacteriology* **180**:6649-6654.

263. **Zhang, A. L., H. Liu, M. M. Yang, Y. S. Gong, and H. Chen.** 2007. Assay and characterization of a strong promoter element from *B. subtilis*. *Biochemical and Biophysical Research Communications* **354**:90-95.
264. **Zhang, X. Z., Z. L. Cui, Q. Hong, and S. P. Li.** 2005. High-level expression and secretion of methyl parathion hydrolase in *Bacillus subtilis* WB800. *Applied and Environmental Microbiology* **71**:4101-4103.
265. **Zukowski, M. M. and L. Miller.** 1986. Hyperproduction of an intracellular heterologous protein in a *sacU<sup>h</sup>* mutant of *Bacillus subtilis*. *Gene* **46**:247-255.



## 7. Appendices

The map of the parental plasmids used in this study.

